Unravelling the role of α_2-adrenoceptors and P2X purinoceptors in vascular sympathetic neurotransmission using a mouse lacking α_1-adrenoceptors

Claire Stevenson BSc (Hons)

Thesis submitted in fulfilment of the requirements for the Degree of Doctor of Philosophy

UNIVERSITY *of* GLASGOW

December 2014

School of Life Sciences

College of Medical, Veterinary and Life Sciences

Abstract

The experiments presented in this thesis describe the roles of the post-junctional α_1, α_2-adrenoceptors (AR) and P2X purinoceptors in response to sympathetic nerve stimulation in mouse mesenteric and tail arteries. Such roles were determined by combining wire myography techniques and nerve stimulation alongside various selective antagonists. The influence of each receptor on the response to nerve stimulation was first defined in wild type (WT) mice before analysis of α_1-AR knock out (KO) mice. Therefore the effect that genetic removal of the α_1-ARs had on vascular response could be investigated. The response is the force generated in milligrams/tension when the nerves are stimulated and correspond to activation of post-junctional receptors and subsequent smooth muscle cell contraction.

Systolic Blood Pressure and the α_1-ARs

The aim of the first study (Chapter Three) was to determine whether systolic blood pressure (BP) was different in the KO mice compared to WT controls. Tail cuff measurements of systolic BP were recorded in WT and AR KO mice. It was found that BP was not affected by loss of the α_{1A}- and α_{1D}-AR subtypes (ADKO) or by loss of all three α_1-AR subtypes (α_1-null). Therefore, the α_1-AR role in maintaining BP may not be as crucial as previously understood or, the remaining receptors may have compensated for the loss.

Calcitonin Gene Related Peptide (CGRP) in Mouse mesenteric and tail arteries

The second study (Chapter Four) examined whether, under the stimulation parameters used, the potent vasodilator CGRP masked the vasoconstrictor response to nerve stimulation in mouse mesenteric and tail arteries. The potent neurotoxin capsaicin depletes the sensory nerves of CGRP. Responses prior to capsaicin incubation were compared with those following capsaicin treatment in WT, ADKO and α_1-null mice. In mesenteric artery from each mouse strain, capsaicin incubation had no significant effect on the peak response to nerve stimulation. Furthermore, in the tail artery, capsaicin treatment had no significant effects on the responses in WT and α_1-null mice. However, in the ADKO mouse tail artery preparations, capsaicin treatment significantly increased the peak response at low frequency

stimulation. These findings may indicate an interaction between the α_1-AR subtypes and the release of CGRP whereby the presence of all or none of the subtypes (WT and α_1-null) has no effect on CGRP release but loss of the α_{1A}- and α_{1D}-AR subtypes alters the balance and reveals a CGRP induced effect.

Response to perivascular nerve stimulation in Mouse mesenteric and tail arteries from Wild Type mice

The aim of Chapter Five was to determine which receptors were involved in the response to nerve stimulation in mouse mesenteric and tail arteries. These results would then act as a comparison with the ADKO and α_1-null responses in the later chapters. A contractile response to nerve stimulation was recorded in each of the studied vessels and abolished by combined blocked with antagonists for the α_1-, α_2-ARs and P2X receptors. Individual receptor blockade and component analysis then revealed the roles of the individual receptors. In the mesenteric arteries, the α_1-ARs were the main contributors to the response followed by the P2X receptors and finally the α_2-ARs which displayed both pre- and post-junctional effects. No interactions were discovered between the α_1-ARs and the other receptors. The P2X receptors initiated the contraction and prolonged the response at the low frequency and contributed to the contractile response at the high frequency. In the tail artery, the α_2-ARs were the dominant receptors but required the presence of the α_1-ARs, and to some extent the P2X receptors in order to produce a full contractile response upon activation. The P2X receptors alone initiated the response at low frequency stimulation with both α_1-ARs and P2X receptors involved in initiation of the contraction at the high frequency.

Response to perivascular nerve stimulation in mesenteric and tail arteries from mice lacking α_{1A}- and α_{1D}-AR subtypes (ADKO)

Chapter Six determined the role of the α_{1B}-ARs in the response to nerve stimulation and therefore examined whether loss of the α_{1A}- and α_{1D}-AR subtypes (ADKO) affected the response. In the mesenteric arteries, at the low frequency, there was a potential interaction between the receptors. However, no single receptor was responsible for the contraction although there was a trend for the P2X receptors to be active at the beginning of the response and the α_2-ARs to be active at the latter stage of the response. This was also true at the higher frequency. The ADKO vessels displayed no evidence of pre-junctional α_2-ARs. In the

mesenteric arteries, there is little role for the α_{1B}-ARs. The overall contribution in the tail artery was reduced in the ADKO, particularly at the higher frequency. Similar to the WT mice, the α_2-ARs were the main contributor to the response. The P2X receptors initiated the contraction but required the α_2-ARs to be active at the low frequency. The α_{1B}-ARs also required an interaction with the other receptors at low frequency stimulation in order to contribute to the initiation of the response. The α_{1B}-ARs also contributed to the initiation of the response at the high frequency without requiring the presence of the other receptors.

Response to perivascular nerve stimulation in mesenteric and tail arteries from mice lacking α_{1A}-, α_{1B}- and α_{1D}-AR subtypes (α_1-null)

In the final study (Chapter Seven), α_1-null mice were utilised in order to determine whether loss of the α_1-ARs had a significant effect on the response to nerve stimulation in mouse mesenteric and tail arteries. Furthermore, the influence of the α_2-ARs and P2X receptors were compared with the response in the WT vessels to determine whether they compensate for the loss of the α_1-ARs. The removal of the α_1-ARs dramatically reduced the response to nerve stimulation in the mesenteric arteries, with no apparent compensation from the α_2-ARs or P2X receptors. There was no evidence of pre-junctional α_2-ARs. The small response recorded at the high frequency was initiated by the P2X receptors and maintained by the α_2-ARs and P2X receptors. The tail artery response was smaller in the α_1-null mice compared with WT, particularly at the higher frequency. However, the response was still mediated largely by the α_2-ARs with an interaction with the P2X receptors likely. A potential compensatory mechanism was recorded at the lower frequency as the response to P2X receptor antagonism was greater in the α_1-null than in the WT mice. As was shown in the WT, activation of the P2X receptors initiated the contraction, particularly at the high frequency.

Findings and Results

Collectively, the findings of the studies presented in this thesis demonstrate that the α_1-, α_2-ARs and P2X receptors are involved in the response to nerve stimulation in the mouse mesenteric and tail arteries. Genetic removal of the α_1-ARs in the ADKO and α_1-null is most effective in the mesenteric arteries with little evidence of any compensatory mechanisms. In the mouse tail artery, the α_2-ARs are the main contributors to the response and so loss of the

α_1-ARs has less of an effect. Interactions between the receptors were most clearly shown in the tail artery with little interaction between the α_1-ARs and the other receptors demonstrated in the mesentery. Furthermore, it has been demonstrated here that systolic BP is unaffected in the KO mice and there is little input from the CGRP nerves using the parameters tested. From these results, the importance of α_1-AR activation in nerve mediated responses was determined. The absence of a compensatory mechanism to match the response lost in the ADKO and α_1-null mice, and the presentation of a normal BP alongside the survival of these transgenic mice challenges the importance of the α_1-ARs being crucial in the maintenance of vascular tone. This therefore complements the knowledge that treatment of primary hypertension with α_1-AR antagonists is largely unsuccessful. The contractile response mediated by α_2-ARs and P2X receptors may be used as potential therapeutic targets in controlling hypertension.

Table of Contents

List of Tables

Chapter Six: ADKO

Chapter Seven: α_1-null

List of Figures

Acknowledgements

I would firstly like to thank my supervisors, Professor Ian McGrath and Dr Craig Daly for the invaluable knowledge and encouragement you have both given throughout the course of my PhD and my Undergraduate studies. A special thanks to Elspeth for your time and patience over the past four years. I would also like to thank the British Heart Foundation for their funding and support of this research.

Thank you to Joyce – your wisdom and enthusiasm knows no bounds – I truly believe that you know everything!

My time in the lab would not have been the same without the company of Anne and Stefanie, particularly over the past few months. Their continuous support and kindness has been greatly appreciated – and their ability to listen to my moans and provide perfect advice! Thank you so much.

To my Aberdeen family – the encouragement and friendship I have received from you all has been overwhelming. I can't thank you enough – for distracting me when I needed a break and for providing plenty food when I've had to work! Kerr - Tha mi fada nur comain.

Calum – thank you for joining me on this journey and listening to my endless chat on all things adrenergic! Your continued support and encouragement is greatly appreciated; as is your ability to make me laugh after a long day at the lab. I couldn't have done this without you.

To my Granny, Gran, Papa, Mum, Dad and Mark – you've always been there for me, had confidence in me, and supported me in all of my decisions. I wouldn't be the person I am today without you all and so thank you for everything! Papa….I've finished writing now ☺

Author's Declaration

I hereby declare that this thesis has been composed by myself, and the work of which it is a record has been done by myself, except where specifically acknowledged. I also confirm that it has not been submitted in any previous application for a higher degree and that all sources of information have been specifically acknowledged by means of references.

Claire Stevenson
December 2014

Abbreviations

α_1-AR	alpha 1 adrenoceptor
α_2-AR	alpha 2 adrenoceptor
α_{1AD}-KO	alpha 1AD adrenoceptors knock out mouse
ACh	Acetylcholine
ANOVA	Analysis of Variance
AR	Adrenoceptor
ATP	Adenosine Tri-Phosphate
BP	Blood Pressure
cAMP	Adenosine 3'-5'cyclic monophosphate
CGRP	Calcitonin gene-related peptide
DAG	Diacylglycerol
DNA	Deoxyribonucleic acid
GDP	Guanosine diphosphate
GTP	Guanosine triphosphate
GPCR	G-protein coupled receptor
IP_3	Inositol-1,4,5-triphosphate
KO	Knock-out
mM	Millimolar
NA	Noradrenaline
NANC	Non-adrenergic Non-cholinergic
nM	Nanomolar
pA_2	affinity estimate of an antagonist derived from a Schild plot

PIP_2	phosphoinositol-4,5-bisphosphate
PKC	Protein kinase C
PLC	Phopholipase C
PS	Prazosin sensitive
RS	Rauwolscine sensitive
SEM	Standard error of the mean
SNS	Sympathetic nervous system
SS	Suramin sensitive
WT	Wild Type
µM	Micromolar
5-HT	5-hydroxytryptamine

Chapter One

General Introduction

1.1 Sympathetic Neurovascular Transmission

The sympathetic nervous system (SNS) forms part of the autonomic nervous system (ANS). The SNS branch is responsible for the 'fight or flight' response and in maintaining homeostasis. In relation to the vasculature, activation of the SNS leads to release of several neurotransmitters that can lead to vasoconstriction and therefore directly affect blood pressure.

1.1.1 Vascular Sympathetic Nerves and Transmitter Release

The sympathetic nerves are mainly adrenergic, originating from the thoracolumbar sections of the spinal cord and project to many target organs including smooth muscle. The preganglionic neurones release acetylcholine (ACh) which binds to nicotinic receptors located on post-ganglionic neurones. The post-ganglionic neurones terminate at the adventitial-media border where activation of the nerves leads to neurotransmitter release from vesicles within the nerve varicosities. The neurotransmitters released include noradrenaline (NA) and adenosine tri-phosphate (ATP) with continued debate as to whether they are released in parallel or via separate mechanisms (Msghina et al., 1992; Msghina et al., 1999; Brock and Cunnane, 1999; Brock and Tan, 2004). The sympathetic nerves located close to vascular smooth muscle cells have been shown to exist alongside sensory nerves that are able to release vasodilators (Kawasaki et al., 1988).

1.1.2 Pre- and Post-Junctional Receptors

When the nerves are stimulated electrically, NA and ATP are released from the nerve terminals where they can then exert their effects on receptors located pre-junctionally, on the nerve terminal or post-junctionally, on smooth muscle cells. Post-junctional α_1- and α_2-ARs can be activated by NA, and ATP can act at post-junctional P2X receptors (Brock and

Cunnane, 1999). Activation of these post-junctional receptors results in vessel constriction. The α_2-ARs have also been shown to exist pre-junctionally and activation of these receptors inhibits further neurotransmitter release from the nerve terminals (Msghina et al., 1992; Starke et al., 1974; Langer, 1974).

1.1.3 Post Receptor Mechanisms of Contraction

The α-ARs belong to the G-protein-coupled receptor (GPCR) superfamily and are made up of 7 transmembrane domains which have three intracellular and three extracellular loops (Graham et al., 1996). The GPCRs are an extensive family of receptors which are involved in numerous processes within the body including regulation of the immune system and behavioural and mood regulation. Physiological mechanisms within the vascular system are regulated by noradrenaline and adrenaline (Vargas and Gorman, 1995).

The α_1-ARs belong to the subset of the GPCRs which also includes the α_2-ARs. Located in the intracellular space is the C-terminus, with the N-terminus located in the extracellular space. The agonist binds to the ligand binding site which is formed by the collection of the 7 α helical domains. When an agonist binds to the extracellular ligand binding site, a signal is passed to an intracellular receptor bound specific G_q subunit (Ruffolo et al., 1991). In the α_1-ARs the specific G protein is either $G_{\alpha q/11}$, $G_{\alpha 14}$ or $G_{\alpha 16}$ depending on the α_1-AR subtype which is being activated. When noradrenaline binds to the α_1-AR it activates the specific G protein. When the G_α sub-unit is in its inactivated state it is associated with β and γ subunits. These subunits dissociate when the adrenoceptors are stimulated and guanosine diphosphate (GDP) is converted into guanosine triphosphate (GTP). This leads to activation of phospholipase C (PLC). PLC cleaves phosphoinositol-4,5-bisphosphate (PIP_2) into 1,2-diaclycerol (DAG) and inositol-1,4,5-triphosphate (IP_3) (Uberti et al., 2003). Phosphoinositide specific-phospholipase C (PI-PLC) β1 is the PLC activated by the $G_{\alpha q/11}$, $G_{\alpha 14}$ or $G_{\alpha 16}$ subunits (Wu et al., 1992). IP_3 interacts with the calcium channel on the endoplasmic reticulum which in turn leads to the release of calcium from the intracellular stores. This increase in $[Ca^{2+}]_i$ leads to vasoconstriction. The release of Ca^{2+} acts synergistically with DAG to activate protein kinase C (PKC). The activation of PKC leads

to phosphorylation of specific target proteins which in turn controls the cell and alters function (Minneman, 1988).

The α_2-ARs also belong to the GPCR superfamily but have a different mechanism upon activation. When an agonist binds to the ligand binding site, the intracellular G_α subunit dissociates from the β and γ subunits and GDP is converted to GTP. The GTP binding protein binds Gi. These proteins are known as inhibitory proteins as the G_i sub-units inhibit adenylyl cyclase enzymes. When the adenylyl cyclase enzyme is in its active form it is responsible for converting ATP into the second messenger cyclic AMP (cAMP). Formation of cAMP leads to activation of protein kinases which allow important cellular functions to be regulated (Tan et al., 2007). Therefore, the inhibition of adenylyl cyclase leads to a decrease in ion transport and ion channel function which increases cell excitability leading to smooth muscle contraction.

It is not yet fully understood how activation of α_2-ARs initiates depolarisation. However, some lab groups have investigated possible mechanisms. Tan et al. published data indicating that the inhibition of the ATP-sensitive K^+ (K_{ATP}) channels is involved in membrane depolarisation in the rat tail artery. NA acting on post-junctional α_2-ARs inhibits the K_{ATP} channels (Tan et al., 2007)

1.2 α-Adrenoceptors (AR)

Knowledge of the adrenoceptors (ARs) has been developing over the last 100 years; from the discovery of a vasoconstriction induced by adrenaline by Dale in 1906 (Dale, 1906) to the present recognition of three major groups of ARs and 9 AR subtypes. The effects on the cardiovascular system of several sympathomimetic amines were tested to advance Dale's early discovery. From these results the terms α and β-adrenoceptors were suggested as the potency values recorded for the studied amines differed between the two proposed receptors (Ahlquist, 1948). The separation into α and β was confirmed in 1957 by the discovery of dichloroisoprenaline which was found to antagonise β- but not α-ARs (Powell and Slater,

1958) and further determined through concentration response curve studies in 1967 (Furchgott, 1967). Langer and Starke et al. both discovered the division of α_1- and α_2-ARs which were then further subdivided in the 1980s (Langer, 1974; Starke et al., 1974). The AR subtypes are now recognised as α_{1A}-, α_{1B}-, α_{1D}-, α_{2A}-, α_{2B}-, α_{2C}-, β_1-, β_2- and β_3-ARs.

1.2.1 α_1-Adrenoceptors

Experiments carried out in the 1980s by different lab groups confirmed evidence that the α_1-ARs can be subdivided further. Coates et al., in 1982, investigated the effects of SGD 101/75 and phenoxybenzamine on the rat anococcygeus. SGD 101/75 is a full agonist at α_1-ARs in the rat anococcygeus. Weetman's group concluded that there must be at least two subtypes present due to the results they obtained (Coates et al., 1982). The varying potencies of the antagonists yohimbine and prazosin on the α_1-ARs of several isolated vessels was shown in 1985 (Drew, 1985). Building on this, Flavahan and Vanhoutte divided the α_1-ARs into the α_{1H}- and α_{1L}-ARs and discovered that the same antagonist could have different affinities at the receptors and so deduced that the adrenoceptor must have different subtypes (Flavahan and Vanhoutte, 1986). Muramatsu et al. (1990) also attempted to classify the α_1-ARs. They employed five competitive α-AR antagonists and the irreversible antagonist chlorethylclonidine. Their results were in line with those from Flavahan and Vanhoutte. However, they presented a new α_1-AR subtype, which they named α_{1N} to represent the results that neither pointed to a high nor low affinity to the antagonists (Muramatsu et al., 1990). As well as the proposed nomenclature from Flavahan and Vanhoutte in 1986, Morrow and Creese also proposed a sub-classification of the α_1-ARs. These were termed α_{1A}- and α_{1B}-ARs and referred to binding sites identified through radioligand binding studies. Competition curves were constructed for [3H]prazosin and [3H]WB4101 which showed a high and low affinity component assigned α_{1A}- and α_{1B}-AR respectively (Morrow and Creese, 1986). Further radioligand binding techniques carried out in rat tissue using urapidil derivatives also established two distinct α_1-AR binding sites. In these results, the rat tissues used gave different affinity constants upon displacement of prazosin from its binding sites by 5-methyl-urapidil (Hanft and Gross, 1989). Molecular cloning in 1990 by Schwinn et al. led to the discovery of the α_{1C}-AR subtype (Schwinn et al., 1990) and prompted lab groups to study the receptor pharmacology.

Competitive antagonists were used to compare their affinities towards the α_{1A}- and α_{1C}-ARs and it was discovered that the affinities were very similar and so the α_{1C}-ARs are now accepted as the α_{1A}-ARs (Ford et al., 1994). Lomasney et al. discovered a further subtype through a cDNA clone that they reported was similar to the α_{1a}-AR subtype yet experiments carried out by Perez et al., discovered that this receptor subtype had a low affinity for 5-methylurapidil and (+)-niguldipine both of which are selective α_{1A}-AR antagonists (Lomasney et al., 1991; Perez et al., 1991). This novel subtype was named as the α_{1d}-AR and was cloned in 1994 (Forray et al., 1994).

The α_{1b}-AR was cloned in 1988 from the cDNA of the Syrian hamster. A 515-residue polypeptide makes up the amino acid sequence. At the time when the affinity binding studies split the α_1-ARs into two subtypes; α_{1A}- and α_{1B}-ARs, the cloned receptor was most similar to the α_{1B}-ARs (Cotecchia et al., 1988). Cloning of the α_{1a}-AR occurred two years later through the use of the bovine cDNA library. The amino acid sequence had a 466-residue polypeptide and the receptor was shown to have a 10-times greater affinity for WB4101 and phentolamine compared to the α_{1B}-ARs. This cloned receptor was linked to the α_{1A}-ARs (Schwinn et al., 1990). A final α_1-AR subtype was cloned in 1991 and was inactivated by chlorethylclonidine. At the time, chlorethylclonidine was thought to act selectively at α_{1B}-ARs. However, the cloned receptor had a 560 amino acid protein which differed from the cloned α_{1b}-AR subtype and so this novel subtype was named the α_{1d}-AR (Perez et al., 1991).

At the time of discovery of post-junctional α_2-ARs, receptor reserves in the arteries were shown to have more α_1-ARs than α_2-ARs. In some cases, the difference was found to be five-fold (Ruffolo and Yaden, 1984). This therefore means that even when the α_2-ARs are being activated at their highest level, it still does not reach the maximum response achieved by the α_1-ARs (Flavahan and McGrath, 1984). It is recognised and accepted that the α_{1A}-ARs are involved in mediating changes in blood flow and regulating blood pressure whereas the α_{1D}-ARs are involved in contraction of the smooth muscle of large conduit vessels. The α_{1B}-ARs are thought to play a minor role in all processes concerning the maintenance of vascular resistance and blood pressure (Daly et al., 2002).

The α_{1A}-AR subtype has been shown to be involved in contraction of the mouse mesenteric arteries. Ibarra's group used the α_{1A}-AR selective agonist A61603 and found it had a 235-fold higher potency at the ARs than phenylephrine. The α_{1B}- and α_{1D}-AR alkylating agent chlorethylclonidine only slightly altered the contraction from A61603 addition (Villalobos-Molina et al., 2006). Further evidence of the role played by the α_{1A}-ARs in the mouse mesentery was published by Methven et al. in 2009. α_{1BD}-AR KO mice were used to isolate the α_{1A}-AR subtype. Pharmacological experiments revealed that there is a greater contraction in the mesenteric arteries through α_{1A}-AR activation compared with the carotid arteries (Methven et al., 2009a). The α_{1A}-AR subtype selective agonist A61603 was utilised in studies concerning the rat tail artery. Vessel contractions in response to NA were found to be due to the activation of at least two α_1-AR subtypes. Pharmacological studies involving A61603 revealed one of the subtypes to be the α_{1A}-AR as vessel response to NA and to A61603 was similar suggesting that the α_{1A}-AR subtype plays a large role in contraction of the rat tail artery (Lachnit et al., 1997).

Cavalli et al. employed α_{1B}-AR KO mice to study the functional role of the α_{1B}-AR subtype and discovered that the mice lacking the α_{1B}-AR had an overall decrease in α_{1B}-AR sites in the liver, heart and cerebral cortex. Results from reverse transcription-PCR and ligand binding studies indicated that the α_{1B}-ARs mediate the control of blood pressure in the mouse (Cavalli et al., 1997). However, published work by Zuscik et al. described the α_{1B}-AR as being associated with metabolic and cellular responses rather than playing a central role in vasoconstriction. Their results were obtained from experiments carried out using transgenic mice overexpressing the α_{1B}-AR subtype (Zuscik et al., 2001).

The α_{1D}-ARs have been shown to be the main α-AR subtype in the conduit arteries with Martinez et al. showing that even after myocardial infarction and with congestive heart failure, the α_{1D}-AR population remains and continues to function in the rat (Martinez et al., 1999). The α_{1D}-ARs have been isolated using α_{1AB}-AR KO mice and the carotid and mesenteric arteries studied. These are examples of conduit and resistance arteries respectively. The α_{1D}-ARs were shown to contribute to vasoconstriction in both vessels but had a larger impact in the conduit artery (Methven et al., 2009b).

As well as adrenaline and noradrenaline being agonists at α_1-ARs; there are more specific agonists and antagonists for the α_1-ARs and the individual subtypes. Agonists selective to the α_1-ARs relative to the α_2-ARs include phenylephrine, methoxamine and cirazoline and the receptors are antagonised by prazosin and corynanthine. There are few selective agonists and antagonists for the individual receptor subtypes with the α_{1B}-AR having no known selective agonists or antagonists. The α_{1A}-ARs are activated by A61603 and antagonised by tamsulosin, sildosin and (+)niguldipine. The α_{1D}-ARs have one accepted antagonist which is BMY7378 (Alexander et al., 2013).

1.2.2 α_2-Adrenoceptors

Docherty and McGrath produced evidence for two types of post-junctional α-AR. They tested known agonists, with dose-response and frequency response curves. Results indicated a 'prazosin-resistant' post-junctional α-AR which did not fit the criteria of the α_1-ARs but did have similarities to the pre-junctional α_2-ARs (Docherty and McGrath, 1980; McGrath, 1982). In 1985, Bylund looked at rodent and non-rodent mammalian species in order to determine the pharmacological properties of the α_2-ARs. He proposed that the α_2-AR could be subdivided into α_{2A}- and α_{2B}-AR based on their relative affinity towards prazosin. This assumption was based on the different affinity values for prazosin between the rodents and the non-rodents (Bylund, 1985). Further pharmacological studies in the rat brain by Petrash and Bylund confirmed the earlier finding of a α_{2A}- and α_{2B}-AR. [^{3}H]yohimbine, an α_2-AR antagonist, was used in experiments to determine how effective prazosin and oxymetazoloine were at inhibiting the binding of [^{3}H]yohimbine to the α_2-ARs. Different inhibition curves were constructed from blood vessels taken from the cerebral cortex, cerebellum and human caudate nucleus that confirmed the concept of more than one α_2-AR (Petrash and Bylund, 1986). As more agonists and antagonists were discovered, more experiments in 1988 and 1989 were carried out to further prove the belief of multiple α_2-AR subtypes (Bylund et al., 1988; Young et al., 1989). Bylund et al. used [^{3}H]yohimbine and oxymetazoline to determine the drug affinities of many α_2-AR antagonists that had been discovered through radio-ligand binding studies. Young et al. furthered these results in 1989 when studying α_2-ARs in rat and human tissues (Young et al., 1989) confirming, along with other labs at the time, that the results from Bylund's experiments were reproducible and taken to be correct. Brown et al. conducted experiments in 1990 which also revealed, through

saturation and displacement studies, that the α_2-ARs could be subdivided into α_{2A}- and α_{2B}-ARs (Brown et al., 1990b; Brown et al., 1990a). Following the discovery of the α_{2A}- and α_{2B}-ARs, the possibility of further subtypes was investigated. In 1988, Murphy and Bylund produced evidence in support of a third receptor subtype; α_{2C}-AR. This receptor is similar to the α_{2B}-AR subtype but has a higher affinity for [^{3}H]rauwolscine (Murphy and Bylund, 1988).

The cloning of the α_2-AR subtypes occurred before the α_1-ARs with the α_{2a}-AR subtype being first cloned in 1987 by Kobilka et al. Xenopus laevis oocytes had the cloned receptor expressed and experiments revealed that the α_2-AR agonists bound. The subtype was found to have a high affinity for yohimbine and rauwolscine and low affinity for prazosin as well as a similar amino acid sequence to that of the β_1-ARs (Kobilka et al., 1987). The α_{2b}-AR subtype was then cloned from human kidney cDNA. The subtype had a similar structure to the α_{1a}-AR subtype. The subtype bound rauwolscine and had an amino acid sequence comparable to the α_{2a}-AR. However, the subtype cloned had a high affinity for prazosin and low affinity for oxymetazoline as compared with the α_{2a}-AR and so was named as being the α_{2B}-AR (Regan et al., 1988). In 1990, the α_{2c}-AR subtype was cloned. Different adrenoceptors ligands were tested which produced different binding properties. These results showed a unique pharmacology which could not be determined as either of the previously cloned α_2-ARs. The subtype is made up of 250 amino acids and is located on chromosome 2 and was designated as the α_{2C}-AR (Lomasney et al., 1990).

The development of knock-out models for each of the α_2-AR subtypes has enabled the function of each of these subtypes to be studied. The α_{2A}-D79N mice have point mutation at position 79 and were developed to gain greater understanding of the signal transduction mechanisms. However, further investigation into these mice revealed that as the receptors were unable to couple to K^+ and Ca^+ channels, the α_{2A}-D79N mice could effectively act as α_{2A}-AR KO mice (Lakhlani et al., 1997). The KO studies have shown the α_{2A}-AR to be the main α_2-AR subtype responsible for maintaining blood pressure. The α_2-ARs have been described as mediating 'Classical Effects' upon activation via agonists with these effects including hypotension and sedation (Kable et al., 2000). In the α_{2A}-AR KO and α_{2a}-D79N mice, the agonist-induced hypotensive effect was abolished and the α_{2A}-D79N mice did not responsd to the α_2-AR selective agonist dexmedetomidine which reduces locomotor activity

in WT mice (Hunter et al., 1997). This discovery highlighted the importance of the α_{2A}-AR subtype as these same experiments carried out in the α_{2B}- and α_{2C}-AR KO mice did not yield the same results (Link et al., 1996; Hunter et al., 1997).

The α_{2B}-AR subtype has been shown to contribute to the hypertensive response in mice as this response is abolished in the α_{2B}-AR KO mice when they are exposed to the α_2-AR agonist dexmedetomidine (Link et al., 1996).

Scheinin's lab has carried out experiments using the α_{2C}-AR KO mice and mice over-expressing (OE) the α_{2C}-AR (α_{2C}-OE) subtype in an attempt to define its functionality. Results suggest that the α_{2C}-ARs are involved in brain regulation of dopamine and its metabolites as the α_{2C}-AR KO mice have decreased levels of dopamine and the α_{2C}-OE mice have raised levels of dopamine (Sallinen et al., 1997). Further studies revealed an indication that the α_{2C}-ARs may be involved in stress-dependent depression as increasing levels in the α_{2C}-AR KO and α_{2C}-OE mice yielded different results (Sallinen et al., 1999). Other than these results, the α_{2C}-AR subtype is believed to be a 'silent' receptor with no definite role in maintaining the homeostasis of the cardiovascular system. Some studies have implicated the subtype in thermoregulation as cold induces a translocation of the α_{2C}-ARs to the cell surface (Bailey et al., 2004).

As well as adrenaline and NA, there are other more specific agonists and antagonists for the α_2-ARs and the individual subtypes. Relative to the α_1-ARs, the agonists UK14304 and BHT920 are selective towards the α_2-ARs. The antagonists selective for the α_2-ARs relative to the α_1-ARs are rauwolscine and yohimbine. For the α_2-AR subtypes, only the agonist oxymetazoline has been found to be selective for the α_{2A}-ARs with no known selective agonists for the other subtypes available. BRL44408 is a selective antagonist at α_{2A}-ARs and imiloxan is selective for the α_{2B}-ARs. The antagonist JP1302 is selective towards the α_{2C}-ARs (Alexander et al., 2013).

1.3 Adenosine Tri-Phosphate (ATP) in Arterial Vessels

ATP, in the early 1970s, was believed to be the non-adrenergic non cholinergic (NANC) neurotransmitter released from the nerves that exerted their effects at the gastrointestinal tract (Burnstock et al., 1970). Following on from this, Burnstock et al. investigated the NANC response from other tissues and compared these responses to those elicited by exogenously added ATP. The results outlined the difference between the vessel response to NA and to ATP; slow and fast respectively and this fast response to ATP was mimicked by non-adrenergic non-cholinergic (NANC) inhibitory nerve stimulation (Burnstock et al., 1972). As well as ATP release from NANC nerves, it was also proposed at the time that ATP could be co-released from vesicles containing NA (Burnstock, 1976; Kasakov and Burnstock, 1983).

1.3.1 P2X Receptors

In 1972, evidence was presented that showed that released ATP stimulated P2 receptors which lead to a depolarisation (Burnstock, 1972). To date, seven P2X purinoceptors have been identified ($P2X_{1\text{-}7}$) and divided into different groups based on their efficacy towards various agonists. Group 1 belongs to the group of P2X receptors with a high affinity for ATP and rapid desensitisation. $P2X_1$ and $P2X_3$ are included in this group. Groups 2 and 3 represent the receptors with low and very low receptor affinity for ATP respectively (Burnstock and Williams, 2000). The predominant P2X receptor subtype in smooth muscle cells is the $P2X_1$ receptor which has been shown to be present in rat tail artery and mouse mesenteric arteries (Evans and Kennedy, 1994; Vial and Evans, 2002). In the mouse mesenteric arteries, the vasoconstriction due to P2X receptor activation is lost in $P2X_1$ deficient mice and the $P2X_1$ receptors have been shown, using immunofluorescence and microscopy techniques, to be grouped together in clusters opposite from the nerve varicosities (Vial and Evans, 2002; Hansen et al., 1999). Patterns of stimulation of low frequency (< 1 Hz) stimulations favours contraction through P2X receptor activation in rat mesenteric arteries (Lamont and Wier, 2002).

The mechanism of action of the P2 receptors is via ion channels which are gated by extracellular ATP. A rapid response ensues upon activation which leads to depolarisation within milliseconds compared to depolarisation via α-ARs which take seconds to initiate. The ATP released from nerve terminal vesicles acts at the post-junctional P2X receptors in the vascular smooth muscle or pre-junctionally to modulate transmitter release. After release and activation of P2X receptors by ATP, ectoATPases hydrolyse the ATP to adenosine and the presence of adenosine has been shown to reduce transmitter output (Huidobro-Toro and Donoso, 2004).

Kasakov and Burnstock demonstrated that the agonist α, β, methylene ATP (αβme-ATP) could act selectively on P2-purinoceptors. This resulted in desensitisation of the receptors due to the slowly degradable nature of αβme-ATP (Kasakov and Burnstock, 1983). Suramin has been shown to effectively antagonise P2 receptors in the mouse vas deferens; tested against the agonist αβme-ATP (Dunn and Blakeley, 1988). Experiments carried out in 1993 by Bao and Stjarne revealed an increased response to NA after desensitisation of P2X receptors by αβme-ATP. They proposed that desensitisation of the P2X receptors removes an ATP inhibitory effect (Bao and Stjarne, 1993).

1.4 Calcitonin Gene-Related Peptide (CGRP)

The sensory nervous system is comprised of cell bodies located in spinal and cranial sensory ganglia with axons projecting centrally and peripherally. To maintain homeostasis, the sensory nerves respond to alterations in the internal and external environments. However, the sensory nerves can also exert effects locally, including vascular smooth muscle relaxation (Lee et al., 1978).

The neuropeptide CGRP was discovered in 1983 by tissue-specific RNA processing (Rosenfeld et al., 1983) with CGRP containing nerves shown to be present throughout the sensory nervous system (Dhall et al., 1986; Tornebrandt et al., 1987). CGRP binding sites were found, by radioligand binding studies, to be numerous in the rat mesenteric arteries

(Wimalawansa and MacIntyre, 1988). The distribution of CGRP containing nerves throughout the guinea pig mesenteric arteries was shown by Uddman et al. who demonstrated that with raised vessel tone, addition of CGRP induced a relaxation which became more pronounced with increasing concentrations of CGRP (Uddman et al., 1986).

Transient receptor potential vanilloid (TRPV) channels are found on sensory nerves and activation of TRPV1 receptors (also known as VR1) via nerve stimulation has been shown to cause release of CGRP (Wang et al., 2006). The VR1 receptor was cloned in 1997 and activation of the channel was shown to be voltage sensitive; having a high permeability to Ca^{2+}. The continued excitation of this receptor, now linked to CGRP release, leads to desensitisation of the receptor whilst in the presence of extracellular Ca^{2+} (Caterina et al., 1997).

As the VR1 receptor can be desensitised, it is possible to deplete the sensory nerves of CGRP and thus remove the vasodilatory effect. The sensory neurotoxin capsaicin is able to do this. CGRP concentrations in the rat have been shown to originate mainly from capsaicin-sensitive perivascular nerves (Zaidi et al., 1985). In perfused rat mesenteric arteries with raised tone, peripheral nerve stimulation elicited a relaxation that could be inhibited by capsaicin pre-treatment (Kawasaki et al., 1988). Fujiwara et al. have now shown this in the mouse mesenteric arteries and conclude that the arteries are densely innervated by CGRP containing nerves (Fujiwara et al., 2012). Excitatory junctional potentials (EJP) in rat mesenteric arteries have been potentiated when pre-incubated with capsaicin to remove CGRP (Dunn et al., 2003). It is therefore possible in the mouse vessels that the full contractile effect to nerve stimulation may be masked by CGRP release.

1.5 Genetically Altered Mice

In the early 1970s, lab groups began experimenting on the genetics of mice in the hope of developing genetically altered mice that could be used to study disease states and investigate which receptors may be specifically involved. This was first achieved in 1974 by Rudolph

Jaenisch who inserted a DNA virus into the mouse embryo. This attempt was not a success as the DNA virus was not present in the next generation of mice bred (Jaenisch and Mintz, 1974). However, following two years of continuing research Jaenisch successfully manipulated a mouse embryo genome with Moloney murine leukaemia virus proviral DNA. The disease was effectively transmitted to the germ line of the resulting adults which was shown by the development of leukaemia in the animals (Jaenisch, 1976; Jaenisch, 1979). This technique has been developed and utilised by many to improve on knowledge of various disease states including cardiovascular disease. Uncovering the roles of the α_1-AR subtypes using overexpression and KO techniques should contribute to this knowledge as the α_1-ARs are believed to be crucial in the maintenance of vascular tone. Of particular interest to the topic of this project is the development of mice lacking the α_{1A}- and α_{1D}-AR subtypes (ADKO) and mice lacking all of the α_1-AR subtypes (α_1-null).

1.5.1 Transgenic Mice

There have been investigations into the α-ARs using mice with an overexpression of a particular receptor subtype. Overexpression of the α_{1B}-AR was achieved by coupling of the mutant gene to a α-myosin heavy chain promoter. Results suggested that the α_{1B}-ARs are involved in the development of cardiac hypertrophy (Milano et al., 1994). Furthermore, the α_{1B}-ARs, through overexpression studies, have also been shown to be implicated in blood pressure regulation as the transgenic mice were hypotensive. However, contractile responses in the mesentery were not altered from WT response (Zuscik et al., 2001). Mice with an α_{1A}-AR overexpression have also been developed with results suggesting these receptors are involved in cardiac contractility (Lin et al., 2001). However, there have been no other overexpression studies which concentrated on vessel contractility and response.

1.5.2 Knock-Out Mice

The mouse is a good candidate for gene knock-out (KO) studies as it has a sequenced genome which is suggested to be 75 % similar to humans (Church et al., 2009) and they have a short

generation time, meaning many experiments can be carried out in a short space of time. The generation of mice lacking either one, two or three α-AR subtypes have been developed.

The first knock-out mouse was developed in 1997 and was the α_{1B}-AR KO. The hamster α_{1b}-AR DNA was used as a probe to screen the 129/Sv mouse genomic library. The first exon of the mouse α_{1b}-AR was replaced by a 1.6 Kb cassette containing the neomycin resistance gene within the pBlueScript vector. The vector was then electroporated into 129 embryonic stem cells (ES). C57Bl/ 6J mouse blastocysts received the ES clone via microinjection before being transferred to pseudopregnant NMRI females. Of the seven mice that were mated, two contained the disrupted allele and were therefore α_{1B}-AR KO mice (Cavalli et al., 1997).

The initial experiments carried out by Cavalli et al. suggested that the α_{1B}-ARs were important mediators of blood pressure and aortic contractility (Cavalli et al., 1997). However, further experiments have suggested more of a minor role for the α_{1B}-ARs in the vasculature. The mouse aorta, carotid, mesenteric and tail arteries were employed alongside known antagonists. They were tested against the agonist phenylephrine and concentration response curves constructed. Results indicated a definite role for the α_{1A}-and α_{1D}-AR subtypes and a minor vasoconstrictor role for the α_{1B}-ARs (Daly et al., 2002). Deighan et al. proposed that the α_{1B}-ARs played a regulatory role in smooth muscle contraction of the mouse carotid arteries (Deighan et al., 2005).

Rokosh and Simpson developed the α_{1A}-AR KO mice utilising the same technique as Cavalli et al. The neomycin resistance gene was located in the vector alongside the Ecoliβ-galactosidase gene Laz C cassette before being electroporated into RW-4 129/SVJ mouse ES. These cells were then transferred into C5Bl/6 blastocysts with the targeted allele successfully transmitted through the germ line (Rokosh and Simpson, 2002).

The initial experiments by Rokosh and Simpson showed the α_{1A}-AR KO mice to be hypotensive and concluded that the α_{1A}-ARs must be important in blood pressure maintenance (Rokosh and Simpson, 2002).

The α_{1D}-AR KO was generated in 2002 by Tanoue et al. who followed a similar protocol to that of Cavalli et al. The first exon of the α_{1D}-AR gene was replaced by the neomycin resistance gene cassette and 129V ES. The ES were microinjected into pseudopregnant females. The male mice produced were mated with C57Bl/ 6J mice with litters genotyped to detect the α_{1D}-AR KO strain (Tanoue et al., 2002).

The initial experiments revealed the α_{1D}-AR KO mice to have a lower systolic and mean arterial blood pressure. Contractile responses in the mesentery and aorta were reduced suggesting a definite role for α_{1D}-ARs in the contractile response (Tanoue et al., 2002). Hosoda et al. also reported a lowered systolic and mean arterial blood pressure in the α_{1D}AR KO mice (Hosoda et al., 2005).

The α_{1AB}-AR KO mouse was developed by crossing both the α_{1A}- and α_{1B}-AR KO mice. The male KO mice had a smaller heart size due to smaller myocytes. However, this did not impact on the blood pressure (O'Connell et al., 2003). Further investigations into the α_{1AB}-AR KOs focussed on the adrenoceptors influence in the carotid and mesenteric arteries. Concentration response curves to phenylephrine were unchanged in the carotid arteries of the KO mouse but the pEC_{50} was altered in the mesenteric arteries. This supports the theory that the α_{1D}-ARs are the main functional subtype in the carotid arteries and the α_{1A}-ARs drive the response in the mesenteric arteries (Methven et al., 2009b).

The α_{1BD}-AR KO mouse has also been generated and systolic and mean arterial BP recorded. The mean arterial BP was significantly reduced in α_{1BD}-AR KO mice as was the response to the phenylephrine induced pressor response in the perfused mesenteric arteries (Hosoda et al., 2005). The development of the α_{1BD}-AR KO allows isolation of the α_{1A}ARs which was then studied in the carotid and mesenteric arteries. The contractile response to phenylephrine was not altered in the mesenteric arteries but was greatly reduced in the carotid arteries, providing further evidence of the α_{1D}-ARs role in being the main contributor in the carotid arteries (Methven et al., 2009a).

The α_{1AD}-AR KOs have now been developed and studies are ongoing to determine the effect of loss of these receptor subtypes has on vascular contractility. Based on previous experiments, these mice would be expected to be hypotensive and display a reduced contractile response in the mesenteric arteries and in the aorta.

The development of α_1-null mice is relatively new and so there have been a limited number of investigations published. Some lab groups have had difficulty in breeding these mice and have published evidence in support of ejaculatory dysfunction in the α_1-null mice. However, the mice that have been bred have been shown to develop normally and survive for at least one year. Aside from ejaculatory dysfunction, the mice also have a lower systolic blood pressure (Sanbe et al., 2007). This lab group have also reported an increase in sensitivity towards 5-hydroxytryptamine (5-HT) in the aorta of α_1-null mice compared with WT response and suggest that the α_1-ARs may play a regulatory role in connection with other vasoconstrictor mechanisms (Sanbe et al., 2009).

1.6 Justification of Utilised Vessels

The mouse and rat mesenteric arteries have been studied extensively; particularly studies utilising agonist and antagonist responses in isolated vessels. Previous studies show that in this vessel the α_1-ARs predominate with some input from P2X receptors and no evidence of post-junctional α_2-ARs (Daly et al., 2002; Martinez-Salas et al., 2007; Rummery et al., 2007). Removal of the α_1-ARs in the α_1-null mice therefore simplifies post-junctional receptor pharmacology and allows isolation of the purinergic response and study of the pre-junctional α_2-AR population.

In the rat tail artery, there are populations of α_1-, α_2-ARs and P2X receptors (Brock and Cunnane, 1999). Little is known of the response in mouse tail artery; particularly to nerve stimulation. It is beneficial to use the mouse tail artery due to the increase in development of genetically modified mice. However, before experiments can be carried out on the α_1-AR deficient mice, WT response to nerve stimulation must be analysed to determine whether it

is similar to that in the rat or different. Removal of the α_1-ARs in this preparation will allow a greater understanding of the α_2-ARs and may uncover interactions between the adrenoceptors and the purinoceptors.

In these WT and KO mouse vessels, results will further contribute to the literature using nerve stimulation techniques and various antagonists to determine which receptors are active throughout the response and in what way these receptors contribute to the response.

1.7 Aims and Objectives

The development and advances in transgenic mouse models has enabled a more direct approach to studying individual receptors. The α_1-ARs are considered to be the main mediators of constriction via vascular nerves. The genetic removal of these receptors should enhance understanding of α-AR function by simplifying the complex pharmacology within the vasculature and so reveal the other mechanisms of vascular neuroeffector control. Therefore, the main objectives of the research were:

(i). To establish whether loss of the α_{1A}- and α_{1D}-ARs in the ADKO or loss of all three α_1-ARs in the α_1-null has an effect on systolic blood pressure.

(ii). To determine whether the vasodilatory neuropeptide CGRP affects the response to perivascular nerve stimulation in WT, ADKO and α_1-null mouse mesenteric and tail artery preparations.

(iii). To verify the post-junctional receptors involved in neurovascular transmission in WT mesenteric and tail arteries.

(iv). To investigate the role of the α_{1B}-ARs in neurovascular transmission in mouse mesenteric and tail arteries by utilising ADKO mice and to establish any compensatory mechanisms loss of the α_{1A}- and α_{1D}-ARs may have on the response.

(v). To determine whether activation of the remaining receptors in the α_1-null mice were able to induce a contractile response in the absence of the α_1-ARs.

Chapter Two

Materials and Methods

This Chapter describes the Methods and Materials used throughout the project. The genotyping of the mice is described in Section 2.2. The techniques used to extract the blood vessels and the measurement of their contractions are described in Sections 2.3 and 2.4. Section 2.5 provides details of the blood pressure monitoring techniques. Lastly, a description of the statistical techniques used for the analysis of the results obtained is given in Section 2.6 with a list of materials used provided in Section 2.7.

2.1 Mice

Mice used as controls were the C57 Black Jackson Wild Type (WT) strain. The genetically modified mice were originally provided as single α_1-adrenoceptor (AR) subtype knockouts (KO). Dr Gregg Rokosh and Professor Paul C Simpson (Veterans Affairs Medical Centre, San Francisco, USA) provided the α_{1A}-AR KO; Professor Susanna Cotecchia (University of Lausanne, Lausanne, Switzerland) provided the α_{1B}-AR KO and Professor Gozoh Tsujimoto (National Children's Medical Research Centre, Tokyo, Japan) provided the α_{1D}-AR KO. The generation and background of the single knockouts have been described in detail (Rokosh and Simpson, 2002; Cavalli et al., 1997; Tanoue et al., 2002).

Initially, double KO mice were generated by crossing the single KO mice with WT mice to produce F1 generation heterozygotes. These mice were then intercrossed to produce the F2 generation which contained a mixture of all potential genotypes. WT mice produced from the F2 generation were bred to produce the control mice and the α_{1AD}-AR KO (ADKO) mice were bred to produce more double KOs (Hosoda et al., 2005). The development of the α_{1D}-AR KO mice allowed the generation of triple KO (α_1-null) mice in the same way as the double KOs. Two strains were bred specifically for the present studies. First, the single KO mice were crossed to produce α_{1AB}-AR KO (ABKO), α_{1BD}-AR KO (BDKO) and α_{1AD}-AR KO (ADKO) mice. The ABKO and BDKO mice were crossed to produce heterozygous α_{1ABD}-AR mice. These mice contained the WT gene and the KO gene for each of the α_1-AR subtypes. The heterozygous mice were crossed and the offspring genotyped to determine whether α_1-null mice had been produced.

All mice used were bred at the University of Glasgow and maintained on a 12:12 hour light/dark schedule at 22-25°C with 45-65% humidity. They had unrestricted access to a standard chow diet and were provided with drinking water. All experiments utilised male mice aged 4-6 months weighing between 26g and 42g (WT 26g - 42g, ADKO 28g - 35g, α_1-null 26g - 35g). Mice were euthanased by the standard Schedule one carbon dioxide asphyxiation. The n numbers shown throughout represents the number of animals used and in each set of experiments only one vessel was used for each protocol. Therefore, where there is an n = 7, this represents seven vessels from seven animals.

2.2 Genotyping

2.2.1 Ear Clip collection

All genetically modified mice were genotyped to ensure that the animals used were receptor knock-outs; either α_{1AD}-AR KO (ADKO) or α_1-null. The method employed involved clipping a small section from the ears of each animal. In cages containing multiple mice the ear clipping pattern was different for each mouse and a note kept of which pattern belonged to which mouse. Each ear clip was stored in a fresh sterile Eppendorf in the freezer ready for genotyping.

2.2.2 Isolation of DNA

Digestion buffer and proteinase K (10mg/1ml) were added to fresh sterile Eppendorfs. It was important to maintain a sterile environment to decrease any chance of contamination. The ear clips were then added to the solution. Proteinase K is an enzyme which breaks peptide bonds and thus frees the nucleic acids. The digestion buffer aids in this reaction, maintaining the pH and enhancing the proteinase K activity (Goldenberger et al., 1995). The Eppendorfs containing the ear clips were then agitated (‘Eppendorf; Thermomixer compact’) at 400 rpm at 55°C for approximately two hours. The samples were then vortexed and centrifuged (10

K for 5 minutes). This ensured that the ear clips were fully digested. A pellet containing those parts which did not digest was discarded following centrifugation.

Fresh sterile Eppendorfs containing the precipitant isopropanol were prepared and the supernatant from the digest added. Since DNA is insoluble in this alcohol the isopropanol causes the precipitation of the nucleic acids. The solution was mixed by inversion until a white strand (nucleic acids) became visible. To isolate the nucleic acids, the Eppendorfs where centrifuged at 14 K for 10 minutes. This resulted in the formation of a pellet of nucleic acids. The isopropanol was replaced by 70% ethanol to aid the drying of the pellet. The samples were then centrifuged (10 K for 5 minutes) before the ethanol was removed. The pellet was then left to air dry. Finally, TE buffer was added to the pellet and it was then warmed to 55 °C for one hour. TE buffer contains tris(hydroxymethyl)aminomethane (Tris) (50 mM) which buffers the pH to 8.0 and ethylenediaminetetraacetic acid (EDTA) (100 mM) which chelates cations. It is a solvent for DNA and prevents its degradation (Ross et al., 1990). The samples were then stored in the fridge.

2.2.3 Polymerase Chain Reaction (PCR)

The PCR technique allows the amplification of a DNA sequence to enable the detection of a particular gene. As each of the α_1-AR KO mice strains have distinct genetic differences it is possible to determine, from analysing the genes of interest, which mice are ADKO and which are α_1-nulls.

The solution required for PCR must contain DNA polymerase, dNTPs (deoxyribonucleotides) (0.2 mM), primers (5 μM), and DNA. A PCR 'Master Mix' contains DNA polymerase which is responsible for the replication, and dNTPs which are the free base pairs required for building replicate strands. The primers are strands of nucleic acids that serve as a starting point for DNA synthesis. The primers are specific for each gene. For these mice, the genes for α_{1A}-, α_{1B}- and α_{1D}-ARs were being targeted. Therefore, primers for each receptor, WT and KO, were required (Table 2-1). The primers for detecting α_{1A}- WT and α_{1A}- KO differ enough in nucleic acid size that the reactions can be run together (within the

same mix). However, the others cannot and so four separate reactions are run. Once the reaction mixtures are prepared, they are pipetted into a PCR plate and the solution containing the DNA added to each well.

Table 2-1: Information from Sigma Aldrich showing primers used in PCR

Target Receptor	Oligo Name	Sequence (5' - 3')
α_{1A}-AR (duplex)	a1A5'COM	AGCTAACCATTTCAGCAAAGAC
	a1A3'1A	CAAGATCACCCCAAGTAGAATG
	a1A3'LACZ	TAACCGTGCATCTGCCAGTTTG
α_{1B}-AR WT	ADRA1BCM159F	CCAAAATGCTCCCAACTCTG
	ADRA1BCM2022R	CCTGCAGGTATGAGGTCTGTG
α_{1B}-AR KO	NEO1A1B	ATTTGTCACGTCCTGCACGAC
	ADRA1BCM2022R	CCTGCAGGTATGAGGTCTGTG
α_{1D}-AR WT	ADRA1DCM013F	GACATCCTGAGCGTCACTTTC
	ADRA1DCM293R	GCTAGGAAGACACCCACTCC
α_{1D}-AR KO	NeoCM2373F	CTTTGTTAAGAAGGGTGAGAACAGAG
	ADRA1DCM293R	GCTAGGAAGACACCCACTCC

The PCR cycle begins by warming up the samples. This denatures the DNA, separating the strands. The temperature is then reduced to allow the annealing of the primers to their target sequences. Taq polymerase then begins to copy the template strands. This cycle is then repeated multiple times to amplify the quantity of DNA in the samples.

2.2.4 Gel Electrophoresis

Gel electrophoresis allows the nucleic acid fragments to be viewed directly therefore, allowing the genotypes to be identified. The gel is made up by dissolving agarose in TAE buffer. This buffer is made up of Tris, acetic acid and EDTA and allows the samples to move through the gel in response to an electrical current. The bands appear separately on the gel due to the nucleic acid composition in each sample. The nucleic acids migrate towards the positive electrode due to the number of negative charges they carry, meaning they are

attracted to the positive electrode when placed in an electrical field. Larger nucleic acids take longer to move through the gel compared to shorter nucleic acids which are able to move through the pores in the gel more easily. Ethidium bromide is added to the mixture as this binds between the DNA bases and fluoresces orange when illuminated with ultraviolet (UV) light. The gel mixture is poured into a tray and plastic combs are inserted to create the wells for the samples.

Once set, the combs are removed and the gel is submerged in TAE buffer in a gel tank. A field of 180V is then set up across the buffer and gel. The samples are run alongside a DNA ladder which acts as a standard and provides information on the size of the nucleic acids. After 30 - 40 minutes, the gel is viewed under UV light. A picture of the gel is taken and the mouse genotype is determined (Figure 2-1).

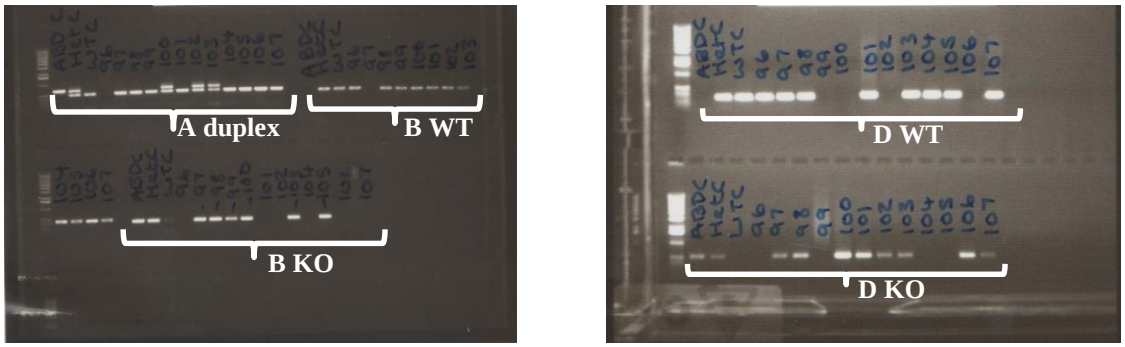

Figure 2-1: Example of gel results photograph detailing each of the PCR mixture outcomes.

2.3 Dissection

2.3.1 Tail Artery

The underside of the mouse tail was marked with a black marker pen, close to the base of the tail, in order to locate the tail artery. The tail was then cut near the base of the tail and pinned to a clean petri dish containing fresh physiological saline solution (PSS). The

composition of the PSS was as follows (in mM): 119 NaCl, 4.7 KCl, 1.2 $MgSO_4.H_20$, 1.2 KH_2PO_4, 24.9 $NaHCO_3$, 2.5 $CaCl_2$ and 11.1 glucose. Pins were placed at the base of the tail and 2 cm from the base to secure. With the aid of a Zeiss dissecting microscope and dissection instruments, the tail skin and membranous sheath were removed to expose the artery. A 4 mm section starting 2 cm from the base of the tail ("proximal segment") was then removed and stored in fresh PSS. Another pin was then placed 5 cm from the base of the tail and the process repeated in order to remove a 4 mm section starting 5 cm from the base of the tail ("distal segment"). Both segments of tail artery were cleared free of fat and cut into two pieces ready for experimental use.

2.3.2 Mesenteric Arteries

A section of the mesentery containing several mesenteric arcades was removed from the abdominal cavity and pinned out in a clean petri dish containing fresh PSS. The superior mesenteric artery was located in order to determine the position of first order mesenteric arteries which branch off from it. Four first order mesenteric arteries were cleared free of fat, removed from their junction with the superior mesenteric artery, and cut into 2 mm pieces ready for experimental use.

2.4 Myography

2.4.1 Wire Myograph

The ability to study mechanical responses in vessels with a small diameter (<300 μm) was facilitated by the introduction of the wire myograph in 1976 by Mulvany and Halpern (Mulvany and Halpern, 1976). The myograph used in all myography experiments contained four stainless steel 8 ml baths (Multi Myograph model 610M, Danish Myotechnology, Aarhus, Denmark) (Figure 2-2). Each bath contained two heads; one attached to a

micrometer allowing length adjustments and the other attached to the force transducer which measures the force produced by the vessel. The term 'the response' is used throughout to describe the force produced by the vessel. Silver plates mounted within the heads functioned as the stimulating electrodes. Each bath contained 8 ml PSS which was continually gassed with 95% O_2/ 5% CO_2 and kept at a temperature of 37°C. A suction tube was used to remove PSS from the baths when fresh PSS was added. Responses were recorded from the transducer via an ADI Powerlab (4/20) and displayed in grams tension using Chart software (Version 7). The equipment was calibrated on a regular basis using a 2 g weight.

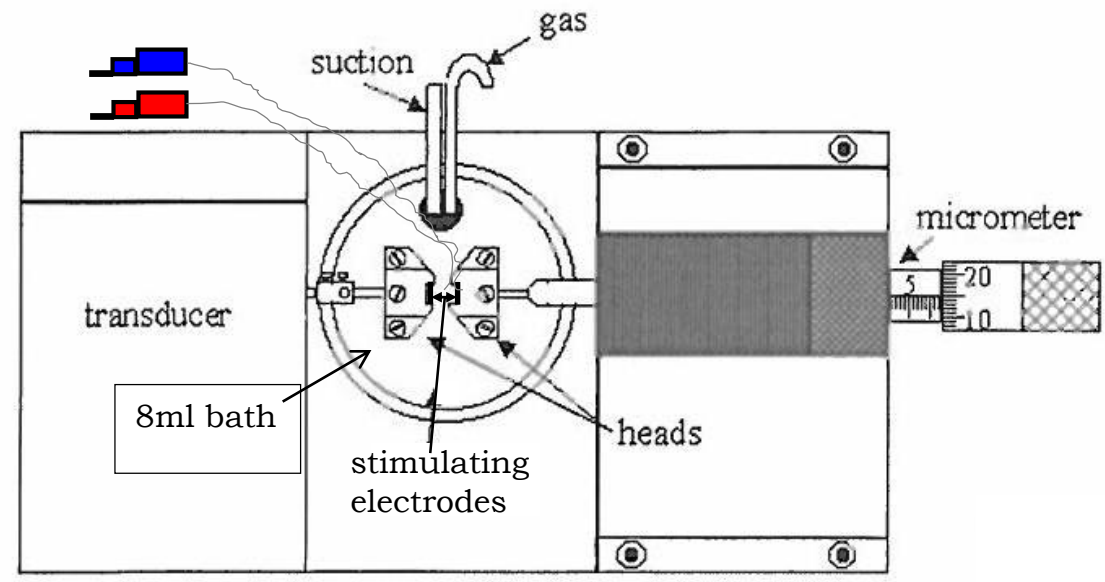

Figure 2-2: The Myograph Bath. Diagram adapted from Morton showing the myograph bath and stimulating electrodes (Morton, 2006).

2.4.2 Vessel Mounting

The vessels for mounting were placed in a clean petri dish containing fresh PSS. One 40 µm stainless steel wire was passed through the lumen of the vessel; with the vessel then being positioned half-way along the wire. The vessel and wire were then transferred to a myograph bath containing fresh PSS and secured to the micrometer head. This was achieved by firstly bringing the two heads together so that the vessel was located in the gap between the two heads. To prevent any damage, the heads were then separated before each end of the wire was coiled round the screws on the myograph head and secured in place. A second wire was

then placed through the lumen of the vessel, alongside the first wire, and the heads were brought together in order for the second wire to be secured to the transducer head. The heads were then opened to the point where the two wires were just touching (Figure 2-3).

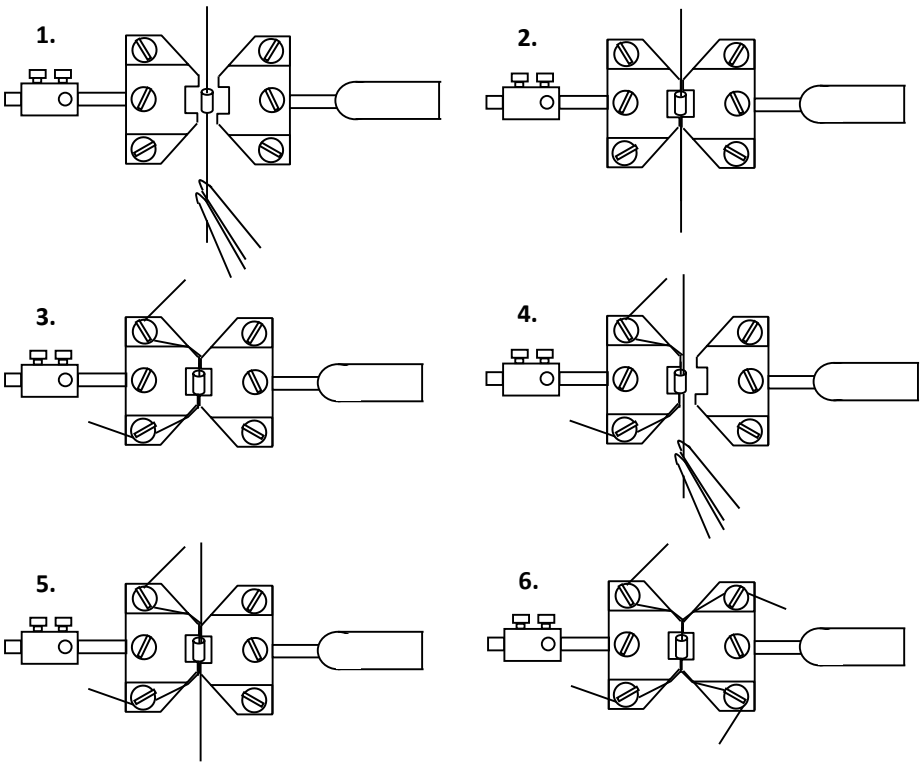

Figure 2-3: Procedure followed for mounting blood vessels: 1. Vessel positioned between the two heads. 2. Micrometer side moved so that both heads touching. 3. Ends of the wire secured to the transducer side using small screws. 4. Heads separated to allow second wire to pass through lumen of vessel. 5. Micrometer side moved so both heads touching. 6. Ends of the wire secured to micrometer side using small screws (Morton, 2006).

2.4.3 Vessel Equilibration

Following the mounting of the vessels into the myograph baths, the PSS solution was changed and the vessels were left to equilibrate for 30 minutes. Following this equilibration period a resting tension of 200 mg for tail artery, and 150 mg for mesenteric arteries was gradually applied to the vessels. This was achieved by slowly turning the micrometer and so separating the wires and stretching the vessel. This tension was chosen due to previous

normalisation experiments carried out on tail artery in the lab (Daly et al., 2002). A resting tension of 150 mg was chosen for the mesenteric arteries as resting tension above this level damaged the vessel and altered the control responses. The vessels were then left to equilibrate for a further 45 minutes with PSS changed every 15 minutes and tension adjusted accordingly.

2.4.4 Determination of Vessel Reactivity

Noradrenaline (NA) was the initial choice of agonist used when testing vessel reactivity. In the WT tail vessels, addition of 1 µM NA to the bath resulted in a strong contraction with a defined plateau (Figure 2-4).

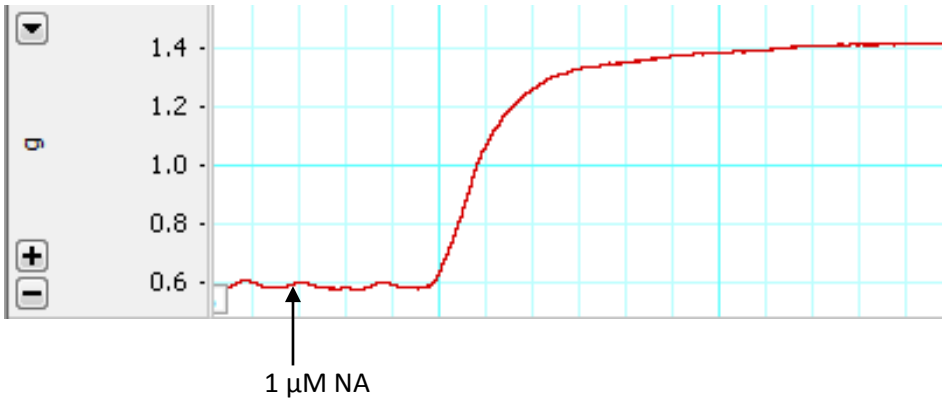

Figure 2-4: Representative trace showing WT mouse tail artery response to NA addition. Time scale; one box represents 10 seconds and is the same on all traces shown throughout.

However, the KO vessels did not respond reliably to NA addition and therefore the serotonergic agonist 5-hydroxytryptamine (5-HT) was used for all experiments in the tail artery. If the vessels were reactive, this drug was able to elicit a strong contraction and defined plateau regardless of strain (Figure 2-5) which disappeared when the PSS in the bath was changed. Following a 10 minute rest, vessels were exposed again to 5-HT, whereby a similar response to the first exposure was displayed (Figure 2-6).

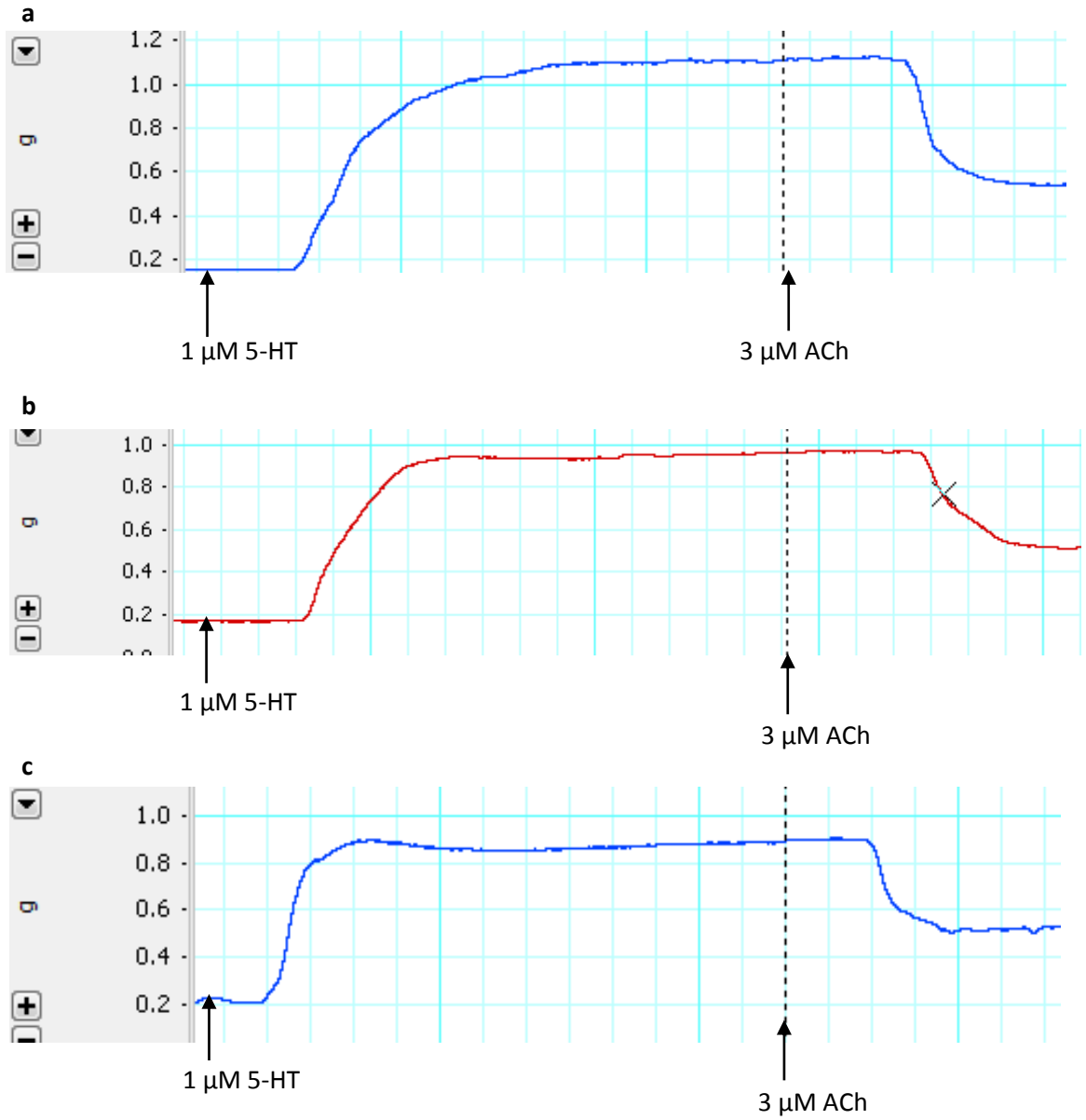

Figure 2-5: Representative traces showing WT (a), ADKO (b) and α_1-null (c) mouse tail artery response to 5-HT and ACh addition.

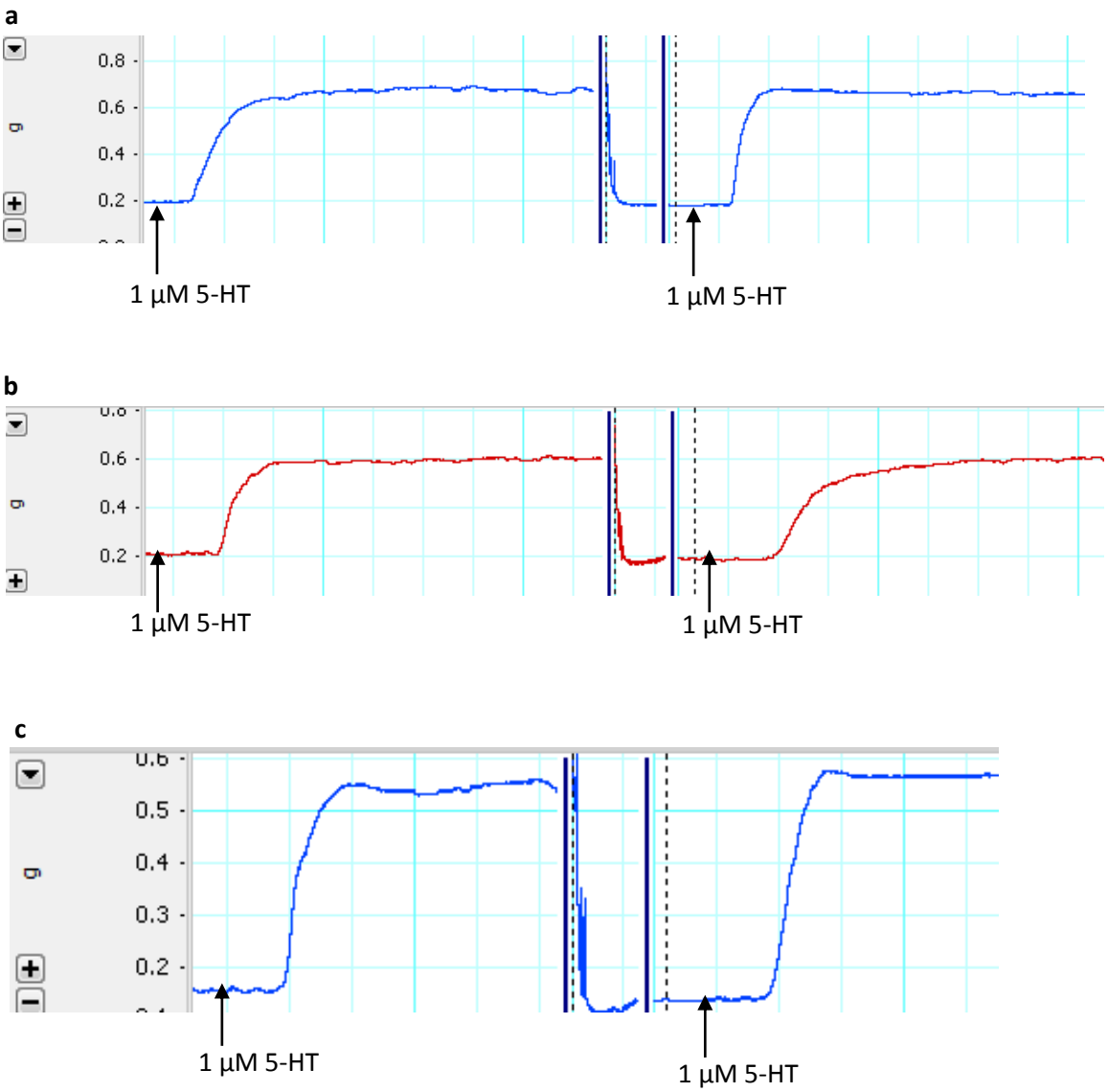

Figure 2-6: Representative traces showing WT (a), ADKO (b) and α_1-null (c) mouse tail artery response to multiple 5-HT exposure. Bath washed between additions with 5 minute rest period.

At the plateau, the response to 3 µM acetylcholine (ACh) was tested. ACh acts at endothelial cells to initiate vessel relaxation – this response ensured that the endothelium was intact and the vessel could be used for experiments (Figure 2-5).

The mesenteric arteries did not respond well to 5-HT incubation; they were unable to maintain the contraction plateau long enough for ACh addition (Figure 2-7). For these vessels, U46619 (U19), the thromboxane mimetic was used to contract the vessels (Figure 2-8). Vessels were then left for 10 minutes before testing responses to perivascular nerve stimulation.

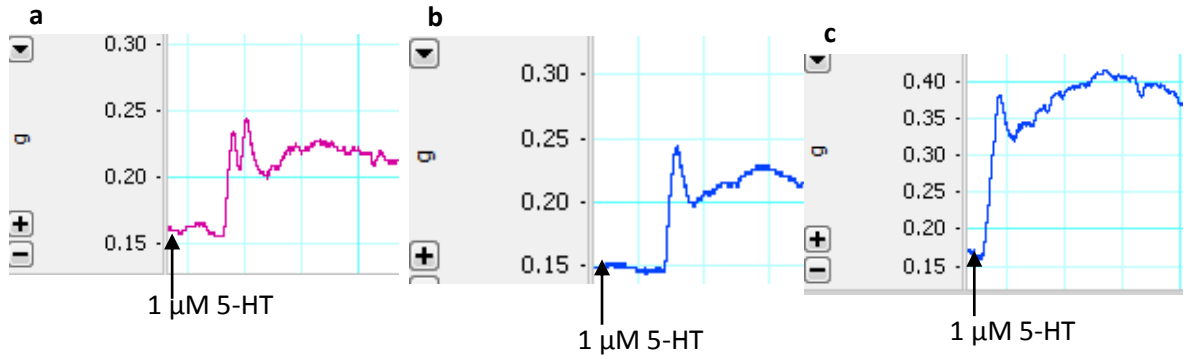

Figure 2-7: Representative traces showing mesenteric arteries from WT (a), ADKO (b) and α_1-null (c) in response to 5-HT exposure.

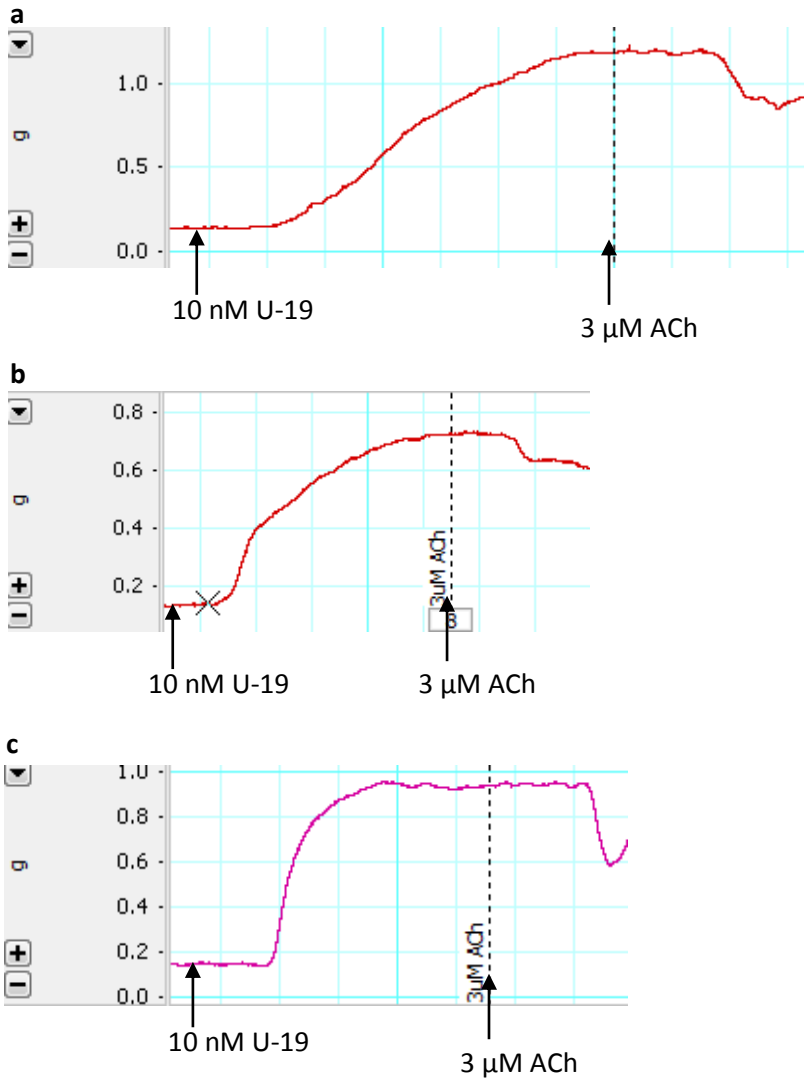

Figure 2-8: Representative traces showing mesenteric arteries from WT (a), ADKO (b) and α_1-null (c) in response to U-19 and ACh exposure.

2.4.5 Parameters of Stimulation

The rat mesenteric arteries have been shown to be surrounded by a plexus of sensory nerves containing calcitonin gene-related peptide (CGRP) (Kawasaki et al., 1988). When activated they release CGRP, which is a potent vasodilator (Brain et al., 1985). Therefore, in order to view only the contractile response of the vessel, the CGRP component must be removed. Incubation with 1 µM capsaicin depletes the sensory nerves of CGRP (Fujimori et al., 1990) thus removing the vasodilatory effect. Capsaicin was tested in the mesenteric arteries by raising vessel tone and adding 1 µM capsaicin to the bath. If the nerves contain CGRP, it would be expected to be released and there would be a relaxation. This did occur in the mesenteric arteries, as shown in Figure 2-9. Consequently, 1 µM capsaicin was added prior to the nerve stimulation protocol in both the mesenteric and tail arteries.

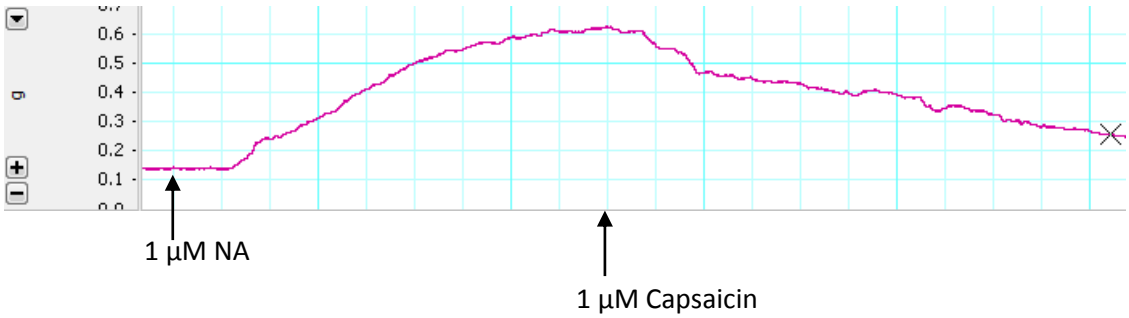

Figure 2-9: Representative trace showing WT mesenteric arteries responding to NA and capsaicin exposure.

2.4.5.1 Tail Artery

From the findings of Jänig and preliminary work carried out in the lab, the following frequencies were chosen to be tested on the vessels: 0.5 Hz, 1 Hz, 2 Hz, 4 Hz and 8 Hz (Janig, 2006). The pulse width was 0.3 ms so as to only excite the smooth muscle cells. Previous studies using pulse widths between 0.2 ms and 0.5 ms have shown that some of the response to 0.5 ms is due to direct stimulation of the smooth muscle as pre-treatment with

tetrodotoxin (TTX), which blocks nerve but not smooth muscle action potentials (Wang et al., 2006), did not abolish the responses to 0.5 ms pulses.

The responses to 20 stimuli became larger with increasing frequency of stimulation. Only the lowest and highest frequencies were used in the main experimental protocols as the intermediate frequencies contractions showed a graded transition in shape between the lower and higher frequencies (Figure 2-10). Both of these frequencies are within the physiological range (Janig, 2006). An intermediate frequency of 2 Hz was chosen to test nerve reactivity before commencement of the main protocol.

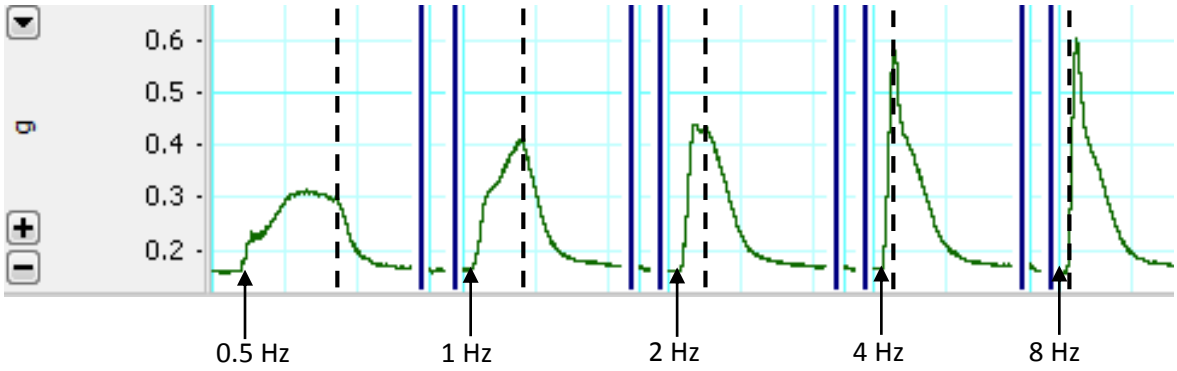

Figure 2-10: Representative traces showing WT tail artery responding to increasing frequencies of nerve stimulation. The dashed vertical line represents the end of the stimulation period.

2.4.5.2 Mesenteric Arteries

Responses in the mesenteric arteries were smaller than those in the tail. Therefore trains of 50 stimuli at frequencies of 2 Hz and 8 Hz were chosen for the main experiments with 4 Hz delivered initially to test vessel reactivity (Figure 2-11).

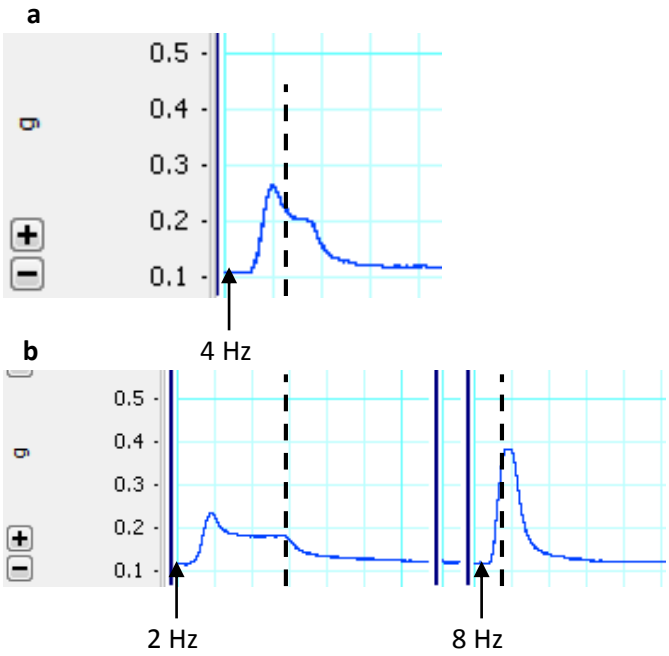

Figure 2-11: Representative traces showing WT mesenteric artery responding to increasing frequencies in nerve stimulation – (a) response to 4 Hz; (b) response to 2 Hz and 8 Hz. The dashed vertical bar represents the end of the stimulation period.

2.4.5.3 Tail and Mesenteric Arteries

All vessels were stimulated with 15 V, 20 V and 30 V initially and 20 V was found to be supramaximal and hence used throughout the protocols. A pulse width of 0.3 ms was used to stimulate the nerves and release neurotransmitters. The tail arteries were stimulated with 20 pulses in 40 seconds at 0.5 Hz and 20 pulses in 2.5 seconds at 8 Hz. The mesenteric arteries were stimulated with 50 pulses at 2 Hz for 25 seconds and at 8 Hz for 6.3 seconds. Following the return to baseline after the lower frequency stimulation, vessels were left for two minutes before commencement of stimulation at the next frequency.

2.4.5.4 Measurement of Parameters from the Averaged Traces

Responses produced at both frequencies in the tail artery contained two components: an initial fast component followed by a second slower component. The following points of the

responses were recorded for analysis: rate of rise, tension at the peak of both components as well as the tension at the end of the period of stimulation, the time taken to reach the peak of the second component (8 Hz) and the time taken for the peak response to reduce in amplitude by 50 % (decay time) (Figure 2-12). The rate of rise was calculated by measuring the change in tension between the beginning of the stimulation period and the peak of the first component and then dividing this tension by the time taken.

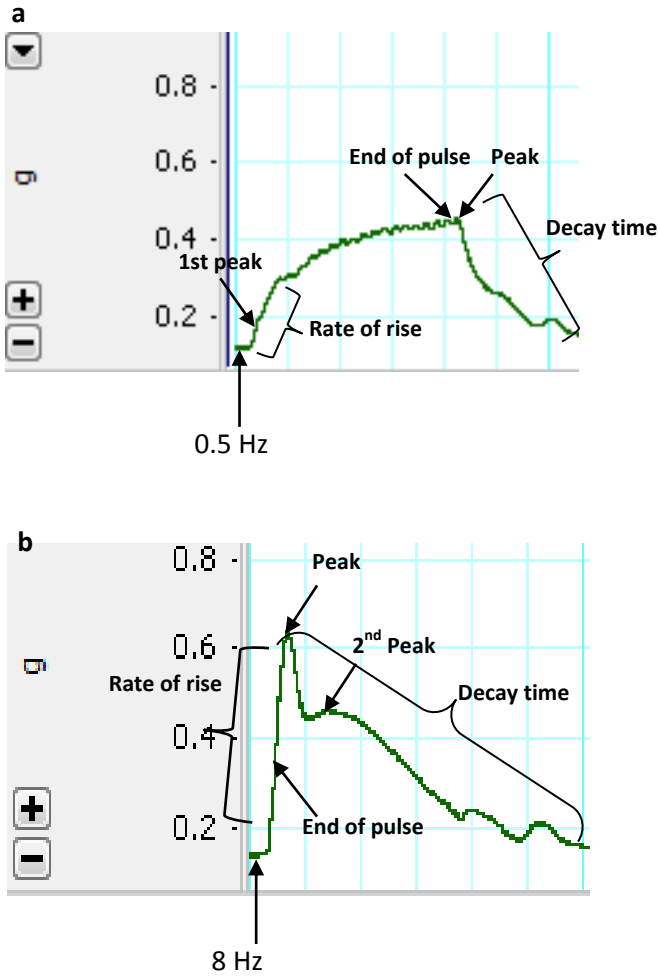

Figure 2-12: Representative traces showing WT tail artery responses at 0.5 Hz (a) and 8 Hz (b) annotated to show which parameters of the trace were measured.

Various measurements from the mesenteric artery responses were also recorded. At 2 Hz and 8 Hz the control responses had one distinct peak. The following points of the responses were recorded for analysis, rate of rise, tension at the peak as well as the tension at the end of the pulse, the time taken to reach the peak and the time taken for the peak response to reduce by 50 % (decay time) (Figure 2-13).

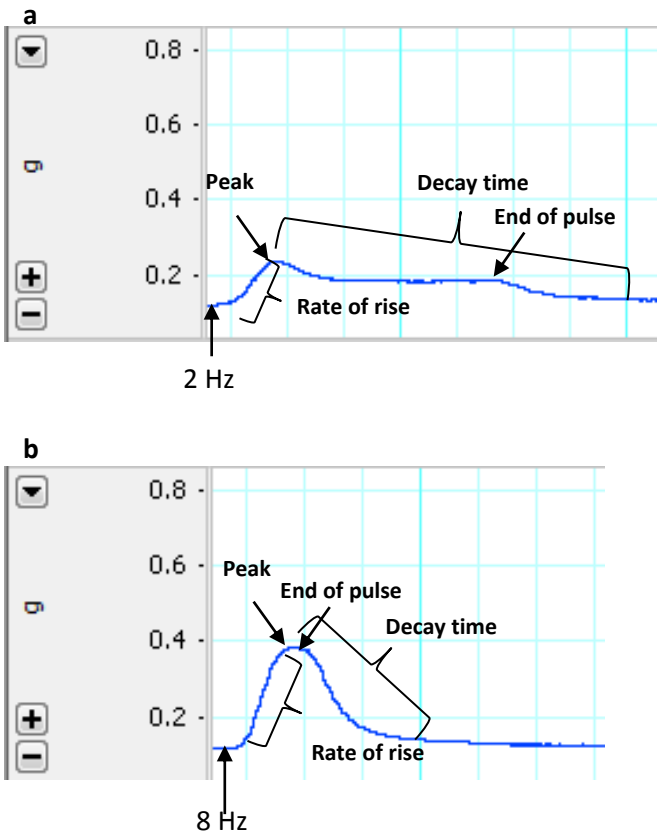

Figure 2-13: Representative traces showing WT mesenteric artery responses at 2 Hz (a) and 8 Hz (b) annotated to show which parameters of the trace were measured.

2.4.6 Antagonists

Both prazosin (α_1-AR antagonist) and rauwolscine (α_2-AR antagonist) have been shown previously to block α_1- and α_2-ARs respectively at 100 nM (Shafaroudi et al., 2005; Methven et al., 2009a). The pA2 value is the negative logarithm of the molar concentration of an antagonist which reduces the effect of a dose of agonist to that of half the dose. The pA2 value for prazosin against the α_1-AR agonist phenylephrine was shown to be 9.9 in rat blood vessels (Hussain and Marshall, 1997) and against the α_2-AR agonist UK14304 was shown to be 5.93 in canine saphenous vein (Guimaraes and Nunes, 1990). The pA2 value for rauwolscine against phenylephrine was 6.00 in the rat mesenteric arterial bed (Pipili, 1986) and against the α_2-AR agonist clonidine was 8.10 in the rabbit vas deferens (Lattimer and Rhodes, 1985). For these reasons, this concentration was used throughout in both the tail artery and mesenteric arteries.

The P2X receptor desensitising agent α, β, methylene ATP (αβme-ATP) has been shown previously to successfully block responses to exogenous ATP in various tissues (Kasakov and Burnstock, 1983). This was also shown to be true when used here in the WT tail artery preparations. The drug acts by binding to, activating and then desensitising the P2X receptors so that further addition of the drug does not elicit a response (Figure 2-14).

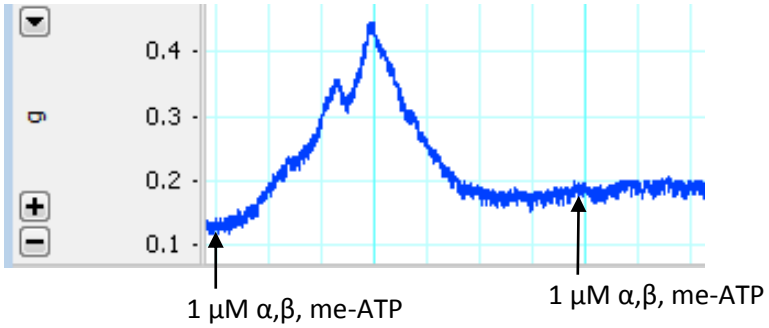

Figure 2-14: Representative trace showing WT tail artery vessel response to α,β,me-ATP.

However, in the α_1-null vessels, regardless of how many times αβme-ATP was applied or the concentration that was used, the vessel continued to respond (Figure 2-15; n = 2). For this reason, the P2X receptor antagonist suramin was used in the main experiment protocols. A concentration of 1 mM was used to ensure all available P2X receptors were blocked (Bao and Stjarne, 1993).

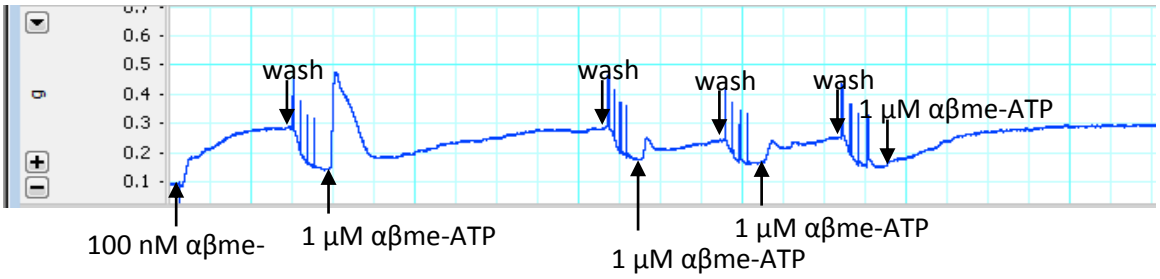

Figure 2-15: Representative trace showing α_1-null tail artery vessel response to α,β,me-ATP.

2.4.7 Spontaneous Activity

In some of the vessel preparations, spontaneous activity was recorded (Figure 2-16) and in some cases the effects can be seen in the averaged traces. The activity occurred following the end of the applied stimulus and did not affect the values recorded and analysed.

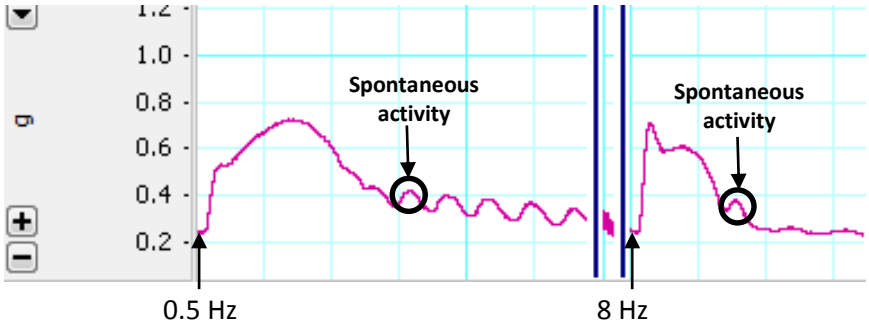

Figure 2-16: Example taken from LabChart showing α_1-null tail artery spontaneous activity.

2.4.8 Control Experiments

During every experiment, a control vessel was set up to show that the peak responses to nerve stimulation did not vary with time. Therefore any change in response following drug incubation was due to the drug itself. Figures 2-17, 2-18 and 2-19 are averaged proximal and distal tail artery and mesenteric artery control traces from six wild type mice. Analysis of % change in each strain showed no significant differences between the strains for all vessels studied. Hence, only the WT traces are shown below. Tables 2-2 and 2-3 detail all of the % changes in each strain.

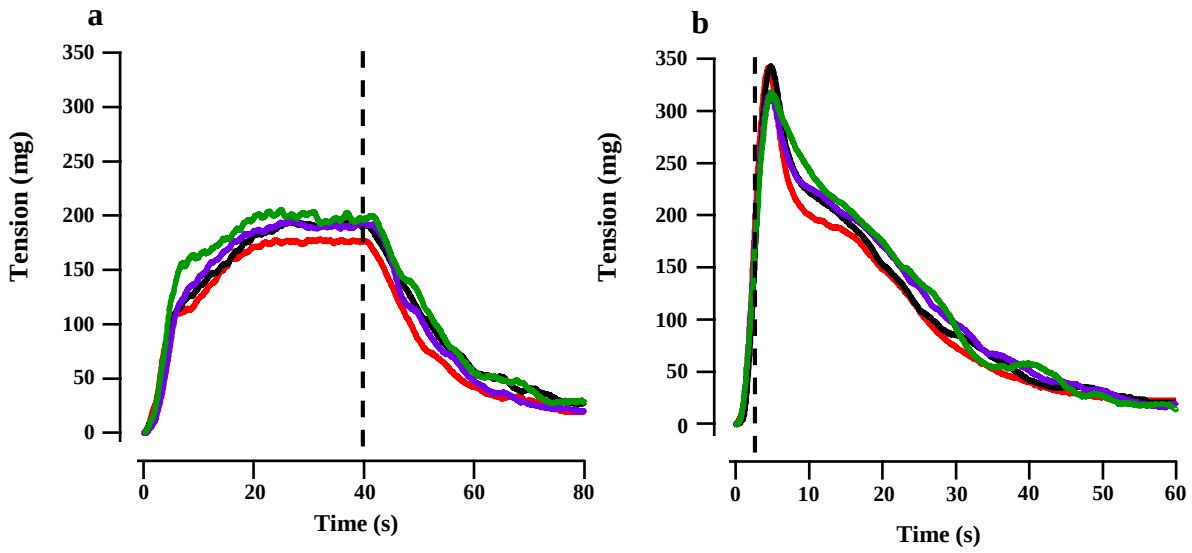

Figure 2-17: Average control traces from WT proximal mouse tail artery at 0.5 Hz (a) and 8 Hz (b). 1st stimulation – red; 2nd stimulation – black; 3rd stimulation – purple; 4th stimulation – green. The dashed line represents the end of the stimulation period.

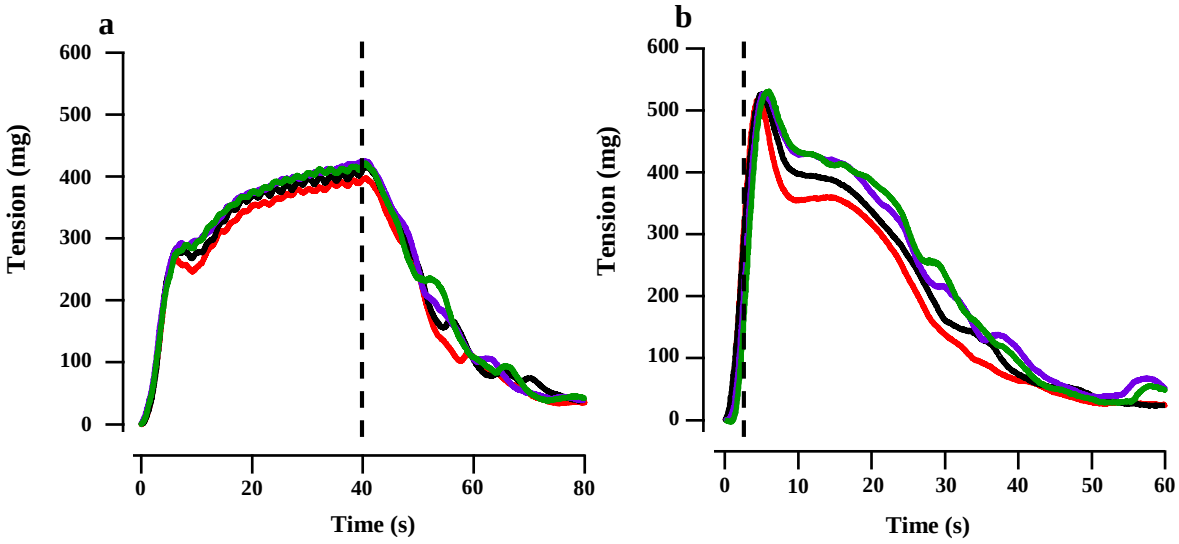

Figure 2-18: Average control traces from WT distal mouse tail artery at 0.5 Hz (a) and 8 Hz (b). 1st stimulation – red; 2nd stimulation – black; 3rd stimulation – purple; 4th stimulation – green. The dashed line represents the end of the stimulation period.

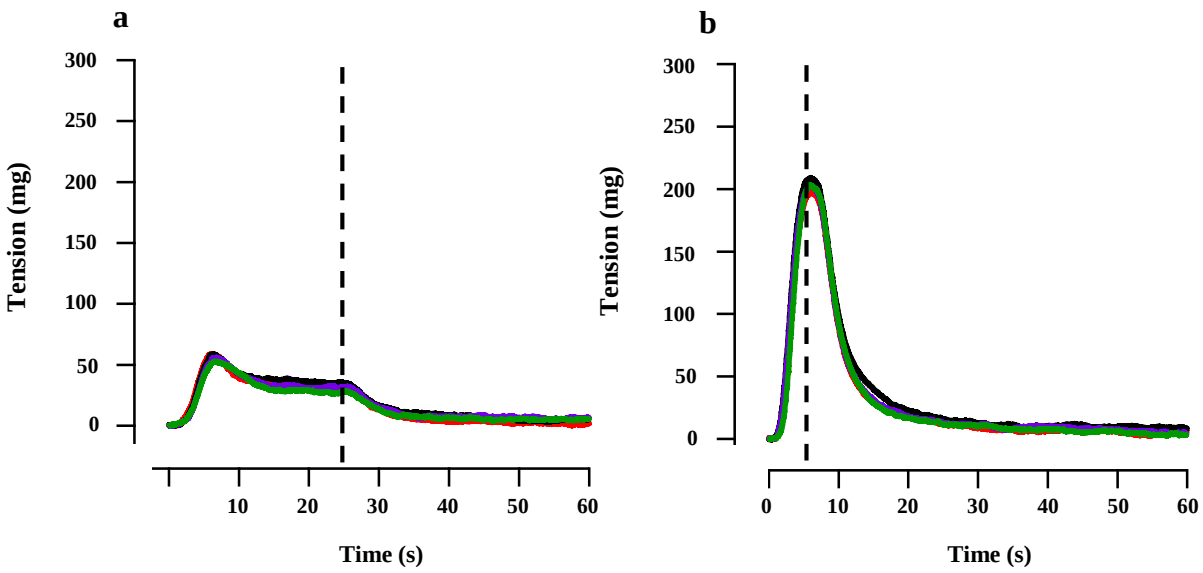

Figure 2-19: Average control traces from WT mouse mesenteric artery at 2 Hz (a) and 8 Hz (b). 1st stimulation – red; 2nd stimulation – black; 3rd stimulation – purple; 4th stimulation – green. The dashed line represents the end of the stimulation period.

Table 2-2: The % change between the peak first and last control nerve stimulations in mouse tail artery at 0.5 Hz and 8 Hz.

Strain	Location	% Change (± S.E.M)	
		0.5 Hz	8 Hz
Wild Type	Proximal	15 ± 5	0.3 ± 3
ADKO	Proximal	3 ± 4	- 1 ± 2
α_1-null	Proximal	5 ± 5	- 4 ± 7
Wild Type	Distal	6 ± 3	2 ± 2
ADKO	Distal	4 ± 2	3 ± 5
α_1-null	Distal	5 ± 6	1 ± 5

Table 2-3: The % change between the peak first and last control nerve stimulations in mouse mesenteric artery at 2 Hz and 8 Hz.

Strain	% Change (± S.E.M)	
	2 Hz	8 Hz
Wild Type	- 2 ± 9	2 ± 4
ADKO	26 ± 18	- 24 ± 11
α_1-null	- 29 ± 33	- 10 ± 19

2.5 Blood Pressure Monitoring

2.5.1 Training of Mice

The apparatus for measuring blood pressure was located in a different animal house to the one where the mice were being housed. Therefore, the mice whose blood pressures were going to be measured were transferred to the animal house containing the apparatus. The animals were left to adjust to their new surroundings for one week before commencement of training. Training was carried out on all mice on three separate days over a one week period. As well as the mice becoming accustomed to being handled they also became familiar with the blood pressure (BP) monitoring equipment. This involved placement of the tail cuff and subsequent inflation of the cuff. No measurements were recorded at this stage. On the same three days the following week, BP measurements were recorded.

2.5.2 Tail Cuff Technique

The LE 5001 Pressure Meter (Panlab Harvard Apparatus) was the tail cuff system used throughout. Mice were handled by the tail, placed on a clean cloth which was then wrapped around the mouse so that only the tail was exposed. The cuff was then slid near to the base

of the tail and inflated. Measurements were recorded using the SeDaCom (Version 1.4.01) software. The tail cuff recorded beats per minute (BPM), systolic pressure and calculated the diastolic pressure from the systolic measurement. Diastolic measurement collection was not reliable and often did not work so only systolic measurements were analysed. The BPM recordings were also not reliable and so were not included in the analysis.

2.5.3 Protocols

On the days where BP measurements were taken, mice were removed from their cages and placed in a polystyrene box with a heated light bulb directed over them. As the tail artery is involved in temperature regulation the mice had to be warm to ensure the artery was not constricted. If the tail artery is constricted, a BP measurement will not be recorded by the cuff. A heat blanket was located under the cloth so that during BP measurements the temperature could be maintained. Following a 10 - 15 minute period in the polystyrene box, each mouse was then wrapped in the cloth and the tail placed through the cuff. Following six reproducible measurements the mice were then placed back in their cages. This was not always possible because the mice became agitated so that they were placed back in their cages sooner.

2.6 Statistical Analysis

GraphPad Prism (Version 5) was used to determine statistical significance in all tests. The Student's paired t-tests were carried out when comparing a control response with an antagonist response and unpaired t-test used when comparing responses with different mouse strains. A one-way ANOVA with Bonferonni's post-test was performed when analysing the time control responses and when comparing the antagonist sensitive components in Chapters 5-7.

IGOR Pro (Version 6) software produced averaged traces which are shown throughout and are displayed in the results sections alongside standard errors of the means (S.E.M). For each set of results, an average (± S.E.M) was generated from an n number of at least six mice and used in comparison studies.

A novel way of analysing vessel response to antagonist incubation was developed whereby the individual 'antagonist-sensitive' portion of the response could be extracted from various incubation sequences and compared. For example, the prazosin-sensitive (PS) component can be obtained by subtracting the response following prazosin treatment from the control response. Similarly, by subtracting the response following rauwolscine plus prazosin treatment from the response following rauwolscine treatment, the prazosin-sensitive component is revealed. Prazosin, rauwolscine and suramin should be successfully blocking the α_1-, α_2-ARs and P2X receptors respectively and so the PS components represent the response due to activation of α_1-ARs. If there are no interactions between the receptors then each of the revealed components would be similar. Therefore this analysis will expose whether the receptors interact with one another and if they are dependent on the presence of the other receptors in order to contribute to vessel constriction. A full worked example of this analysis is shown in the results section of Chapter 5 for both mesenteric and tail artery responses.

2.7 Materials

Physiological salt solution (PSS) with the following composition (in mM) was used: 119 NaCl, 4.7 KCl, 1.2 $MgSO_4.H_20$, 1.2 KH_2PO_4, 24.9 $NaHCO_3$, 2.5 $CaCl_2$ and 11.1 glucose. The following stock solutions were dissolved in distilled water (dH_2O) to the required concentrations unless otherwise stated. Materials were sourced from: Sigma Aldrich (Poole, UK), Tocris (Bristol, UK), Thermo Scientific (Loughborough, UK) and Invitrogen (Paisley, UK). To minimise any solvent effects on the responses, those drugs dissolved in solvents were made at higher concentrations before being diluted down using dH_2O. The concentrations of the stock solutions are shown below in brackets.

2.7.1 Drugs used in the Nerve Stimulation Protocol

Noradrenaline hydrochloride – SIGMA (10^{-2} M)

5-hydroxytryptamine – SIGMA (10^{-2} M)

U46619 – Available from TOCRIS – dissolved in ethanol (10^{-2} M)

Acetylcholine chloride – SIGMA (10^{-2} M)

Capsaicin – SIGMA – dissolved in ethanol (10^{-2} M)

Prazosin hydrochloride – SIGMA – required sonication (10^{-3} M)

Rauwolscine hydrochloride – SIGMA (10^{-3} M)

Suramin sodium salt – SIGMA (10^{-2} M)

2.7.2 Solutions used in the Genotyping Protocol

Primers (Table 2-1) – THERMO SCIENTIFIC

Readymix PCR Mastermix – THERMO SCIENTIFIC

Digestion Buffer – Prepared in Lab

Proteinase K – PROMEGA

TE Buffer – INVITROGEN

Agarose – INVITROGEN

TAE Buffer – INVITROGEN

Ethidium Bromide – SIGMA

DNA Ladder - INVITROGEN

Chapter Three

The effect of α_1-adrenoceptor deletion on mouse blood pressure

3.1 Introduction

3.1.1 Sympathetic control of Blood Pressure

Stimulation of the neurovascular nerves results in release of noradrenaline (NA) and adenosine tri-phosphate (ATP) from the nerve terminals (Sneddon and Burnstock, 1984). These neurotransmitters act post-junctionally on α_1- and α_2-adrenoceptors (ARs) and P2X purinoceptors located on smooth muscle cells. Activation of these receptors alters vessel tone and therefore influences blood pressure. Historically, α_1-AR blockers effect on reducing arteriolar resistance have been used to treat hypertension and so genetic removal of some or all of the α_1-AR subtypes would be expected to have an effect on blood pressure.

3.1.2 Genetically Modified Mice

The generation of genetically modified mice lacking either one, two or three α_1-AR subtypes have been developed in order to simplify the complex pharmacology (Cavalli et al., 1997; Rokosh and Simpson, 2002; Tanoue et al., 2002; Hosoda et al., 2005; Sanbe et al., 2007; Methven et al., 2009b). The α_{1AD}-AR knock out (ADKO) and the α_{1ABD}-KO (α_1-null) mouse strains have been utilised presently in the study of systolic blood pressure (SBP).

3.1.3 Measuring Blood Pressure

The tail-cuff method is one way in which SBP can be measured in mice. This is a low cost, non-invasive procedure that utilises a sphygmomanometer together with a pulse signal which determines blood pressure (BP) in conscious mice. Various lab groups have utilised this method in BP recording of wild type (WT) and genetically modified mice. SBP measured in WT mice was found to range between 99 mm Hg and 109 mm Hg (Tanoue et al., 2002; Hosoda et al., 2005; Sanbe et al., 2007). The α_{1D}-AR KO was found to have a

significantly lower SBP compared to WT mice (Tanoue et al., 2002; Hosoda et al., 2005) as did the α_{1BD}-AR KO and the α_1-null mice (Hosoda et al., 2005; Sanbe et al., 2007). Where cardiac function was investigated, no change was detected between the WT mice and the KO mice (Tanoue et al., 2002; Hosoda et al., 2005).

Other labs employed a carotid catheter to establish mean arterial pressure (MAP) in KO mice. With this method, the α_{1A}-AR KO mice were found to be hypotensive (Rokosh and Simpson, 2002). The α_{1B}-AR KO mice were shown to have a similar MAP to their WT controls (Cavalli et al., 1997). However, in mice with an overexpression of α_{1B}-ARs, basal hypertension and bradycardia occurred alongside reproductive problems and weight loss which are characteristics of autonomic failure (Zuscik et al., 2001). Additionally, the α_{1D}-AR KO mice were also found to have a significantly lowered BP compared to the WT controls.

In this study, the effect genetic removal of the α_1-ARs had on SBP was investigated using the tail-cuff method in WT, ADKO and α_1-null mice.

3.2 Methods

A full description on how the measurements were recorded can be found in Chapter 2. Briefly, six WT, six ADKO and five α_1-null male mice aged 4 – 6 months had their SBP measured using the motorised tail cuff system. Mice were placed on a heat mat to ensure tail artery vasodilation before placing the cuff close to the base of the tail and recording pressure. On average, six measurements were recorded in each mouse. Measurements were taken from each mouse on five days over a two week period following three days of training. The equipment used did not reliably record diastolic pressures or heart rate (HR) and so only results from the systolic pressure measurements are shown here.

Results were analysed using a one way ANOVA with Bonferonni's post-test. Significance was taken as $P < 0.05$.

3.3 Results

Analysis of recorded SBP did not reveal any significant differences between the strains (Table 3-1).

Table 3-1: Average systolic blood pressure measurements from WT, ADKO and α_1-null mice.

	Strain		
	WT n = 6	**ADKO n = 6**	**α_1-null n = 5**
Systolic Blood Pressure mm Hg (± S.E.M)	140 ± 2 mm Hg	139 ± 2 mm Hg	145 ± 2 mm Hg

3.4 Discussion

The results recorded here suggest that removal of the α_{1A}- and α_{1D}-ARs, or removal of all α_1-AR subtypes has no impact on the SBP. However, when comparing the values with those of the lab groups mentioned in the introduction (Hosoda et al., 2005; Sanbe et al., 2007; Tanoue et al., 2002), the values recorded presently are higher. Therefore, it is possible that the present acclimatisation/training protocol was not long enough for the animals to produce a resting SBP. If the mice were agitated it would suggest that under pressure, the effect on vascular tone is similar between the strains. Conversely, this group of mice may have had isolated systolic hypertension; a potential consequence of having to be moved from one animal house to another. Determination of aortic stiffness could have confirmed this theory.

The results presented here differ from previously published results which show resting SBP to be lower in α_1-AR KO mice. This correlates with the effects seen in patients using α_1-AR blockers in hypertension; where the systolic and diastolic pressures are reduced to lessen strain on the myocardium. However, currently α_1-AR antagonists are generally only

prescribed as an additive measure in patients with uncontrolled blood pressure. This is partly due to the adverse effects reported in some clinical trials where major cardiovascular events occurred (Chapman et al., 2010). Combined with present results, resting SBP may rely on α_1-AR input. However, whilst under pressure/ agitated, the vessels respond in a similar way, regardless of strain.

Chapter Four

Does the sensory neurotoxin capsaicin affect response to sympathetic nerve stimulation in mouse tail and mesenteric arteries?

4.1 Introduction

As well as a dense plexus of sympathetic nerve terminals, primary afferent sensory nerve terminals are present in the adventitia of many arterial vessels (Kawasaki et al., 1988; Sneddon and Burnstock, 1984). Recently, mouse models lacking one or more α_1-adrenoceptor (AR) subtype (α_1-AR KO) have been developed which allows a greater understanding of the postjunctional receptors. However, sensory nerves can release potent vasodilators which may mask the full contractile effect of postjunctional receptor activation when all of the perivascular nerves are stimulated electrically. The vasodilator effect could be altered in the genetically modified mice as loss of α_1-ARs may have a potential effect on the vasoconstrictor response and so may reveal a vasodilator response.

The sensory nervous system is comprised of cell bodies located in spinal and cranial sensory ganglia with axons projecting centrally and peripherally. To maintain homeostasis, the sensory nerves respond to alterations in the internal and external environment. However, the sensory nerves can also exert effects locally, including vascular smooth muscle relaxation (Lee et al., 1978).

Determination of the relationship between sensory nerves and vessel relaxation has been ongoing since the 1960's. Discovery of the neuropeptide calcitonin gene-related peptide (CGRP) occurred in 1983 by tissue-specific RNA processing (Rosenfeld et al., 1983) and was suggested to be a potential modulator of noradrenergic sympathetic outflow in the peripheral nervous system (PNS) (Fisher et al., 1983). Intradermal injection of CGRP was shown to vasodilate certain blood vessels in a potent manner (Brain et al., 1985) with CGRP containing nerves shown to be present throughout the sensory nervous system and in some cases present before the development of noradrenergic nerves (Dhall et al., 1986; Tornebrandt et al., 1987). The distribution of CGRP containing nerves throughout the guinea pig mesenteric arteries was shown by Uddman et al. who demonstrated that with raised vessel tone, addition of CGRP induced a relaxation which became more pronounced with increasing concentration of CGRP (Uddman et al., 1986). CGRP binding sites were found, by radioligand binding studies, to be numerous in the rat mesenteric arteries (Wimalawansa and MacIntyre, 1988).

Caterina et al., (1997) cloned the VR1 receptor and noted that activation of this receptor, which is voltage sensitive, was found to have a high permeability to Ca^{2+} and continued excitation of the receptor could lead to desensitisation but only in the presence of extracellular Ca^{2+}. These results provided the link between the VR1 receptor and the transient receptor potential vanilloid (TRPV) superfamily of ion channels (Caterina et al., 1997). TRPV channels are found on sensory nerves and activation of the TRPV1 via nerve stimulation has been shown to cause release of calcitonin gene-related peptide (CGRP) (Wang et al., 2006). The TRPV1 channels are voltage sensitive and so membrane depolarisation through electrical field stimulation (EFS) can stimulate the release of CGRP (Voets et al., 2004).

As CGRP can act as a potent vasodilator following nerve stimulation, it may be masking the vasoconstrictor effect of sympathetic activity and so a blockade of CGRP release could augment postjunctional receptor activation. One such substance able to desensitise the CGRP containing nerves is capsaicin, a sensory neurotoxin derived from capsicum peppers. Capsaicin has been shown to have multiple actions on sensory nerves including excitation of the nerves and a prolonged neurotoxic effect (Caterina et al., 1997). CGRP concentrations in the rat have been shown to originate mainly from capsaicin-sensitive perivascular nerves (Zaidi et al., 1985). The link between CGRP activity and capsaicin was further shown in 1986 by Wharton et al. who used capsaicin injections to show a reduced CGRP content in the rat superior mesenteric arteries (Wharton et al., 1986). In 1988, Kawasaki et al. utilised peripheral nerve stimulation (PNS) in perfused rat mesenteric arteries. They showed that with raised tone, PNS elicited a relaxation that could be inhibited by capsaicin pre-treatment and that the relaxation shown was due to release of CGRP. Immunohistochemistry studies also revealed CGRP containing nerves (Kawasaki et al., 1988). Fujiwara et al. have now shown this in the mouse mesenteric arteries and conclude that the arteries are densely innervated by CGRP containing nerves (Fujiwara et al., 2012).

It is therefore possible that pre-treatment with capsaicin will result in an increased peak response to EFS as the ‘masking’ vasodilation will be removed. The effect of capsaicin on excitatory junctional potentials (EJP) in rat mesenteric arteries was investigated by Dunn et al. who reported an increase in EJP amplitude following removal of CGRP (Dunn et al., 2003). It is unknown whether EFS response in the mouse mesenteric arteries or tail artery

will be altered by capsaicin. However, previous data suggests that as both tissues contain CGRP, a difference may be recorded (Morrison et al., 2009).

In this study, the effects of capsaicin treatment on the amplitude of contractile responses to EFS were tested on mesenteric and tail arteries from WT, ADKO and α_1-null mice.

4.2 Methods

A full description of the methods used can be found in Chapter Two. Briefly, six male mice, aged four to six months from each strain (WT; ADKO; α_1-null) were utilised. First order mesenteric arteries and proximal and distal tail artery were removed and set up in myograph baths. Capsaicin's vasodilatory effect was tested by raising mesenteric artery vessel tone with 1 µM NA and then applying 1 µM capsaicin. Following the vessel reactivity tests, vessels were stimulated with various patterns of perivascular electrical stimuli before and after capsaicin treatment. The amplitudes of the responses were recorded and analysed using a paired t-test with a P value < 0.05 taken as significant and shown alongside standard error of the mean (S.E.M).

4.3 Results

4.3.1 Mesenteric Arteries

When vessel tone was raised using 1 µM NA, 1 µM capsaicin was added and the vessel relaxed by 73 % 5 minutes following administration - indicating the presence of CGRP containing sensory nerves (Figure 4-1). Regardless of strain or frequency, the addition of capsaicin was not shown to alter the response significantly to nerve stimulation (Figures 4-2 – 4-4; Table 4-1). For example, the amplitude of the WT response following capsaicin treatment decreased, on average, by 7.3 % ± 6.8 for each frequency. Furthermore, the shape

of the response does not alter following the addition of capsaicin to the bath (Figures 4-2 - 4-4).

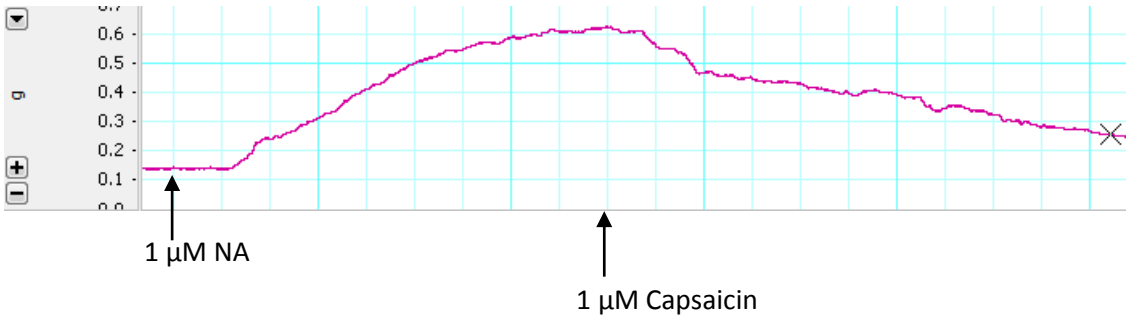

Figure 4-1: Representative trace showing WT mesenteric arteries responding to NA and capsaicin exposure. Vessel relaxed to 73 % of the peak response 5 minutes following administration.

Table 4-1: Comparison of nerve responses before and after capsaicin treatment (1 µM for 30 minutes) in mouse mesenteric arteries from WT, ADKO and α_1-null strains.

Strain	Frequency	Contractile Response (mg ± S.E.M)	
		Before Capsaicin	Following Capsaicin
WT n = 6	**2 Hz**	62 ± 8	60 ± 16
	8 Hz	197 ± 14	189 ± 21
	16 Hz	273 ± 13	264 ± 20
ADKO n = 6	**2 Hz**	22 ± 5	16 ± 5
	8 Hz	66 ± 13	45 ± 15
	16 Hz	92 ± 12	67 ± 12
α_1-null n = 6	**2 Hz**	13 ± 7	9 ± 4
	8 Hz	30 ± 18	22 ± 10
	16 Hz	40 ± 19	34 ± 12

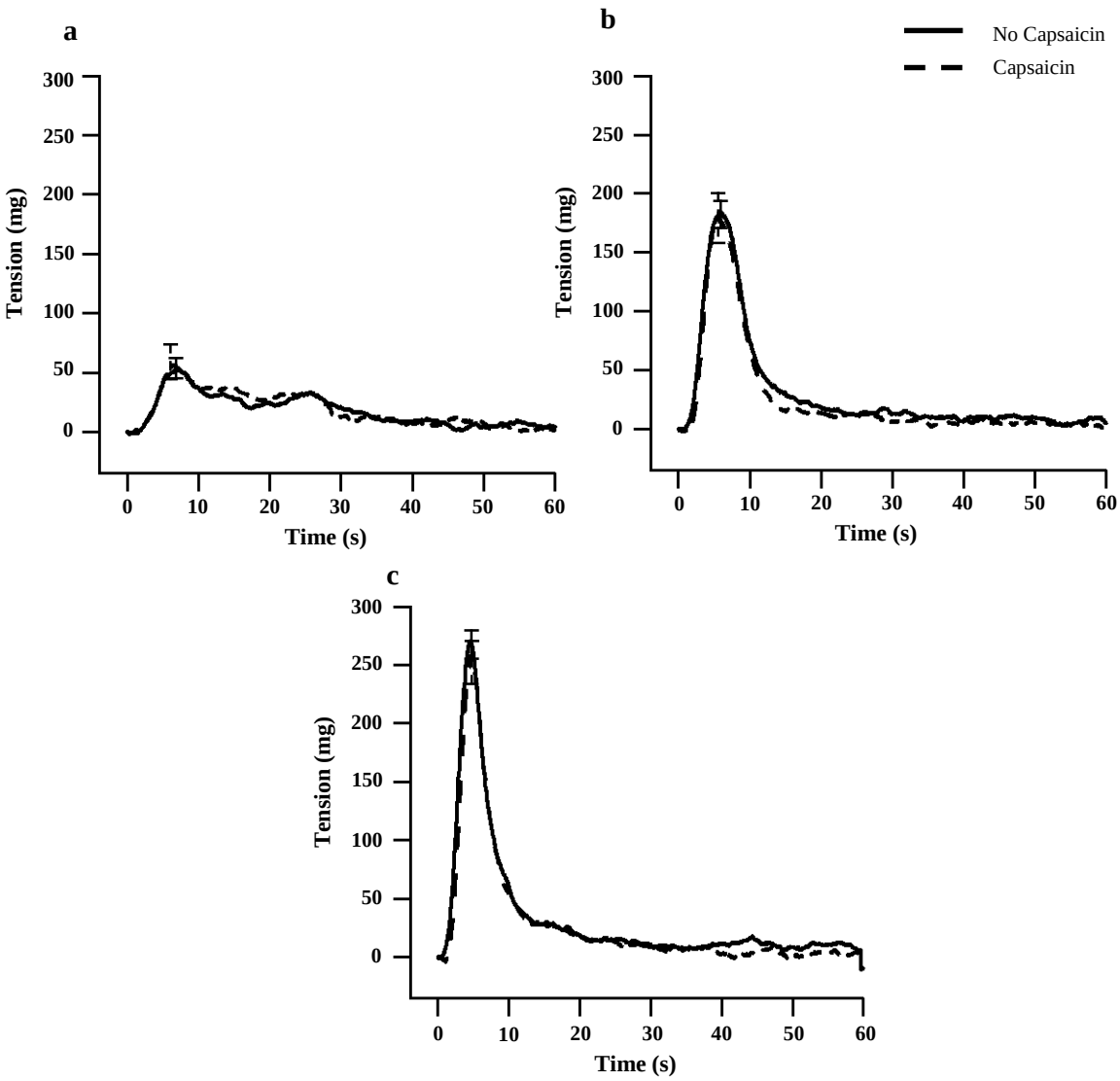

Figure 4-2: Averaged traces from 6 wild type mouse mesenteric arteries taken before capsaicin treatment and following capsaicin treatment (1 µM for 30 minutes) at 2 Hz (a), 8 Hz (b) and 16 Hz (c). Responses in mg tension with error bars at the peak responses ± S.E.M. —— **No Capsaicin** – – **Capsaicin**

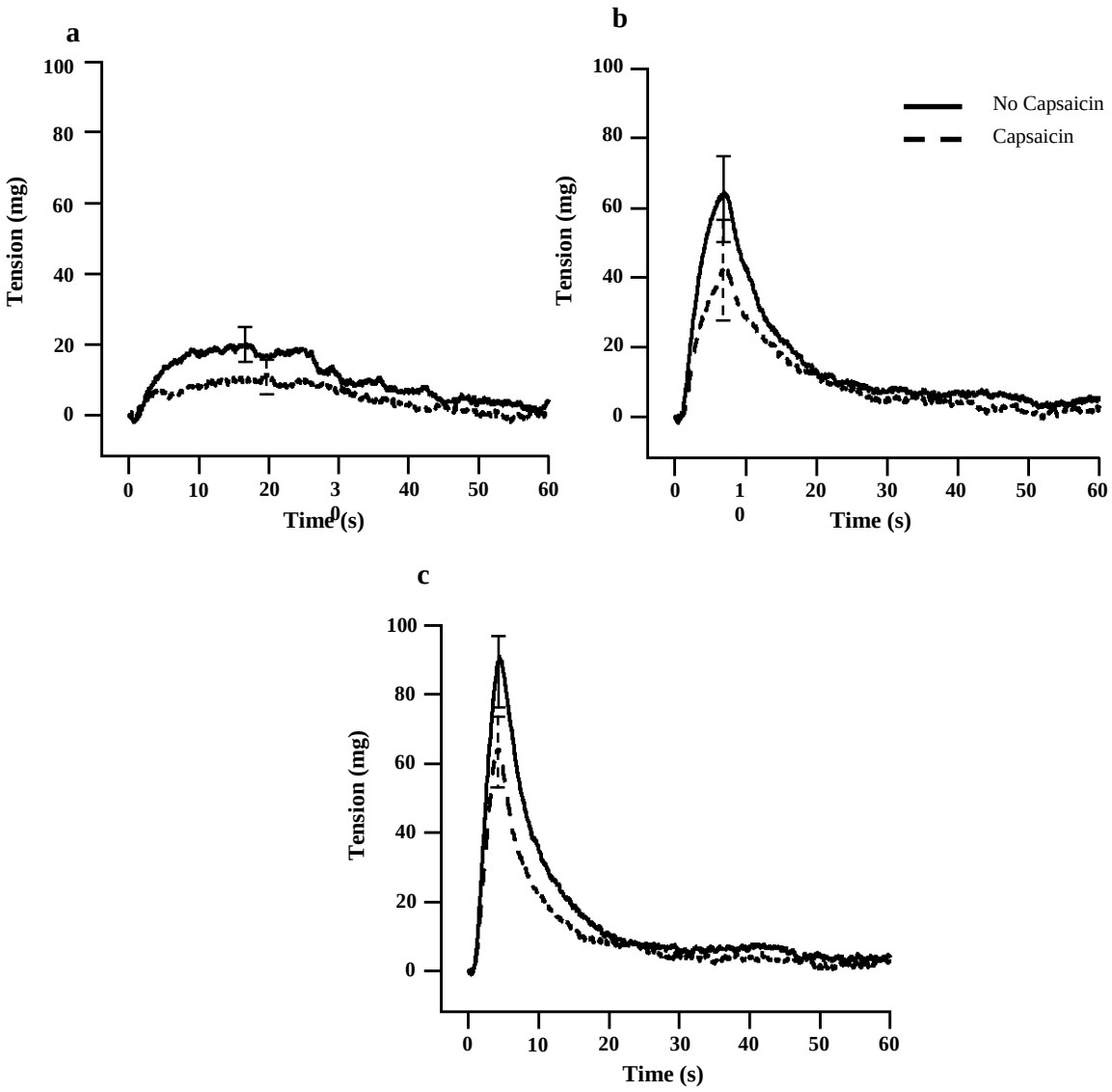

Figure 4-3: Averaged traces from 6 ADKO mouse mesenteric arteries taken before capsaicin treatment and following capsaicin treatment (1 µM for 30 minutes) at 2 Hz (a), 8 Hz (b) and 16 Hz (c). Responses in mg tension with error bars at the peak responses ± S.E.M. ——— No Capsaicin – – – Capsaicin

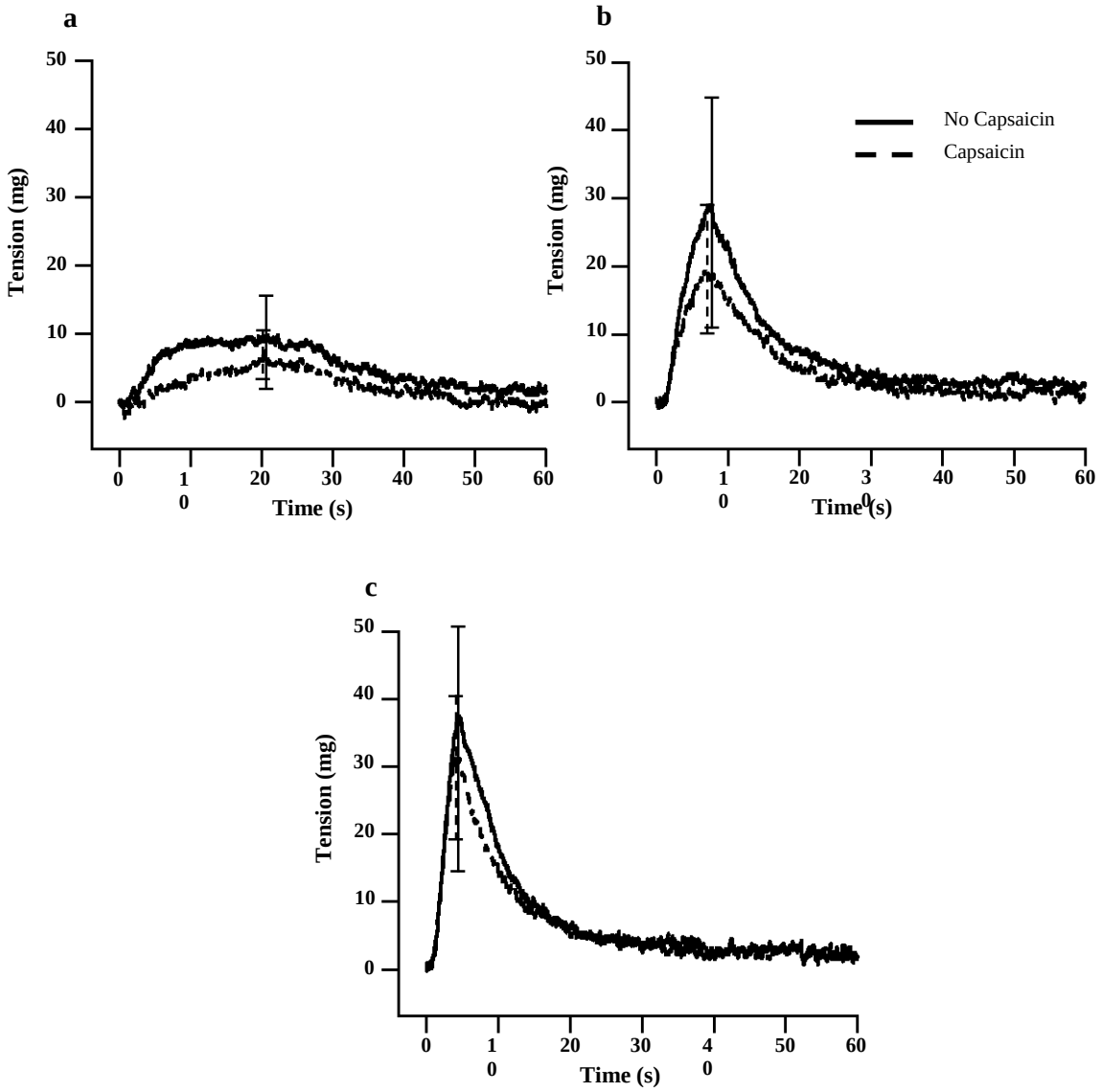

Figure 4-4: Averaged traces from 6 α_1-null mouse mesenteric arteries taken before capsaicin treatment and following capsaicin treatment (1 µM for 30 minutes) at 2 Hz (a), 8 Hz (b) and 16 Hz (c). Responses in mg tension with error bars at the peak responses ± S.E.M. —— **No Capsaicin** – – **Capsaicin**

4.3.2 Tail Artery

When vessel tone was raised using 1 µM 5-HT, 1 µM capsaicin was added and the vessel did not relax; suggesting that CGRP is not released from the nerves under these stimulation parameters (Figure 4-5). In WT and α_1-null tail arteries, the addition of capsaicin to the myograph baths did not significantly alter their responses to nerve stimulation, regardless of location. However, the mean graphs were always larger than before capsaicin although this change was only significant in the ADKO, in which the addition of capsaicin increased the responses to 0.5 Hz in both proximal and distal sections (Figures 4-6 – 4-11; Table 4-2). At 0.5 Hz proximal tissue response before capsaicin was 140 ± 27 mg and following capsaicin this increased to 211 ± 35 mg (n = 6). Distally, the initial response was 234 ± 43 mg and this increased to 299 ± 33 mg following capsaicin incubation (n = 6).

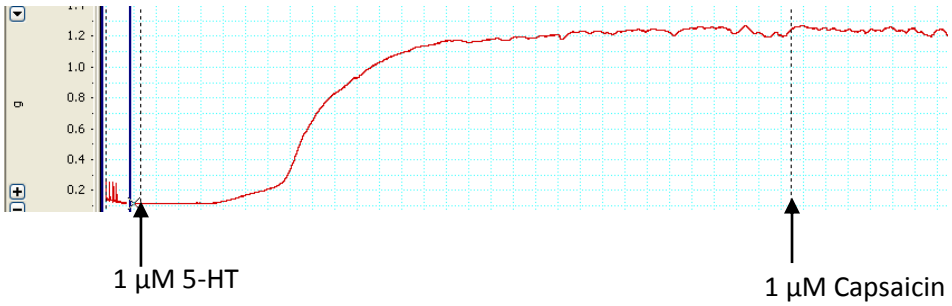

Figure 4-5: Representative trace showing WT tail artery responding to 5-HT and capsaicin exposure.

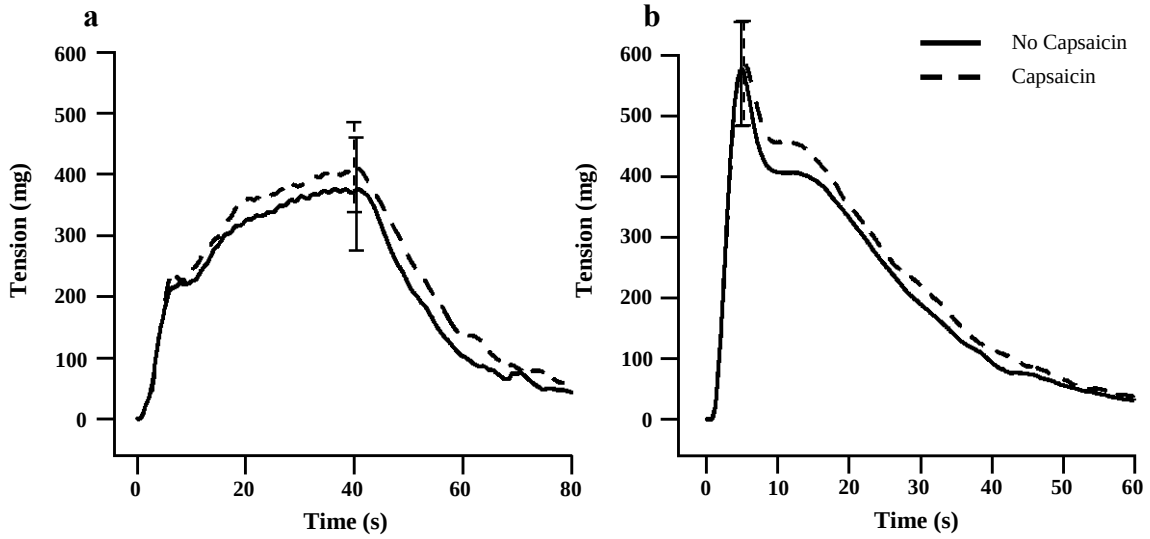

Figure 4-6: Averaged traces from 6 proximal WT mouse tail arteries taken before capsaicin treatment and following capsaicin treatment (1 µM for 30 minutes) at 0.5 Hz (a) and 8 Hz (b). Responses in mg tension with error bars at the peak responses ± S.E.M. —— **No Capsaicin** – – **Capsaicin**

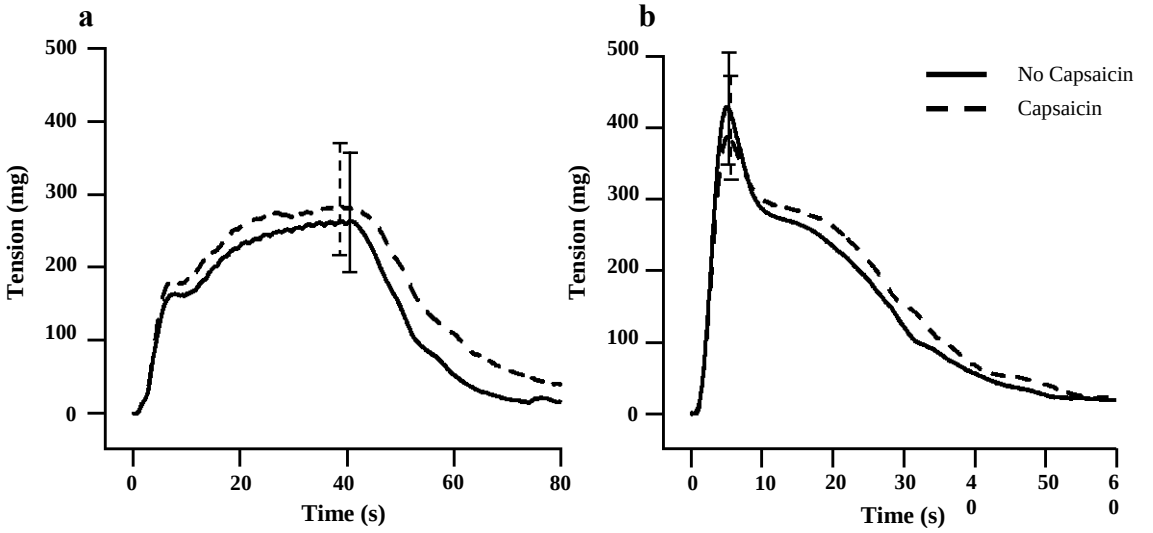

Figure 4-7: Averaged traces from 6 distal WT mouse tail arteries taken before capsaicin treatment and following capsaicin treatment (1 µM for 30 minutes) at 0.5 Hz (a) and 8 Hz (b). Responses in mg tension with error bars at the peak responses ± S.E.M. —— **No Capsaicin** – – **Capsaicin**

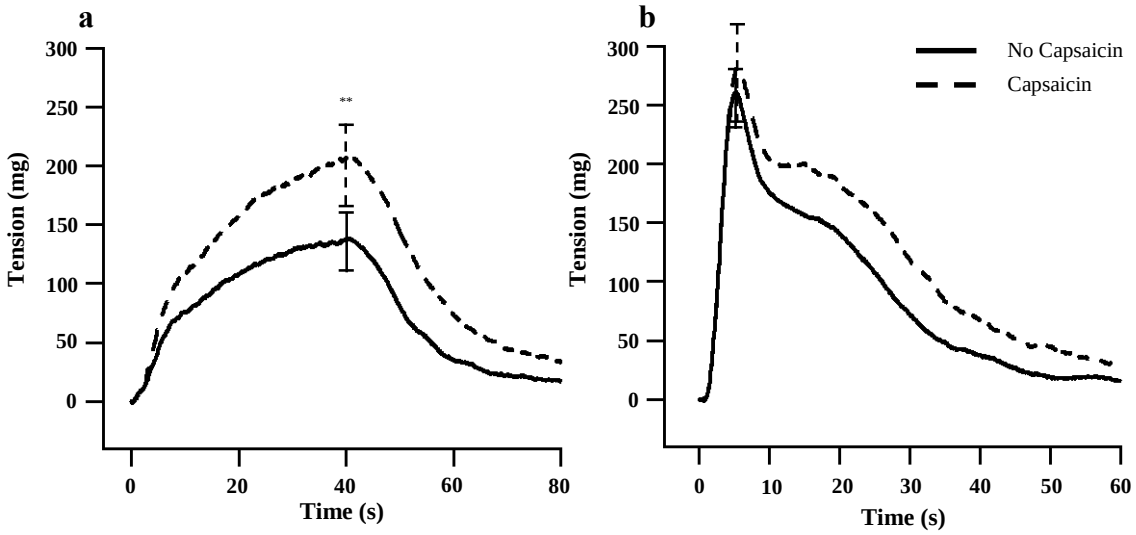

Figure 4-8: Averaged traces from 6 proximal ADKO mouse tail arteries taken before capsaicin treatment and following capsaicin treatment (1 µM for 30 minutes) at 0.5 Hz (a) and 8 Hz (b). Responses in mg tension with error bars at the peak responses ± S.E.M. ** indicates a significant difference in peak tension before and after capsaicin treatment. ——— No Capsaicin – – – Capsaicin

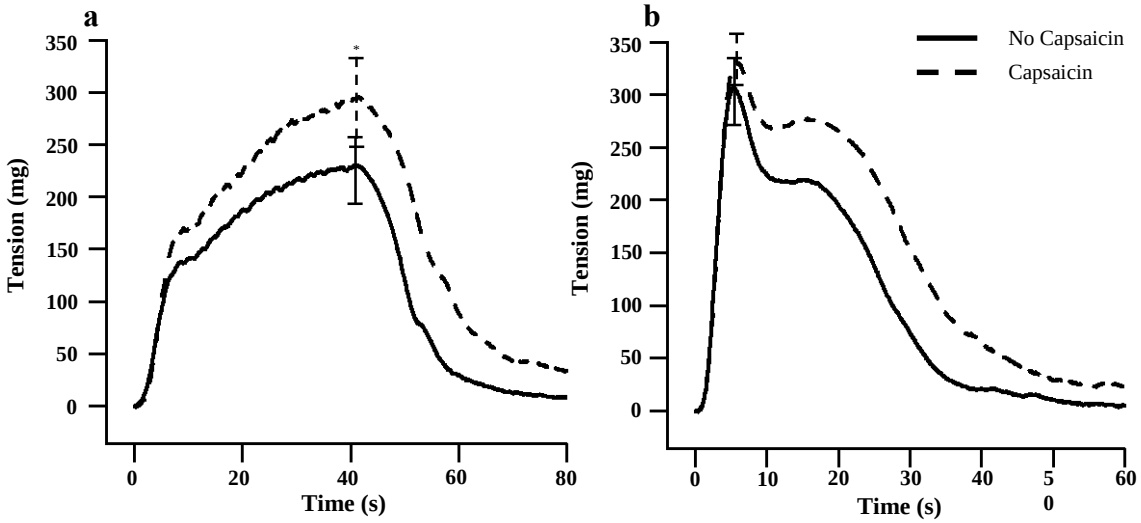

Figure 4-9: Averaged traces from 6 distal ADKO mouse tail arteries taken before capsaicin treatment and following capsaicin treatment (1 µM for 30 minutes) at 0.5 Hz (a) and 8 Hz (b). Responses in mg tension with error bars at the peak responses ± S.E.M. * indicates a significant difference in peak tension before and after capsaicin treatment. ——— No Capsaicin – – – Capsaicin

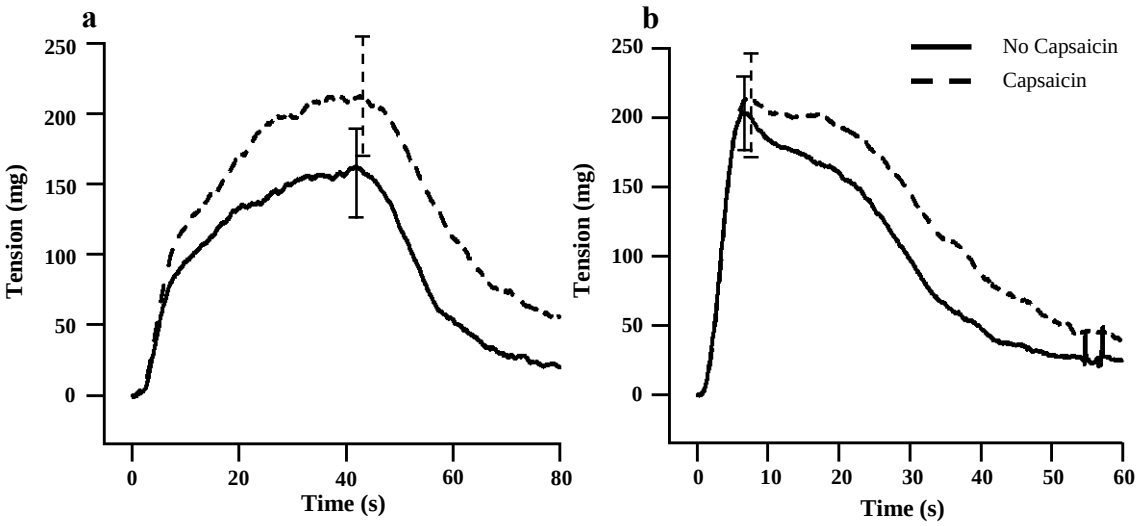

Figure 4-10: Averaged traces from 6 proximal α_1-null mouse tail arteries taken before capsaicin treatment and following capsaicin treatment (1 µM for 30 minutes) at 0.5 Hz (a) and 8 Hz (b). Responses in mg tension with error bars at the peak responses ± S.E.M. —— **No Capsaicin** – – **Capsaicin**

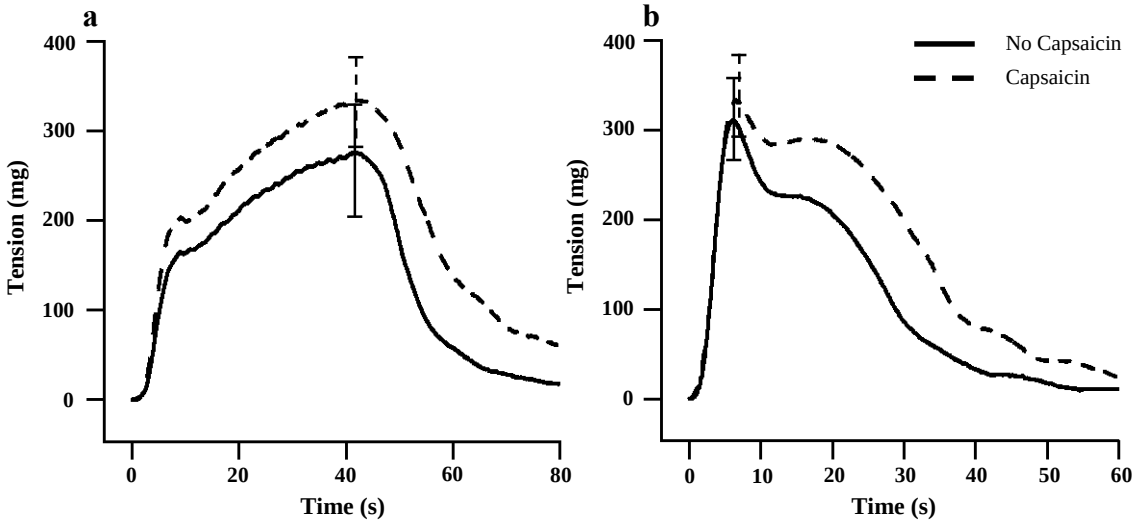

Figure 4-11: Averaged traces from 6 distal α_1-null mouse tail arteries taken before capsaicin treatment and following capsaicin treatment (1 µM for 30 minutes) at 0.5 Hz (a) and 8 Hz (b). Responses in mg tension with error bars at the peak responses ± S.E.M.
—— **No Capsaicin** – – **Capsaicin**

Table 4-2: Comparison of nerve responses before and after capsaicin treatment (1 μM for 30 minutes) in mouse tail arteries from WT, ADKO and α_1-null strains.

Strain	Location	Frequency	Response (mg ± S.E.M)	
			Before Capsaicin	Following Capsaicin
WT n = 6	Proximal	0.5 Hz	385 ± 97	413 ± 77
		8 Hz	589 ± 86	599 ± 87
	Distal	0.5 Hz	270 ± 82	291 ± 79
		8 Hz	445 ± 79	403 ± 72
ADKO n = 6	Proximal	0.5 Hz	140 ± 27	211 ± 35 **
		8 Hz	264 ± 27	284 ± 42
	Distal	0.5 Hz	234 ± 43	299 ± 33 *
		8 Hz	314 ± 34	335 ± 27
α_1-null n = 6	Proximal	0.5 Hz	165 ± 33	218 ± 44
		8 Hz	208 ± 28	219 ± 39
	Distal	0.5 Hz	279 ± 65	337 ± 53
		8 Hz	324 ± 50	352 ± 50

*** P < 0.05, ** P < 0.01 compared with response before capsaicin treatment. Paired t-test.**

4.4 Discussion

The nonadrenergic noncholinergic (NANC) response in the vasculature is now known to be mediated, in part, by CGRP-containing sensory nerves. These nerves are capable of contributing to the maintenance of homeostasis by monitoring the vessels environment and responding to changes. They are also sensitive to capsaicin, which induces peptide release and results in subsequent desensitisation of the nerves (Caterina et al., 1997). Capsaicin has also been shown to inhibit ATP release from the nerves following EFS in the guinea pig vas deferens through a suggested action on a pre-junctional receptor (Ellis and Burnstock, 1989). The actions of the sympathetic and sensory nerves are not completely separate and therefore may be able to influence the actions of either group of receptors. It has been suggested that CGRP release may be inhibited by NA acting on α_2-ARs located on sensory nerves. This study was conducted using the rat mesenteric arteries and utilised EFS. The response to various antagonists including yohimbine (α_2-AR antagonist) revealed an inhibition in CGRP release when yohimbine was present (Kawasaki et al., 1990).

4.4.1 Mouse Mesenteric Arteries

Initial tests with capsaicin whilst tone was raised in the vessels suggest that CGRP containing nerves are present in mouse mesenteric arteries. This supports the experiments carried out by Fujiwara et al. in the mouse mesentery (Fujiwara et al., 2012). However, effects on nerve-mediated responses have not been reported. Here, peak response to perivascular nerve stimulation was not affected by capsaicin. Using capsaicin revealed that nerve stimulation within the aforementioned parameters does not expose a vasodilatory effect. Therefore simultaneous activation of the CGRP containing nerves present in the mesentery does not influence the contractile response to sympathetic nerve stimulation. However, a recent paper by Sheykhzade et al., (2011) showed that, in the mouse vas deferens, there is a triphasic response to capsaicin. This variation in vessel reaction to capsaicin is dependent on the concentration of capsaicin administered. At low doses (1 nM – 300 nM) capsaicin induced CGRP release decreased the response to nerve stimulation; at an intermediate dose (100 nM – 10 µM) the response was augmented and at high doses (10 µM – 1 mM) the response was again decreased. If a similar response occurs in the mesentery then at 1 µM, capsaicin incubation may be exerting a dual effect whereby released CGRP leads to desensitisation and augments the response but the non-specific effects of capsaicin attenuates the response. This could result in little change being seen in the response (Sheykhzade et al., 2011).

Interestingly, Fujii et al. have shown that exogenously added 5-hydroxytryptamine (5-HT) can be stored in adrenergic nerves and exert an inhibitory effect on CGRP containing nerves upon release (Fujii et al., 2012). The vessel reactivity tests performed at the beginning of these experiments include response to 1 µM 5-HT. Consequently, if this 5-HT can be stored in the same way as in the rat it is possible that any vasodilatory effect would be lost. Repeating the experiments without 5-HT addition would determine whether it was having an inhibitory effect.

4.4.2 Mouse Tail Artery

Few studies have investigated the effect of CGRP release in the rat tail artery and none have investigated the mouse tail artery. If CGRP is released following nerve stimulation, the full contractile effect of postjunctional receptor activation will not be seen. This complicates the investigation of neurotransmitter release. However, it has been shown here that capsaicin incubation has no significant effects on the peak response to nerve stimulation in both WT and α_1-null mice. This suggests that under the parameters tested, CGRP is not released in significant enough quantities to produce a vasodilatory effect. In the ADKO mice, responses both proximally and distally at 0.5 Hz were significantly increased following capsaicin exposure. To date, there has been no correlation reported between the α_1-ARs and CGRP activity. In the WT and α_1-null mouse tail artery, there was a trend to increase the response following capsaicin treatment. Further investigations, including increasing the number of experiments, utilising α_1-AR antagonists and immunohistochemistry (IHC) would contribute to revealing capsaicin's effect.

Furthermore, as suggested in the mesenteric arteries, capsaicin may have a dual effect in response to sympathetic nerve stimulation in the tail artery. A 1 μM administration of capsaicin may result in the release of CGRP to augment the response but may also result in non-specific actions of capsaicin which may attenuate the response. Non-specific actions of capsaicin include altering voltage dependent sodium channel regulation at high capsaicin concentrations (Lundbaek et al., 2005; Sheykhzade et al., 2011).

4.4.3 Conclusion

It has been shown here that nerve stimulation induced responses are not alone masked by a vasodilatory action of CGRP release from sensory nerves in mesenteric arteries from each mouse strain or in WT and α_1-null tail arteries. This may be due to a dual capsaicin effect on the blood vessels. Whereby capsaicin is able to stimulate release of CGRP and desensitise the nerves as well as initiate non-specific effects which may alter voltage dependent sodium channels and trigger vessel contraction. In the mouse tail artery, capsaicin incubation results

in an increase in peak response in the ADKO strain suggesting that CGRP release can reveal a vasodilatory effect. This may be due to an interaction between the α_{1A}- and α_{1B}-ARs that is masked in the WT mice, lost in the α_1-null mice and revealed in the ADKO mice. However, as both the WT and α_1-null tail artery preparations showed a trend to increase in response following capsaicin treatment, further investigations are required to clarify capsaicin's effect.

Chapter Five

Pharmacological analysis of post junctional receptors in mouse mesenteric and tail arteries involved in contractions evoked by short trains of perivascular nerve impulses.

5.1 Introduction

Sympathetic neurovascular transmission involves the release of neurotransmitters from the nerve terminals and subsequent activation of receptors located pre- and post-junctionally. Activation of such receptors modulates vascular tone and can therefore increase blood pressure via narrowing of the blood vessels caused by smooth muscle cell contraction. Release of noradrenaline (NA) from the nerve terminals can act at post-junctional α_1- and α_2-ARs to initiate vasoconstriction or act pre-junctionally at α_2-ARs to inhibit further neurotransmitter release (Msghina et al., 1992; Brock and Cunnane, 1999). Adenosine Tri-phosphate (ATP) is also released from the nerve terminals and acts post-junctionally at P2X receptors to initiate vasoconstriction (Burnstock, 1972).

Studies in rat mesenteric and tail arteries have been extensive and have demonstrated the presence of the α_1-, α_2-ARs and P2X receptors. Nerve stimulation experiments in the rat mesenteric arteries revealed α_1-AR activation to be dominant in constricting the vessels with the P2X receptors also contributing and in some instances interacting with the α_1-ARs. There is also a population of pre-junctional α_2-ARs which, when activated by NA, inhibit further neurotransmitter release (Angus et al., 1988; Gitterman and Evans, 2001; Brock et al., 2006). More recently, evidence of an adrenergic component in the response to nerve stimulation in the mouse mesenteric arteries has been published (Fujiwara et al., 2012). In the rat tail artery, the α_1- and α_2-ARs have been shown to contribute to the slow portion of the nerve response, with activation of the P2X receptors producing the initial contraction (Sneddon and Burnstock, 1984; Bao et al., 1990). There is also evidence to show that ATP release has a dual effect, activating P2X receptors and inhibiting the adrenergic response (Bao and Stjarne, 1993). Evidence of α_2-AR involvement has been shown pre- and post-junctionally, with increased α_2-AR sensitivity shown in distal tail artery segments (Msghina et al., 1999; Weiss et al., 1983; Medgett, 1985).

The development of transgenic mice and, in particular, the α_1-AR KO mice, has allowed the functional pharmacology in the mouse vasculature to be simplified (Cavalli et al., 1997; Rokosh and Simpson, 2002; Tanoue et al., 2002). The α_1-ARs are considered to be crucial

in the maintenance of vascular tone and so these KO mice will contribute to the understanding of how the blood vessels are regulated when these receptors are missing. Before responses to nerve stimulation in these mice can be studied in depth, the roles the receptors play must first be elucidated in WT mice. Presently, the mouse mesenteric arteries and tail artery have been employed and the responses to perivascular nerve stimulation studied. Therefore the aims of the following study were:

- To characterise the roles of the α_1-, α_2-ARs and P2X receptors in the response to nerve stimulation in mouse mesenteric arteries.
- To characterise the roles of the α_1-, α_2-ARs and P2X receptors in the response to nerve stimulation in the mouse proximal and distal tail artery
- To determine whether there are any interactions between the receptors in either the mouse mesenteric arteries or the tail artery.

5.2 Methods

A full description of the methods used can be found in Chapter Two (Materials and Methods). Briefly, wire myography studies were conducted using mouse mesenteric arteries and proximal and distal tail artery segments. The vessels were contained within two stimulating electrodes which could be controlled to deliver pulses of varying parameters of stimulation. All vessels were incubated with 1 µM capsaicin in order to deplete the sensory nerves of CGRP; a potent vasodilator. Control response to 2 Hz and 8 Hz (mesenteric arteries) and 0.5 Hz and 8 Hz (tail artery) were recorded before incubation with one of the following antagonists: 100 nM prazosin (α_1-AR antagonist), 100 nM rauwolscine (α_2-AR antagonist) or 1 mM suramin (P2X receptor antagonist). The vessels were then stimulated again using the same parameters.

Statistical analysis was performed using GraphPad Prism (Version 5) with paired t-tests used when comparing control response with antagonist response and one way ANOVA with Bonferonni's post-test utilised for comparing the antagonist sensitive components. A worked example of the component analysis, which revealed the antagonist sensitive response in

different incubation sequences is shown at the beginning of the mesenteric and tail artery results sections in Chapter Five.

5.3 Results

5.3.1 Mouse Mesenteric Artery

Combined incubation with prazosin (100 nM), rauwolscine (100 nM) and suramin (1 mM) effectively blocked the α_1-, α_2-ARs and P2X receptors respectively in response to nerve stimulation at 2 Hz and 8 Hz in the mesenteric arteries and completely abolished the response (Figures 5-1 and 5-2).

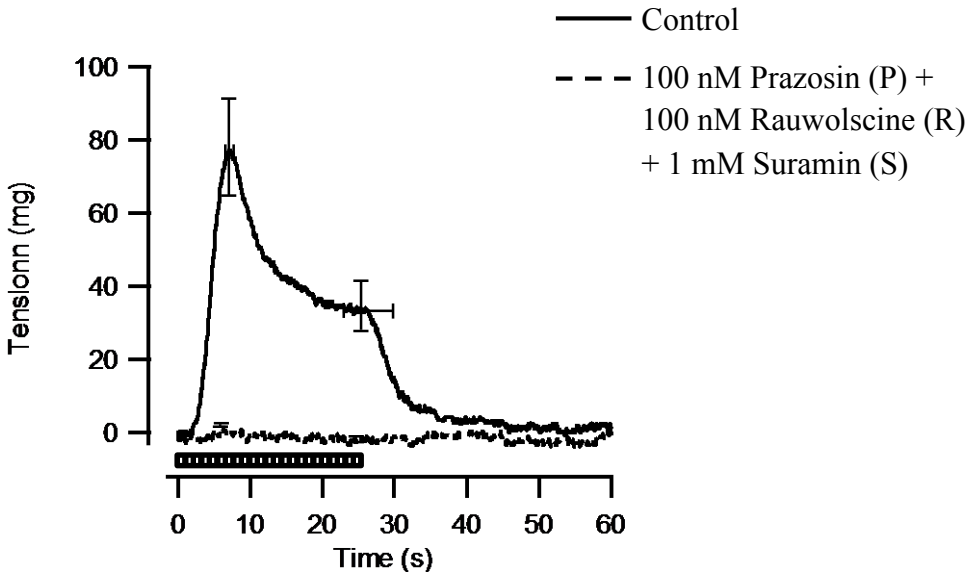

Figure 5-1: WT Mouse mesenteric artery response to nerve stimulation at 2 Hz in control vessels and in the presence of the following antagonists: 100 nM prazosin, 100 nM rauwolscine, 1 mM suramin (n = 4).

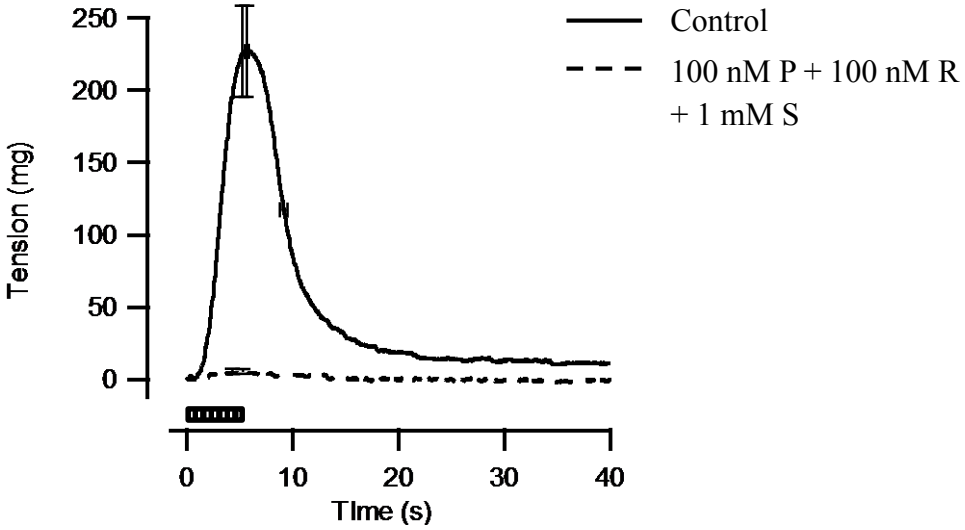

Figure 5-2: WT Mouse mesenteric artery response to nerve stimulation at 8 Hz in control vessels and in the presence of the following antagonists: 100 nM prazosin, 100 nM rauwolscine, 1 mM suramin (n = 4).

5.3.1.1 Revealing the α_1-ARs role in the response to sympathetic nerve stimulation at 2 Hz.

Following incubation with 100 nM prazosin (α_1-AR antagonist), the response to stimulation of the sympathetic nerves was reduced; statistically affecting the rate of rise and both the peak tension and the tension recorded at the end of the stimulation period (Figure 5-3; Table 5-1).

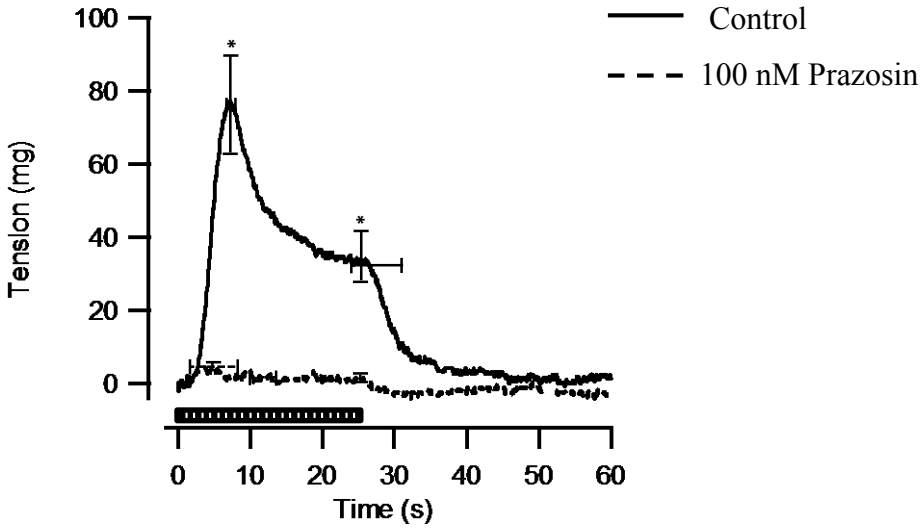

Figure 5-3: WT Mouse mesenteric artery response to nerve stimulation at 2 Hz in control vessels and in the presence of the α_1-AR antagonist prazosin (100 nM) (n =4).

*** P < 0.05 compared with control response. Paired t-test.**

Table 5-1: WT Mouse mesenteric artery response to nerve stimulation in control and prazosin (100 nM) incubated vessels at 2 Hz.

2 Hz	Contractile Response (average ± S.E.M)		
	Control	100 nM Prazosin (P) (n = 4)	% change following P incubation
Time to Peak (seconds)	6.8 ± 0.5	7.5 ± 3.7	- 16 ± 24
Peak Tension (mg)	81 ± 16	7 ± 1 *	- 91 ± 1
Rate of Rise (mg/s)	10.4 ± 1.4	1 ± 0.4 *	- 88 ± 3
Tension at End of pulse (mg)	34 ± 8	1 ± 1 *	- 94 ± 4
50 % Decay Time (seconds)	10.8 ± 3.9	3.2 ± 2.0	- 59 ± 29

*** P < 0.05 compared with control response. Paired t-test.**

When investigating the different receptors involved in the formation of the response, a novel approach was taken in analysing the data. This allowed the data collected to be utilised fully and permitted the isolation of the receptor components in different ways. This was achieved by incubating the arteries in selected antagonists in different sequences. This analysis allowed investigation of whether there was any interaction between the three post-junctional receptors. If there were no interactions, then all of the components revealed would be similar. If there was synergy as has been shown for NA and ATP in the mesenteric artery (Ralevic and Burnstock, 1990), the sizes (or shapes) of the contractions would not be identical.

The first analysis is shown in Figure 5-4 whereby the prazosin-sensitive (PS) component was isolated in three different ways. The PS component was identified by subtracting averaged traces in several incubation sequences as follows:

1. The PS component was revealed as the difference between the control trace and the trace following prazosin incubation – when both the α_2-ARs and P2X receptors were still activated by nerve-released transmitters (Figure 5-4a). The difference is shown in the shading and the key indicates that it is the PS component.

2. The PS component in the absence of α_2-AR activation was revealed by the difference between the trace in rauwolscine and that following rauwolscine plus prazosin

(Figure 5-4b). Shown in brackets are the additional antagonists present; in this example, rauwolscine.

3. Finally, when the arteries were incubated in both suramin and rauwolscine, so that neither P2X receptors nor α_2-ARs were activated, the PS component was revealed (Figure 5-4c). Shown in brackets are the additional antagonists present and in the order the tissues were incubated; in this example, suramin plus rauwolscine.

The trapezoidal methods for calculating the area under the curve was used to determine the shaded areas which were taken to represent the total magnitude of the response due to activation of the α_1-ARs. The values calculated are represented as a percentage of the control response (Figure 5-5). There was no statistical significance between the PS components derived in the three different conditions (Table 5-2).

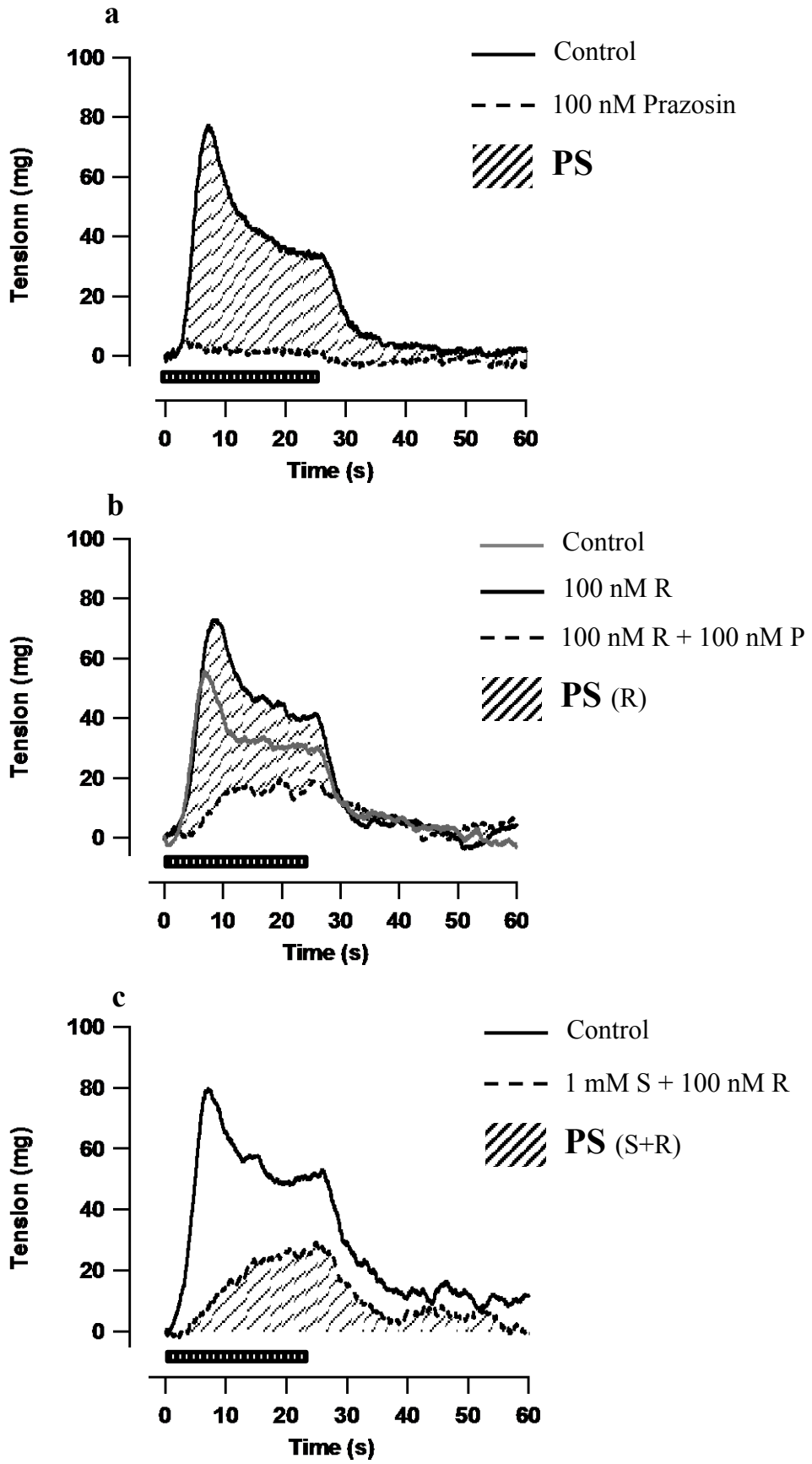

Figure 5-4: Traces showing the revealed prazosin sensitive (PS) components at 2 Hz isolated in three different ways – (a) shows the PS component when the α_2-ARs and P2X receptors are active; (b) shows the PS component when the α_2-ARs are blocked and the P2X receptors are active; (c) shows the PS component when the P2X receptors and α_2-ARs are blocked.

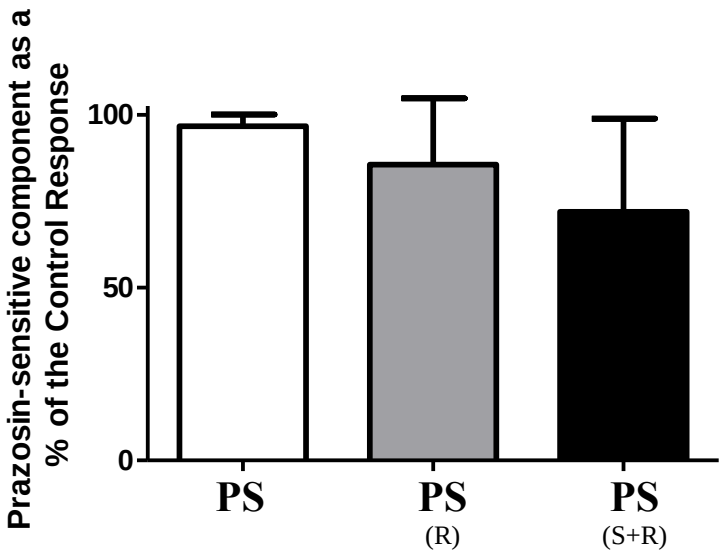

Figure 5-5: WT mouse mesenteric artery – the prazosin sensitive (PS) component at 2 Hz when the α_2-ARs and P2X receptors are functional (white) (n=4), α_2-ARs are blocked (grey) (n=7), P2X receptors and α_2-ARs are blocked (black) (n=6). The presence of additional antagonists are shown in brackets.

Table 5-2: WT mouse mesenteric artery response - revealing the prazosin sensitive component as a % of control area under the curves. Data taken from Figures 5-5 and 5-7.

	Prazosin-sensitive component as a % of the Control Response	
	2 Hz	**8 Hz**
PS	97 ± 3	87 ± 4
PS (R)	86 ± 19	85 ± 15
PS (S+R)	72 ± 27	36 ± 9 *

*** P < 0.05 compared with PS component when the α_2-ARs are blocked. One way ANOVA with Bonferonni's post-test.**

5.3.1.2 Revealing the α_1-ARs role in the response to sympathetic nerve stimulation at 8 Hz.

At 8 Hz, the response to EFS following blockade of α_1-ARs reduced the peak tension and the tension recorded at the end of the stimulation period with the time taken to reach the peak and the rate of rise also being reduced (Figure 5-6; Table 5-3).

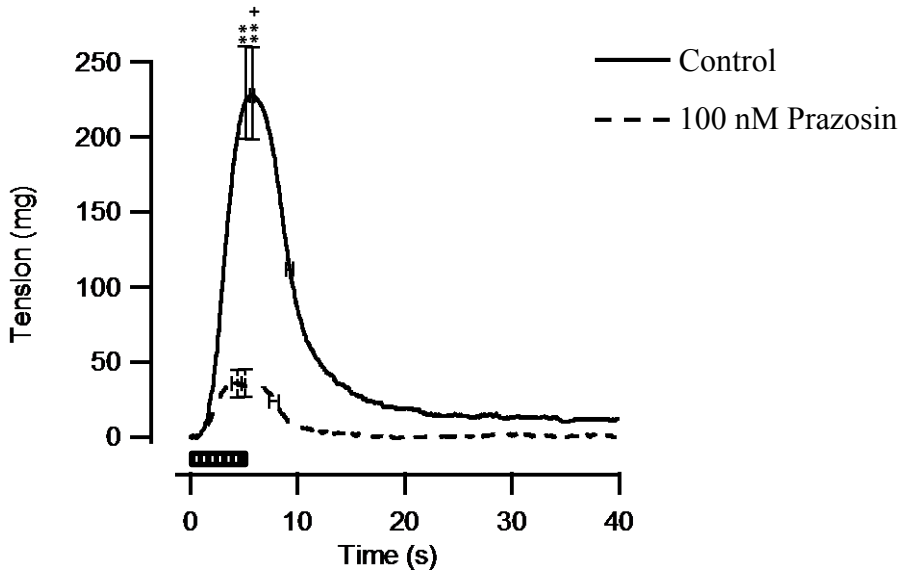

Figure 5-6: WT Mouse mesenteric artery response to nerve stimulation at 8 Hz in control vessels and in the presence of the α_1-AR antagonist prazosin (100 nM) (n = 4).

**** P < 0.01 compared with control response. Paired t-test.**

+ P < 0.05 compared with control time. Paired t-test.

Table 5-3: WT Mouse mesenteric artery response to nerve stimulation in control and prazosin (100 nM) incubated vessels at 8 Hz.

8 Hz	Contractile Response (average ± S.E.M)		
	Control	100 nM Prazosin (P) (n = 4)	% change following P incubation
Time to Peak (seconds)	5.5 ± 0.1	3.7 ± 0.4 +	- 33 ± 8
Peak Tension (mg)	228 ± 36	38 ± 10 **	- 83 ± 3
Rate of Rise (mg/s)	37 ± 3	10 ± 1 **	- 75 ± 3
Tension at End of pulse (mg)	225 ± 36	33 ± 10 **	- 85 ± 3
50 % Decay Time (seconds)	3.8 ± 0.3	4.4 ± 0.5	13 ± 7

**** P < 0.01 compared with control response. Paired t-test.**

+ P < 0.05 compared with control time. Paired t-test.

The prazosin-sensitive components revealed at 8 Hz show that when the P2X receptors and α_2-ARs are blocked, the resulting prazosin-sensitive component response is smaller than the component when only the α_2-ARs are blocked (Figure 5-7; Table 5-2).

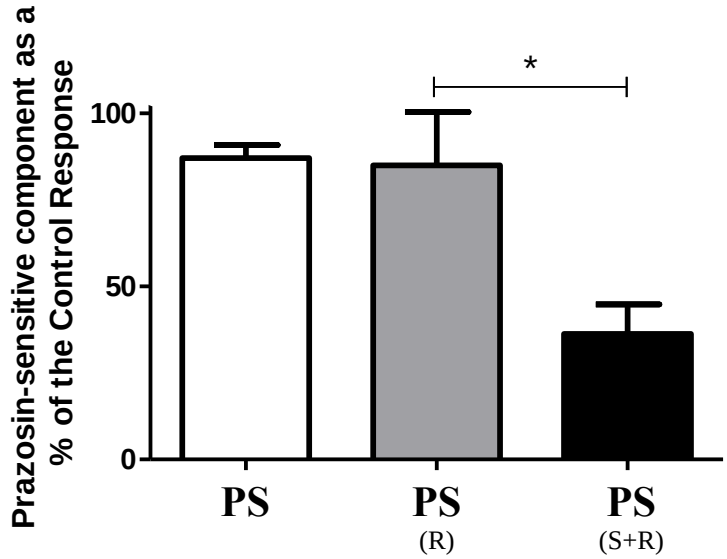

Figure 5-7: WT mouse mesenteric artery – the prazosin-sensitive (PS) component at 8 Hz when the α_2-ARs and P2X receptors are functional (white) (n=4), α_2-ARs are blocked (grey) (n=7), P2X receptors and α_2-ARs are blocked (black) (n=6). The presence of additional antagonists are shown in brackets.

*** P < 0.05 compared with PS component when the P2X receptors and α_2-ARs are blocked. One way ANOVA with Bonferonni's post-test.**

5.3.1.3 Revealing the α_2-ARs role in the response to sympathetic nerve stimulation at 2 Hz.

Following incubation with 100 nM rauwolscine (α_2-AR antagonist), the response to stimulation of the sympathetic nerves is not significantly altered (Figure 5-8; Table 5-4). The graph shows that at 2 Hz, although not statistically significant, there is a trend to potentiate the response following blockade of the α_2-ARs.

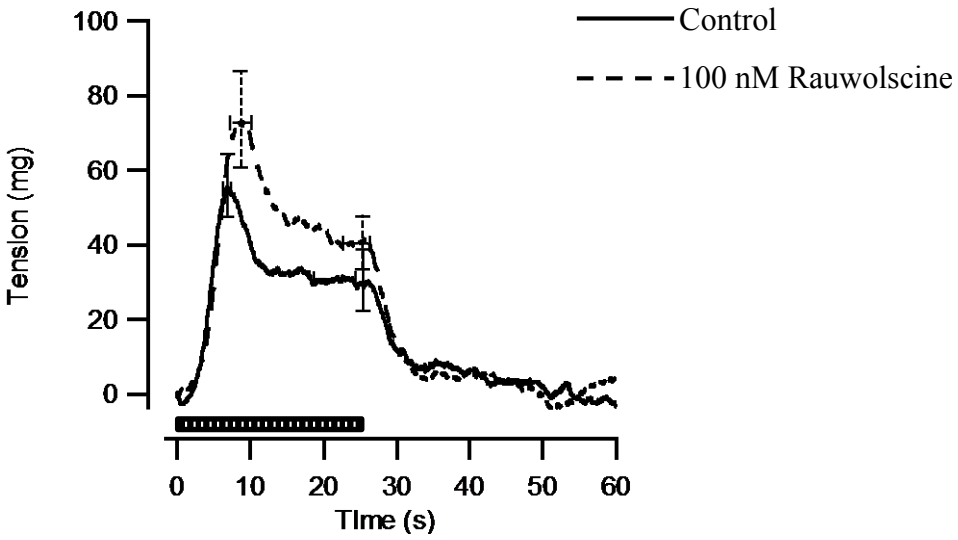

Figure 5-8: WT Mouse mesenteric artery response to nerve stimulation at 2 Hz in control vessels and in the presence of the α_2-AR antagonist rauwolscine (100 nM) (n = 7).

Table 5-4: WT Mouse mesenteric artery response to nerve stimulation in control and rauwolscine (100 nM) incubated vessels at 2 Hz.

2 Hz	Contractile Response (average ± S.E.M)		
	Control	100 nM Rauwolscine (R) (n = 7)	% change following R incubation
Time to Peak (seconds)	7.3 ± 0.5	9.8 ± 1.7	20 ± 6
Peak Tension (mg)	59 ± 10	77 ± 16	17 ± 11
Rate of Rise (mg/s)	10 ± 1	10 ± 2	1 ± 13
Tension at End of pulse (mg)	30 ± 10	41 ± 9	28 ± 17
50 % Decay Time (seconds)	10.2 ± 3.3	12.6 ± 2.0	28 ± 19

Figure 5-9 displays the α_2-AR components that were revealed under various conditions. There is a trend for the area under the curve to be smallest when the α_1-ARs are blocked and the P2X receptors are functional (Figure 5-9; Table 5-5).

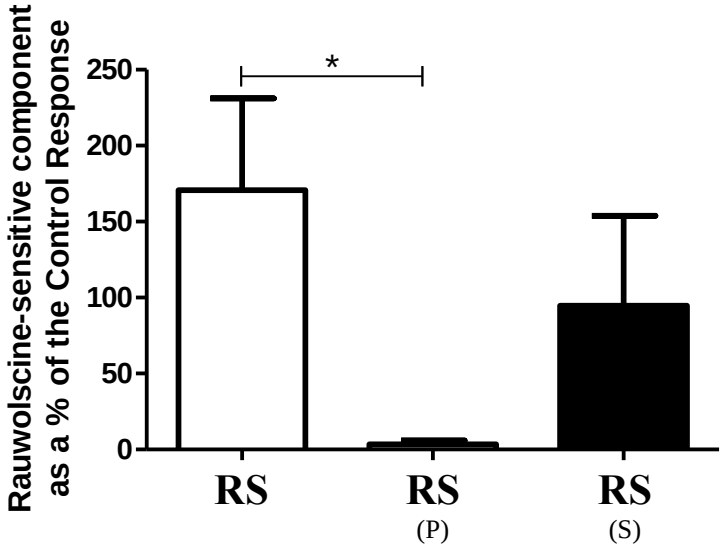

Figure 5-9: WT mouse mesenteric artery – the rauwolscine-sensitive component at 2 Hz when the α_1-ARs and P2X receptors are functional (white) (n=7), α_1-ARs are blocked (grey) (n=4), P2X receptors are blocked (black) (n=6). The presence of additional antagonists are shown in brackets.

*** P < 0.05 compared with the RS component when the α_1-ARs and P2X receptors were functional. One way ANOVA with Bonferonni's post-test.**

Table 5-5: WT mouse mesenteric artery response - revealing the rauwolscine sensitive component as a % of control area under the curves. Data taken from Figures 5-9 and 5-11.

	Rauwolscine-sensitive component as a % of Control Response	
	2 Hz	**8 Hz**
RS	199 ± 63	130 ± 29
RS (P)	3 ± 2 *	108 ± 4
RS (S)	95 ± 59	72 ± 22

*** P < 0.05 compared with RS component when the α_1-ARs and P2X receptors are functional. One way ANOVA with Bonferonni's post-test.**

5.3.1.4 Revealing the α_2-ARs role in the response to sympathetic nerve stimulation at 8 Hz.

At 8 Hz, the response to EFS following blockade of α_2-ARs significantly impacted all of the points studied. The peak tension and the tension recorded at the end of the stimulation period were significantly increased following rauwolscine incubation with the time taken to reach the peak prolonged, the decay time reduced and the rate of rise increased (Figure 5-10; Table 5-6).

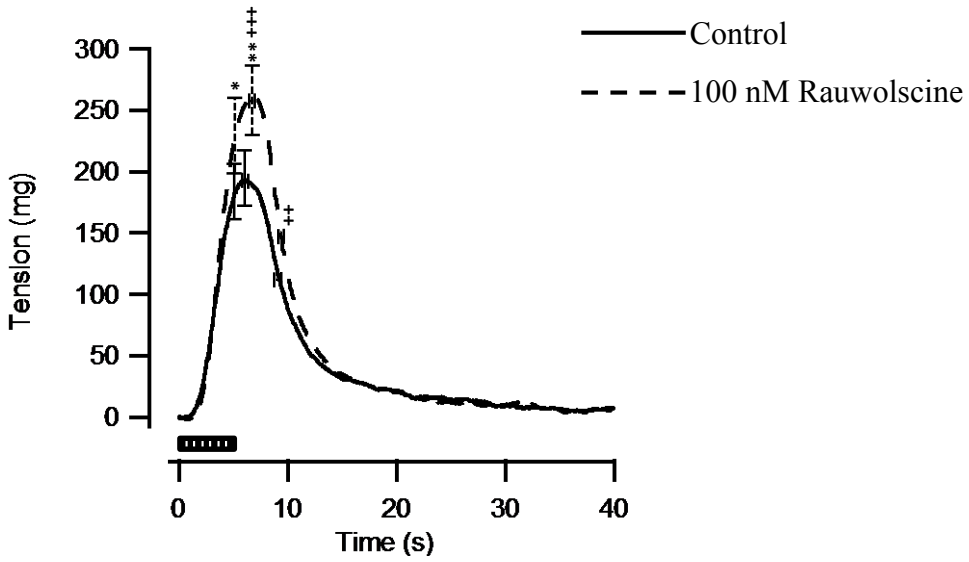

Figure 5-10: WT Mouse mesenteric artery response to nerve stimulation at 8 Hz in control vessels and in the presence of the α_2-AR antagonist rauwolscine (100 nM) (n = 7).

*** P < 0.05, ** P < 0.01 compared with control response. Paired t-test.**

++ P < 0.01; +++ P < 0.001 compared with control time. Paired t-test.

Table 5-6: WT Mouse mesenteric artery response to nerve stimulation in control and rauwolscine (100 nM) incubated vessels at 8 Hz.

8 Hz	Contractile Response (average ± S.E.M)		
	Control	100 nM Rauwolscine (R) (n = 7)	% change following R incubation
Time to Peak (seconds)	6.0 ± 0.2	6.6 ± 0.2 +++	11 ± 2
Peak Tension (mg)	197 ± 26	265 ± 33 **	24 ± 5
Rate of Rise (mg/s)	37 ± 3	40 ± 6 *	16 ± 6
Tension at End of pulse (mg)	192 ± 26	285 ± 35 *	23 ± 7
50 % Decay Time (seconds)	3.8 ± 0.3	3.0 ± 0.1 ++	- 19 ± 4

*** P < 0.05, ** P < 0.01, *** P < 0.001 compared with control response. Paired t-test.**

++ P < 0.01; +++ P < 0.001 compared with control time. Paired t-test.

The rauwolscine-sensitive components were determined and analysis revealed no significant differences between the conditions (Figure 5-11; Table 5-5).

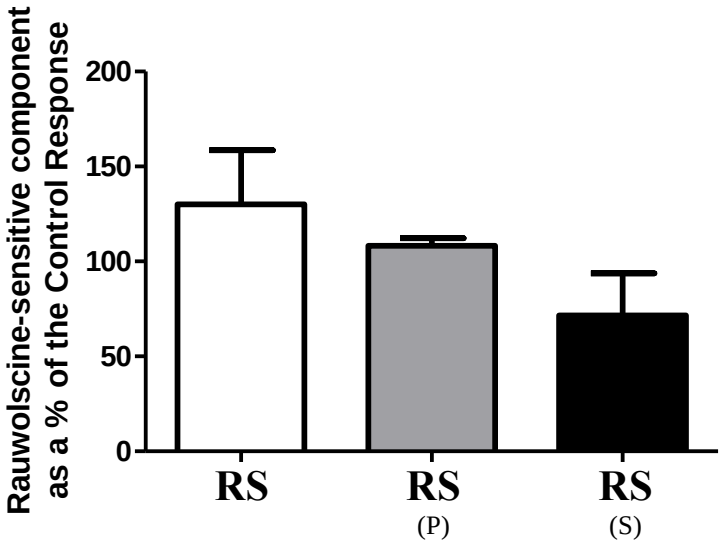

Figure 5-11: WT mouse mesenteric artery – rauwolscine-sensitive component at 8 Hz when the α_1-ARs and P2X receptors are functional (white) (n=7), α_1-ARs are blocked (grey) (n=4), P2X receptors are blocked (black) (n=6). The presence of additional antagonists are shown in brackets.

5.3.1.5 Revealing the P2X receptor role in the response to sympathetic nerve stimulation at 2 Hz.

Following incubation with 1 mM suramin (P2X receptor antagonist), the response to stimulation of the sympathetic nerves resulted in a reduction in peak tension and rate of rise as well as a prolonged time to reach the peak and a shortened decay time (Figure 5-12; Table 5-7).

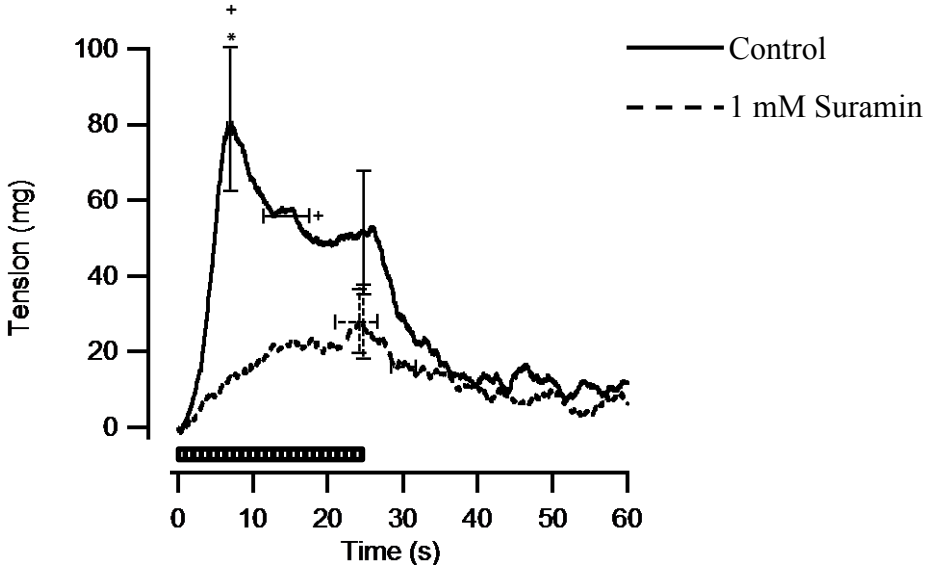

Figure 5-12: WT Mouse mesenteric artery response to nerve stimulation at 2 Hz in control vessels and in the presence of the P2X receptor antagonist suramin (1 mM) (n =6).

*** P < 0.05 compared with control response. Paired t-test.**

+ P < 0.05 compared with control time. Paired t-test.

Table 5-7: Mouse mesenteric artery response to nerve stimulation in control and suramin (1 mM) incubated vessels at 2 Hz.

2 Hz	Contractile Response (average ± S.E.M)		
	Control	1 mM Suramin (S) (n = 6)	% change following S incubation
Time to Peak (seconds)	7.3 ± 0.3	18.4 ± 3.3 +	51 ± 13
Peak Tension (mg)	83 ± 22	31 ± 10 *	- 50 ± 25
Rate of Rise (mg/s)	10 ± 1	2 ± 0.4 *	- 72 ± 17
Tension at End of pulse (mg)	52 ± 19	26 ± 11	- 46 ± 27
50 % Decay Time (seconds)	15.3 ± 3.6	4.6 ± 1.8 +	- 73 ± 7

*** P < 0.05 compared with control response. Paired t-test.**

+ P < 0.05 compared with control time. Paired t-test.

The suramin-sensitive components were determined and analysis revealed is shown in Figure 5-13 (Table 5-8).

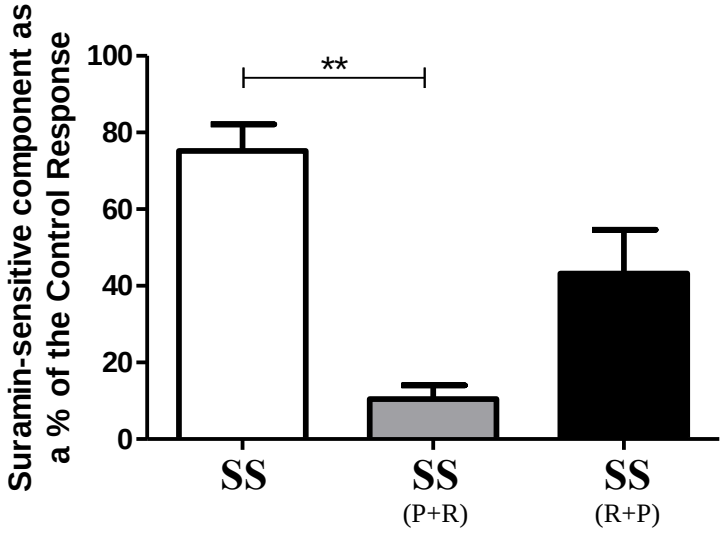

Figure 5-13: WT mouse mesenteric artery – the suramin-sensitive component at 2 Hz when the α_1- and α_2-ARs are functional (white) (n=6), α_1- and α_2-ARs are blocked (grey) (n=4), α_2-ARs and α_1-ARs are blocked (black) (n=7).

**** P < 0.01 compared with SS component when the α_1- and α_2-ARs are functional. One way ANOVA with Bonferonni's post-test.**

Table 5-8: WT mouse mesenteric artery response - revealing the suramin-sensitive component as a % of control area under the curves. Data taken from Figures 5-13 and 5-15.

	Suramin-sensitive component as a % of Control Response	
	2 Hz	**8 Hz**
SS	75 ± 7	90 ± 13
SS (P+R)	10 ± 4 **	21 ± 6 **
SS (R+P)	43 ± 11	46 ± 11 *

*** P < 0.05; ** P < 0.01 compared with SS component when the α_1- and α_2-ARs were functional. One way ANOVA with Bonferonni's post-test.**

5.3.1.6 Revealing the P2X receptors role in the response to sympathetic nerve stimulation at 8 Hz.

At 8 Hz, the response to EFS following blockade of P2X receptors significantly impacted the peak tension, the tension at the end of the stimulation period and the rate of rise. The peak tension and the tension recorded at the end of the stimulation period were significantly reduced following suramin incubation with the rate of rise also being reduced (Figure 5-14; Table 5-9).

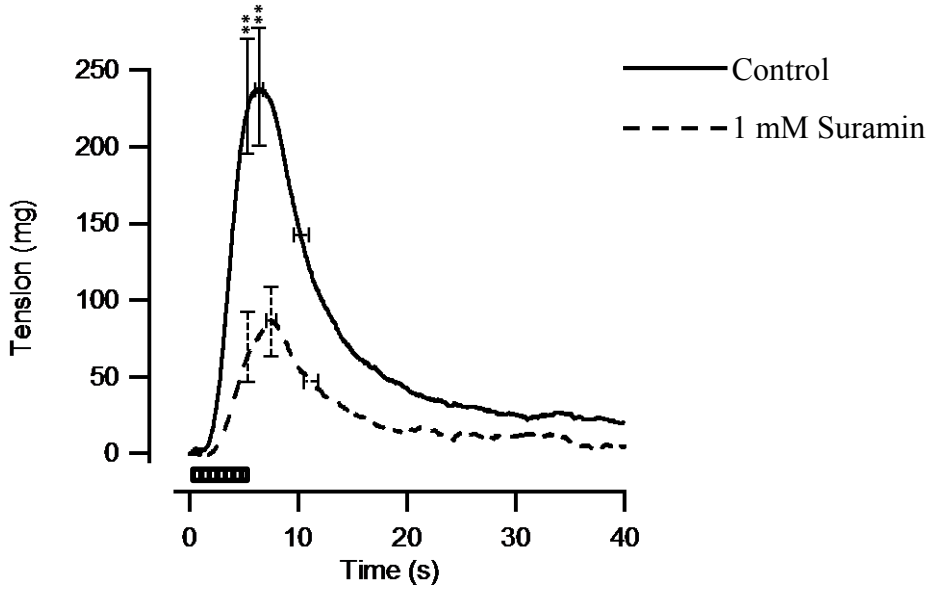

Figure 5-14: WT Mouse mesenteric artery response to nerve stimulation at 8 Hz in control vessels and in the presence of the P2X receptor antagonist suramin (1 mM) (n = 6).

**** P < 0.01 compared with control response. Paired t-test.**

Table 5-9: WT Mouse mesenteric artery response to nerve stimulation in control and suramin (1 mM) incubated vessels at 8 Hz.

8 Hz	Contractile Response (average ± S.E.M)		
	Control	1 mM Suramin (S) (n = 6)	% change following S incubation
Time to Peak (seconds)	6.4 ± 0.3	7.1 ± 0.4	8 ± 5
Peak Tension (mg)	248 ± 45	87 ± 27 **	- 61 ± 13
Rate of Rise (mg/s)	37 ± 3	12 ± 4 **	- 65 ± 11
Tension at End of pulse (mg)	237 ± 44	75 ± 27 **	- 66 ± 11
50 % Decay Time (seconds)	4.5 ± 0.7	4.1 ± 0.7	- 12 ± 11

**** P < 0.01 compared with control response. Paired t-test.**

Analysis of the suramin-sensitive (SS) components show the largest area to be when the α_1- and α_2-ARs are functional. This response is significantly larger than the responses recorded when α_1- and α_2-ARs are blocked; in either order (Figure 5-15; Table 5-8).

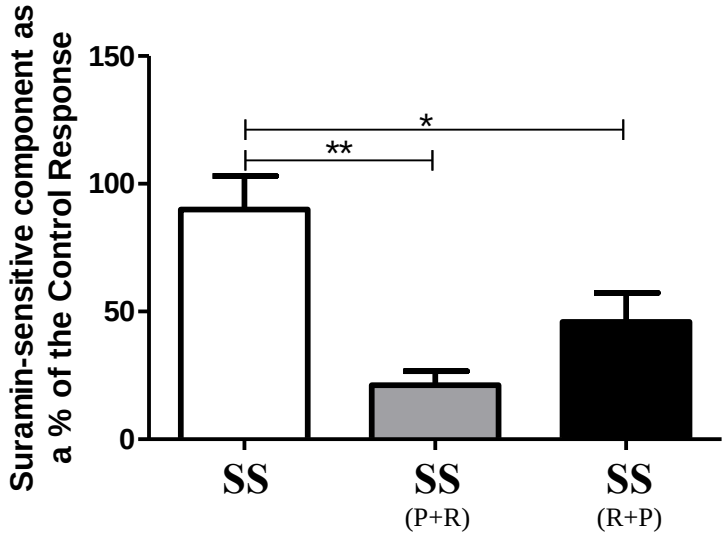

Figure 5-15: WT mouse mesenteric artery – the suramin-sensitive component at 8 Hz when the α_1- and α_2-ARs are functional (white) (n=6), α_1- and α_2-ARs are blocked (grey) (n=4), α_2-ARs and α_1-ARs are blocked (black) (n=7).

*** P < 0.05; ** P < 0.01 compared with SS component when the α_1- and α_2-ARs are functional. One way ANOVA with Bonferonni's post-test.**

5.3.2 Proximal and Distal Mouse Tail Artery

The present results in the mouse tail artery indicate little difference between the proximal and distal segments (Tables 5-10 and 5-11). At the points studied, only the tension recorded at the second peak of the 8 Hz stimulation was lower in the distal segments compared to the proximal response. For this reason, the results section includes only graphs from one area of the tail and only discrepancies in results were noted.

Table 5-10: WT Proximal and Distal mouse tail artery response to nerve stimulation at 0.5 Hz.

0.5 Hz	Contractile Response (average ± S.E.M)	
	Proximal	**Distal**
Time to Peak (1st) (seconds)	2.4 ± 0.4	2.9 ± 0.4
Peak Tension (1st) (mg)	50 ± 19	58 ± 17
Rate of Rise (mg/s)	17 ± 4	17 ± 3
Time to Peak (seconds)	37.6 ± 1.1	37.0 ± 2.8
Peak Tension (mg)	344 ± 44	316 ± 46
Tension at End of pulse (mg)	330 ± 43	303 ± 45
50 % Decay Time (seconds)	15.0 ± 1.6	12.1 ± 2.9

Table 5-11: WT Proximal and Distal mouse tail artery response to nerve stimulation at 8 Hz.

8 Hz	Contractile Response (average ± S.E.M)	
	Proximal	**Distal**
Tension at End of pulse (mg)	240 ± 32	183 ± 14
Time to Peak (seconds)	4.9 ± 0.1	4.9 ± 0.1
Peak Tension (mg)	563 ± 51	494 ± 29
Rate of Rise (mg/s)	117 ± 11	85 ± 9
Time to Peak (2nd) (seconds)	11.2 ± 0.5	12.3 ± 0.3
Peak Tension (2nd) (mg)	369 ± 48	285 ± 22 *
50 % Decay Time (seconds)	15.4 ± 1.8	13.3 ± 1.2

*** P < 0.05 compared with proximal response. Un-paired t-test.**

Combined incubation with prazosin (100 nM), rauwolscine (100 nM) and suramin (1 mM) effectively blocked the α_1-, α_2-ARs and P2X receptors respectively in response to nerve stimulation at 0.5 Hz and 8 Hz in the tail artery and completely abolished the response (Figures 5-16 and 5-17).

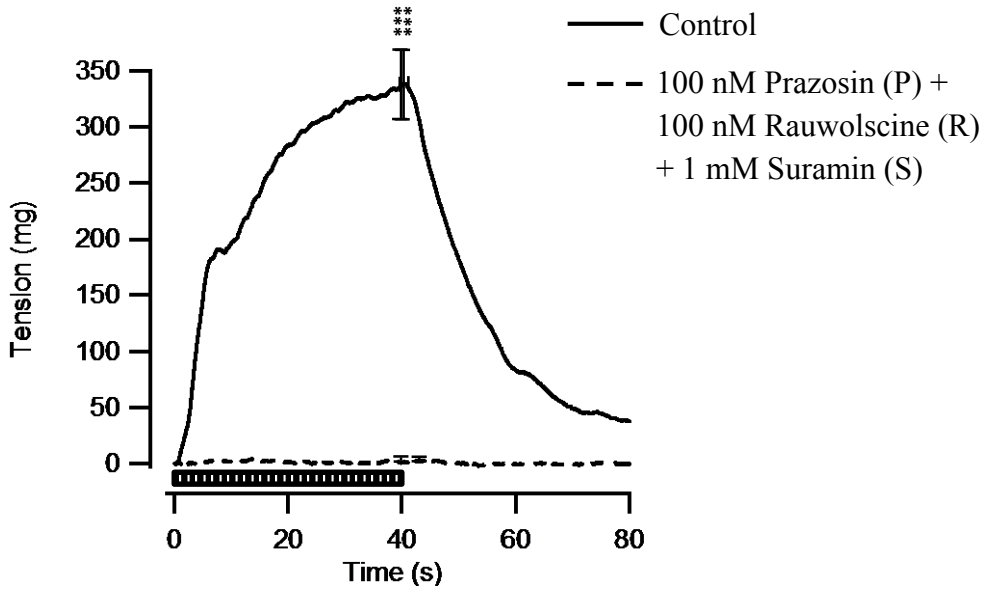

Figure 5-16: WT Proximal mouse tail artery response to nerve stimulation at 0.5 Hz in control vessels and in the presence of the following antagonists: 100 nM prazosin, 100 nM rauwolscine, 1 mM suramin (n = 6).

***** P < 0.001 compared with control response. Paired t-test.**

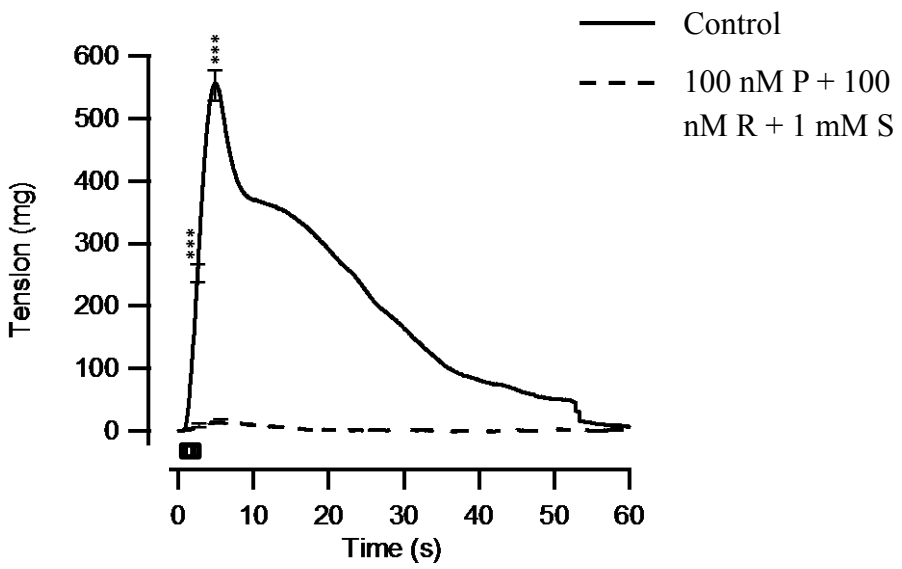

Figure 5-17: WT Proximal mouse tail artery response to nerve stimulation at 8 Hz in control vessels and in the presence of the following antagonists: 100 nM prazosin, 100 nM rauwolscine, 1 mM suramin (n = 6).

***** P < 0.001 compared with control response. Paired t-test.**

5.3.2.1 Revealing the α_1-ARs role in the response to sympathetic nerve stimulation at 0.5 Hz.

Following incubation with 100 nM prazosin (α_1-AR antagonist), the response to stimulation of the sympathetic nerves was reduced; statistically affecting the rate of rise and both the peak tension and the tension recorded at the end of the stimulation period (Figure 5-18; Table 5-12). In the distal tail artery, the tension recorded at the first peak was also significantly reduced following prazosin incubation (Table 5-13).

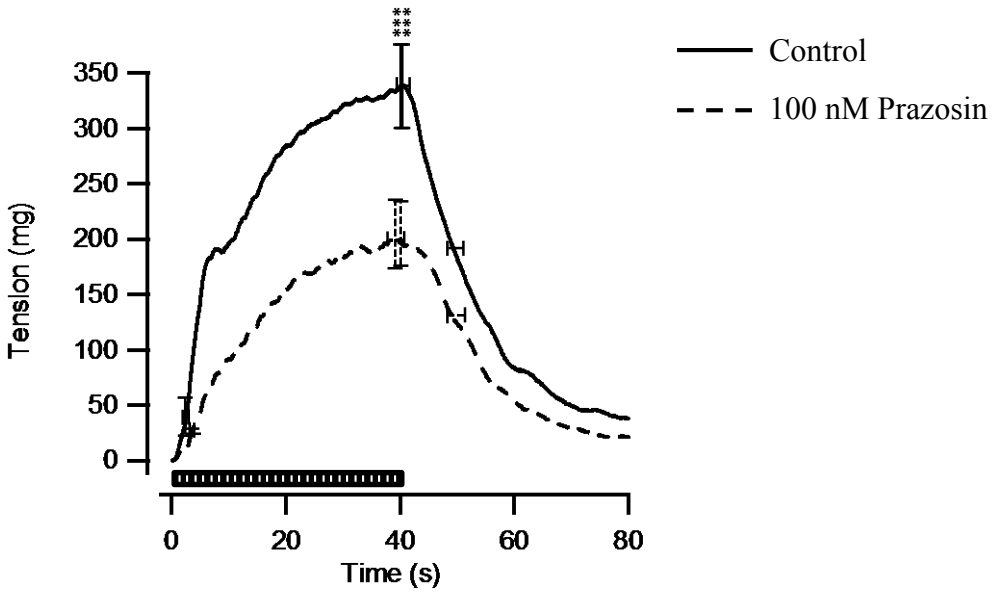

Figure 5-18: WT Proximal mouse tail artery response to nerve stimulation at 0.5 Hz in control vessels and in the presence of the α_1-AR antagonist prazosin (100 nM) (n = 12).

***** P < 0.001 compared with control response. Paired t-test.**

Table 5-12: WT Proximal mouse tail artery response to nerve stimulation in control and prazosin (100 nM) incubated vessels at 0.5 Hz.

Proximal 0.5 Hz	Contractile Response (average ± S.E.M)		
	Control	100 nM Prazosin (P) (n = 12)	% change following P incubation
Time to Peak (1st) (seconds)	2.4 ± 0.4	1.9 ± 0.3	- 21 ± 6
Peak Tension (1st) (mg)	50 ± 19	14 ± 2	- 44 ± 14
Rate of Rise (mg/s)	17 ± 4	8 ± 1 *	- 42 ± 9
Time to Peak (seconds)	37.6 ± 1.1	37.6 ± 1.5	6 ± 4
Peak Tension (mg)	344 ± 44	206 ± 35 ***	- 33 ± 10
Tension at End of pulse (mg)	330 ± 43	195 ± 33 ***	- 34 ± 10
50 % Decay Time (seconds)	15.0 ± 1.6	14.4 ± 1.7	6 ± 11

*** P < 0.05, *** P < 0.001 compared with control response. Paired t-test.**

Table 5-13: WT Distal mouse tail artery response to nerve stimulation in control and prazosin (100 nM) incubated vessels at 0.5 Hz.

Distal 0.5 Hz	Contractile Response (average ± S.E.M)		
	Control	100 nM Prazosin (P) (n = 12)	% change following P incubation
Time to Peak (1st) (seconds)	2.9 ± 0.4	2.2 ± 0.2	7 ± 13
Peak Tension (1st) (mg)	58 ± 17	16 ± 3 *	- 22 ± 21
Rate of Rise (mg/s)	17 ± 3	8 ± 2 *	- 44 ± 13
Time to Peak (seconds)	37.0 ± 2.8	36.5 ± 1.5	8 ± 15
Peak Tension (mg)	316 ± 46	227 ± 34 ***	- 23 ± 6
Tension at End of pulse (mg)	303 ± 45	217 ± 34 ***	- 24 ± 7
50 % Decay Time (seconds)	12.1 ± 2.9	14.9 ± 1.6	8 ± 9

*** P < 0.05, *** P < 0.001 compared with control response. Paired t-test.**

Figure 5-19 displays the prazosin-sensitive (PS) components that were isolated in five different ways. The PS component was identified by subtracting averaged traces in several incubation sequences as follows:

1. The PS component was revealed as the difference between the control trace and the trace following prazosin incubation – when both the α_2-ARs and P2X receptors were still activated by nerve-released transmitters (Figure 5-19a). The difference is shown in the shading and the key indicates that it is the PS component.

2. The PS component in the absence of α_2-AR activation was revealed by the difference between the trace in rauwolscine and that following rauwolscine plus prazosin (Figure 5-19b). Shown in brackets are the additional antagonists present; in this example, rauwolscine.

3. The PS component in the absence of P2X receptor activation was revealed by the difference between the trace in suramin and that following suramin plus prazosin (Figure 5-19c). Shown in brackets are the additional antagonists present; in this example, suramin.

4. When the arteries were incubated in both rauwolscine and suramin, so that neither the α_2-ARs nor the P2X receptors were activated, the PS component was revealed

(Figure 5-19d). Shown in brackets are the additional antagonists present and in the order the tissues were incubated; in this example, rauwolscine plus suramin.

5. When the arteries were incubated in both suramin and rauwolscine, so that neither the P2X receptors nor the α_2-ARs were activated, the PS component was revealed (Figure 5-19e). Shown in brackets are the additional antagonists present and in the order the tissues were incubated; in this example, suramin plus rauwolscine.

The trapezoidal methods for calculating the area under the curve was used to determine the shaded areas which were taken to represent the total magnitude of the response due to activation of the α_1-ARs. The values calculated are represented as a percentage of the control response (Figure 5-20; Table 5-14). The distal tail artery results produced the same significant differences as those in the proximal segments (Table 5-15).

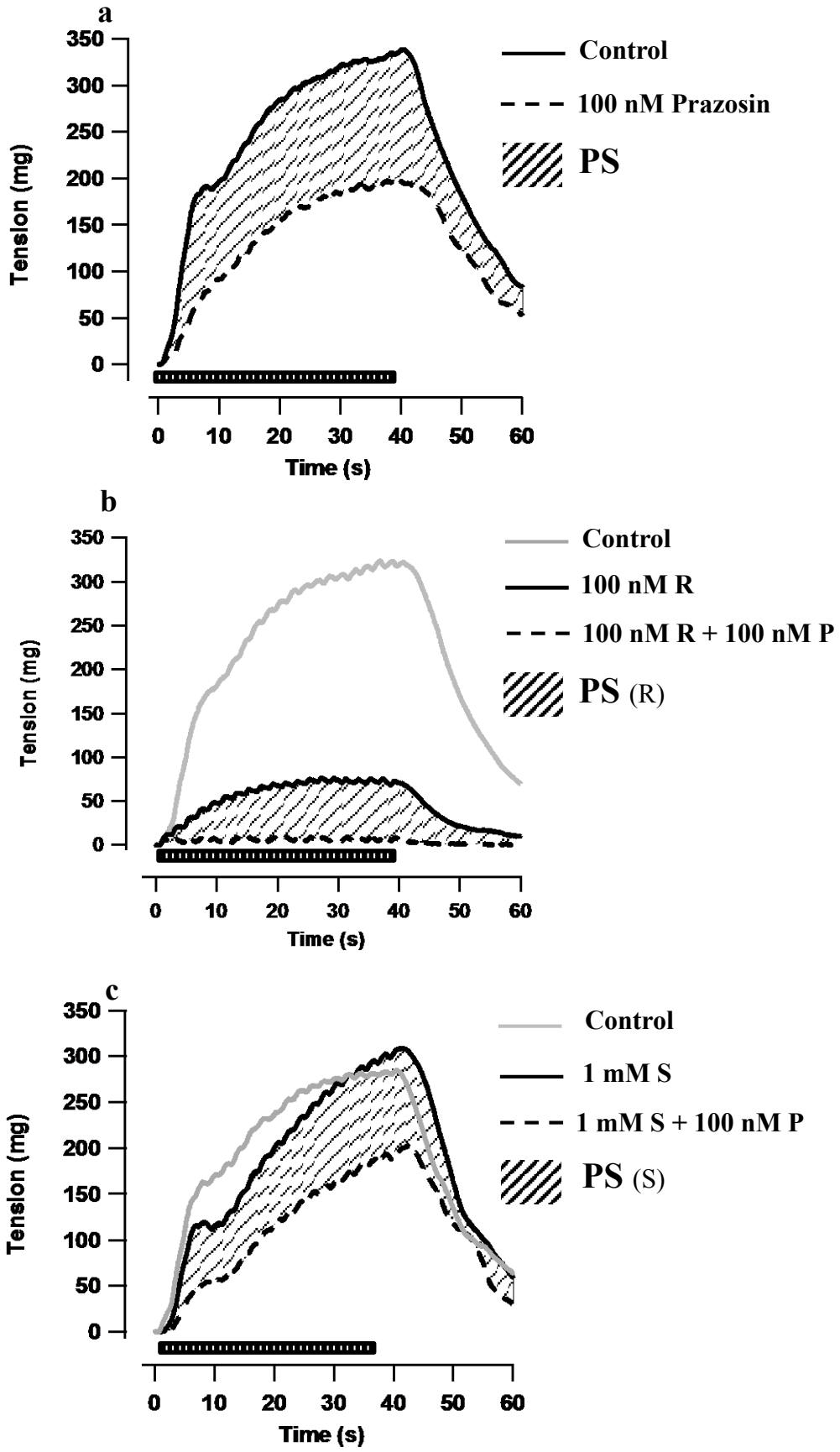

Figure 5-19: Traces showing the revealed prazosin sensitive (PS) components isolated in five different ways (a-e).

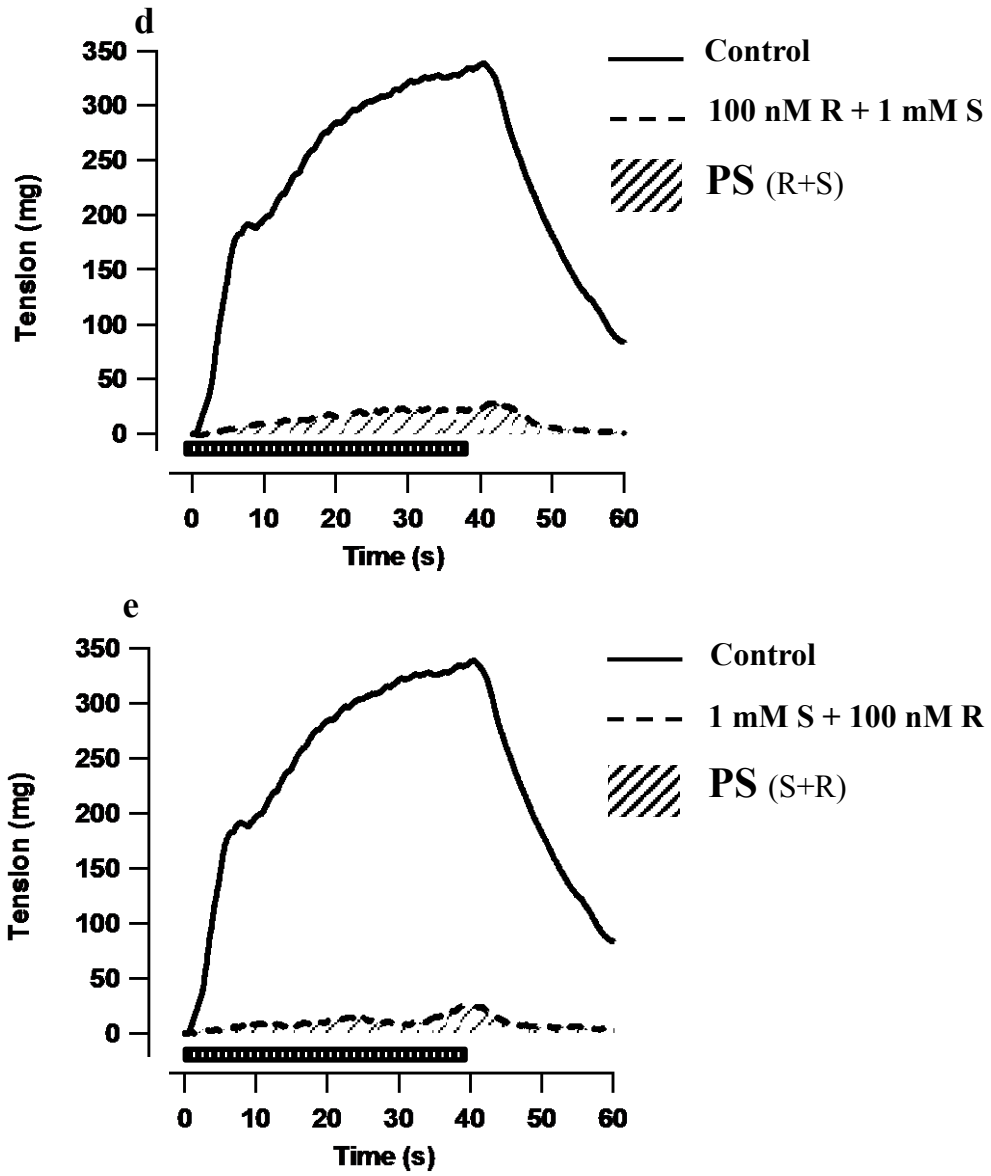

Figure 5-19: Traces showing the revealed prazosin sensitive (PS) components isolated in five different ways – (a) shows the PS component when the α_2-ARs and P2X receptors are active; (b) shows the PS component when the α_2-ARs are blocked; (c) shows the PS component when the P2X receptors are blocked; (d) shows the PS component when the α_2-ARs and P2X receptors are blocked; (e) shows the PS component when the P2X receptors and α_2-ARs are blocked.

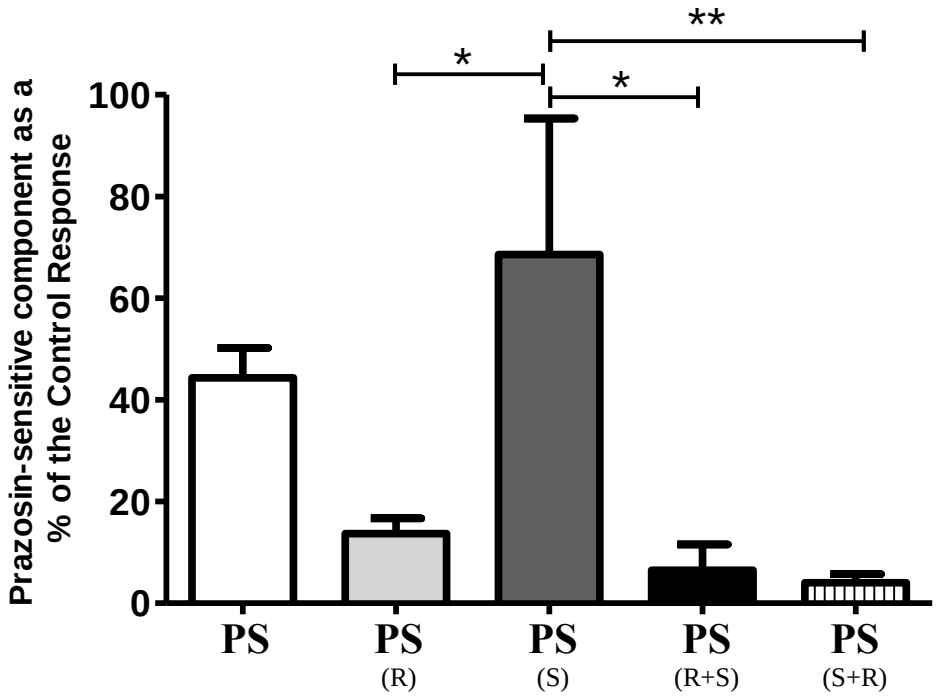

Figure 5-20: WT Proximal mouse tail – the prazosin-sensitive component at 0.5 Hz when the P2X receptors and α_2-ARs are functional (white) (n=13), α_2-ARs are blocked (light grey) (n=8), P2X receptors blocked (dark grey) (n=7), the α_2-ARs and P2X receptors are blocked (black) (n=6), P2X receptors and α_2-ARs are blocked (striped) (n=7).

*** P < 0.05; ** P < 0.01 compared with PS component when the P2X receptors are blocked. One way ANOVA with Bonferonni's post-test.**

Table 5-14: WT Proximal mouse tail artery – the prazosin-sensitive component as a % of control area under the curves. Data taken from Figures 5-20 and 5-22.

	Prazosin-sensitive component as a % of the Control Response	
	0.5 Hz	**8 Hz**
PS	44 ± 6	47 ± 3.6
PS (R)	14 ± 3 *	38 ± 7
PS (S)	69 ± 27	99 ± 31
PS (R+S)	7 ± 5 *	20 ± 9 **
PS (S+R)	4 ± 2 **	24 ± 13 **

*** P < 0.05; ** P < 0.01 compared with the PS component when the P2X receptors are blocked. One way ANOVA with Bonferonni's post-test.**

Table 5-15: WT Distal mouse tail artery – the prazosin-sensitive component as a % of control area under the curves

	Prazosin-sensitive component as a % of the Control Response	
	0.5 Hz	**8 Hz**
PS	31 ± 4 ***	38 ± 7 ***
PS (R)	31 ± 6 ***	35 ± 3 ***
PS (S)	112 ± 16	118 ± 24
PS (R+S)	22 ± 13 ***	38 ± 7 **
PS (S+R)	11 ± 4 ***	38 ± 7 ***

**** P < 0.01; *** P < 0.001 compared with the PS component when the P2X receptors are blocked. One way ANOVA with Bonferonni's post-test.**

5.3.2.2 Revealing the α_1-ARs role in the response to sympathetic nerve stimulation at 8 Hz.

At 8 Hz, the response to EFS following blockade of α_1-ARs results in reduced peak tensions, and the tension recorded at the end of the stimulation with the time taken to reach both peaks occurring later (Figure 5-21; Table 5-16). This was true also for the distal tail artery responses (Table 5-17).

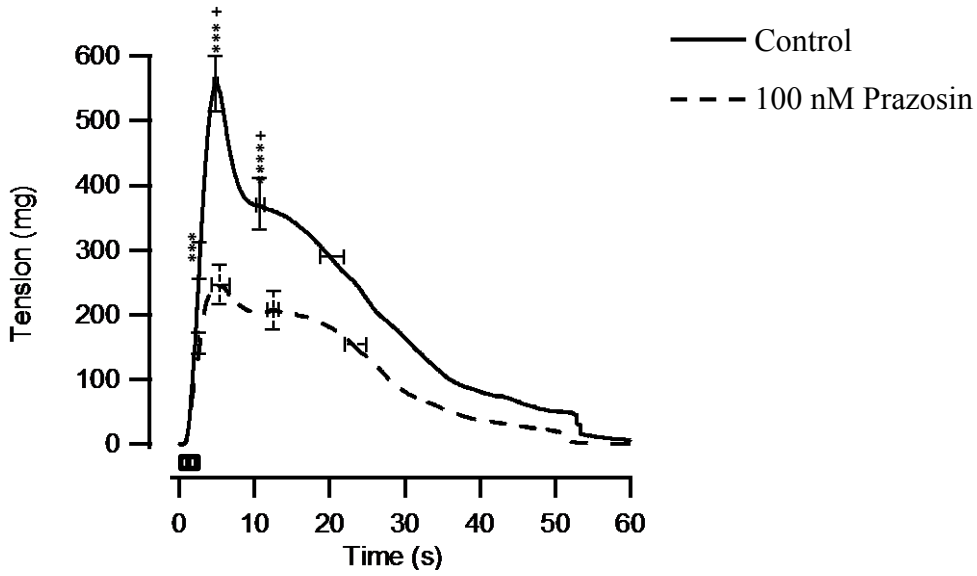

Figure 5-21: WT Proximal mouse tail artery response to nerve stimulation at 8 Hz in control vessels and in the presence of the α_1-AR antagonist prazosin (100 nM) (n = 12).

***** P < 0.001 compared with control response. Paired t-test.**

+ P < 0.05 compared with control time. Paired t-test.

Table 5-16: Proximal mouse tail artery response to nerve stimulation in control and prazosin (100 nM) incubated vessels at 8 Hz.

Proximal 8 Hz	Contractile Response (average ± S.E.M)		
	Control	100 nM Prazosin (P) (n = 12)	% change following P incubation
Tension at End of pulse (mg)	240 ± 32	135 ± 21 ***	- 35 ± 8
Time to Peak (seconds)	4.9 ± 0.1	7.7 ± 1.3 +	29 ± 17
Peak Tension (mg)	563 ± 51	267 ± 34 ***	- 53 ± 5
Rate of Rise (mg/s)	117 ± 11	42 ± 6 ***	- 65 ± 4
Time to Peak (2^{nd}) (seconds)	11.2 ± 0.5	13.4 ± 0.7 +	11 ± 5
Peak Tension (2^{nd}) (mg)	369 ± 48	212 ± 34 ***	- 40 ± 7
50 % Decay Time (seconds)	15.4 ± 1.8	15.4 ± 1.6	4 ± 9

***** P < 0.001 compared with control response.**

Paired t-test. + P < 0.05 compared with control time. Paired t-test.

Table 5-17: Distal mouse tail artery response to nerve stimulation in control and prazosin (100 nM) incubated vessels at 8 Hz.

Distal 8 Hz	Contractile Response (average ± S.E.M)		
	Control	100 nM Prazosin (P) (n = 12)	% change following P incubation
Tension at End of pulse (mg)	183 ± 14	93 ± 16 **	- 52 ± 6
Time to Peak (seconds)	4.9 ± 0.1	7.4 ± 1.0 +	38 ± 10
Peak Tension (mg)	494 ± 29	269 ± 35 ***	- 39 ± 7
Rate of Rise (mg/s)	85 ± 9	44 ± 7 ***	- 52 ± 5
Time to Peak (2^{nd}) (seconds)	12.3 ± 0.3	15.6 ± 0.6 +++	26 ± 6
Peak Tension (2^{nd}) (mg)	285 ± 22	217 ± 35 **	- 29 ± 6
50 % Decay Time (seconds)	13.3 ± 1.2	16.6 ± 1.9	4 ± 8

**** P < 0.01, *** P < 0.001 compared with control response. Paired t-test.**

+ P < 0.05, +++ P < 0.001 compared with control time. Paired t-test.

The influence of the α_1-ARs on the response to nerve stimulation depends on the antagonist incubation sequence (Figure 5-22). The prazosin-sensitive component was greatest when prazosin was incubated following P2X receptor blockade; when the α_2-ARs are still functional. The prazosin-sensitive component was smaller following blockade of the α_2-ARs and the P2X receptors (Table 5-14). Distally, the prazosin-sensitive components were similar (Table 5-15).

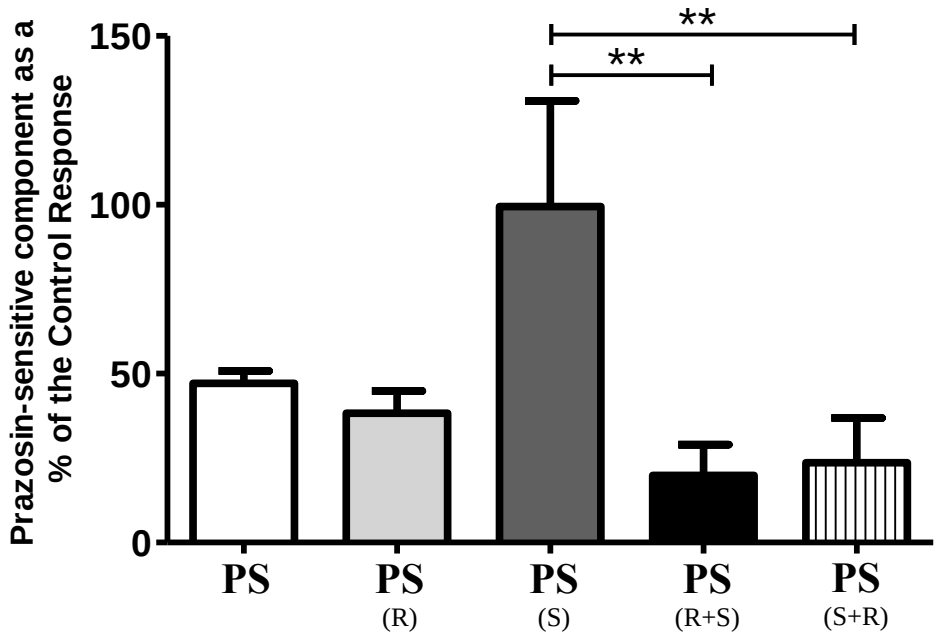

Figure 5-22: WT Proximal mouse tail – the prazosin-sensitive component at 8 Hz when the P2X receptors and α_2-ARs are functional (white) (n=13), α_2-ARs are blocked (light grey) (n=8), P2X receptors blocked (dark grey) (n=7), the α_2-ARs and P2X receptors are blocked (black) (n=6), P2X receptors and α_2-ARs are blocked (striped) (n=7).

**** P < 0.01 compared with the PS component when the P2X receptors are blocked. One way ANOVA with Bonferonni's post-test.**

5.3.2.3 Revealing the α_2-ARs role in the response to sympathetic nerve stimulation at 0.5 Hz.

Following incubation with 100 nM rauwolscine (α_2-AR antagonist), the response to stimulation of the sympathetic nerves was reduced (Figure 5-23; Table 5-18). Distally, the peak tension, the tension at the end of the stimulation period and the time to reach the first peak were all reduced (Table 5-19).

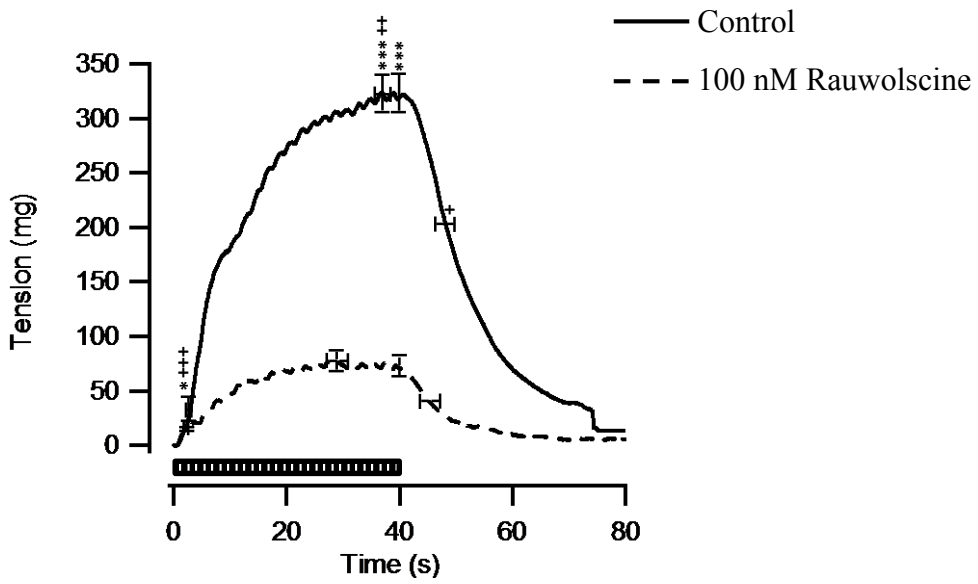

Figure 5-23: WT Proximal mouse tail artery response to nerve stimulation at 0.5 Hz in control vessels and in the presence of the α_2-AR antagonist rauwolscine (100 nM) (n = 13).

*** P < 0.05; *** P < 0.001 compared with control response. Paired t-test.**

+ P < 0.05; ++ P < 0.01; +++ P < 0.001 compared with control time. Paired t-test.

Table 5-18: WT Proximal mouse tail artery response to nerve stimulation in control and 100 nM rauwolscine incubated vessels at 0.5 Hz.

Proximal 0.5 Hz	Contractile Response (average ± S.E.M)		
	Control	100 nM Rauwolscine (R) (n = 13)	% change following R incubation
Time to Peak (1st) (seconds)	3.1 ± 0.3	1.6 ± 0.1 +++	- 42 ± 5
Peak Tension (1st) (mg)	42 ± 12	12 ± 1 *	- 56 ± 6
Rate of Rise (mg/s)	12 ± 2	8 ± 1 *	- 24 ± 10
Time to Peak (seconds)	37.6 ± 1.4	27.4 ± 2.1 ++	- 26 ± 6
Peak Tension (mg)	328 ± 20	81 ± 11 ***	- 75 ± 3
Tension at End of pulse (mg)	317 ± 20	74 ± 11 ***	- 77 ± 3
50 % Decay Time (seconds)	12.6 ± 1.8	17.3 ± 1.9 +	19 ± 10

*** P < 0.05; *** P < 0.001 compared with control response. Paired t-test.**

+ P < 0.05; ++ P < 0.01; +++ P < 0.001 compared with control time. Paired t-test.

Table 5-19: WT Distal mouse tail artery response to nerve stimulation in control and rauwolscine (100 nM) incubated vessels at 0.5 Hz.

Distal 0.5 Hz	Contractile Response (average ± S.E.M)		
	Control	100 nM Rauwolscine (R) (n = 13)	% change following R incubation
Time to Peak (1st) (seconds)	2.5 ± 0.2	2.1 ± 0.1 ++	- 17 ± 4
Peak Tension (1st) (mg)	52 ± 22	21 ± 3	- 35 ± 9
Rate of Rise (mg/s)	17 ± 5	10 ± 1	- 25 ± 10
Time to Peak (seconds)	36 ± 3.3	35.1 ± 1.1	1 ± 10
Peak Tension (mg)	324 ± 40	111 ± 17 ***	- 64 ± 4
Tension at End of pulse (mg)	307 ± 40	103 ± 16 ***	- 64 ± 4
50 % Decay Time (seconds)	18.3 ± 2.6	10.6 ± 1.3 +	- 32.3 ± 9.0

***** P < 0.001 compared with control response. Paired t-test.**

+ P < 0.05; ++ P < 0.01 compared with control time. Paired t-test.

The prazosin-sensitive components that were revealed differed depending on whether the α_2-ARs and P2X receptors were blocked or active. This result occurred both proximally and distally (Figure 5-24; Table 5-20 and 5-21).

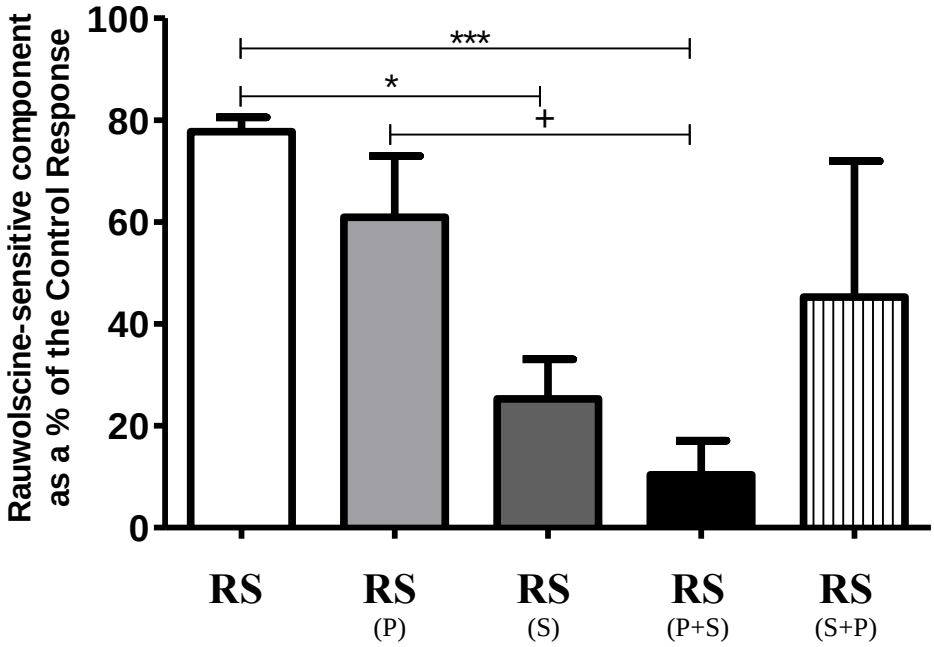

Figure 5-24: WT Proximal mouse tail – the rauwolscine-sensitive component at 0.5 Hz when the P2X receptors and α_1-ARs are functional (white) (n=14), α_1-ARs are blocked (light grey) (n=7), P2X receptors are blocked (dark grey) (n=7), when α_1-ARs and P2X receptors are blocked (black) (n=6), P2X receptors and α_1-ARs are blocked (striped) (n=7).

*** P < 0.05, *** P < 0.001 compared with the RS component when the α_1-ARs and the P2X receptors are functional. One way ANOVA with Bonferonni's post-test.**

+ P < 0.05 compared with the RS component when the α_1-ARs and P2X receptors are blocked. One way ANOVA with Bonferonni's post-test.

Table 5-20: WT Proximal mouse tail artery - revealing the rauwolscine-sensitive component as a % of control area under the curves. Data taken from Figures 5-24 and 5-26.

	Rauwolscine-sensitive component as a % of the Control Response	
	0.5 Hz	**8 Hz**
RS	77 ± 3	48 ± 6
RS (P)	61 ± 12	49 ± 7
RS (S)	25 ± 8 *	16 ± 5
RS (P+S)	10 ± 7 *** +	14 ± 5
RS (S+P)	45 ± 27	46 ± 21

+ P < 0.05 compared with the RS component when the α_1-ARs are blocked. One way ANOVA with Bonferonni's post-test.

*** P < 0.05; *** P < 0.001 compared with the RS component when the P2X receptors and α_1-ARs are functional. One way ANOVA with Bonferonni's post-test.**

Table 5-21: WT Distal mouse tail artery - revealing the rauwolscine-sensitive component as a % of control area under the curves.

	Rauwolscine-sensitive component as a % of the Control Response	
	0.5 Hz	**8 Hz**
RS	65 ± 4	46 ± 5 ***
RS (P)	70 ± 5	65 ± 3 *
RS (S)	86 ± 17 +	62 ± 7 *
RS (P+S)	40 ± 9	48 ± 11 **
RS (S+P)	80 ± 13	126 ± 30

+ P < 0.05 compared with the RS component when the α_1-ARs and P2X receptors are blocked (in that order). One way ANOVA with Bonferonni's post-test.

*** P < 0.05; ** P < 0.01; *** P < 0.001 compared with the RS component when the P2X receptors and α_1-ARs are blocked (in that order). One way ANOVA with Bonferonni's post-test.**

5.3.2.4 Revealing the α_2-ARs role in the response to sympathetic nerve stimulation at 8 Hz.

Following incubation with 100 nM rauwolscine, the proximal response to stimulation of the sympathetic nerves was reduced (Figure 5-25; Table 5-22). The distal response was similar; however the time to reach the peak response was statistically reduced by rauwolscine whereas the time taken to reach the second peak was not (Table 5-23).

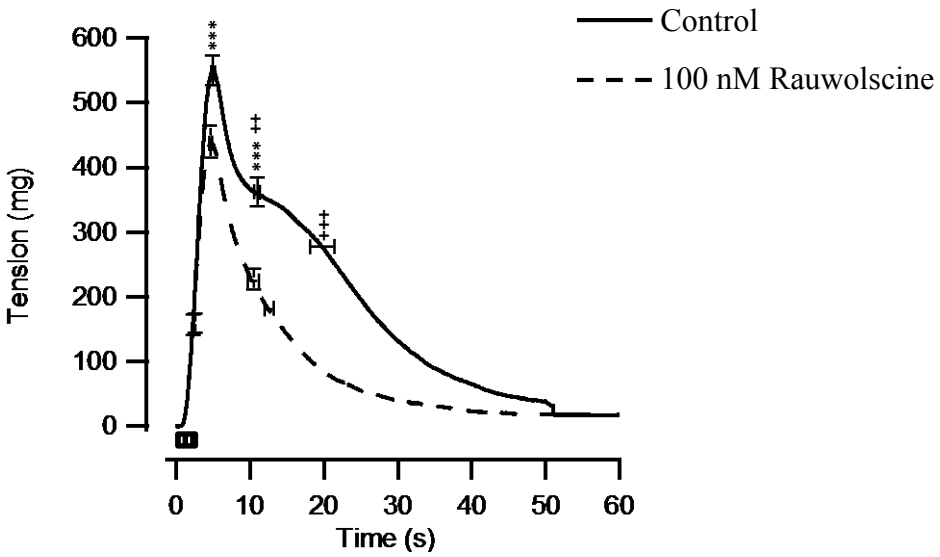

Figure 5-25: WT Proximal mouse tail artery response to nerve stimulation at 8 Hz in control vessels and in the presence of the α_2-AR antagonist rauwolscine (100 nM) (n = 13).

***** P < 0.001 compared with control response. Paired t-test.**

++ P < 0.01; +++ P < 0.001 compared with control time. Paired t-test.

Table 5-22: WT Proximal mouse tail artery response to nerve stimulation in control and 100 nM rauwolscine incubated vessels at 8 Hz.

Proximal 8 Hz	Contractile Response (average ± S.E.M)		
	Control	100 nM Rauwolscine (R) (n = 13)	% change following R incubation
Tension at End of pulse (mg)	189 ± 18	194 ± 17	2 ± 11
Time to Peak (seconds)	5.0 ± 0.1	4.6 ± 0.1	- 7 ± 4
Peak Tension (mg)	554 ± 27	446 ± 30 ***	- 19 ± 4
Rate of Rise (mg/s)	112 ± 6	97 ± 5.8 *	- 13 ± 5
Time to Peak (2nd) (seconds)	11.4 ± 0.4	13.9 ± 0.8 ++	16 ± 4
Peak Tension (2nd) (mg)	352 ± 25	149 ± 17 ***	- 56 ± 6
50 % Decay Time (seconds)	12.5 ± 1.9	5.8 ± 0.6 +++	- 49 ± 8

*** P < 0.05, *** P < 0.001 compared with control response. Paired t-test.**

++ P < 0.01; +++ P < 0.001 compared with control time. Paired t-test.

Table 5-23: WT Distal mouse tail artery response to nerve stimulation in control and 100 nM rauwolscine incubated vessels at 8 Hz.

Distal 8 Hz	Contractile Response (average ± S.E.M)		
	Control	100 nM Rauwolscine (R) (n = 14)	% change following R incubation
Tension at End of pulse (mg)	232 ± 24	229 ± 21	1 ± 11
Time to Peak (seconds)	4.9 ± 0.1	4.5 ± 0.1 ++	- 10 ± 2
Peak Tension (mg)	622 ± 32	483 ± 34 ***	- 22 ± 4
Rate of Rise (mg/s)	127 ± 7	109 ± 8 *	- 13 ± 5
Time to Peak (2nd) (seconds)	12.3 ± 0.5	12.9 ± 0.4	5 ± 3
Peak Tension (2nd) (mg)	317 ± 32	147 ± 19 ***	- 52 ± 5
50 % Decay Time (seconds)	12.9 ± 2.2	3.6 ± 0.3 +++	- 53 ± 8

*** P < 0.05, *** P < 0.001 compared with control response. Paired t-test.**

++ P < 0.01; +++ P < 0.001 compared with control time. Paired t-test.

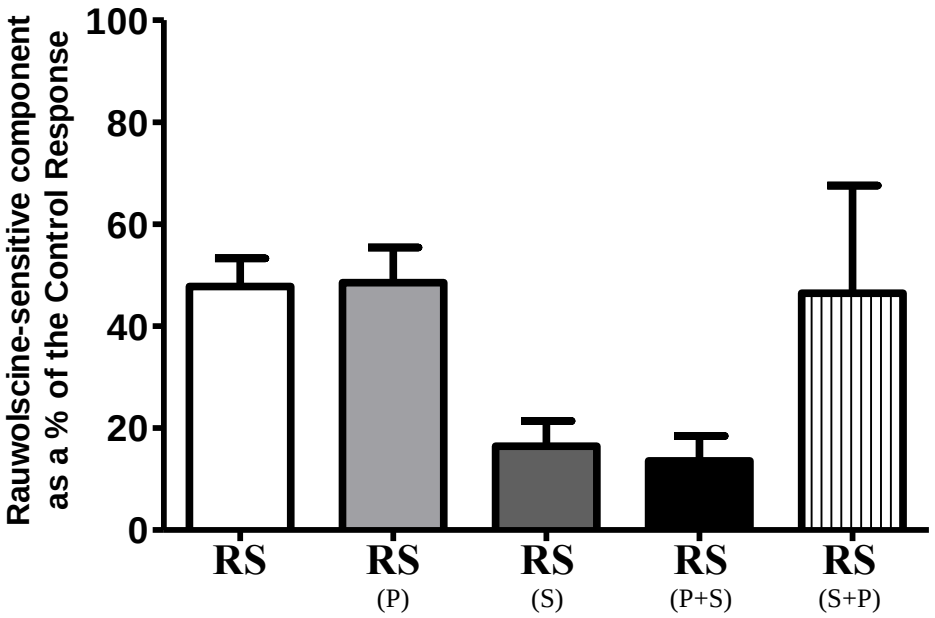

Figure 5-26: WT Proximal mouse tail – the rauwolscine-sensitive component at 8 Hz when the P2X receptors and α_1-ARs are functional (white) (n=14), α_1-ARs are blocked (light grey) (n=7), P2X receptors are blocked (dark grey) (n=7), when α_1-ARs and P2X receptors are blocked (black) (n=6), P2X receptors and α_1-ARs are blocked (striped) (n=7).

Figure 5-26 shows the individual proximal rauwolscine sensitive components (Figure 5-25; Table 5-20) and the distal rauwolscine sensitive components are shown in Figure 5-27 as these were different to the proximal results (Table 5-21; Figure 5-27).

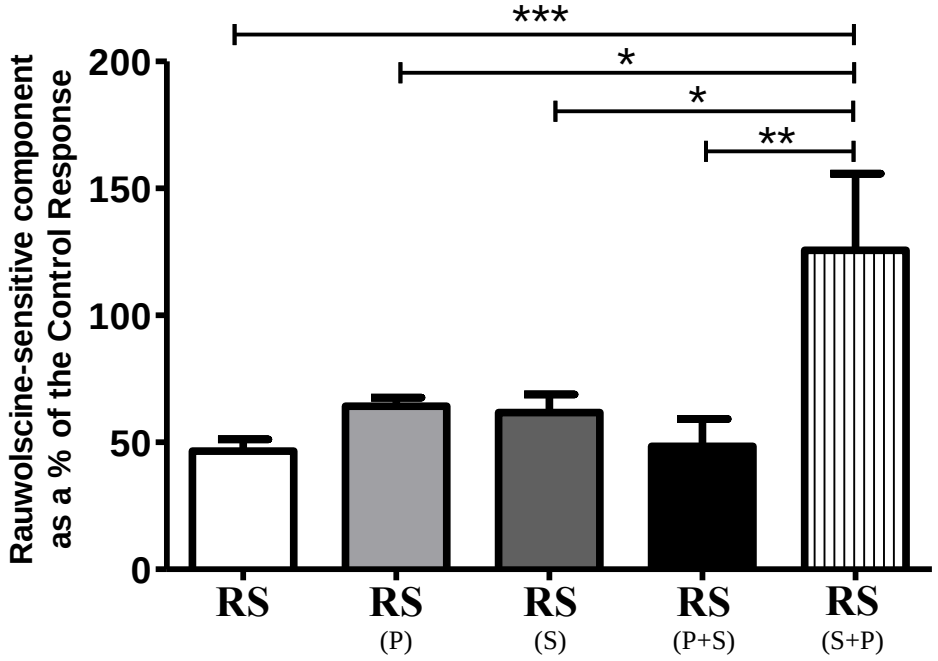

Figure 5-27: WT Distal mouse tail – the rauwolscine-sensitive component at 8 Hz when the P2X receptors and α_1-ARs are functional (white) (n=14), α_1-ARs are blocked (light grey) (n=6), P2X receptors are blocked (dark grey) (n=6), when α_1-ARs and P2X receptors are blocked (black) (n=7), P2X receptors and α_1-ARs are blocked (striped) (n=7).

*** P < 0.05; ** P < 0.01; *** P < 0.001 compared with the RS component when the P2X receptors and α_1-ARs are blocked. One way ANOVA with Bonferonni's post-test.**

5.3.2.5 Revealing the P2X receptor role in the response to sympathetic nerve stimulation at 0.5 Hz.

Blockade of the P2X receptors proximally with 1 mM suramin results in a prolonged time to reach the 1st peak (Figure 5-28; Table 5-24). Distally, the time to reach the 1st peak is not significantly affected by suramin incubation. However, the rate of rise and the time to reach the peak response are both significantly altered (Table 5-25).

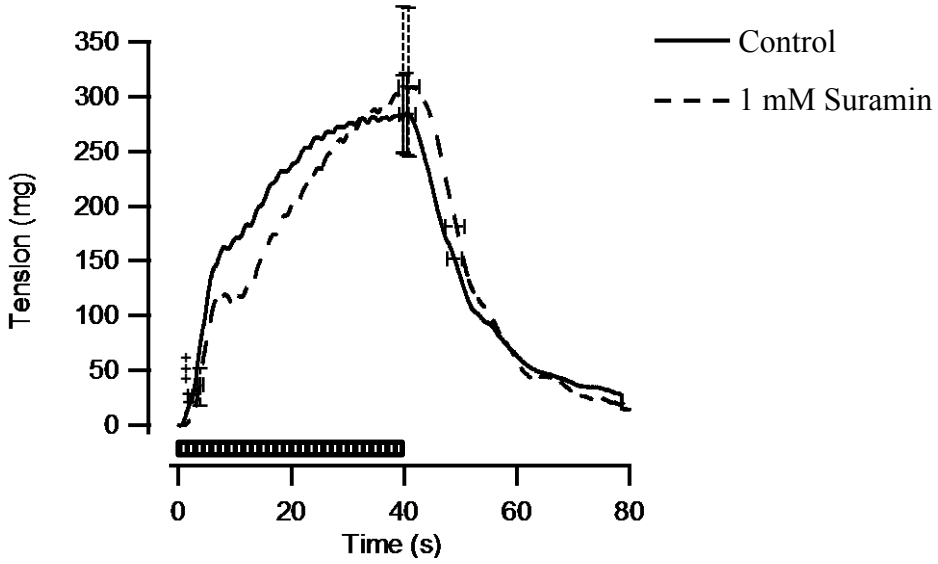

Figure 5-28: WT Proximal mouse tail artery response to nerve stimulation at 0.5 Hz in control vessels and in the presence of the P2X receptor antagonist suramin (1 mM) (n = 13).

+++ P < 0.001 compared with control time. Paired t-test.

Table 5-24: WT Proximal mouse tail artery response to nerve stimulation in control and suramin (1 mM) incubated vessels at 0.5 Hz.

Proximal 0.5 Hz	Contractile Response (average ± S.E.M)		
	Control	1 mM Suramin (S) (n = 13)	% change following S incubation
Time to Peak (1st) (seconds)	2.1 ± 0.1	4.4 ± 0.3 +++	50 ± 6
Peak Tension (1st) (mg)	21 ± 4	59 ± 20	13 ± 24
Rate of Rise (mg/s)	10 ± 2	13 ± 4	- 13 ± 17
Time to Peak (seconds)	36.2 ± 1.4	28.5 ± 1.9	9 ± 6
Peak Tension (mg)	295 ± 44	308 ± 81	- 38 ± 17
Tension at End of pulse (mg)	285 ± 43	293 ± 80	- 40 ± 17
50 % Decay Time (seconds)	10.9 ± 1.3	10.5 ± 1.8	- 14 ± 13

+++ P < 0.001 compared with control time. Paired t-test.

Table 5-25: WT Distal mouse tail artery response to nerve stimulation in control and suramin (1 mM) incubated vessels at 0.5 Hz.

Distal 0.5 Hz	Contractile Response (average ± S.E.M)		
	Control	1 mM Suramin (S) (n = 13)	% change following S incubation
Time to Peak (1st) (seconds)	2.3 ± 0.1	3.0 ± 0.4	23 ± 12
Peak Tension (1st) (mg)	34 ± 7	29 ± 9	- 8 ± 26
Rate of Rise (mg/s)	14 ± 3	8 ± 2 **	- 43 ± 12
Time to Peak (seconds)	33 ± 2.3	37.0 ± 2.7 ++	3 ± 9
Peak Tension (mg)	270 ± 42	216 ± 42	- 8 ± 13
Tension at End of pulse (mg)	260 ± 41	203 ± 39	- 6 ± 14
50 % Decay Time (seconds)	11.8 ± 2.2	14.2 ± 2.9	- 21 ± 9

**** P < 0.01 compared with control response. Paired t-test.**

++ P < 0.01 compared with control time. Paired t-test.

The suramin-sensitive component of the response differed depending on whether suramin was incubated alone or following incubation with one or more antagonists (Figure 5-29; Table 5-26 and 5-27).

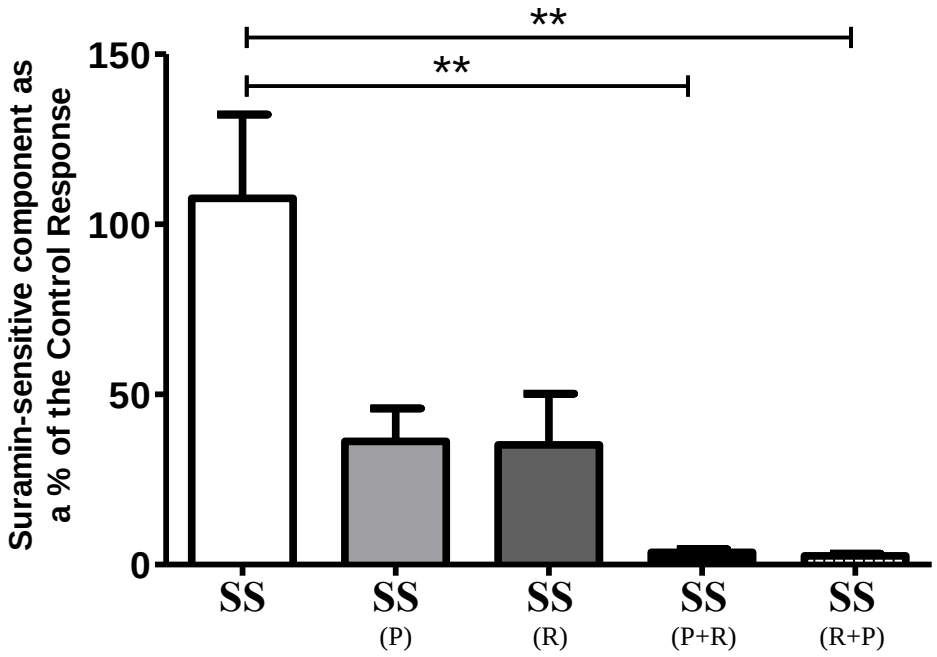

Figure 5-29: WT Proximal mouse tail – the suramin-sensitive component at 0.5 Hz when the α_1- and α_2-ARs are functional (white) (n=14), α_1-ARs are blocked (light grey) (n=6), α_2-ARs are blocked (dark grey) (n=6) α_1- and α_2-ARs are blocked (black) (n=7), α_2- and α_1-ARs are blocked (striped) (n=8).

**** P < 0.01 compared with SS component when the α_1- and α_2-ARs are functional. One way ANOVA with Bonferonni's post-test.**

Table 5-26: WT Proximal mouse tail artery response - the suramin-sensitive (SS) component as a % of control area under the curves. Data taken from Figures 5-29 and 5-31.

	Suramin-sensitive component as a % of the Control Response	
	0.5 Hz	**8 Hz**
SS	108 ± 25	54 ± 9
SS (P)	36 ± 10	31 ± 8
SS (R)	35 ± 15	37 ± 11
SS (P+R)	4 ± 1 **	10 ± 3 *
SS (R+P)	3 ± 1 **	7 ± 1 *

*** P < 0.05; ** P < 0.01 compared with area under the curve when the α_1- and α_2-ARs are functional. One way ANOVA with Bonferonni's post-test.**

Table 5-27: WT Distal mouse tail artery response - the suramin-sensitive (SS) component as a % of control area under the curves.

	Suramin-sensitive component as a % of the Control Response	
	0.5 Hz	**8 Hz**
SS	60 ± 16	35 ± 7 *
SS (P)	48 ± 16	36 ± 6 *
SS (R)	15 ± 2	20 ± 3
SS (P+R)	45 ± 25	4 ± 1
SS (R+P)	11 ± 2	17 ± 4

*** P < 0.05 compared with area under the curve when the α_1- and α_2-ARs are blocked. One way ANOVA with Bonferonni's post-test.**

5.3.2.6 Revealing the P2X receptor role in the response to sympathetic nerve stimulation at 8 Hz.

At 8 Hz, the response following block of the P2X receptors is more greatly affected than the response at 0.5 Hz. In both proximal and distal segments, the peak amplitude and the tension at the end of the stimulation period were both significantly reduced. These changes led to a

reduction in the rate of rise. The time taken to reach the 2nd peak was prolonged following suramin incubation. (Figure 5-30; Table 5-28 and 5-29).

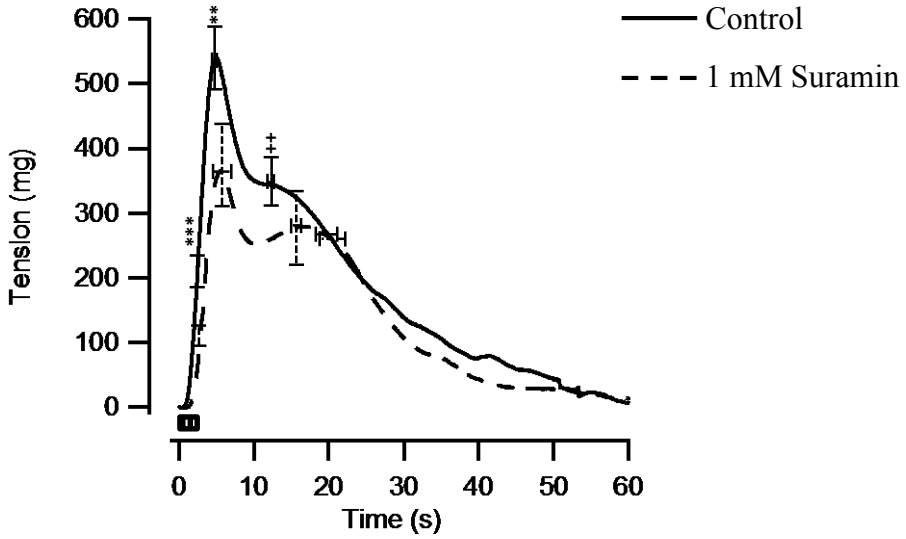

Figure 5-30: WT Proximal mouse tail artery response to nerve stimulation at 8 Hz in control vessels and in the presence of the P2X receptor antagonist suramin (1 mM) (n = 13).

**** P < 0.01, *** P < 0.001 compared with control response. Paired t-test.**

++ P < 0.01 compared with control time. Paired t-test.

Table 5-28: WT Proximal mouse tail artery response to nerve stimulation in control and suramin (1 mM) incubated vessels at 8 Hz.

Proximal 8 Hz	Contractile Response (average ± S.E.M)		
	Control	1 mM Suramin (S) (n = 13)	% change following S incubation
Tension at End of pulse (mg)	208 ± 28	62 ± 18 ***	- 79 ± 7
Time to Peak (seconds)	5.1 ± 0.2	7.1 ± 1.3	12 ± 10
Peak Tension (mg)	554 ± 58	376 ± 76 **	- 49 ± 11
Rate of Rise (mg/s)	110 ± 12	59 ± 13 ***	- 52 ± 8
Time to Peak (2nd) (seconds)	12.0 ± 0.4	15.0 ± 0.7 ++	12 ± 6
Peak Tension (2nd) (mg)	350 ± 45	280 ± 68	- 44 ± 17
50 % Decay Time (seconds)	13.4 ± 1.7	13.0 ± 1.9	- 3 ± 16

**** P < 0.01, *** P < 0.001 compared with control response. Paired t-test.**

++ P < 0.01 compared with control time. Paired t-test.

Table 5-29: WT Distal mouse tail artery response to nerve stimulation in control and suramin (1 mM) incubated vessels at 8 Hz.

Distal 8 Hz	Contractile Response (average ± S.E.M)		
	Control	1 mM Suramin (S) (n = 13)	% change following S incubation
Tension at End of pulse (mg)	164 ± 24	45 ± 12 ***	- 58 ± 9
Time to Peak (seconds)	4.8 ± 0.1	7.2 ± 1.3	19 ± 10
Peak Tension (mg)	410 ± 50	272 ± 44 **	- 30 ± 8
Rate of Rise (mg/s)	86 ± 10	46 ± 9 ***	- 48 ± 8
Time to Peak (2^{nd}) (seconds)	11.9 ± 0.6	15.7 ± 0.7 +++	32 ± 7
Peak Tension (2^{nd}) (mg)	246 ± 37	204 ± 36	- 9 ± 15
50 % Decay Time (seconds)	12.2 ± 2.0	15.8 ± 2.6	10 ± 13

**** P < 0.01, *** P < 0.001 compared with control response. Paired t-test.**

+++ P < 0.001 compared with control time. Paired t-test.

The suramin-sensitive components were shown to have similar areas at 8 Hz in both proximal and distal segments (Figure 5-31, Tables 5-26 and 5-27).

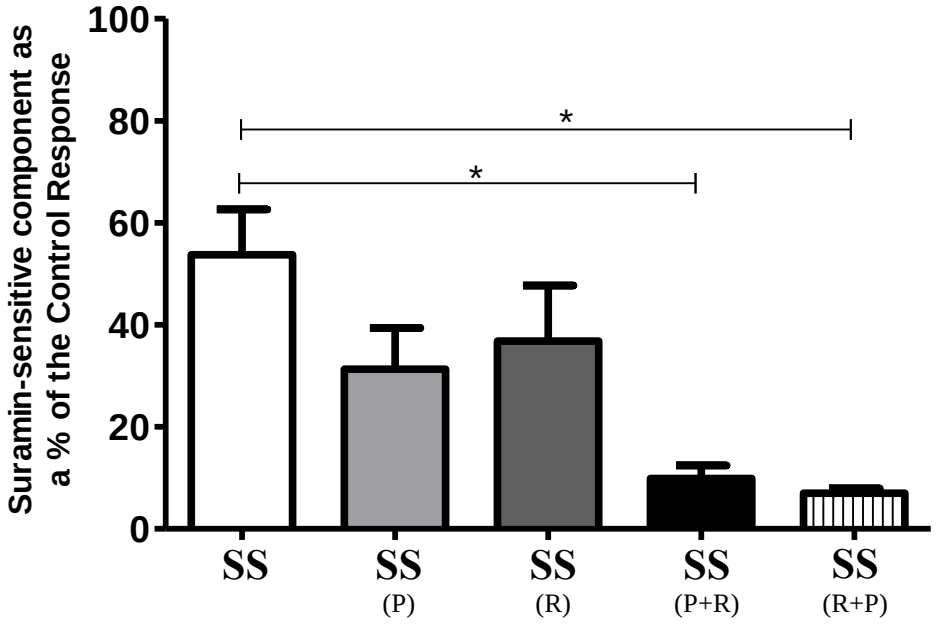

Figure 5-31: WT Proximal mouse tail – the suramin-sensitive component at 8 Hz when the α_1- and α_2-ARs are functional (white) (n=14), α_1-ARs are blocked (light grey) (n=6), α_2-ARs are blocked (dark grey) (n=6) α_1- and α_2-ARs are blocked (black) (n=7), α_2- and α_1-ARs are blocked (striped) (n=8).

*** P < 0.05 compared with the SS component when the α_1- and α_2-ARs are functional. One way ANOVA with Bonferonni's post-test.**

5.4 Discussion

The present study was set out to determine the post-junctional receptors involved in mediating the response to nerve stimulation in WT mesenteric and tail arteries.

5.4.1 Mouse Mesenteric Arteries

Antagonists for α_1-, α_2-ARs and P2X receptors abolished the response to nerve stimulation at 2 Hz and 8 Hz. Therefore, the receptors involved in mediating the response to nerve stimulation may involve the α_1-, α_2-ARs and P2X receptors. This suggests a release of NA and ATP from the nerve terminals which has been shown by others in the rat mesenteric arteries. Previous studies have shown activation of post-junctional α_1-ARs and P2X receptors to be responsible for vasoconstriction, with blockade of pre-junctional α_2-ARs enhancing the response (Angus et al., 1988; Gitterman and Evans, 2001). The adrenergic nerves have also been shown to be involved in nerve stimulation in the mouse mesenteric arteries (Fujiwara et al., 2012). Presently, stimulation of the mouse mesenteric arteries produced frequency dependent responses. Therefore the response at 2 Hz was smaller than the response at 8 Hz. This is similar to the nerve responses in the rat mesenteric arteries (Gitterman and Evans, 2001). In these arteries, responses at low frequency were dominated by ATP (non-adrenergic) and at high frequencies are dominated by adrenergic receptor activation (Sjoblom-Widfeldt et al., 1990).

By employing selective antagonists for the α_1-, α_2-ARs and P2X receptors, it was possible to isolate each component of the response to nerve stimulation. A novel way of analysing the results, as described in the General Methods and Results section, allowed each component to be viewed whilst the other receptors were either active or blocked. This therefore provided information on whether the receptors can produce a response independently or whether they rely on the other receptors. No evidence of post-junctional interactions in the mouse mesenteric arteries have been published. However, in the rat, it has

been suggested that NA and ATP can produce a synergistic post-junctional response (Brock et al., 2006).

Various points during the response to nerve stimulation were studied to determine the roles each receptor played in the response. The results from incubation with a single antagonist were compared to the control responses and significant differences calculated. Firstly, the time taken to reach the peak tension provides information on which receptors are involved in initiating the contraction and ensuring it reached the peak. Secondly, the tension at the peak demonstrates which receptors are involved in producing the peak amplitude. Thirdly, the tension at the end of the stimulation period indicates which receptors are active at the end of the stimulation. Finally, the time for the peak amplitude to reduce by 50 % reveals the receptors still active or the signalling processes when there is no longer a stimulus, and so provides information on the active receptors that prolong the response. Combined, these points provide valuable information concerning the whole response. Furthermore, where the peak tensions are similar, the rate of rise could detect differences in the generation of the response.

5.4.2 α_1-AR role in Mouse Mesenteric Arteries

Of the three antagonists utilised, prazosin had the greatest effect on reducing the response to nerve stimulation at both frequencies. This highlights the role of the α_1-ARs in vasoconstriction which has been shown in the rat, whereby continuous stimulation of the nerves can be effectively reduced by prazosin incubation (Sjoblom-Widfeldt et al., 1990). Presently, under each incubation condition, various points during the response were recorded for analysis. At 2 Hz, prazosin incubation reduced the peak tension and the tension recorded at the end of the stimulation period by 91 % ± 1 and 94 % ± 4 respectively. The remaining response was minimal, yet its time to peak response was not significantly different to the control. These results show the α_1-ARs to be the main receptor responsible for producing the amplitude of the response. At 8 Hz, prazosin incubation still reduced the peak tensions recorded but it also reduced the time taken to reach the peak tension. This response may be due to the decrease in tension; allowing a faster initial increase. However, it may reveal an inhibitory action of the α_1-ARs in prolonging the time taken to reach the peak tension.

The component analysis aimed to determine whether the α_1-ARs act independently or whether they can interact with the other receptors by isolating the prazosin-sensitive component. This component was investigated when the α_2-ARs and P2X receptors were active, when only the P2X receptors were active and when the α_2-ARs and P2X receptors were blocked. At 2 Hz, the components were similar, suggesting that the α_1-ARs do not require interaction with the other receptors at low frequency in order to produce a contraction. At 8 Hz, the α_1-AR component that remained following α_2-AR and P2X receptor blockade was significantly smaller than the component when only the P2X receptors were active. The component when the α_2-ARs and P2X receptors were active showed a similar trend. It is the loss of active P2X receptors which leads to the smaller α_1-AR component and thus suggests an interaction between these two receptors. Evidence of synergy has been reported in the rat mesenteric arteries where the reduction in nerve response following prazosin or suramin incubation was ~ 80 % and 40 – 70 % respectively (Brock et al., 2006). A value exceeding 100 % occurs when these results are combined and so the loss of one receptor impacts the remaining response.

5.4.3 α_2-AR role in Mouse Mesenteric Arteries

The role of the α_2-ARs was first recognised pre-junctionally as a mediator of neurotransmitter release before being accepted also as a post-junctional receptor, capable of producing a vasoconstriction (Docherty et al., 1979). Previous studies in the rat mesenteric arteries show α_2-ARs to be limited to a pre-junctional location and so blockade of the receptors results in potentiation of the response due to increase transmitter output (Angus et al., 1988). In the present study, stimulation at 2 Hz in the presence of rauwolscine showed a trend to increase the peak response. At 8 Hz, this potentiation of the response was significantly larger than the control thus providing evidence that pre-junctional α_2-ARs are present and activation with NA inhibits transmitter release. Interestingly, blockade of the α_2-ARs prolongs the time to peak suggesting that these receptors (most likely post-junctional) are involved in initiation of the contraction before the pre-junctional effect occurs. Furthermore, as the time taken for the peak response to decrease by 50 % was reduced, this would suggest again that post-junctional α_2-ARs are present and, when activated by NA they can prolong the response. These results suggest that there are both pre- and post-junctional α_2-ARs that are active at different times during the response. It is possible that initial NA

release following nerve stimulation acts at post-junctional α_2-ARs to initiate the contraction. Then, during the pulse duration, NA acts at pre-junctional α_2-ARs to modulate NA release. Following the end of the stimulation period, NA still present at the junction then acts at post-junctional α_2-ARs to prolong the contraction.

The potentiation of the peak response is shown clearly in the component analysis. The rauwolscine sensitive component (when the α_1-ARs and P2X receptors are active) is greater than the control response at both frequencies. This is due to increased transmitter output that can then act at post-junctional α_1ARs and P2X receptors. There is some debate over whether NA and ATP are released together in similar quantities and whether release of ATP can also be mediated by pre-junctional α_2-ARs. In the guinea pig mesenteric arteries, modulation of ATP release via pre-junctional α_2-ARs occurred mainly at lower frequencies which included 8 Hz (Mutafova-Yambolieva and Keef, 2001). The present results, at 2 Hz, show that when the α_1-ARs are blocked, the rauwolscine sensitive component is significantly smaller than when the α_1-ARs and P2X receptors are active. There is a trend to a similar result when the P2X receptors have been blocked but this change in component size is not as effective as when the α_1-ARs are blocked. Therefore, this result suggests that the post-junctional α_1-ARs are more greatly affected by pre-junctional α_2-AR activity compared to the P2X receptors. Interestingly, this variation in component magnitude is less obvious at 8 Hz. Here, the increase in transmitter output does not favour either receptor and the rauwolscine sensitive components are similar, regardless of which receptors are active or blocked. As mentioned previously, synergy has been suggested in rat mesenteric arteries (Brock et al., 2006). This could also be true in the mouse as blockade of one receptor may be compensated for by another thus enabling the effect of pre-junctional α_2-ARs to be maintained.

5.4.4 P2X receptor role in Mouse Mesenteric Arteries

Present results show activation of post-junctional P2X receptors are involved in initiation of the response to nerve stimulation, particularly at 2 Hz. This result can be expected as the P2X receptors are fast acting ion channels. Activation of the P2X receptors also contributes

to the amplitude of the response. Furthermore, at 2 Hz, the P2X receptor role continues beyond the end of the stimulation period with the receptors involved in prolonging the response and therefore lengthening the decay time. This is demonstrated by the shortened decay time when the vessels are incubated with suramin.

The suramin sensitive component differed depending on the active receptors and the antagonist incubation sequences. At both frequencies, when the α_1- and α_2-ARs were active, the suramin sensitive component was greater than when the α_1- and α_2-ARs were blocked. This therefore indicates an interaction between the receptors whereby the P2X receptor response is partly dependent on the presence of the α-ARs. The sequence of blockade also appears to be important. When the α_1-ARs are blocked before the α_2-ARs the resulting P2X component shows a trend to be smaller than when blocked in the opposite order. In the mesenteric arteries interaction is most likely between the α_1-ARs and the P2X receptors due to the large α_1-AR involvement in this tissue (Brock et al., 2006). Furthermore, a synergy between these receptors has been demonstrated in the rat mesenteric arteries (Brock et al., 2006).

5.4.5 Proximal and Distal Mouse Tail Artery

Co-incubation of prazosin, rauwolscine and suramin effectively blocked the α_1-, α_2-ARs and P2X receptors respectively and abolished the response to nerve stimulation at 0.5 Hz and 8 Hz in proximal and distal tail artery. These same receptors have been shown to be responsible for the response to nerve stimulation in rat tail artery with simultaneous blockade abolishing the response (Bao et al., 1993b). In the present study, stimulation at 0.5 Hz and 8 Hz produced responses with two distinct peaks; an initial fast peak and a second slower peak. At 0.5 Hz, 20 pulses were delivered within 40 seconds and the peak response always occurred close to the end of the stimulation period. At 8 Hz, 20 pulses were delivered within 2.5 seconds and the peak response always followed the end of the stimulation period. Various points from each response were analysed to determine which receptors were involved and at what part of the response. In the proximal rat tail artery, the initial response is due to activation of the P2X receptors, followed by α_1-AR activation and finally α_2-AR activation (Bao and Stjarne, 1993).

Initially, the response to nerve stimulation in mouse proximal and distal tail artery segments was investigated to determine whether the response changed along the length of the tail. This was shown to be true in the rat tail artery where the response to electrical stimulation was lower in distal compared to proximal segments (Medgett, 1985). Medgett also showed that proximally, the α_1-ARs were more sensitive than distally and also indicated a role of pre-junctional α_2-ARs. This changes in distal segments, where the post-junctional effect of the α_2-ARs are seen, but only when the α_1-ARs are blocked; suggesting an interaction between these two receptors (Medgett, 1985). The present results in the mouse tail artery indicate little difference between the proximal and distal segments. At the points studied, only the tension recorded at the second peak of the 8 Hz stimulation was lower in the distal segments compared to the proximal response. This difference between mouse and rat tail artery could be due to the mouse tail being smaller, and therefore receptor population is similar so as to help maintain a homeostatic environment. The mouse tail artery has been implicated in thermoregulation whereby changes in tail artery constriction act as a protective measure against heat loss (Chotani et al., 2000). Therefore it may be more important to have consistent receptor input along the length of the tail. As few differences were found between proximal and distal segments, the results section included only graphs from one area of the tail and only discrepancies in results were noted.

5.4.6 α_1-AR role in Mouse Tail Artery

In the present study, incubation with prazosin reduced the response to nerve stimulation at 0.5 Hz and 8 Hz but not to the same degree as shown in the mesenteric arteries. The α_1-ARs were shown to be involved throughout the response, particularly at 8 Hz where the receptors contributed to the initiation of the contraction. This was shown by prazosin prolonging the time taken to reach the peak and reducing the tension at the end of the stimulation period. These results differ from those shown in the rat whereby the post-junctional α_1-ARs are believed to be responsible for the latter part of the response (Sneddon and Burnstock, 1984; Bao and Stjarne, 1993). However, the α_1-ARs have also been shown to have a larger involvement at higher frequencies in the rat tail artery (Bao et al., 1993a). Presently, both proximal and distal results were similar.

The prazosin sensitive component at 0.5 Hz differed depending on the incubation sequence. The greatest component occurred when the P2X receptors had been blocked and the α_2-ARs were active. When the P2X receptors and the α_2-ARs were both blocked, the remaining α_1-AR component was small. This represents an example of interaction between all three of the receptors. Blockade of the P2X receptors enhances the α_1-AR component but this component can only be enhanced if the α_2-ARs are active. The same effect was seen at 8 Hz suggesting this is not frequency dependent. In the rat tail artery, studies have indicated an inhibitory role for the P2X receptors as αβme-ATP was able to enhance the second component of the response (Bao and Stjarne, 1993).

5.4.7 α_2-ARs role in Mouse Tail Artery

Unlike the rat tail artery, where the α_2-AR influence has been found to be secondary to the α_1-AR response, in mouse tail artery the current study indicates a strong α_2-AR component. At 0.5 Hz and 8 Hz, incubation with rauwolscine reduces the overall response and alters the time course of the response. At 0.5 Hz the time taken to reach both peaks is reduced by α_2-AR blockade suggesting that these receptors are involved in delaying vessel contraction and in inhibiting initiation of the response. This role has not been described previously in the rat tail artery. Conventionally, the α_2-ARs have been shown to exist both pre- and post-junctionally with pre-junctional block enhancing the response and post-junctional blockade inhibiting the response to nerve stimulation (Msghina et al., 1999; Bao and Stjarne, 1993; Weiss et al., 1983; Brock and Tan, 2004; Bao et al., 1993a). Interestingly, in proximal but not distal segments, there was evidence of pre-junctional α_2-ARs; revealed when α_2-AR blockade prolonged the time taken for the peak response to decay by 50 %. This could be explained by block of pre-junctional α_2-ARs and subsequent enhancement of transmitter output. The opposite occurs distally whereby the decay time is reduced in the presence of rauwolscine. It is possible that blockade of pre-junctional α_2-ARs and enhancement of transmitter output may either prolong the response by ensuring the post-junctional receptors remain active or the increase in transmitter output may accelerate transmitter uptake and smooth muscle relaxation via an unknown mechanism.

At 8 Hz, the α_2-ARs have little involvement in the initiation of the contraction as the tension at the end of the stimulation period was not affected by rauwolscine incubation. Both of the peak tensions were reduced and so the α_2-ARs play a definite role in contributing to the peak amplitude of the response, again more so than in the rat tail artery. A pre-junctional α_2-AR presence is evident during the second peak component as rauwolscine incubation prolonged the time taken to reach this peak. However, the peak tension was not enhanced. Furthermore, when the vessels were incubated with rauwolscine, the decay time was reduced, again suggesting an alternative role for α_2-ARs in smooth muscle relaxation.

As these experiments focussed only on the smooth muscle, it is possible that this response to α_2-AR antagonism was due to an endothelium dependent mechanism. Such a mechanism has been suggested by Crassous et al. who studied the effect α_2-AR antagonism had on various agonists in the mouse tail artery. When the endothelium was present, α_2-AR antagonism, in the presence of AR agonist, caused a vasodilation (Crassous et al., 2009).

The rauwolscine sensitive component was found to vary depending on frequency, location and presence of the other receptors, therefore displaying complicated interactions with the other receptors. Proximally, at 0.5 Hz, the greatest rauwolscine sensitive component was revealed whilst the α_1-ARs and P2X receptors were active, with this component being larger than when the P2X receptors were blocked and also when the α_1-ARs and P2X receptors were both blocked. Therefore, although the α_2-ARs have been shown to contribute most to the response, they are somewhat dependent on the presence of the other receptors, particularly the P2X receptors. Further evidence of this was shown when comparing the rauwolscine sensitive component when the P2X receptors were active (and α_1-ARs blocked) and when both receptors were blocked. The loss of P2X receptor activity reduced the rauwolscine sensitive component significantly.

Distally, at 0.5 Hz, the rauwolscine sensitive components were mostly similar, indicating that at this location, the α_2-ARs are not dependent on the presence or absence of the other receptors. However, the component revealed when the α_1-ARs and P2X receptors were blocked (in that order) was smaller than the component revealed when the α_1-ARs were active (and P2X receptors blocked). This is opposite to the proximal response which suggests

that the α_2-ARs could be somewhat dependent on the α_1-ARs. Furthermore, this difference only occurs when the α_1-ARs have been blocked first. This introduces a further complication by suggesting that the incubation sequence is important and so when prazosin is incubated first, it is in the bath for a longer period of time and may therefore exert a more profound antagonism than if incubated for a shorter time as is the case when the P2X receptors are blocked first.

At 8 Hz, the proximal rauwolscine sensitive components were all found to be similar, although there was a trend for the components when the α_1-ARs and P2X receptors were blocked to be smaller. As this did not reach significance the α_2-ARs can be described as being able to produce a similar response that is independent of the other receptors. Distally, the response remaining following blockade of the P2X receptors and α_1-ARs was greater than the initial control response and all of the other revealed components. This was due to an enhancement of the second slower component of the response which has been shown to occur in the rat tail artery (Bao and Stjarne, 1993; Bao et al., 1990). This effect did not occur when the α_1-ARs were blocked first, again demonstrating the importance of the incubation sequence and suggesting that when the P2X receptors are antagonised for a longer period, the response can be enhanced. The other revealed components were all of a similar magnitude indicating little interaction between the receptors.

The component analysis performed here to reveal the rauwolscine component highlights the complex interactions that occur between the receptors and show these interactions can change by altering the frequency or studying a different location. The α_2-ARs could independently cause a contraction of proximal mouse tail artery when the nerves were stimulated at 8 Hz; these would be the most useful parameters for studying the α_2-AR response without input from the other receptors.

5.4.8 P2X receptor role in Mouse Tail Artery

In the rat tail artery, ATP released from the nerve terminals has been indicated in activation of post-junctional P2X receptors and subsequent fast initiation of a contractile response

(Sneddon and Burnstock, 1984; Bao and Stjarne, 1993). The present results indicate that this also occurs in the mouse tail artery as P2X receptor antagonism with suramin prolonged the time taken to reach the peak tensions at both frequencies and also contributed more to the overall contractile response at 8 Hz.

The suramin sensitive components differed depending on the activity of the α-ARs. When both receptors were active, the suramin sensitive component was greatest and significantly larger than when the α-ARs were blocked indicating an interaction between all three receptors. This response occurred at both frequencies.

5.4.9 Conclusion

In summary, the presence of α_1-, α_2-ARs and P2X receptors has been confirmed in the mouse mesenteric and tail arteries. There are complicated interactions between all three receptors that can differ with frequency and vessel type. The α_1-ARs dominated the response to nerve stimulation in the mesenteric arteries with little interaction with the other receptors. Conversely, the α_2-ARs dominated the response in the tail artery but had more of an interaction/dependence on the other receptors. Evidence of pre-junctional α_2-ARs was more clearly shown in the mesenteric arteries compared to the tail artery and the P2X receptors mainly contributed to the initiation of the contractile responses in both vessels. These results provide a framework for future studies in the α_1-null and ADKO mice with which the WT results could be compared. The complicated nature of the responses provides reasoning for the poor performance of α_1-AR antagonists in the treatment of primary hypertension and highlights the requirement for further investigation into the other receptors and the mechanisms with which they interact. This should enhance knowledge in this area and provide novel therapies for the treatment of hypertension. The development of α_1-AR KO mice should simplify the complex pharmacology and such mice have been utilised in the following two studies.

Chapter Six

Role of α_{1B}-AR in nerve-evoked contractions in tail and mesenteric arteries revealed by comparison of tissues from knock-out and wild-type mice.

6.1 Introduction

In Chapter Five, the receptors involved in the response to sympathetic nerve stimulation were characterised. The results suggested that in the mesenteric arteries, the α_1-ARs are the main receptors involved in contraction. In the tail artery, α_2-AR activation predominates with interactions between all three of the receptors studied. The findings from Chapter Five can now be used as controls for the present study in which mice lacking the α_{1A}- and α_{1D}-AR subtypes were utilised.

Stimulation of the perivascular sympathetic nerves can induce the release of the neurotransmitters noradrenaline (NA) and adenosine tri-phosphate (ATP). These exert effects on smooth muscle post-junctional receptors in order to initiate vessel contraction (Bao and Stjarne, 1993) and can also activate pre-junctional receptors which mediate the further release of neurotransmitters from the nerve terminals (Msghina et al., 1999).

The majority of studied vessels in the vasculature, including the mesenteric arteries, have been shown to constrict mainly through activation of post-junctional α_1-ARs by NA (Angus et al., 1988). Other receptors have also been implicated in vessel contraction including post-junctional α_2-ARs and P2X receptors which are stimulated by NA and ATP respectively (Weiss et al., 1983; Gitterman and Evans, 2001). Activation of pre-junctional α_2-ARs inhibits transmitter release (Brock and Tan, 2004).

There is some evidence of post-junctional α_2-ARs in mouse mesenteric arteries and there is a definite α_2-AR mediated contraction in the rat tail artery (Fujiwara et al., 2012; Rajanayagam and Medgett, 1987). The exact roles of the mentioned receptors have been difficult to define due to limited selective antagonists and complex pharmacology. The development of transgenic mice and in particular α_1-AR knock-out (KO) mice allows the effect of genetic removal of these receptors to be studied. This should reduce the complex pharmacology and allow an enhanced study of the remaining receptors and show how they responde to the loss of the α_1-ARs.

Studies thus far on the α_1-AR KO mice have mainly focussed on post-junctional response to selective and non-selective agonists and antagonists. The results presented in Chapter Three suggest that the α_1-ARs are not as important in blood pressure maintenance as was previously believed as systolic blood pressure responses from WT, ADKO and α_1-null mice were similar. The interaction with the sensory nerves was investigated in Chapter Four whereby the responses before and after the neurotoxin capsaicin were compared. Capsaicin depletes the sensory nerves of the potent vasodilator calcitonin gene-related peptide (CGRP). The WT and α_1-null responses were similar before and after capsaicin treatment. However, in the ADKO a complex balance between the individual α_1-ARs was noted as the response following capsaicin treatment increased (see Chapter Four).

Presently, the ADKO mouse was employed which lacks the dominant α_{1A}- and α_{1D}-AR subtypes and therefore only the α_{1B}-AR remained functional. This provides an opportunity to study the α_{1B}-AR which is believed to only play a minor modulating role in the vessels. Furthermore, the impact on the α_2-ARs and P2X receptors response in the ADKO can be studied thus determining whether either vessel compensates for the loss in the mouse mesenteric and tail arteries. Therefore the aims of the following study were:

- To determine whether loss of the α_{1A+D}-ARs prevents the response to nerve stimulation in the mouse mesenteric or tail arteries occurring.
- To investigate the difference in response between WT and ADKO mesenteric and tail arteries.
- To establish the role of the α_{1B}-ARs in the response to nerve stimulation in mesenteric and tail arteries.
- To determine whether there are any changes in the interactions between the receptors compared to those seen in the WT responses and therefore establish any compensatory mechanisms.

6.2 Methods

A full description of the methods used can be found in Chapter Two (Materials and Methods). Briefly, wire myography studies were conducted using mouse mesenteric arteries and proximal and distal tail artery segments. The vessels were mounted between two stimulating electrodes which could be used to deliver square wave pulses of varying parameters. All vessels were incubated with 1 μM capsaicin in order to deplete the sensory nerves of CGRP; a potent vasodilator. Control response to 2 Hz and 8 Hz (mesenteric arteries) and 0.5 Hz and 8 Hz (tail artery) were recorded before incubation with one of the following antagonists: 100 nM prazosin (α_1-AR antagonist), 100 nM rauwolscine (α_2-AR antagonist) or 1 mM suramin (P2X receptor antagonist). The vessels were then stimulated again using the same parameters.

Statistical analysis was performed using GraphPad Prism (Version 5) with paired t-tests used when comparing control response with antagonist response and one way ANOVA with Bonferonni's post-test utilised for comparing the antagonist sensitive components. A worked example of the component analysis, which revealed the antagonist sensitive response in different incubation sequences is shown at the beginning of the mesenteric and tail artery results sections in Chapter Five. The analyses of the antagonist sensitive components were only conducted in the tail artery responses as the mesenteric artery responses were too small to produce reliable statistics.

6.3 Results

6.3.1 Mesenteric Artery

6.3.1.1 Comparison of WT and ADKO response to nerve stimulation.

Both WT and ADKO mesenteric arteries responded to nerve stimulation at 2 Hz and 8 Hz (Figure 6-1 and 6-2). At both frequencies the peak tension and the tension at the end of the stimulation periods were reduced in the ADKO mice. At 2 Hz, the time to reach the peak tension was altered in the ADKO mice (Figure 6-1 and 6-2; Tables 6-1 and 6-2).

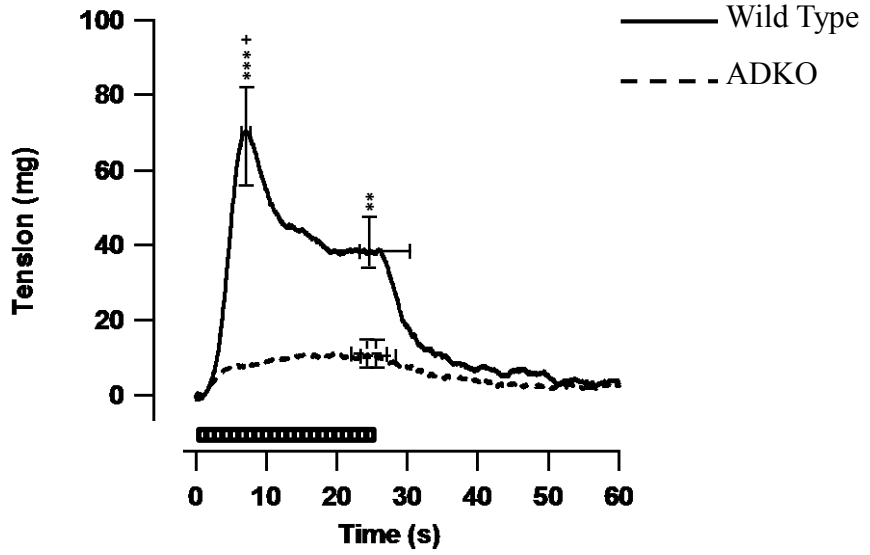

Figure 6-1: WT and ADKO mouse mesenteric arteries - response to nerve stimulation at 2 Hz (WT: n=17; ADKO: n=20).

**** P < 0.01; *** P < 0.001 compared with WT response. Un-paired t-test.**

+ P < 0.05 compared with WT time. Un-paired t-test.

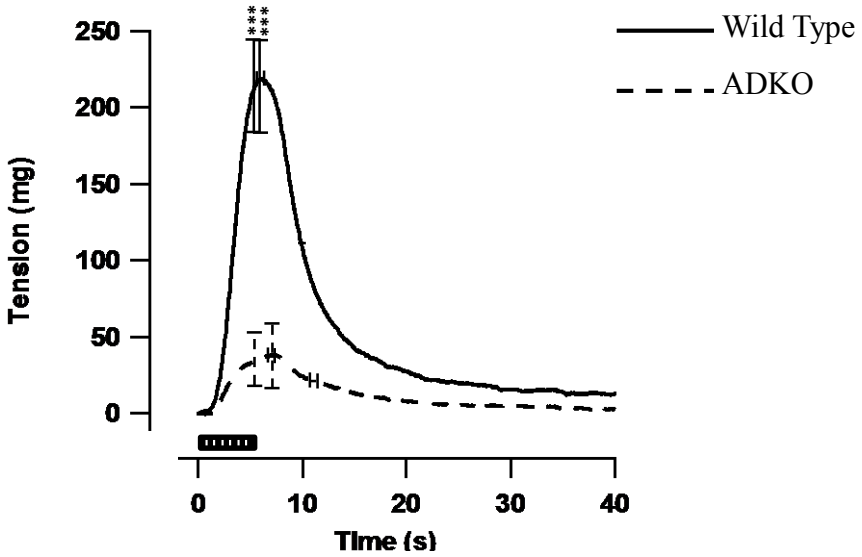

Figure 6-2: WT and ADKO mouse mesenteric arteries - response to nerve stimulation at 8 Hz (WT: n=17; ADKO: n=20).

***** P < 0.001 compared with WT response. Un-paired t-test.**

Table 6-1: WT and ADKO mouse mesenteric arteries - response to nerve stimulation at 2 Hz.

2 Hz	Contractile Response (average ± S.E.M)	
	WT (n=17)	ADKO (n=20)
Time to Peak (seconds)	7.2 ± 0.2	13.0 ± 2.0 +
Peak Tension (mg)	72 ± 9	15 ± 3 ***
Rate of Rise (mg/s)	10 ± 1	2 ± 0.4 ***
Tension at End of pulse (mg)	38 ± 8	11 ± 3 **
50 % Decay Time (seconds)	12.2 ± 2.0	7.5 ± 1.8

**** P < 0.01; *** P < 0.001 compared with WT response. Un-paired t-test.**

+ P < 0.05 compared with WT time. Un-paired t-test.

Table 6-2: WT and ADKO mouse mesenteric arteries - response to nerve stimulation at 8 Hz.

8 Hz	Contractile Response (average ± S.E.M)	
	WT (n=17)	**α_1-null (n=20)**
Time to Peak (seconds)	6.0 ± 0.2	5.8 ± 0.4
Peak Tension (mg)	223 ± 20	42 ± 6 ***
Rate of Rise (mg/s)	40 ± 3	7 ± 1 ***
Tension at End of pulse (mg)	215 ± 20	36 ± 5 ***
50 % Decay Time (seconds)	4.1 ± 0.3	5.0 ± 0.4

***** P < 0.001 compared with WT response. Un-paired t-test.**

Combined incubation with prazosin (100 nM), rauwolscine (100 nM) and suramin (1 mM) in the ADKO animals effectively blocked the α_1-, α_2-ARs and P2X receptors respectively in response to nerve stimulation at 2 Hz and 8 Hz in the mesenteric arteries and completely abolished the response (Figures 6-3 and 6-4).

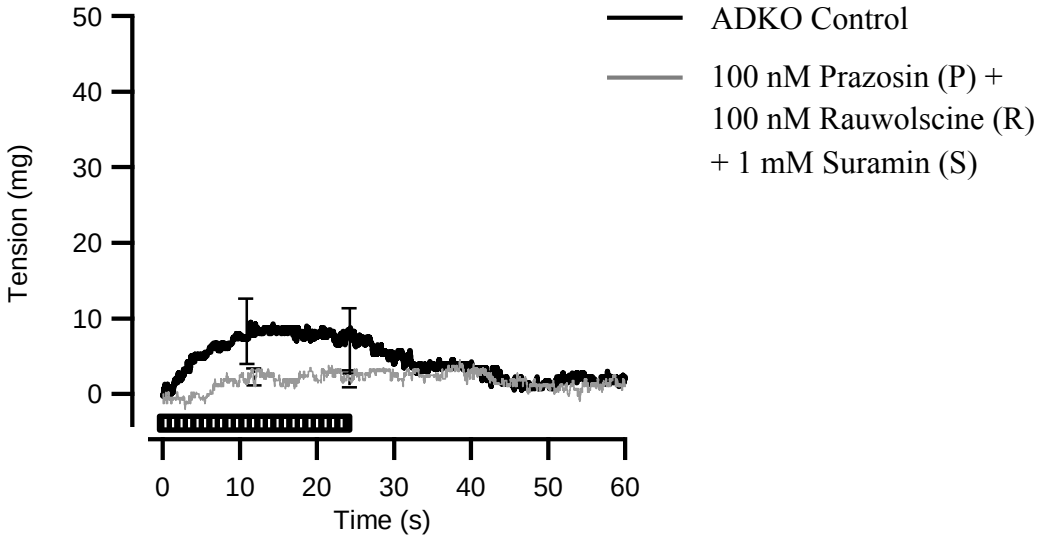

Figure 6-3: ADKO Mouse mesenteric artery response to nerve stimulation at 2 Hz in control vessels and in the presence of the following antagonists: prazosin (100 nM), rauwolscine (100 nM), suramin (1 mM) (n = 4).

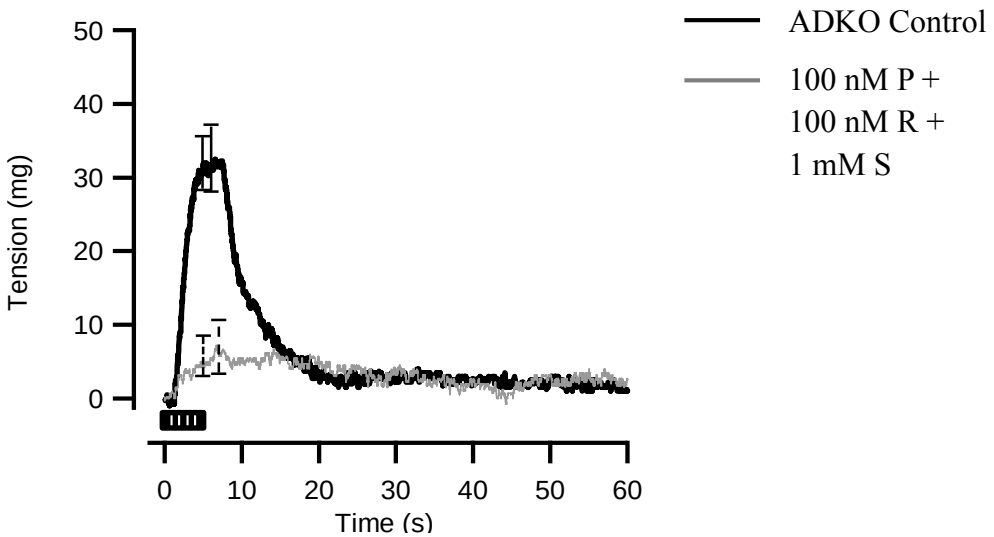

Figure 6-4: ADKO Mouse mesenteric artery response to nerve stimulation at 8 Hz in control vessels and in the presence of the following antagonists: prazosin (100 nM), rauwolscine (100 nM), suramin (1 mM) (n = 4).

6.3.1.2 Revealing the response to sympathetic nerve stimulation at 2 Hz.

Individual incubations with 100 nM prazosin, 100 nM rauwolscine and 1 mM suramin did not result in a significant change in the response compared with the ADKO control response (Figure 6-5; Tables 6-3 – 6-5).

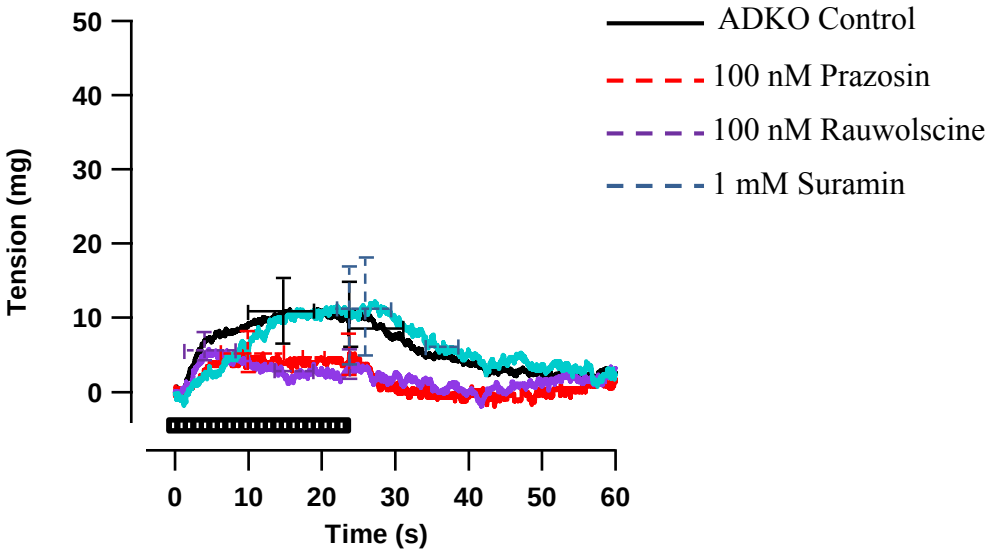

Figure 6-5: ADKO Mouse mesenteric artery response to nerve stimulation at 2 Hz in control vessels and in the presence of 100 nM prazosin (red) (n=6); 100 nM rauwolscine (purple) (n=7); 1 mM suramin (blue) (n=7).

Table 6-3: ADKO Mouse mesenteric artery response to nerve stimulation in control and prazosin (100 nM) incubated vessels at 2 Hz.

2 Hz	Contractile Response (average ± S.E.M)		
	Control	100 nM Prazosin (P) (n = 4)	% change following P incubation
Time to Peak (seconds)	11.1 ± 5.0	9.9 ± 4.9	- 7 ± 35
Peak Tension (mg)	11 ± 5	8 ± 3	- 20 ± 24
Rate of Rise (mg/s)	1 ± 0.4	1 ± 0.1	- 18 ± 31
Tension at End of pulse (mg)	7 ± 5	4 ± 3	- 33 ± 47
50 % Decay Time (seconds)	8.6 ± 4.1	3.8 ± 1.4	- 8 ± 45

Table 6-4: ADKO Mouse mesenteric artery response to nerve stimulation in control and rauwolscine (100 nM) incubated vessels at 2 Hz.

2 Hz	Contractile Response (average ± S.E.M)		
	Control	100 nM Rauwolscine (R) (n = 9)	% change following R incubation
Time to Peak (seconds)	17.4 ± 2.8	12.0 ± 3.7	- 25 ± 18
Peak Tension (mg)	12 ± 2	8 ± 2	- 24 ± 16
Rate of Rise (mg/s)	1 ± 0.3	1 ± 0.3	- 4 ± 20
Tension at End of pulse (mg)	8 ± 2	3 ± 2	- 54 ± 29
50 % Decay Time (seconds)	6.2 ± 2.5	4.2 ± 2.9	- 40 ± 25

Table 6-5: ADKO Mouse mesenteric artery response to nerve stimulation in control and suramin (1 mM) incubated vessels at 2 Hz.

2 Hz	Contractile Response (average ± S.E.M)		
	Control	1 mM Suramin (S) (n = 7)	% change following S incubation
Time to Peak (seconds)	8.5 ± 2.5	10.5 ± 4.5	- 30 ± 23
Peak Tension (mg)	23 ± 8	15 ± 8	- 51 ± 17
Rate of Rise (mg/s)	3 ± 1	1 ± 0.4	- 40 ± 15
Tension at End of pulse (mg)	17 ± 9	10 ± 8	- 80 ± 25
50 % Decay Time (seconds)	8.5 ± 3.5	5.7 ± 2.7	- 61 ± 15

When the mesenteric arteries where incubated with more than one antagonist, there was greater statistical significance in the response compared to incubation with one antagonist (Table 6-6).

Table 6-6: The significant changes to the response at 2 Hz when incubation was with more than one antagonist.

2 Hz	Contractile Response (average ± S.E.M)		
Part of response affected by antagonist incubation	Antagonist Incubation sequence		
	1 mM S + 100 nM R	100 nM R, 100 nM P, 1 mM S	1 mM S, 100 nM R, 100 nM P
Time to Peak (seconds)			+++
Rate of Rise (mg/s)	*		*
Tension at End of pulse (mg)		*	
50 % Decay Time (seconds)	+		

*** P < 0.05 compared with control response. Paired t-test.**

+ P < 0.05; +++ P < 0.001 compared with control time. Paired t-test.

6.3.1.3 Revealing the response to sympathetic nerve stimulation at 8 Hz.

Prazosin incubated alone did not result in a significant change in the response compared with the ADKO control response. However, incubation with 100 nM rauwolscine reduced the time to reach the peak tension and incubation with 1 mM suramin significantly reduced the peak tension, the tension at the end of the stimulation period and the rate of rise (Figure 6-6; Tables 6-7 – 6-9).

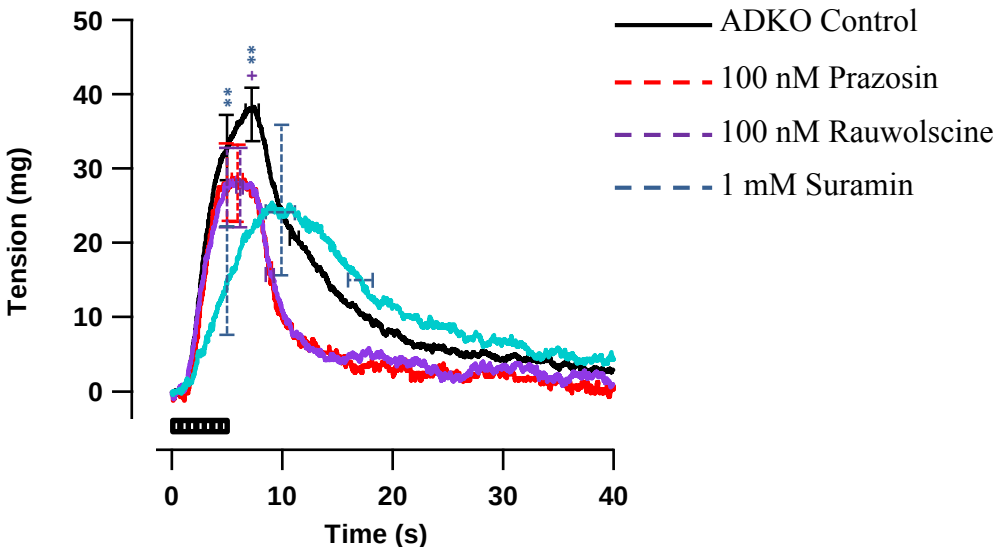

Figure 6-6: ADKO Mouse mesenteric artery response to nerve stimulation at 8 Hz in control vessels and in the presence of 100 nM prazosin (red) (n=6); 100 nM rauwolscine (purple) (n=7); 1 mM suramin (blue) (n=7).

**** P < 0.01 compared with control response. Paired t-test.**

+ P < 0.05 compared with control time. Paired t-test.

Table 6-7: ADKO Mouse mesenteric artery response to nerve stimulation in control and prazosin (100 nM) incubated vessels at 8 Hz.

8 Hz	Contractile Response (average ± S.E.M)		
	Control	100 nM Prazosin (P) (n = 4)	% change following P incubation
Time to Peak (seconds)	4.8 ± 0.9	4.8 ± 0.8	3 ± 11
Peak Tension (mg)	36 ± 5	31 ± 6	- 13 ± 15
Rate of Rise (mg/s)	8 ± 1	7 ± 1	- 18 ± 7
Tension at End of pulse (mg)	32 ± 4	28 ± 5	- 11 ± 17
50 % Decay Time (seconds)	5.7 ± 0.6	4.6 ± 0.2	- 17 ± 8

Table 6-8: ADKO Mouse mesenteric artery response to nerve stimulation in control and rauwolscine (100 nM) incubated vessels at 8 Hz.

8 Hz	Contractile Response (average ± S.E.M)		
	Control	100 nM Rauwolscine (R) (n = 9)	% change following R incubation
Time to Peak (seconds)	6.5 ± 0.4	5.5 ± 0.3 +	- 13 ± 6
Peak Tension (mg)	33 ± 5	30 ± 6	- 13 ± 13
Rate of Rise (mg/s)	5 ± 1	5 ± 1	- 3 ± 12
Tension at End of pulse (mg)	29 ± 4	28 ± 6	- 11 ± 5
50 % Decay Time (seconds)	3.8 ± 0.4	3.0 ± 0.4	- 17 ± 11

+ P < 0.05 compared with control response. Paired t-test.

Table 6-9: ADKO Mouse mesenteric artery response to nerve stimulation in control and suramin (1 mM) incubated vessels at 8 Hz.

8 Hz	Contractile Response (average ± S.E.M)		
	Control	1 mM Suramin (S) (n = 7)	% change following S incubation
Time to Peak (seconds)	5.4 ± 0.8	7.4 ± 2.0	4 ± 17
Peak Tension (mg)	56 ± 16	28 ± 14 **	- 64 ± 10
Rate of Rise (mg/s)	9 ± 1	3 ± 1 ***	- 66 ± 9
Tension at End of pulse (mg)	47 ± 12	18 ± 10 **	- 76 ± 12
50 % Decay Time (seconds)	6.2 ± 0.9	4.7 ± 1.8	- 38 ± 20

**** P < 0.01; *** P < 0.001 compared with control response. Paired t-test.**

When the mesenteric arteries where incubated with more than one antagonist, there were additional changes in the response compared to incubation with one antagonist (Table 6-10).

Table 6-10: The significant changes to the response at 8 Hz when incubation was with more than one antagonist.

8 Hz	Contractile Response (average ± S.E.M)					
Part of response affected by antagonist incubation	Antagonist Incubation sequence					
	100 nM P 100 nM R	100 nM R 100 nM P	1 mM S 100 nM R	100 nM P 100 nM R 1 mM S	100 nM R 100 nM P 1 mM S	1 mM S 100 nM R 100 nM P
Time to Peak (seconds)		+				
Peak Tension (mg)			**	**	**	*
Rate of Rise (mg/s)	**		***	*	***	***
Tension at End of pulse (mg)			**	**	***	**

*** P < 0.05; ** P < 0.01; *** P < 0.001 compared with control response. Paired t-test.**

+ P < 0.05 compared with control time. Paired t-test.

6.3.2 Mouse Tail Artery

6.3.2.1 Comparison of WT and ADKO response to nerve stimulation.

Both WT and ADKO tail artery responded to nerve stimulation at 0.5 Hz and 8 Hz with the response in the ADKO smaller than in the WT (Figure 6-7 and 6-8; Tables 6-11 and 6-12).

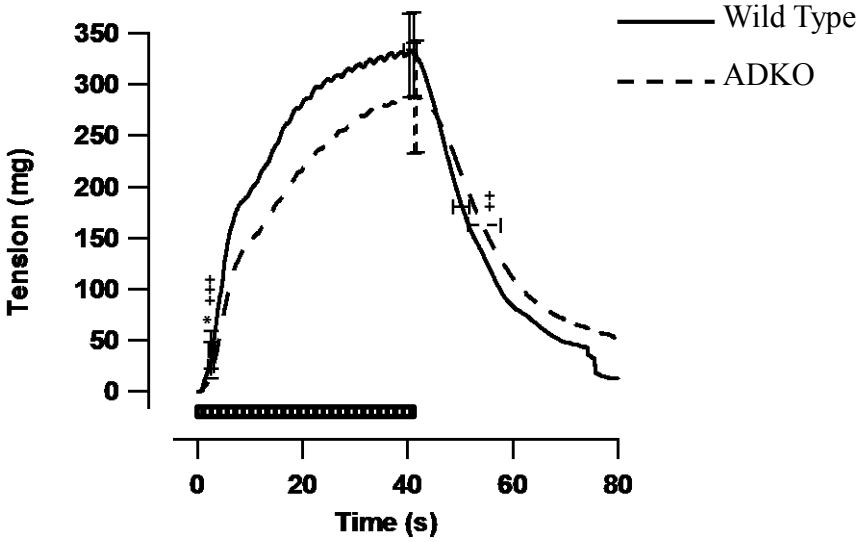

Figure 6-7: WT and ADKO mouse tail artery - response to nerve stimulation at 0.5 Hz (WT: n=26; ADKO: n=25).

*** P < 0.05 compared with WT response. Un-paired t-test.**

++ P < 0.01; +++ P < 0.001 compared with WT time. Un-paired t-test.

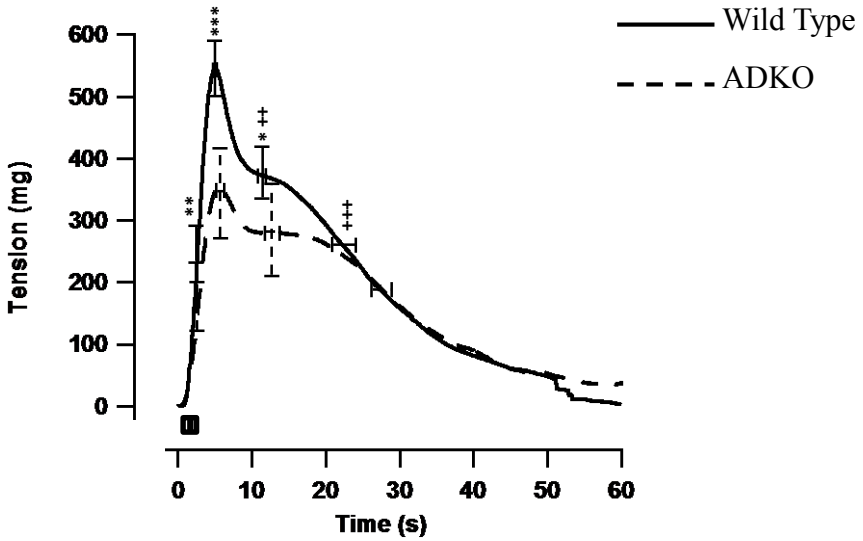

Figure 6-8: WT and ADKO mouse tail artery - response to nerve stimulation at 8 Hz (WT: n=26; ADKO: n=25).

*** P < 0.05; ** P < 0.01; *** P < 0.001 compared with WT response. Un-paired t-test.**

++ P < 0.01; +++ P < 0.001 compared with WT time. Un-paired t-test.

Table 6-11: WT and ADKO mouse tail arteries - response to nerve stimulation at 0.5 Hz.

0.5 Hz	Contractile Response (average ± S.E.M)	
	WT (n=26)	ADKO (n=25)
Time to Peak (1st) (seconds)	2.6 ± 0.2	4.4 ± 0.2 +++
Peak Tension (1st) (mg)	34 ± 7	63 ± 10 *
Rate of Rise (mg/s)	16 ± 3	15 ± 2
Time to Peak (seconds)	37.2 ± 1.0	38.5 ± 1.0
Peak Tension (mg)	338 ± 27	283 ± 31
Tension at End of pulse (mg)	327 ± 26	283 ± 31
50 % Decay Time (seconds)	12.8 ± 0.9	17.3 ± 1.3 ++

*** P < 0.05 compared with WT response. Un-paired t-test.**

++ P < 0.01; +++ P < 0.01 compared with WT time. Un-paired t-test.

Table 6-12: WT and ADKO mouse tail arteries - response to nerve stimulation at 8 Hz.

8 Hz	Contractile Response (average ± S.E.M)	
	WT (n=26)	ADKO (n=25)
Tension at End of pulse (mg)	210 ± 19	135 ± 15 **
Time to Peak (seconds)	5.0 ± 0.1	6.5 ± 0.8
Peak Tension (mg)	552 ± 32	365 ± 36 ***
Rate of Rise (mg/s)	114 ± 6	67 ± 8 ***
Time to Peak (2nd) (seconds)	11.8 ± 0.3	13.6 ± 0.5 ++
Peak Tension (2nd) (mg)	372 ± 29	284 ± 30 *
50 % Decay Time (seconds)	13.7 ± 1.0	20.7 ± 0.9 +++

*** P < 0.05; ** P < 0.01; *** P < 0.001 compared with WT response. Un-paired t-test.**

++ P < 0.01; +++ P < 0.001 compared with WT time. Un-paired t-test.

6.3.2.2 Revealing the effect of prazosin on the response to sympathetic nerve stimulation at 0.5 Hz.

When the mouse tail artery was incubated with 100 nM prazosin, the response to nerve stimulation was similarly affected in both proximal and distal segments. Both showed a

reduction in tension at the first peak. Proximally, the time to reach this peak was reduced (Figure 6-9; Table 6-13). Distally, the rate of rise was reduced (Table 6-14).

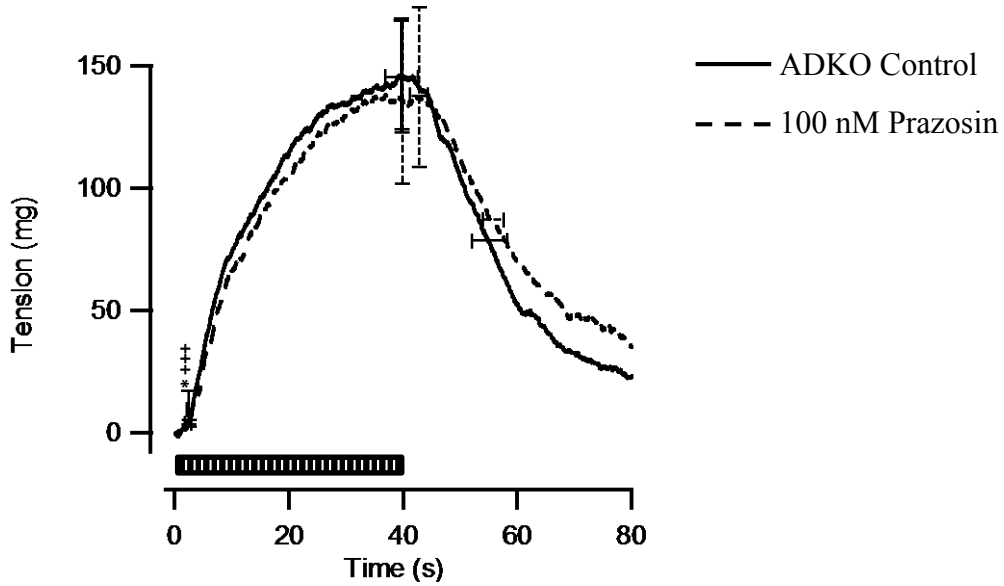

Figure 6-9: ADKO Proximal mouse tail artery response to nerve stimulation at 0.5 Hz in control vessels and in the presence of the α_1-AR antagonist prazosin (100 nM) (n = 6).

*** P < 0.05 compared with control response. Paired t-test.**

+++ P < 0.001 compared with control time. Paired t-test.

Table 6-13: ADKO Proximal mouse tail artery response to nerve stimulation in control and prazosin (100 nM) incubated vessels at 0.5 Hz.

Proximal 0.5 Hz	Contractile Response (average ± S.E.M)		
	Control	100 nM Prazosin (P) (n = 6)	% change following P incubation
Time to Peak (1st) (seconds)	4.3 ± 0.3	1.7 ± 0.4 +++	- 62 ± 8
Peak Tension (1st) (mg)	26 ± 8	5 ± 1 *	- 69 ± 13
Rate of Rise (mg/s)	6 ± 1	3 ± 0.4	- 29 ± 17
Time to Peak (seconds)	35.4 ± 3.1	39.5 ± 1.5	9 ± 10
Peak Tension (mg)	150 ± 26	145 ± 38	- 9 ± 10
Tension at End of pulse (mg)	143 ± 27	136 ± 39	- 11 ± 11
50 % Decay Time (seconds)	19.3 ± 3.4	16.8 ± 1.8	- 2 ± 17

*** P < 0.05 compared with control response. Paired t-test.**

+++ P < 0.001 compared with control time. Paired t-test.

Table 6-14: ADKO Distal mouse tail artery response to nerve stimulation in control and prazosin (100 nM) incubated vessels at 0.5 Hz.

Distal 0.5 Hz	Contractile Response (average ± S.E.M)		
	Control	100 nM Prazosin (P) (n = 7)	% change following P incubation
Time to Peak (1st) (seconds)	3.2 ± 0.5	2.6 ± 0.4	- 13 ± 14
Peak Tension (1st) (mg)	22 ± 6	9 ± 2 *	- 53 ± 11
Rate of Rise (mg/s)	7 ± 1	3 ± 1 *	- 46 ± 8
Time to Peak (seconds)	39.6 ± 0.9	41.2 ± 0.5	4 ± 3
Peak Tension (mg)	196 ± 30	169 ± 29	- 14 ± 8
Tension at End of pulse (mg)	189 ± 30	162 ± 28	- 15 ± 8
50 % Decay Time (seconds)	14.8 ± 1.7	14.0 ± 1.3	- 3 ± 8

*** P < 0.05 compared with control response. Paired t-test.**

The prazosin sensitive components did not differ significantly from one another at either proximal or distal ends. However, there was a trend for the greatest prazosin sensitive component to be seen when the α_2-ARs and P2X receptors were functional (Figure 6-10; Tables 6-15 and 6-16).

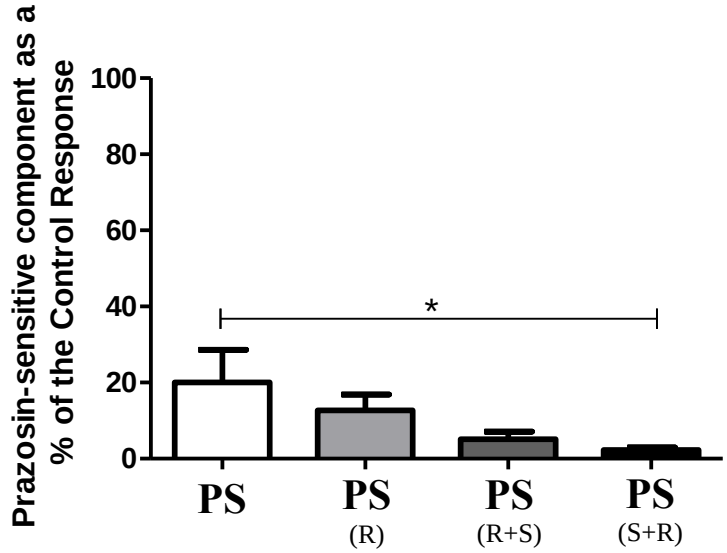

Figure 6-10: ADKO Proximal mouse tail – the prazosin sensitive (PS) component at 0.5 Hz when the P2X receptors and α_2-AR are functional (white) (n=6), α_2-ARs are blocked (light grey) (n=6), when the α_2-ARs and P2X receptors are blocked (dark grey) (n=6), when the P2X receptors and α_2-ARs are blocked (black) (n=7=).

*** P < 0.05 compared with PS component when the α_2-ARs and P2X receptors are functional. One way ANOVA with Bonferonni's post-test.**

Table 6-15: ADKO Proximal mouse tail artery response – the prazosin sensitive (PS) component as a % of control area under the curves. Data taken from Figures 6-10 and 6-12.

	Prazosin-sensitive component as a % of the Control Response	
	0.5 Hz	**8 Hz**
PS	20 ± 9	17 ± 3
PS (R)	13 ± 4	30 ± 6
PS (R+S)	5 ± 2	14 ± 8
PS (S+R)	2 ± 1 *****	15 ± 5

*** P < 0.05 compared with the PS component when the α_2-ARs and P2X receptors are functional. One way ANOVA with Bonferonni's post-test.**

Table 6-16: ADKO Distal mouse tail artery response - the prazosin sensitive (PS) component as a % of control area under the curves.

	Prazosin-sensitive component as a % of the Control Response	
	0.5 Hz	**8 Hz**
PS	35 ± 15	36 ± 18
PS (R)	15 ± 2	26 ± 4
PS (R+S)	12 ± 5	22 ± 7
PS (S+R)	7 ± 4	23 ± 11

6.3.2.3 Revealing the effect of prazosin on the response to sympathetic nerve stimulation at 8 Hz.

At 8 Hz prazosin (100 nM) was shown to reduce the peak tension and rate of rise in both proximal and distal segments as well as prolonging the time to reach the peak in proximal tail artery segments (Figure 6-11; Tables 6-17 and 6-18).

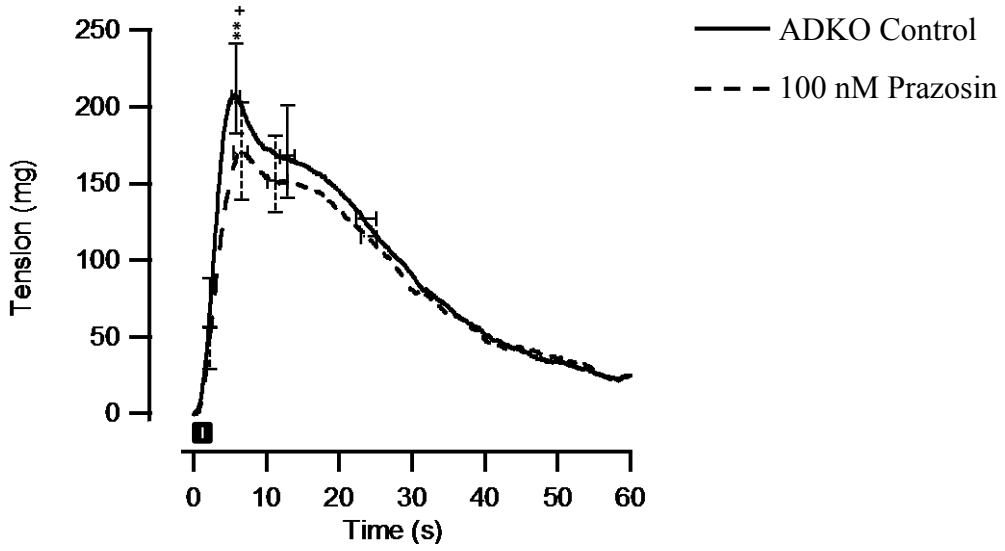

Figure 6-11: ADKO Proximal mouse tail artery response to nerve stimulation at 8 Hz in control vessels and in the presence of the α_1-AR antagonist prazosin (100 nM) (n = 6).

**** P < 0.01 compared with control response. Paired t-test.**

+ P < 0.05 compared with control time. Paired t-test.

Table 6-17: ADKO Proximal mouse tail artery response to nerve stimulation in control and prazosin (100 nM) incubated vessels at 8 Hz.

Proximal 8 Hz	Contractile Response (average ± S.E.M)		
	Control	100 nM Prazosin (P) (n = 6)	% change following P incubation
Tension at End of pulse (mg)	81 ± 18	58 ± 15	- 31 ± 14
Time to Peak (seconds)	5.6 ± 0.5	7.1 ± 1.0 +	19 ± 5
Peak Tension (mg)	219 ± 33	180 ± 37 **	- 21 ± 5
Rate of Rise (mg/s)	40 ± 6	26 ± 5 **	- 36 ± 5
Time to Peak (2^{nd}) (seconds)	13.3 ± 1.1	14.7 ± 1.5	7 ± 12
Peak Tension (2^{nd}) (mg)	168 ± 34	138 ± 28	- 18 ± 6
50 % Decay Time (seconds)	19.9 ± 1.5	22.5 ± 1.0	12 ± 6

**** P < 0.01 compared with control response. Paired t-test.**

+ P < 0.05 compared with control time. Paired t-test.

Table 6-18: ADKO Distal mouse tail artery response to nerve stimulation in control and prazosin (100 nM) incubated vessels at 8 Hz.

Distal 8 Hz	Contractile Response (average ± S.E.M)		
	Control	100 nM Prazosin (P) (n = 7)	% change following P incubation
Tension at End of pulse (mg)	78 ± 10	58 ± 14	- 28 ± 17
Time to Peak (seconds)	5.3 ± 0.2	6.8 ± 0.7	18 ± 7
Peak Tension (mg)	250 ± 38	203 ± 36 **	- 21 ± 5
Rate of Rise (mg/s)	46 ± 6	31 ± 6 **	- 36 ± 6
Time to Peak (2nd) (seconds)	13.3 ± 0.7	14.6 ± 0.5	9 ± 6
Peak Tension (2nd) (mg)	185 ± 37	171 ± 35	- 10 ± 7
50 % Decay Time (seconds)	19.8 ± 1.8	20.2 ± 12	3 ± 7

**** P < 0.01 compared with control response. Paired t-test.**

The prazosin sensitive components were similar for each of the incubation sequences in both proximal and distal tail artery segments (Figure 6-12; Tables 6-15 and 6-16).

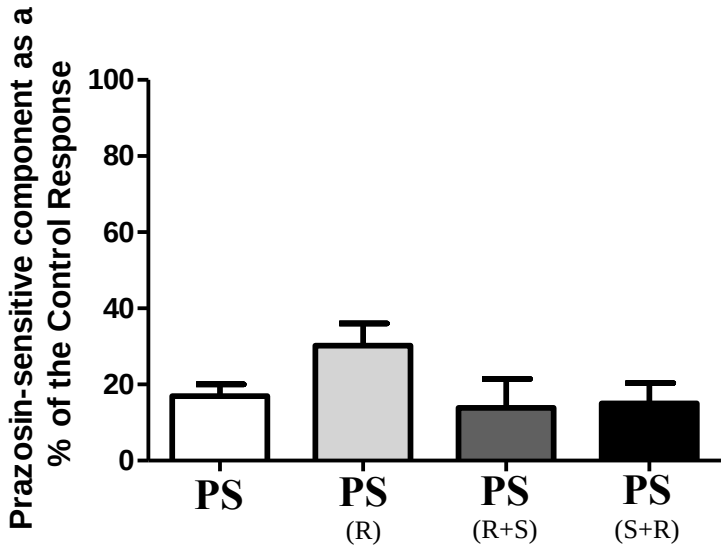

Figure 6-12: ADKO Proximal mouse tail – the prazosin sensitive (PS) component at 8 Hz when the P2X receptors and α_2-AR are functional (white) (n=6), α_2-ARs are blocked (light grey) (n=6), when the α_2-ARs and P2X receptors are blocked (dark grey) (n=6), when the P2X receptors and α_2-ARs are blocked (black) (n=7).

6.3.2.4 Revealing the α_2-ARs role in the response to sympathetic nerve stimulation at 0.5 Hz.

In proximal and distal segments, the response to nerve stimulation at 0.5 Hz when the vessels were incubated with 100 nM rauwolscine reduced both peak tensions and the tension at the end of the stimulation period (Tables 6-19 and 6-20). Additionally, in proximal segments, the rate of rise and time to reach the first peak were both reduced (Figure 6-13; Table 6-19).

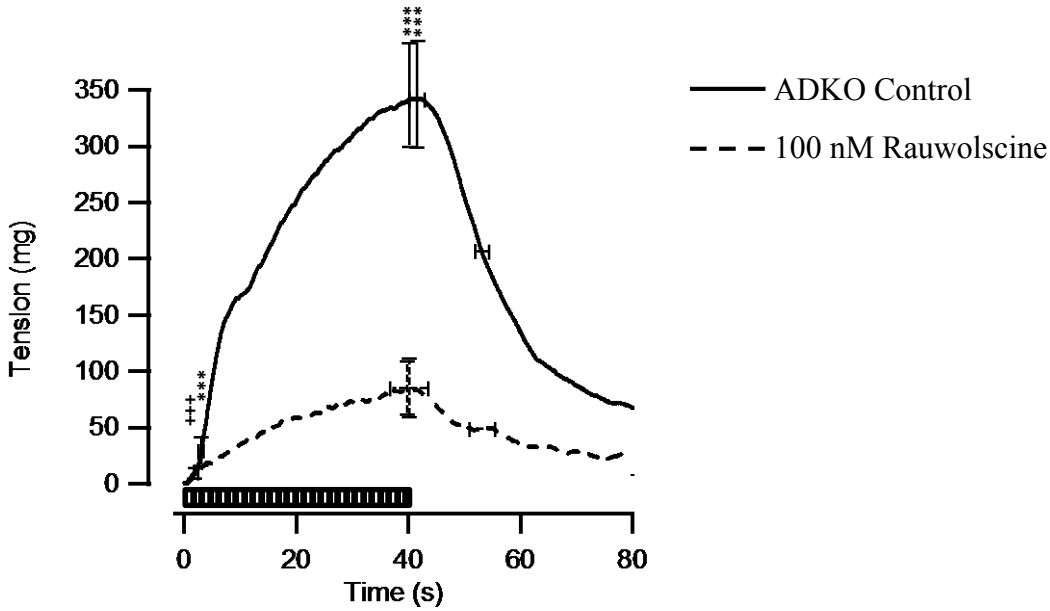

Figure 6-13: ADKO Proximal mouse tail artery response to nerve stimulation at 0.5 Hz in control vessels and in the presence of the α_2-AR antagonist rauwolscine (100 nM) (n = 12).

***** P < 0.001 compared with control response. Paired t-test.**

+++ P < 0.001 compared with control time. Paired t-test.

Table 6-19: ADKO Proximal mouse tail artery response to nerve stimulation in control and rauwolscine (100 nM) incubated vessels at 0.5 Hz.

Proximal 0.5 Hz	Contractile Response (average ± S.E.M)		
	Control	100 nM Rauwolscine (R) (n = 12)	% change following R incubation
Time to Peak (1st) (seconds)	4.5 ± 0.3	1.8 ± 0.1 +++	- 59 ± 4
Peak Tension (1st) (mg)	69 ± 13	11 ± 4 ***	- 84 ± 3
Rate of Rise (mg/s)	16 ± 3	6 ± 2 ***	- 62 ± 8
Time to Peak (seconds)	39.6 ± 1.2	31.7 ± 3.5	- 19 ± 9
Peak Tension (mg)	326 ± 53	91 ± 28 ***	- 76 ± 4
Tension at End of pulse (mg)	335 ± 52	81 ± 26 ***	- 79 ± 4
50 % Decay Time (seconds)	16.4 ± 1.2	15.5 ± 2.3	- 18 ± 13

***** P < 0.001 compared with control response. Paired t-test.**

+++ P < 0.001 compared with control time. Paired t-test.

Table 6-20: ADKO Distal mouse tail artery response to nerve stimulation in control and rauwolscine (100 nM) incubated vessels at 0.5 Hz.

Distal 0.5 Hz	Contractile Response (average ± S.E.M)		
	Control	100 nM Rauwolscine (R) (n = 14)	% change following R incubation
Time to Peak (1st) (seconds)	3.4 ± 0.4	2.5 ± 0.3	- 19 ± 11
Peak Tension (1st) (mg)	69 ± 15	15 ± 4 **	- 56 ± 11
Rate of Rise (mg/s)	19 ± 3	6 ± 2	- 57 ± 9
Time to Peak (seconds)	36.4 ± 2.4	35.0 ± 1.8	- 2 ± 6
Peak Tension (mg)	306 ± 17	83 ± 9 ***	- 72 ± 3
Tension at End of pulse (mg)	299 ± 18	75 ± 10 ***	- 75 ± 3
50 % Decay Time (seconds)	16.5 ± 2.4	12.4 ± 1.4	- 21 ± 8

**** P < 0.01; *** P < 0.001 compared with control response. Paired t-test.**

In proximal segments the rauwolscine sensitive (RS) component when the α_1-ARs and the P2X receptors were blocked was smaller when compared to the other incubation conditions (Figure 6-14; Table 6-21). In distal segments, the areas under the curves where shown to be similar (Table 6-22).

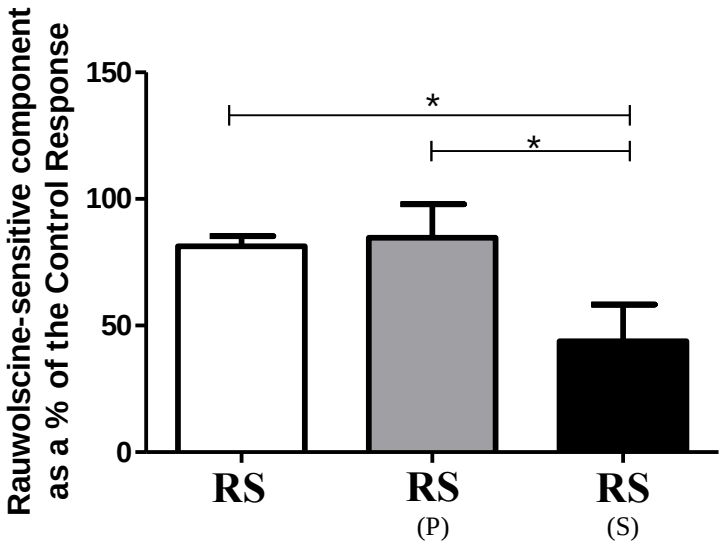

Figure 6-14: ADKO Proximal mouse tail – the rauwolscine sensitive (RS) component at 0.5 Hz when the P2X receptors and α_1-AR are functional (white) (n=12), α_1-ARs are blocked (light grey) (n=6), P2X receptors are blocked (dark grey) (n=7).

*** P < 0.05 compared with RS component when the P2X receptors are blocked. One way ANOVA with Bonferonni's post-test.**

Table 6-21: ADKO Proximal mouse tail artery - revealing the rauwolscine-sensitive component as a % of control area under the curves. Data taken from Figures 6-14 and 6-16.

	Rauwolscine-sensitive component as a % of the Control Response	
	0.5 Hz	**8 Hz**
RS	81 ± 4 *****	49 ± 7
RS (P)	85 ± 13 *****	68 ± 6
RS (S)	44 ± 14	42 ± 11

*** P < 0.05 compared with the RS component when the the P2X receptors are blocked. One way ANOVA with Bonferonni's post-test.**

Table 6-22: ADKO Distal mouse tail artery response - revealing the rauwolscine-sensitive component as a % of control area under the curves.

	Rauwolscine-sensitive component as a % of the Control Response	
	0.5 Hz	**8 Hz**
RS	77 ± 3	53 ± 3
RS (P)	65 ± 11	69 ± 5
RS (S)	57 ± 10	50 ± 8

6.3.2.5 Revealing the α_2-ARs role in the response to sympathetic nerve stimulation at 8 Hz.

The response to nerve stimulation at 8 Hz was reduced in the presence of 100 nM rauwolscine at both proximal and distal segments of the tail artery. In both segments the peak tensions, decay times and the time to reach the second peak were reduced. Proximally, the tension at the end of the stimulation period was also reduced (Figure 6-15; Table 6-23). Distally, the rate of rise was also reduced (Table 6-24).

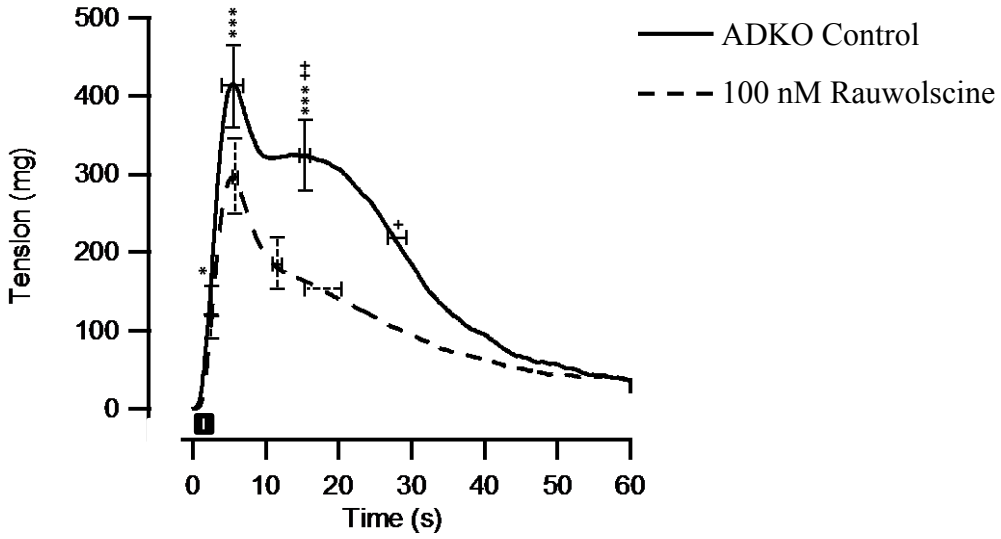

Figure 6-15: ADKO Proximal mouse tail artery response to nerve stimulation at 8 Hz in control vessels and in the presence of the α_2-AR antagonist rauwolscine (100 nM) (n = 12).

*** P < 0.05; *** P < 0.001 compared with control response. Paired t-test.**

+ P < 0.05; ++ P < 0.01 compared with control time. Paired t-test.

Table 6-23: ADKO Proximal mouse tail artery response to nerve stimulation in control and rauwolscine (100 nM) incubated vessels at 8 Hz.

Proximal 8 Hz	Contractile Response (average ± S.E.M)		
	Control	100 nM Rauwolscine (R) (n = 12)	% change following R incubation
Tension at End of pulse (mg)	148 ± 21	105 ± 14 *	- 25 ± 10
Time to Peak (seconds)	7.6 ± 1.6	4.9 ± 0.3	- 18 ± 8
Peak Tension (mg)	420 ± 63	309 ± 55 ***	- 29 ± 4
Rate of Rise (mg/s)	72 ± 12	60 ± 9	8 ± 20
Time to Peak (2nd) (seconds)	14.7 ± 0.7	11.2 ± 0.6 ++	- 22 ± 6
Peak Tension (2nd) (mg)	339 ± 54	181 ± 38 ***	- 49 ± 5
50 % Decay Time (seconds)	20.9 ± 1.4	11.8 ± 2.8 +	- 45 ± 11

*** P < 0.05; *** P < 0.001 compared with control response. Paired t-test.**

+ P < 0.05; ++ P < 0.01 compared with control time. Paired t-test.

Table 6-24: ADKO Distal mouse tail artery response to nerve stimulation in control and rauwolscine (100 nM) incubated vessels at 8 Hz.

Distal 8 Hz	Contractile Response (average ± S.E.M)		
	Control	100 nM Rauwolscine (R) (n = 14)	% change following R incubation
Tension at End of pulse (mg)	144 ± 19	109 ± 10	- 13 ± 10
Time to Peak (seconds)	6.2 ± 1.1	4.9 ± 0.1	- 9 ± 6
Peak Tension (mg)	407 ± 26	271 ± 21 ***	- 34 ± 3
Rate of Rise (mg/s)	78 ± 7	55 ± 4 ***	- 24 ± 7
Time to Peak (2nd) (seconds)	15.6 ± 0.6	12.6 ± 0.3 +++	- 18 ± 3
Peak Tension (2nd) (mg)	277 ± 17	131 ± 13 ***	- 53 ± 4
50 % Decay Time (seconds)	21.2 ± 1.6	8.6 ± 1.6 +++	- 51 ± 8

***** P < 0.001 compared with control response. Paired t-test.**

+++ P < 0.001 compared with control response. Paired t-test.

Under all conditions and at both proximal and distal segments, the rauwolscine sensitive component forms a large portion of the control response (Figure 6-16; Tables 6-21 and 6-22).

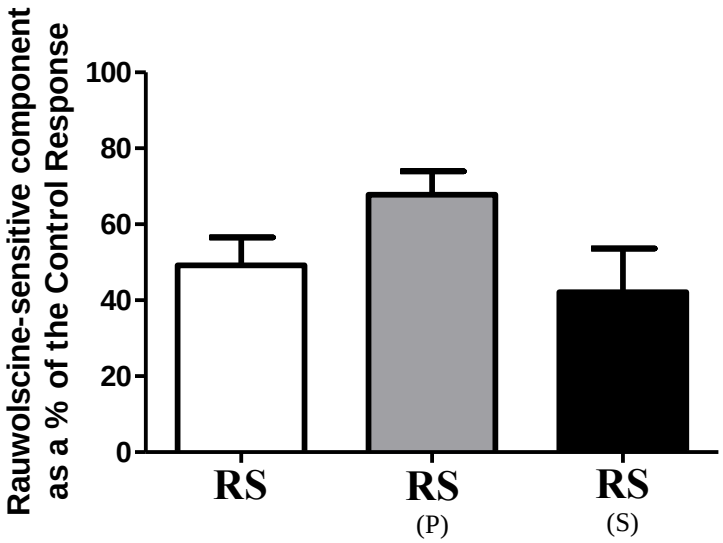

Figure 6-16: ADKO Proximal mouse tail – the rauwolscine sensitive (RS) component at 8 Hz when the P2X receptors and α_1-AR are functional (white) (n=12), α_1-ARs are blocked (light grey) (n=6), P2X receptors are blocked (dark grey) (n=7).

6.3.2.6 Revealing the P2X receptor role in the response to sympathetic nerve stimulation at 0.5 Hz.

In both proximal and distal segments, the peak tension and the tension at the end of the stimulation period were reduced by 1 mM suramin incubation. Additionally, in proximal segments, the first peak tension and the rate of rise were also reduced (Figure 6-17; Table 6-25 and 6-26).

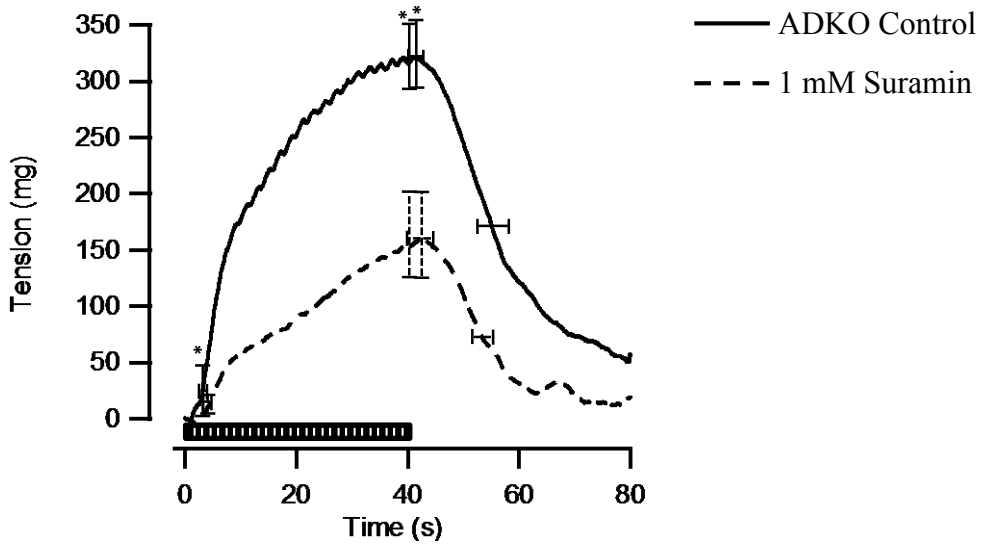

Figure 6-17: ADKO Proximal mouse tail artery response to nerve stimulation at 0.5 Hz in control vessels and in the presence of the P2X receptor antagonist suramin (1 mM) (n = 7).

*** P < 0.05 compared with control response. Paired t-test.**

Table 6-25: ADKO Proximal mouse tail artery response to nerve stimulation in control and suramin (1 mM) incubated vessels at 0.5 Hz.

Proximal 0.5 Hz	Contractile Response (average ± S.E.M)		
	Control	1 mM Suramin (S) (n = 7)	% change following S incubation
Time to Peak (1st) (seconds)	4.5 ± 0.5	4.3 ± 0.6	- 4 ± 15
Peak Tension (1st) (mg)	83 ± 25	17 ± 9 *	- 66 ± 18
Rate of Rise (mg/s)	16 ± 4	3 ± 1 *	- 73 ± 13
Time to Peak (seconds)	39.3 ± 1.3	36.8 ± 2.3	- 6 ± 6
Peak Tension (mg)	325 ± 35	162 ± 44 *	- 48 ± 15
Tension at End of pulse (mg)	316 ± 33	147 ± 43 *	- 51 ± 15
50 % Decay Time (seconds)	17.1 ± 3.0	16.4 ± 1.8	0.2 ± 12

*** P < 0.05 compared with control response. Paired t-test.**

Table 6-26: ADKO Distal mouse tail artery response to nerve stimulation in control and suramin (1 mM) incubated vessels at 0.5 Hz.

Distal 0.5 Hz	Contractile Response (average ± S.E.M)		
	Control	1 mM Suramin (S) (n = 7)	% change following S incubation
Time to Peak (1st) (seconds)	2.4 ± 0.3	3.0 ± 0.1	15 ± 12
Peak Tension (1st) (mg)	28 ± 12	9 ± 3	- 30 ± 22
Rate of Rise (mg/s)	10 ± 4	3 ± 1	- 50 ± 15
Time to Peak (seconds)	40.6 ± 1.6	42.3 ± 1.0	4 ± 2
Peak Tension (mg)	298 ± 55	214 ± 53 *	- 31 ± 11
Tension at End of pulse (mg)	286 ± 54	197 ± 51 *	- 33 ± 11
50 % Decay Time (seconds)	16.7 ± 1.3	11.9 ± 1.1	- 19 ± 8

*** P < 0.05 compared with control response. Paired t-test.**

In both proximal and distal segments the suramin sensitive component isolated when the α_1- and α_2-ARs were functional was greater in comparison to the other incubation conditions (Figure 6-18; Table 6-27 and 6-28).

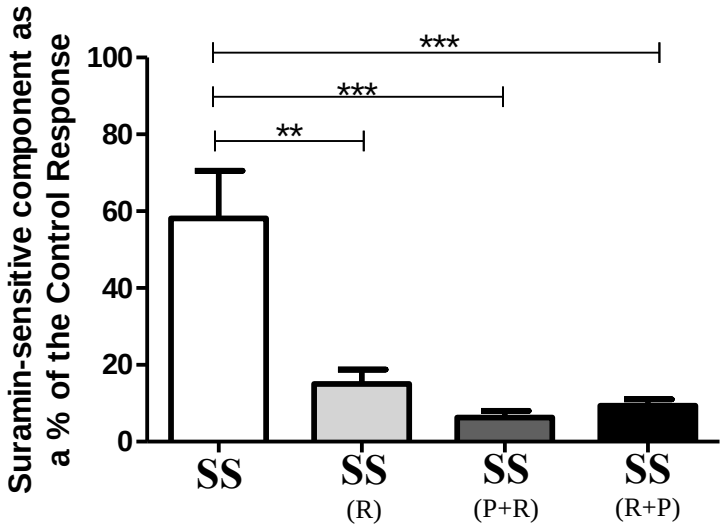

Figure 6-18: ADKO Proximal mouse tail – the suramin sensitive component at 0.5 Hz when the α_1- and α_2-ARs are functional (white) (n=7), α_2-ARs are blocked (light grey) (n=6), α_1- and α_2-ARs are blocked (dark grey) (n=6), α_2-ARs and α_1-ARs are blocked (black) (n=6).

**** P < 0.01; *** P < 0.001 compared with the SS component when the α_1-ARs and P2X receptors are functional. One way ANOVA with Bonferonni's post-test.**

Table 6-27: ADKO Proximal mouse tail artery response - the suramin-sensitive (SS) component as a % of control area under the curves. Data taken from Figures 6-18 and 6-20.

	Suramin-sensitive component as a % of the Control Response	
	0.5 Hz	**8 Hz**
SS	58 ± 14	46 ± 13
SS (R)	15 ± 4 **	33 ± 9
SS (P+R)	6 ± 2 ***	22 ± 4
SS (R+P)	9 ± 2 ***	24 ± 5

**** P < 0.01; ***** P < 0.001 compared with the SS component when the α_1- and α_2-ARs are functional. One way ANOVA with Bonferonni's post-test.**

Table 6-28: ADKO Distal mouse tail artery response - the suramin-sensitive (SS) component as a % of control area under the curves.

	Suramin-sensitive component as a % of the Control Response	
	0.5 Hz	**8 Hz**
SS	39 ± 10	60 ± 19
SS (R)	10 ± 3 **	23 ± 5
SS (P+R)	7 ± 1 ***	20 ± 5
SS (R+P)	10 ± 1 **	23 ± 2

**** P < 0.01; ***** P < 0.001 compared with the SS component when the α_1- and α_2-ARs are functional. One way ANOVA with Bonferonni's post-test.**

6.3.2.7 Revealing the P2X receptor role in the response to sympathetic nerve stimulation at 8 Hz.

The response to nerve stimulation at 8 Hz in proximal and distal tail artery segments was significantly altered in the presence of 1 mM suramin. Both the peak tension and the rate of rise were significantly reduced (Table 6-30). Additionally, in proximal segments, the tension at the end of the stimulation period was reduced and the time to reach the second peak was prolonged (Figure 6-19; Table 6-29).

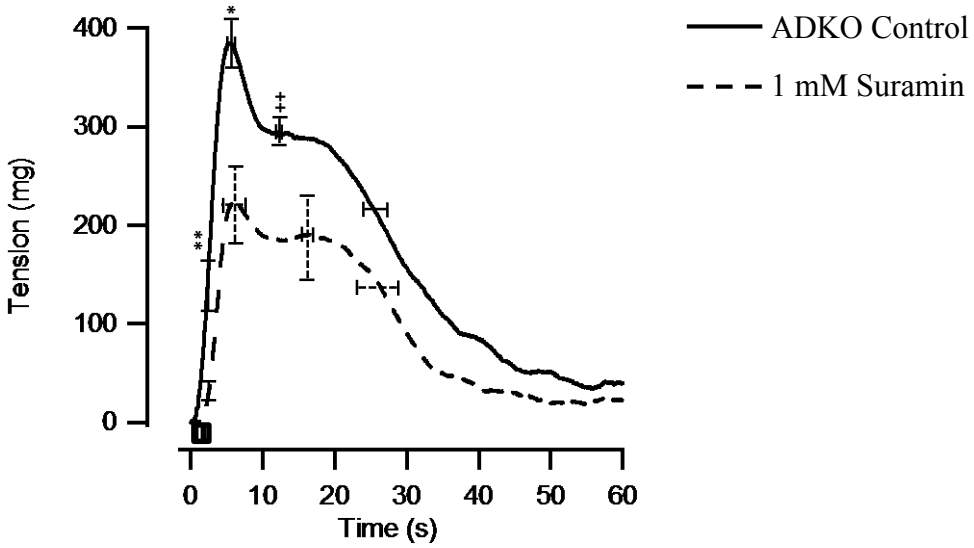

Figure 6-19: ADKO Proximal mouse tail artery response to nerve stimulation at 8 Hz in control vessels and in the presence of the P2X receptor antagonist suramin (1 mM) (n = 7).

*** P < 0.05, ** P < 0.01 compared with control response. Paired t-test.**

++ P < 0.01 compared with control time. Paired t-test.

Table 6-29: ADKO Proximal mouse tail artery response to nerve stimulation in control and suramin (1 mM) incubated vessels at 8 Hz.

Proximal 8 Hz	Contractile Response (average ± S.E.M)		
	Control	1 mM Suramin (S) (n = 7)	% change following S incubation
Tension at End of pulse (mg)	160 ± 29	31 ± 10 **	- 78 ± 7
Time to Peak (seconds)	5.5 ± 0.4	7.6 ± 1.8	17 ± 9
Peak Tension (mg)	394 ± 28	232 ± 46 *	- 41 ± 12
Rate of Rise (mg/s)	76 ± 9	34 ± 7 **	- 55 ± 8
Time to Peak (2nd) (seconds)	11.9 ± 0.3	14.8 ± 0.8 ++	18 ± 5
Peak Tension (2nd) (mg)	290 ± 15	192 ± 49	- 36 ± 16
50 % Decay Time (seconds)	21.0 ± 1.9	15.3 ± 3.2	- 32 ± 13

*** P < 0.05; ** P < 0.01 compared with control response. Paired t-test.**

++ P < 0.01 compared with control time. Paired t-test.

Table 6-30: ADKO Distal mouse tail artery response to nerve stimulation in control and suramin (1 mM) incubated vessels at 8 Hz.

Distal 8 Hz	Contractile Response (average ± S.E.M)		
	Control	1 mM Suramin (S) (n = 7)	% change following S incubation
Tension at End of pulse (mg)	100 ± 34	37 ± 6	- 36 ± 18
Time to Peak (seconds)	5.8 ± 0.4	5.7 ± 0.4	- 2 ± 6
Peak Tension (mg)	335 ± 57	243 ± 51 **	- 30 ± 7
Rate of Rise (mg/s)	59 ± 11	41 ± 7 *	- 29 ± 4
Time to Peak (2^{nd}) (seconds)	15.3 ± 0.7	14.4 ± 0.9	- 6 ± 4
Peak Tension (2^{nd}) (mg)	270 ± 47	199 ± 49	- 29 ± 12
50 % Decay Time (seconds)	17.2 ± 0.8	21.8 ± 2.4	- 4 ± 8

*** P < 0.05, ** P < 0.01 compared with control response. Paired t-test.**

At both proximal and distal segments there was a trend for the suramin sensitive component when the α_1- and α_2-ARs were functional to be greater than the other components. However, this did not reach significance (Figure 6-20; Table 6-27 and 6-28).

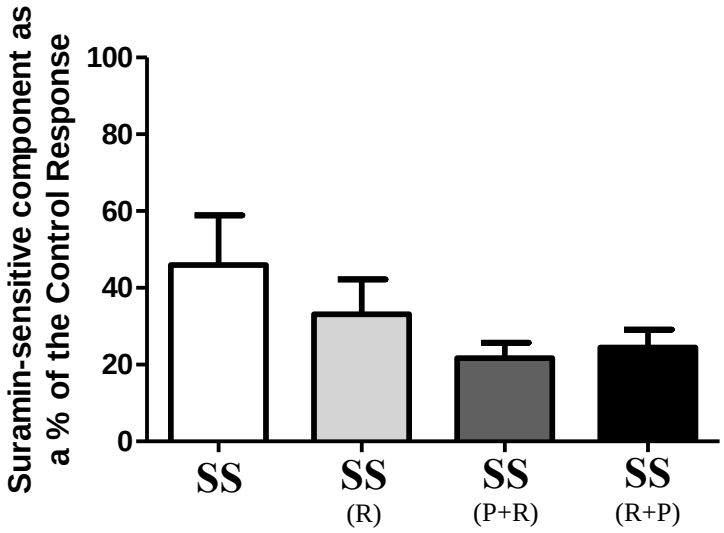

Figure 6-20: ADKO Proximal mouse tail – the suramin sensitive component at 8 Hz when the α_1- and α_2-ARs are functional (white) (n=7), α_2-ARs are blocked (light grey) (n=6), α_1- and α_2-ARs are blocked (dark grey) (n=6), α_2-ARs and α_1-ARs are blocked (black) (n=6).

6.4 Discussion

The present study was set out to investigate the effect genetic removal of the α_{1A}- and α_{1D}-ARs had on the response to nerve stimulation. Furthermore, the ADKO allows isolation of the α_{1B}-ARs, of which little is known of its role in the vasculature.

6.4.1 Mouse Mesenteric Arteries

6.4.1.1 Comparison with WT response

The loss of the α_{1AD}-ARs has an effect at both frequencies. This supports previous knowledge of the α_1-ARs dominating the contraction in the mesenteric arteries (Sjoblom-Widfeldt et al., 1990) and in particular, the α_{1A}-ARs (Methven et al., 2009a). The response in the ADKO vessels, which still display a fast onset, of transmitter induced contraction, may be due to activation of the remaining α_{1B}-ARs or the α_2-ARs and P2X receptors. In the WT, the response was due mainly to activation of the α_1-ARs with a definite P2X receptor component and a minor post-junctional α_2-AR influence.

6.4.1.2 ADKO Control Response to Nerve Stimulation

Blockade of the α_{1B}-ARs, α_2-ARs and P2X receptors abolished the response to nerve stimulation at both frequencies. Therefore, loss of the α_{1AD}-ARs has not resulted in the emergence of a different receptor influence.

6.4.1.3 Receptor Role in Mouse Mesenteric Arteries

As the responses to nerve stimulation were small, the response following treatment with any one of the antagonists did not reduce the response at 2 Hz. In some instances, even incubating the vessels with all three antagonists did not produce a significant reduction in response. This was most likely due to the size of the response which produced large error bars. However, there were some incubation sequences where treatment with two or three antagonists did affect the response. When the vessels were incubated with suramin and then rauwolscine, to block the P2X receptors and α_2-ARs respectively, the rate of rise and 50 % decay time were reduced. This suggests a combined role for these receptors in initiating the response and ensuring the response continued beyond the end of the stimulation period. When the vessels were incubated with all three antagonists there were examples of reduced tension at the end of the stimulation period, decreased rate of rise and a prolonged time to reach each peak. The results at 2 Hz suggest that the vessels require interactions between at least two receptor types before the vessels can contract. This differs from the WT results shown in Chapter Five, where the α_1-ARs dominated the contraction regardless of the presence of the other receptors.

At 8 Hz, the response to nerve stimulation was greater and individual antagonist effects were recorded. The results suggest little α_{1B}-AR influence as vessel incubation with prazosin did not alter the response. When the vessels were incubated with rauwolscine, the time taken to reach the peak response was reduced. Interestingly, this effect is opposite to the WT response. This is most likely due to the loss of active post-junctional α_1-ARs as increased transmitter output following pre-junctional α_2-AR block will have fewer receptors to act at. The response to vessel incubation with suramin was similar to that in the WT; reducing the peak tension, the tension at the end of the stimulation period and the rate of rise. Therefore, in the ADKO mesenteric arteries, there is little role for the α_{1B}-ARs, the α_2-ARs are mainly pre-junctional and the P2X receptors are the main receptors involved in vessel contraction.

6.4.2 Mouse Proximal and Distal Tail Artery

Similar to the WT results, the ADKO data from only one location of the tail is shown and only discrepancies between the segments are shown. When comparing WT with ADKO response, the proximal results were used.

6.4.2.1 Comparison with WT response

At 0.5 Hz and 8 Hz, the ADKO vessels responded to nerve stimulation. At 0.5 Hz the ADKO response took longer to reach the first peak compared to the WT response and the tension at this peak was greater in the ADKO; although this is not clear from the Figure (6-7). The time for the peak response to decay by 50 % was prolonged in the ADKOs. These results suggest that the α_{1AD}-ARs are important in initiating the contraction and ensuring vessel relaxation. At 8 Hz, the loss of the α_{1AD}-ARs is seen more clearly on the response. All of the recorded tensions in the ADKO were reduced and the time to reach the second peak and the decay time were prolonged compared to the WT control response. This would suggest the α_{1AD}-ARs are important in the over-all response to nerve stimulation; contributing to the initiation and maintenance of the response.

6.4.2.2 α_{1B}-AR role in Mouse Tail Artery

The effect of prazosin treatment was examined in the ADKO mice whereby prazosin should effectively block the remaining α_{1B}-ARs. At 0.5 Hz, there was no noticeable change in the peak tension. However, a reduction in the time taken to reach the first peak tension and a reduced tension at this peak revealed a role for the α_{1B}-ARs at the beginning of the contraction. The results suggest a modulatory or inhibitory role for these receptors which is not shown in the WT prazosin incubated vessels. The α_{1B}-ARs have been described previously as having a modulatory role (Deighan et al., 2005) in response in the mouse carotid arteries. Therefore, presently, the α_{1B}-AR modulatory role may be revealed due to

loss of the α_{1AD}-ARs and, under normal conditions, these three subtypes may be in a balance. This also appears to be true of the systolic blood pressure measurements as described in Chapter Three. As was shown in the WT results, the available α_1-AR subtypes can interact with the other receptors and when these receptors are active the prazosin sensitive component of the response is larger.

At 8 Hz, the α_{1B}-ARs are shown to be involved in initiation of the contraction as the time taken to reach the peak is prolonged and the peak tension is reduced following prazosin treatment. The initiation of the contractile response via α_{1B}-ARs has been suggested previously in the mouse tail artery (Daly et al., 1998). The small prazosin sensitive component does not differ regardless of which of the other receptors are active and so do not depend on the α_2-ARs or P2X receptors to produce this response. This is different to the WT response where the α_1-ARs did interact with the α_2-ARs suggesting that this interaction occurred between the α_{1A}- or α_{1D}-ARs.

6.4.2.3 α_2-AR role in Mouse Tail Artery

Similar to the WT results, the main receptors involved in vessel contraction in the ADKOs were the α_2-ARs. In the WT, each of the points studied at 0.5 Hz were altered following rauwolscine treatment whereas in the ADKO the time taken to reach the peak and the decay time were unaffected by rauwolscine treatment. This again highlights an interaction between the α_{1AD}-ARs and the α_2-ARs which is lost in the ADKOs. The presence of pre-junctional α_2-ARs was evident as rauwolscine treatment reduced the time taken to reach the first peak. The potential for an interaction between the α_2-ARs and P2X receptors was revealed by analyses of the rauwolscine sensitive components of the response. The component was greater when the P2X receptors were active compared to when they have been blocked by suramin.

At 8 Hz, the ADKO response to rauwolscine treatment was similar to the WT response. However, the tension at the end of the stimulation period, which occurred at 2.5 seconds, was reduced in the ADKO but not the WT mice. In the WT vessels the reduction in response

occurred due to prazosin treatment and so in the ADKO, the α_2-AR effect may be compensatory. Furthermore, at 8 Hz, activation of the α_2-ARs occurred independently of the other receptors and was the main receptor involved in vessel contraction.

6.4.2.4 P2X receptor role in Mouse Tail Artery

When the ADKO tail artery segments were incubated with suramin, the reduction in response at 0.5 Hz appears to be greater than that shown in the WT vessels. In the WT, the P2X receptors are responsible for initiation of the response whereas in the ADKO, activation of P2X receptors accounts for the overall contraction. However, this influence on the contraction of the vessel is dependent on the presence of active α_2-ARs as blockade of these receptors reduced the suramin sensitive component of the response. As this interaction was not revealed in the WT vessels, it could represent a compensatory mechanism for the loss of the α_{1AD}-ARs which were shown to interact with the α_2-ARs in the WT vessels.

At 8 Hz, the response following suramin treatment was similar to that shown in the WT results confirming a role for the P2X receptors in initiation of the response. Unlike at 0.5 Hz, and the WT results, the suramin sensitive component at 8 Hz in the ADKO was similar regardless of which of the other receptors were active thus suggesting the P2X receptor response occurs independently.

6.4.3 Conclusion

In summary, the presence of α_{1B}-ARs, α_2-ARs and P2X receptors has been confirmed in the both mouse mesenteric arteries and tail artery in ADKO mice. The isolation of the α_{1B}-AR subtype allowed its role in the response to be elucidated. Although activation of these receptors did not contribute greatly to the contractile response, there was evidence to suggest these receptors are involved in initiation of the contraction and, at the lower frequency they can interact with the α_2-ARs. In comparison with the WT results, loss of the α_{1AD}-ARs is more clearly shown in the mesenteric arteries. This is understandable as the WT results show

the α_1-ARs predominate in the mesentery and the α_2-ARs in the tail. Evidence of compensatory mechanisms are shown in the tail artery. At 0.5 Hz, in the WT tail artery, the α_1- and α_2-ARs interacted and this enhanced the α_1-AR response. In the ADKO, this relationship occurred instead between the α_2-ARs and P2X receptors. Furthermore, at 8 Hz, the initiation of the contraction in WT segments was due, in part, to activation of α_1-ARs and this is lost in the ADKO. However, it appears that this role is supported by the α_2-ARs in the ADKO vessels. In conclusion, the development of the ADKO strain simplified the pharmacology somewhat and revealed the potential for compensatory mechanisms. These results can now be studied alongside the α_1-null and WT results in order to determine the effects removal of all three AR subtypes has on the nerve response.

Chapter Seven

Comparison of pharmacological blockade of nerve-evoked contractions in tail and mesenteric arteries of WT and α_1-null mice

7.1 Introduction

The previous two chapters have highlighted the roles of the α_1-, α_2-ARs and P2X receptors in response to sympathetic nerve stimulation. Chapter Five characterised the roles these receptors play in the WT and Chapter Six discussed the effects removal of two of the α_1-AR subtypes had on the response. These results can now be compared with those presented here where mice lacking all three α_1-AR subtypes have been utilised.

Evidence has been shown in the rat and mouse vessels to support the findings shown in Chapters five and six; that the pharmacology in mouse mesenteric and tail arteries is complex, due to multiple receptors available and receptor interactions (Brock et al., 2006; Bao and Stjarne, 1993; Methven et al., 2009a). The development of transgenic mice lacking at least one of the α_1-AR subtypes aims to simplify the pharmacology. In the ADKO mice, where only the α_{1B}-ARs are present, the response in the mesenteric arteries is dramatically reduced, demonstrating that there is no mechanism able to fully compensate for the loss of the α_{1A}- and α_{1D}-ARs. A role in initiation of the contraction was revealed for the α_{1B}-ARs (see Chapter Six). The α_{1B}-AR has previously been reported as playing a modulatory role in the vasculature (Daly et al., 2002) and so the development of the ADKO has allowed a previously unknown mechanism to be revealed. There was no evidence of compensatory mechanisms. Loss of the α_{1AD}-ARs does affect responses in the tail artery but not to the same degree as in the mesenteric arteries. The α_{1B}-ARs are also shown here to contribute to the initiation of the response (Chapter Six). Furthermore, the results presented in Chapter Three show that loss of α_1-AR activation via genetic deletion of the receptors does not alter systolic blood pressure in these mice. Therefore, the results presented thus far offer conflicting evidence on the importance of the α_1-ARs in the vasculature. The blood pressure results suggest little requirement of the α_1-ARs in order to maintain a normal blood pressure. A minor change in the overall response to nerve stimulation in ADKO tail artery supports this. However, the change in response to nerve stimulation in the mesenteric arteries of ADKO mice compared with WT suggests a large input from the α_1-ARs in maintaining vascular tone.

Presently, mice lacking all three AR subtypes (α_1-null) have been utilised and the responses to nerve stimulation in mesenteric and tail arteries studied. These experiments have not been performed elsewhere and so the results should allow a greater understanding into the role the α_1-ARs play in response to nerve stimulation. Therefore the aims of the following study were:

- To determine whether loss of the α_1-ARs prevents the response to nerve stimulation in the mouse mesenteric or tail arteries from occurring.
- To investigate the difference in response between WT, ADKO and α_1-null mesenteric and tail arteries.
- To determine whether there are any changes in the interactions between the receptors compared to those seen in the WT responses and therefore establish any compensatory mechanisms.

7.2 Methods

A full description of the methods used can be found in Chapter Two (Materials and Methods). Briefly, vessels were set up in myograph baths between two stimulating electrodes incubated with 1 µM capsaicin and with control responses to 2 Hz and 8 Hz (mesenteric arteries) and 0.5 Hz and 8 Hz (tail artery) recorded before incubation with one of the following antagonists: 100 nM prazosin (α_1-AR antagonist), 100 nM rauwolscine (α_2-AR antagonist) or 1 mM suramin (P2X receptor antagonist). The vessels were then stimulated again using the same parameters.

Statistical analysis was performed using GraphPad Prism (Version 5) with paired t-tests used when comparing control response with antagonist response and one way ANOVA with Bonferonni's post-test utilised for comparing the antagonist sensitive components. A worked example of the component analysis, which revealed the antagonist sensitive response in difference incubation sequences is shown at the beginning of the mesenteric and tail artery results sections in Chapter Five. The analyses of the antagonist sensitive components was only conducted in the tail artery responses as the mesenteric artery responses were too small to produce reliable statistics.

7.3 Results

7.3.1 Mesenteric Artery

7.3.1.1 Comparison of WT and α1-null response to nerve stimulation.

Both WT and α_1-null mesenteric arteries responded to nerve stimulation at 2 Hz and 8 Hz (Figure 7-1 and 7-2). At both frequencies the peak tension and the tension at the end of the stimulation periods were significantly reduced in the α_1-null mice. At 2 Hz, the time to reach the peak tension and the time to 50 % decay was also significantly altered in the α_1-null mice (Figure 7-1 and 7-2; Tables 7-1 and 7-2).

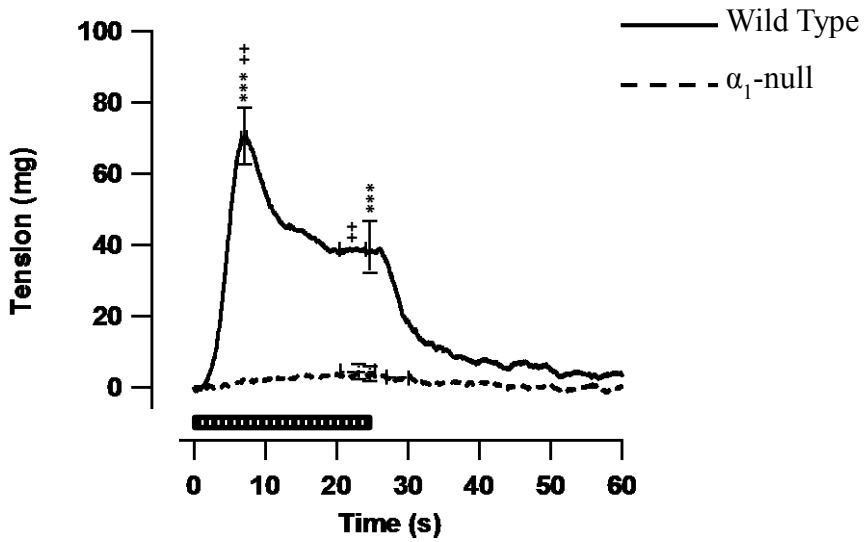

Figure 7-1: WT and α_1-null mouse mesenteric arteries - response to nerve stimulation at 2 Hz (WT: n=17; α_1-null: n=20).

***** P < 0.001 compared with WT response. Un-paired t-test.**

++ P < 0.01 compared with WT time. Un-paired t-test.

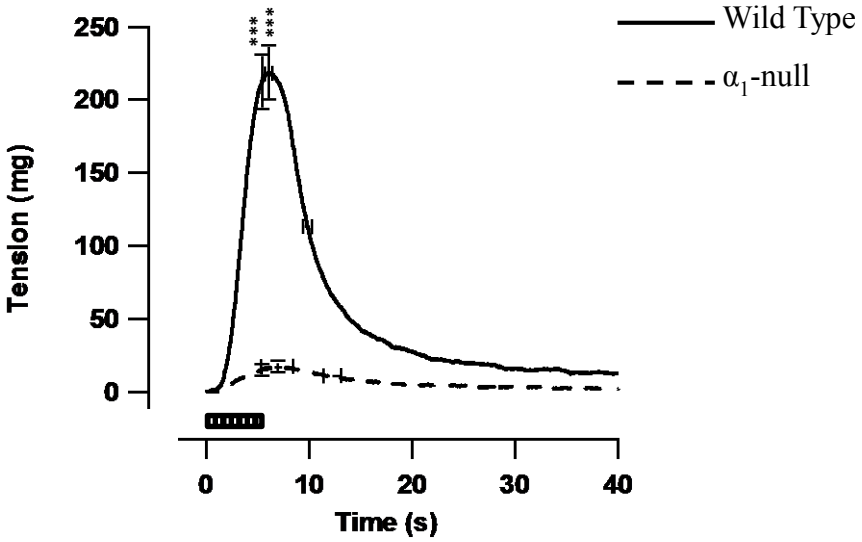

Figure 7-2: WT and α_1-null mouse mesenteric arteries - response to nerve stimulation at 8 Hz (WT: n=17; α_1-null: n=20).

***** P < 0.001 compared with WT response. Un-paired t-test.**

Table 7-1: WT and α_1-null mouse mesenteric arteries - response to nerve stimulation at 2 Hz.

2 Hz	Contractile Response (average ± S.E.M)	
	WT (n=17)	α_1-null (n=20)
Time to Peak (seconds)	7.2 ± 0.2	17.1 ± 2.9 ++
Peak Tension (mg)	72 ± 9	9 ± 2 ***
Rate of Rise (mg/s)	10 ± 1	4 ± 3
Tension at End of pulse (mg)	38 ± 8	3 ± 2 ***
50 % Decay Time (seconds)	12.2 ± 2.0	4.7 ± 1.6 ++

***** P < 0.001 compared with WT response. Un-paired t-test.**

++ P < 0.01 compared with WT time. Un-paired t-test.

Table 7-2: WT and α_1-null mouse mesenteric arteries - response to nerve stimulation at 8 Hz.

8 Hz	Contractile Response (average ± S.E.M)	
	WT (n=17)	**α_1-null (n=20)**
Time to Peak (seconds)	6.0 ± 0.2	7.7 ± 1.7
Peak Tension (mg)	223 ± 20	20 ± 4 ***
Rate of Rise (mg/s)	37 ± 3	3 ± 1 ***
Tension at End of pulse (mg)	215 ± 20	16 ± 4 ***
50 % Decay Time (seconds)	4.1 ± 0.3	4.3 ± 0.8

***** P < 0.001 compared with WT response. Un-paired t-test.**

Combined incubation with prazosin (100 nM), rauwolscine (100 nM) and suramin (1 mM) effectively blocked the α_1-, α_2-ARs and P2X receptors respectively in response to nerve stimulation at 2 Hz and 8 Hz in the KO mesenteric arteries and completely abolished the response (Figures 7-3 and 7-4). Figure 7-4 displays the effect of incubation with prazosin, rauwolscine and suramin on the response at 8 Hz. Although there is a response left following block of the α_1-, α_2-ARs and P2X receptors it is very small, as indicated by the y-axis values.

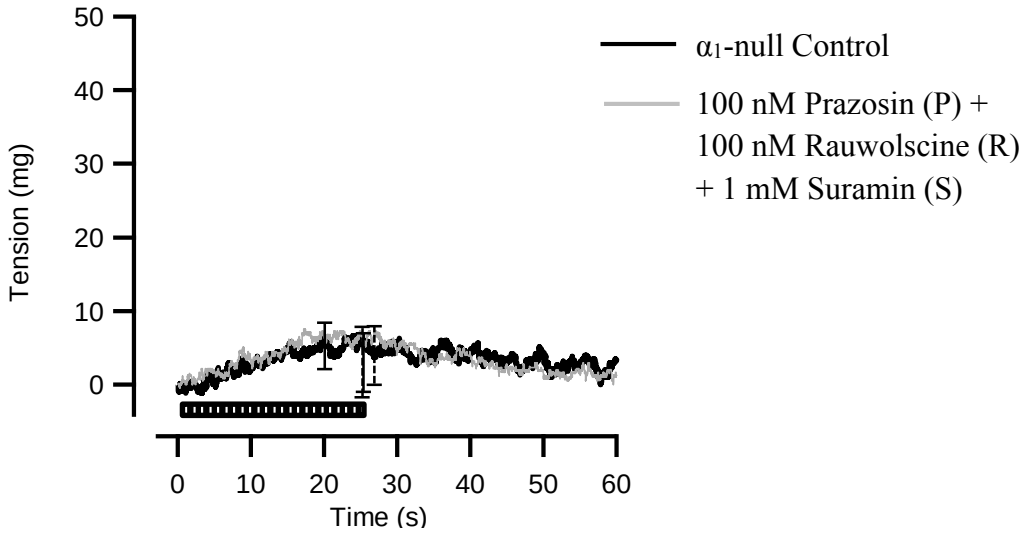

Figure 7-3: α_1-null Mouse mesenteric artery response to nerve stimulation at 2 Hz in control vessels and in the presence of the following antagonists: 100 nM prazosin, 100 nM rauwolscine, 1 mM suramin (n = 6).

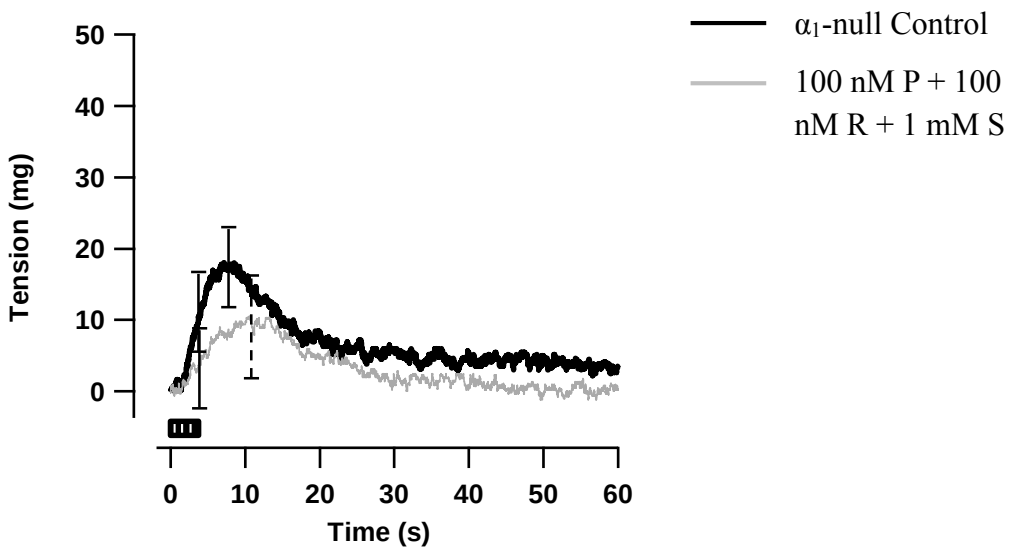

Figure 7-4: α_1-null Mouse mesenteric artery response to nerve stimulation at 8 Hz in control vessels and in the presence of the following antagonists: 100 nM prazosin, 100 nM rauwolscine, 1 mM suramin (n = 6).

7.3.1.2 Revealing the response to sympathetic nerve stimulation at 2 Hz.

Individual incubations with 100 nM prazosin, 100 nM rauwolscine and 1 mM suramin did not result in a significant change in the response compared with the control response (Figure 7-5; Tables 7-3 – 7-5).

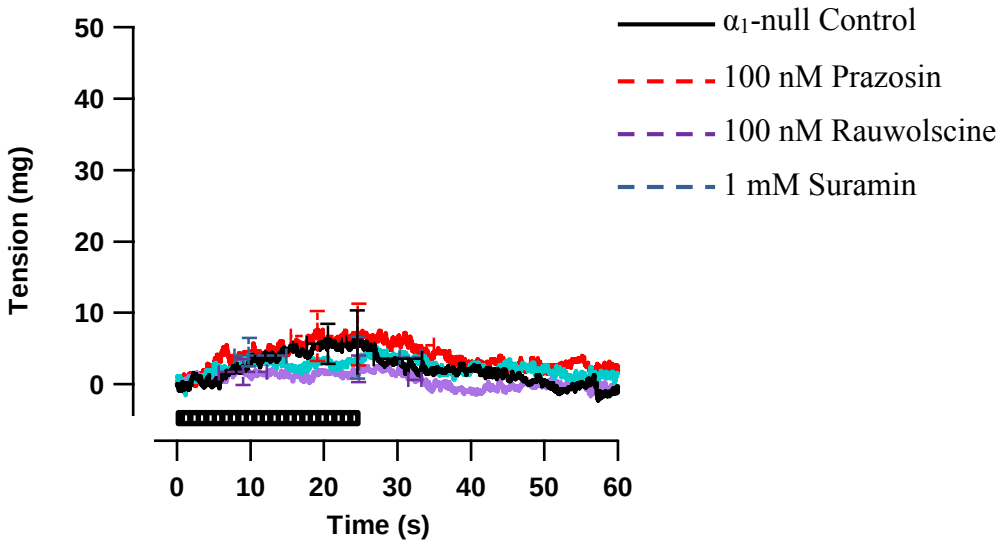

Figure 7-5: α_1-null Mouse mesenteric artery response to nerve stimulation at 2 Hz in control vessels and in the presence of 100 nM prazosin (red) (n=6); 100 nM rauwolscine (purple) (n=7); 1 mM suramin (blue) (n=7).

Table 7-3: α_1-null Mouse mesenteric artery response to nerve stimulation in control and prazosin (100 nM) incubated vessels at 2 Hz.

2 Hz	Contractile Response (average ± S.E.M)		
	Control	100 nM Prazosin (P) (n = 6)	% change following P incubation
Time to Peak (seconds)	24.0 ± 5.5	17.4 ± 4.4	- 8 ± 24
Peak Tension (mg)	11 ± 4	11 ± 4	3 ± 16
Rate of Rise (mg/s)	4 ± 3	1 ± 0.3	- 2 ± 26
Tension at End of pulse (mg)	6 ± 5	6 ± 5	- 49 ± 19
50 % Decay Time (seconds)	4.2 ± 2.8	4.1 ± 3.3	- 3 ± 20

Table 7-4: α_1-null Mouse mesenteric artery response to nerve stimulation in control and rauwolscine (100 nM) incubated vessels at 2 Hz.

2 Hz	Contractile Response (average ± S.E.M)		
	Control	100 nM Rauwolscine (R) (n = 7)	% change following R incubation
Time to Peak (seconds)	13.6 ± 5.3	8.7 ± 3.6	- 19 ± 27
Peak Tension (mg)	4 ± 1	6 ± 2	10 ± 19
Rate of Rise (mg/s)	7 ± 7	2 ± 1	29 ± 26
Tension at End of pulse (mg)	- 1 ± 3	2 ± 2	- 24 ± 44
50 % Decay Time (seconds)	2.0 ± 1.5	1.2 ± 0.8	- 8 ± 28

Table 7-5: α_1-null Mouse mesenteric artery response to nerve stimulation in control and suramin (1 mM) incubated vessels at 2 Hz.

2 Hz	Contractile Response (average ± S.E.M)		
	Control	1 mM Suramin (S) (n = 7)	% change following S incubation
Time to Peak (seconds)	14.5 ± 3.9	10.3 ± 3.8	- 38 ± 14
Peak Tension (mg)	11 ± 3	8 ± 2	- 1 ± 20
Rate of Rise (mg/s)	2 ± 1	8 ± 5	26 ± 24
Tension at End of pulse (mg)	6 ± 5	4 ± 3	- 62 ± 17
50 % Decay Time (seconds)	7.7 ± 3.6	2.2 ± 1.5	- 9 ± 26

Regardless of antagonist incubation sequence or the number of antagonists incubated at the one time, the response to nerve stimulation at 2 Hz in the mesenteric arteries was not significantly changed.

7.3.1.3 Revealing the response to sympathetic nerve stimulation at 8 Hz.

Individual incubations with either prazosin or rauwolscine did not result in a significant change in the response compared with the control response (Figure 7-6; Tables 7-6 and 7-7). However, incubation with 1 mM suramin significantly reduced the force of contraction at the end of the stimulation period and the rate of rise (Figure 7-6; Table 7-8).

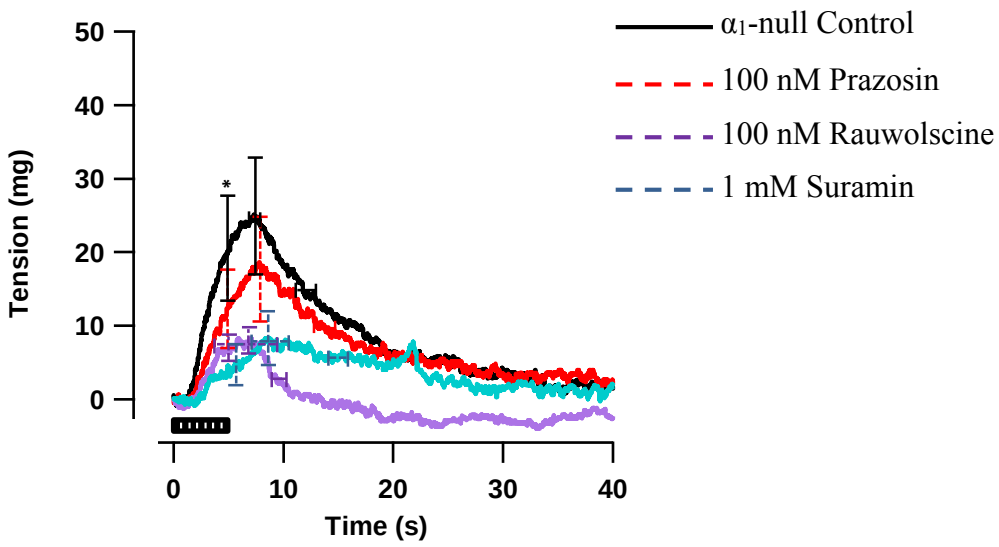

Figure 7-6: α_1-null Mouse mesenteric artery response to nerve stimulation at 8 Hz in control vessels and in the presence of 100 nM prazosin (red) (n=6); 100 nM rauwolscine (purple) (n=7); 1 mM suramin (blue) (n=7).

*** P < 0.05 refers to significant difference between control response at the end of the stimulation period and the response following 1 mM suramin at the same point.**

Table 7-6: α_1-null Mouse mesenteric artery response to nerve stimulation in control and prazosin (100 nM) incubated vessels at 8 Hz.

8 Hz	Contractile Response (average ± S.E.M)		
	Control	100 nM Prazosin (P) (n = 6)	% change following P incubation
Time to Peak (seconds)	7.8 ± 1.6	5.9 ± 1.0	- 9 ± 17
Peak Tension (mg)	22 ± 6	20 ± 8	- 24 ± 16
Rate of Rise (mg/s)	3 ± 1	3 ± 1	- 7 ± 15
Tension at End of pulse (mg)	16 ± 6	15 ± 6	- 3 ± 15
50 % Decay Time (seconds)	4.8 ± 1.5	4.3 ± 1.2	- 16 ± 24

Table 7-7: α_1-null Mouse mesenteric artery response to nerve stimulation in control and rauwolscine (100 nM) incubated vessels at 8 Hz.

8 Hz	Contractile Response (average ± S.E.M)		
	Control	100 nM Rauwolscine (R) (n = 7)	% change following R incubation
Time to Peak (seconds)	9.8 ± 4.6	9.4 ± 4.7	- 5 ± 25
Peak Tension (mg)	11 ± 3	9 ± 3	- 17 ± 12
Rate of Rise (mg/s)	2 ± 1	2 ± 0.5	- 3 ± 25
Tension at End of pulse (mg)	8 ± 3	8 ± 2	- 1 ± 21
50 % Decay Time (seconds)	3.7 ± 1.3	2.8 ± 0.9	0.4 ± 32

Table 7-8: α_1-null Mouse mesenteric artery response to nerve stimulation in control and suramin (1 mM) incubated vessels at 8 Hz.

8 Hz	Contractile Response (average ± S.E.M)		
	Control	1 mM Suramin (S) (n = 7)	% change following S incubation
Time to Peak (seconds)	5.5 ± 0.7	12.6 ± 2.7	41 ± 13
Peak Tension (mg)	28 ± 9	13 ± 4	- 25 ± 21
Rate of Rise (mg/s)	4 ± 1	1 ± 0.4 *	- 60 ± 12
Tension at End of pulse (mg)	23 ± 8	4 ± 3 *	- 67 ± 18
50 % Decay Time (seconds)	4.6 ± 1.4	3.5 ± 1.4	- 31 ± 22

*** P < 0.05 compared with control response. Paired t-test.**

When the mesenteric arteries were incubated with more than one antagonist, there were more significant changes in the response compared to incubation with one antagonist (Table 7-9).

Table 7-9: The significant changes to the response at 8 Hz when incubation was with more than one antagonist.

8 Hz	Contractile Response (average ± S.E.M)		
Part of response affected by antagonist incubation	Antagonist Incubation sequence		
	1 mM S + 100 nM R	1 mM S, 100 nM R + 100 nM P	100 nM P, 100 nM R + 1 mM S
Rate of Rise (mg/s)	*	*	-
Tension at End of pulse (mg)	*	*	*

*** P < 0.05 compared with control response. Paired t-test.**

7.3.2 Proximal and Distal Mouse Tail Artery

7.3.2.1 Comparison of WT and α_1-null response to nerve stimulation.

Both WT and α_1-null tail artery responded to nerve stimulation at 0.5 Hz and 8 Hz (Figure 7-7 and 7-8). At both frequencies the peak tension and the tension at the end of the stimulation periods were significantly reduced and the decay time was prolonged in the α_1-null mice. At 8 Hz, all of the points studied were significantly altered in the α_1-null mice (Figure 7-7 and 7-8; Tables 7-10 and 7-11).

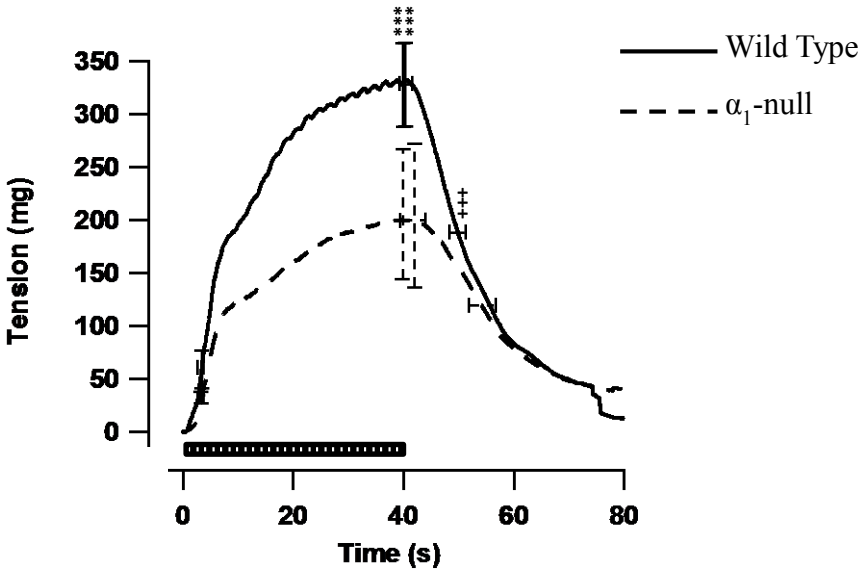

Figure 7-7: WT and α_1-null mouse tail artery - response to nerve stimulation at 0.5 Hz (WT: n=26; α_1-null: n=24).

***** P < 0.001 compared with WT response. Un-paired t-test.**

+++ P < 0.001 compared with WT time. Un-paired t-test.

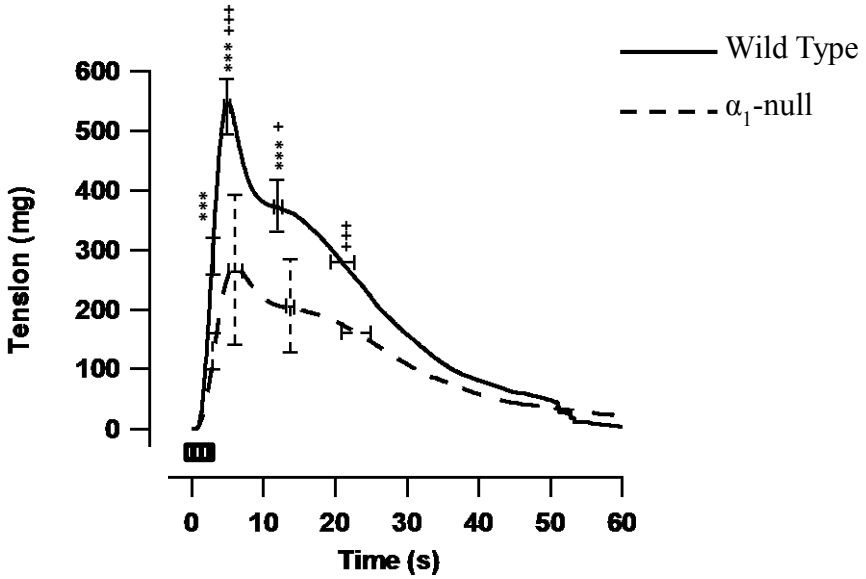

Figure 7-8: WT and α_1-null mouse tail artery - response to nerve stimulation at 8 Hz (WT: n=26; α_1-null: n=24).

***** P < 0.001 compared with WT response. Un-paired t-test.**

+ P < 0.05; +++ P < 0.001 compared with WT time. Un-paired t-test.

Table 7-10: WT and α_1-null mouse tail artery - response to nerve stimulation at 0.5 Hz.

0.5 Hz	Contractile Response (average ± S.E.M)	
	WT (n=26)	α_1-null (n=24)
Time to Peak (1st) (seconds)	2.6 ± 0.2	2.9 ± 0.2
Peak Tension (1st) (mg)	34 ± 7	21 ± 5
Rate of Rise (mg/s)	16 ± 3	9 ± 1 *
Time to Peak (seconds)	37.2 ± 1.0	38.0 ± 0.9
Peak Tension (mg)	338 ± 27	213 ± 20 ***
Tension at End of pulse (mg)	327 ± 26	206 ± 20 ***
50 % Decay Time (seconds)	12.8 ± 0.9	19.4 ± 1.3 +++

*** P < 0.05; *** P < 0.001 compared with WT response. Un-paired t-test.**

+++ P < 0.01 compared with WT time. Un-paired t-test.

Table 7-11: WT and α_1-null mouse tail artery - response to nerve stimulation at 8 Hz.

8 Hz	Contractile Response (average ± S.E.M)	
	WT (n=26)	α_1-null (n=24)
Tension at End of pulse (mg)	210 ± 19	88 ± 14 ***
Time to Peak (seconds)	5.0 ± 0.1	7.3 ± 0.5 +++
Peak Tension (mg)	552 ± 32	280 ± 29 ***
Rate of Rise (mg/s)	114 ± 6	43 ± 5 ***
Time to Peak (2nd) (seconds)	11.8 ± 0.3	13.7 ± 6 +
Peak Tension (2nd) (mg)	372 ± 29	214 ± 21 ***
50 % Decay Time (seconds)	13.7 ± 1.0	20.0 ± 1.4 +++

***** P < 0.001 compared with WT response. Un-paired t-test.**

+ P < 0.05; +++ P < 0.001 compared with WT time. Un-paired t-test.

7.3.2.2 Revealing the effect of prazosin on the response to sympathetic nerve stimulation at 0.5 Hz.

In proximal mouse tail artery, 100 nM prazosin incubation only significantly affects the rate of rise (Table 7-12). However in distal segments, 100 nM prazosin incubation results in a

prolonged time to reach the first peak and both the peak tension and the tension at the end of the stimulation period are significantly reduced (Figure 7-9; Table 7-13).

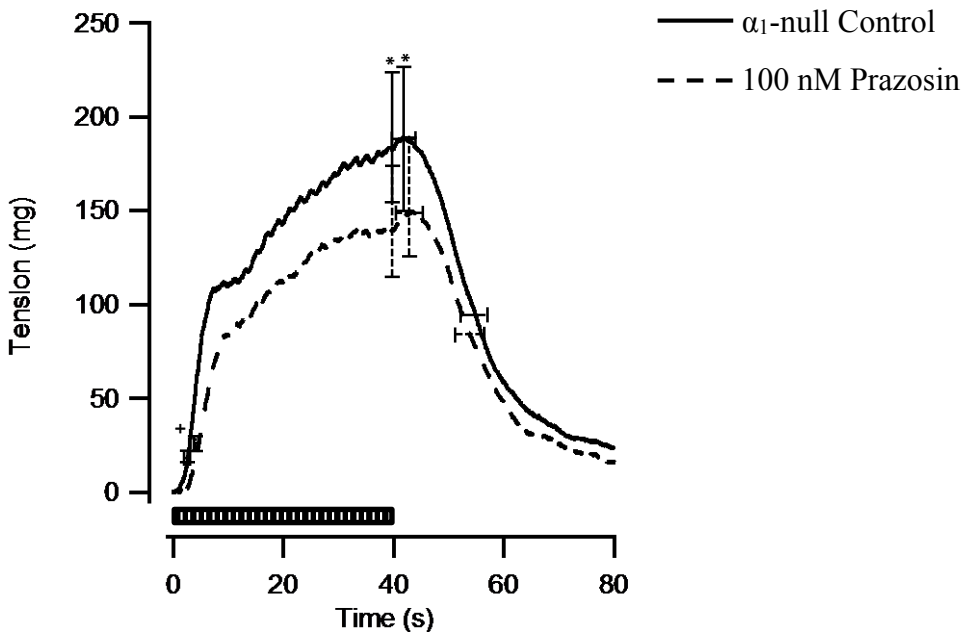

Figure 7-9: α_1-null Distal mouse tail artery response to nerve stimulation at 0.5 Hz in control vessels and in the presence of the α_1-AR antagonist prazosin (100 nM) (n = 9).

*** P < 0.05 compared with control response. Paired t-test.**

+ P < 0.05 compared with control time. Paired t-test.

Table 7-12: α_1-null Proximal mouse tail artery response to nerve stimulation in control and prazosin (100 nM) incubated vessels at 0.5 Hz.

Proximal 0.5 Hz	Contractile Response (average ± S.E.M)		
	Control	100 nM Prazosin (P) (n = 6)	% change following P incubation
Time to Peak (1st) (seconds)	3.2 ± 0.3	2.8 ± 0.7	- 15 ± 16
Peak Tension (1st) (mg)	16 ± 7	9 ± 6	- 52 ± 11
Rate of Rise (mg/s)	5 ± 2	3 ± 1 *	- 43 ± 7
Time to Peak (seconds)	36.8 ± 2.9	41.0 ± 1.1	10 ± 7
Peak Tension (mg)	171 ± 49	140 ± 38	- 18 ± 4
Tension at End of pulse (mg)	165 ± 49	232 ± 92	- 2 ± 18
50 % Decay Time (seconds)	23.0 ± 3.1	22.0 ± 2.5	1 ± 12

*** P < 0.05 compared with control response. Paired t-test.**

Table 7-13: α_1-null Distal mouse tail artery response to nerve stimulation in control and prazosin (100 nM) incubated vessels at 0.5 Hz.

Distal 0.5 Hz	Contractile Response (average ± S.E.M)		
	Control	100 nM Prazosin (P) (n = 9)	% change following P incubation
Time to Peak (1st) (seconds)	2.8 ± 0.3	3.6 ± 0.4 +	54 ± 36
Peak Tension (1st) (mg)	13 ± 3	11 ± 4	- 15 ± 16
Rate of Rise (mg/s)	5 ± 2	3 ± 1	- 31 ± 14
Time to Peak (seconds)	37.3 ± 2.4	37.8 ± 2.6	1 ± 5
Peak Tension (mg)	192 ± 42	155 ± 37 *	- 11 ± 13
Tension at End of pulse (mg)	180 ± 40	139 ± 34 *	- 20 ± 8
50 % Decay Time (seconds)	18.5 ± 2.5	18.3 ± 2.8	- 3 ± 7

*** P < 0.05 compared with control response. Paired t-test.**

+ P < 0.05 compared with control time. Paired t-test.

Traces showing the isolation of the prazosin sensitive component from the various incubation conditions were analysed therefore establishing whether the prazosin sensitive component can be altered depending on what other receptors are still functional. The areas were expressed as a % of the control area. In both proximal and distal segments, the prazosin sensitive component was greatest when the α_2-ARs and P2X receptors were functional compared to when these receptors where blocked (Figure 7-10; Tables 7-14 and 7-15).

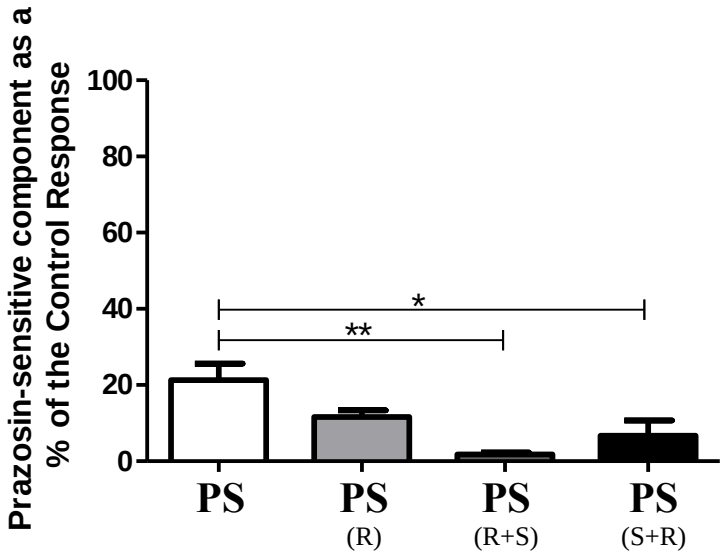

Figure 7-10: α_1-null Proximal mouse tail – the prazosin sensitive (PS) component at 0.5 Hz when the P2X receptors and α_2-ARs are functional (white) (n=6), α_2-ARs are blocked (light grey) (n=12), when the α_2-ARs and P2X receptors were blocked (dark grey) (n=6), the P2X receptors and α_2-ARs were blocked (black) (n=6).

*** P < 0.05; ** P < 0.01 compared with PS component when the α_2-ARs and P2X receptors are functional. One way ANOVA with Bonferonni's post-test.**

Table 7-14: α_1-null Proximal mouse tail artery – revealing the prazosin sensitive (PS) component as a % of control area under the curves. Data taken from Figures 7-10 and 7-12.

	Prazosin-sensitive component as a % of the Control Response	
	0.5 Hz	**8 Hz**
PS	21 ± 4	22 ± 3
PS (R)	12 ± 2	19 ± 7
PS (R+S)	2 ± 1 **	4 ± 2
PS (S+R)	7 ± 4 *	13 ± 6

*** P < 0.05; ** P < 0.01 compared with the PS component when the α_2-ARs and P2X receptors are functional. One way ANOVA with Bonferonni's post-test.**

Table 7-15: α_1-null Distal mouse tail artery response - revealing the prazosin sensitive (PS) component as a % of control area under the curves.

	Prazosin-sensitive component as a % of the Control Response	
	0.5 Hz	**8 Hz**
PS	43 ± 15	24 ± 6
PS (R)	15 ± 5	27 ± 9
PS (R+S)	3 ± 1 *	7 ± 3
PS (S+R)	9 ± 2 *	20 ± 5

*** P < 0.05 compared with PS component when the α_2-ARs and P2X receptors are functional. One way ANOVA with Bonferonni's post-test.**

7.3.2.3 Revealing the effect of prazosin on the response to sympathetic nerve stimulation at 8 Hz.

At 8 Hz, the proximal segments incubated with 100 nM prazosin had significantly lower peak tensions compared to control responses (Table 7-16). Distally, prazosin had more of an effect on the response; reducing the peak tension, the tension at the end of the stimulation period, the rate of rise and prolonging the time to reach the peak tension (Figure 7-11; Table 7-17).

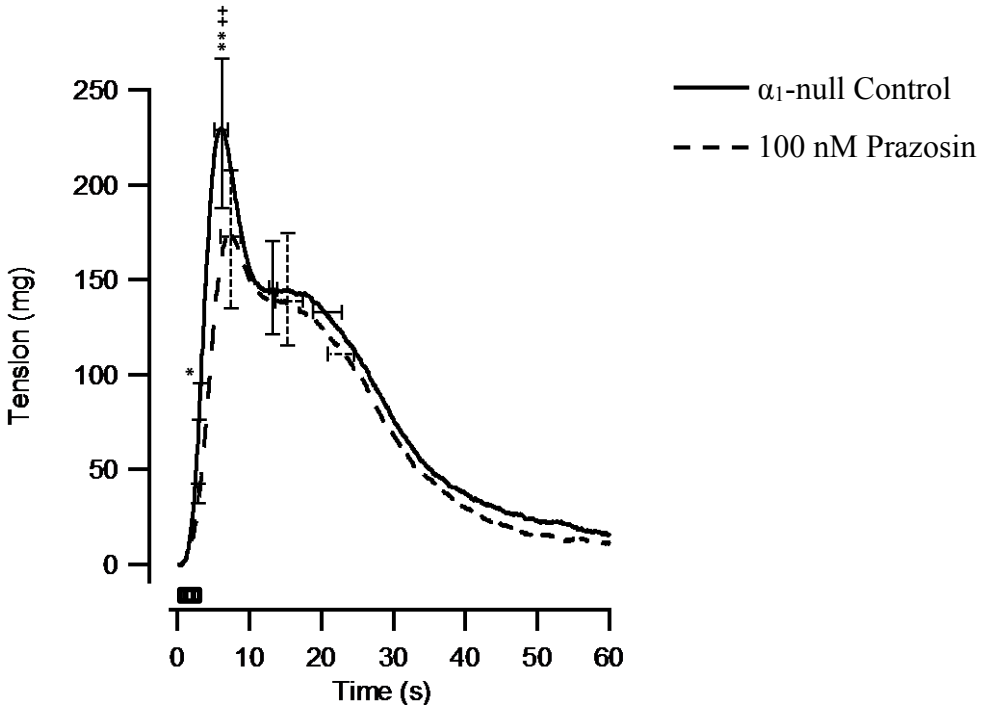

Figure 7-11: α_1-null Distal mouse tail artery response to nerve stimulation at 8 Hz in control vessels and in the presence of the α_1-AR antagonist prazosin (100 nM) (n = 9).

*** P < 0.05, ** P < 0.01 compared with control response. Paired t-test.**

++ P < 0.01 compared with control time. Paired t-test.

Table 7-16: α_1-null Proximal mouse tail artery response to nerve stimulation in control and prazosin (100 nM) incubated vessels at 8 Hz.

Proximal 8 Hz	Contractile Response (average ± S.E.M)		
	Control	100 nM Prazosin (P) (n = 6)	% change following P incubation
Tension at End of pulse (mg)	40 ± 10	42 ± 16	- 9 ± 10
Time to Peak (seconds)	9.4 ± 1.5	9.1 ± 0.8	0.5 ± 9
Peak Tension (mg)	188 ± 39	155 ± 36 **	- 20 ± 2
Rate of Rise (mg/s)	24 ± 7	18 ± 5	- 19 ± 8
Time to Peak (2nd) (seconds)	15.5 ± 1.9	17.3 ± 1.3	11 ± 7
Peak Tension (2nd) (mg)	160 ± 34	139 ± 34 **	- 16 ± 4
50 % Decay Time (seconds)	22.8 ± 2.1	23.4 ± 2.1	2 ± 5

**** P < 0.01 compared with control response. Paired t-test.**

Table 7-17: α_1-null Distal mouse tail artery response to nerve stimulation in control and prazosin (100 nM) incubated vessels at 8 Hz.

Distal 8 Hz	Contractile Response (average ± S.E.M)		
	Control	100 nM Prazosin (P) (n = 9)	% change following P incubation
Tension at End of pulse (mg)	47 ± 11	23 ± 6 *	- 42 ± 12
Time to Peak (seconds)	7.5 ± 1.1	9.5 ± 1.5 ++	19 ± 4
Peak Tension (mg)	234 ± 45	183 ± 41 **	- 22 ± 5
Rate of Rise (mg/s)	39 ± 9	24 ± 6 ***	- 37 ± 4
Time to Peak (2^{nd}) (seconds)	14.6 ± 0.5	18.6 ± 2.2	17 ± 7
Peak Tension (2^{nd}) (mg)	146 ± 28	135 ± 33	- 14 ± 7
50 % Decay Time (seconds)	17.1 ± 2.3	17.5 ± 1.9	6 ± 8

*** P < 0.05, ** P < 0.01, *** P < 0.001 compared with control response. Paired t-test.**

++ P < 0.01 compared with control time. Paired t-test.

The analysis of the prazosin sensitive components was similar for each component and at each segment studied (Figure 7-12; Tables 7-14 and 7-15).

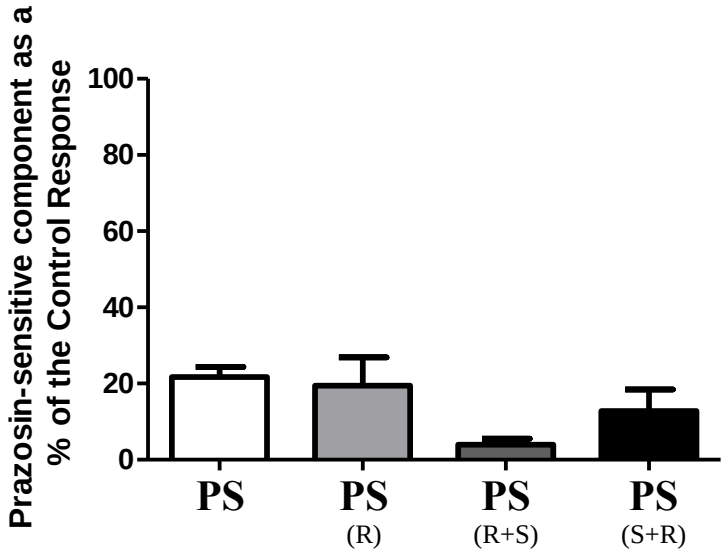

Figure 7-12: α_1-null Proximal mouse tail – the prazosin sensitive (PS) component at 8 Hz when the P2X receptors and α_2-ARs are functional (white) (n=6), α_2-ARs are blocked (light grey) (n=12), when the α_2-ARs and P2X receptors were blocked (dark grey) (n=6), the P2X receptors and α_2-ARs were blocked (black) (n=6).

7.3.2.4 Revealing the α_2-ARs role in the response to sympathetic nerve stimulation at 0.5 Hz.

When rauwolscine (100 nM) was incubated, the response to nerve stimulation in the proximal and distal segments was altered. Proximally and distally, the peak tension and the tension at the end of the stimulation period were reduced in amplitude (Table 7-18). Furthermore, distally, the tension at the first peak and the rate of rise were also reduced (Figure 7-13; Table 7-19).

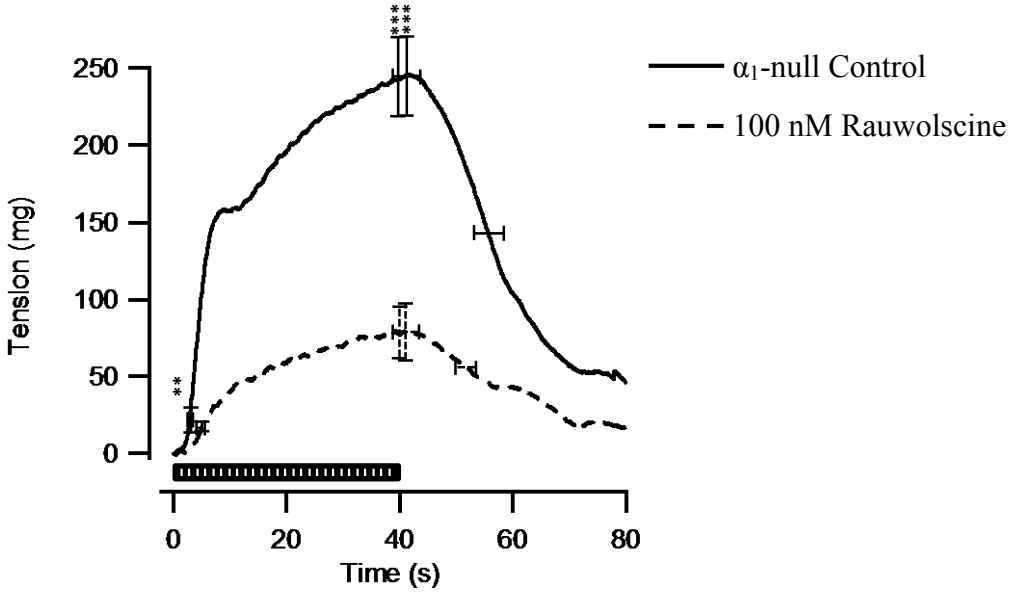

Figure 7-13: α_1-null Distal mouse tail artery response to nerve stimulation at 0.5 Hz in control vessels and in the presence of the α_2-AR antagonist rauwolscine (n = 13).

**** P < 0.01; *** P < 0.001 compared with control response. Paired t-test.**

Table 7-18: α_1-null Proximal mouse tail artery response to nerve stimulation in control and rauwolscine (100 nM) incubated vessels at 0.5 Hz.

Proximal 0.5 Hz	Contractile Response (average ± S.E.M)		
	Control	100 nM Rauwolscine (R) (n = 12)	% change following R incubation
Time to Peak (1st) (seconds)	2.7 ±0.3	3.4 ± 0.7	6 ± 12
Peak Tension (1st) (mg)	23 ± 8	9 ± 2	- 38 ± 12
Rate of Rise (mg/s)	8 ± 2	4 ± 1	- 38 ± 13
Time to Peak (seconds)	38.8 ± 0.9	33.1 ± 3.1	- 15 ± 9
Peak Tension (mg)	240 ± 19	63 ± 8 ***	- 73 ± 3
Tension at End of pulse (mg)	231 ± 19	56 ± 8 ***	- 75 ± 3
50 % Decay Time (seconds)	19.0 ± 1.9	16.7 ± 1.4	- 5 ± 9

***** P < 0.001 compared with control response. Paired t-test.**

Table 7-19: α_1-null Distal mouse tail artery response to nerve stimulation in control and rauwolscine (100 nM) incubated vessels at 0.5 Hz.

Distal 0.5 Hz	Contractile Response (average ± S.E.M)		
	Control	100 nM Rauwolscine (R) (n = 13)	% change following R incubation
Time to Peak (1st) (seconds)	3.2 ± 0.3	3.9 ± 0.6	7 ± 11
Peak Tension (1st) (mg)	38 ± 9	12 ± 3 **	- 61 ± 7
Rate of Rise (mg/s)	11 ± 2	3 ± 1 **	- 65 ± 7
Time to Peak (seconds)	37.8 ± 2.6	33.7 ± 2.4	- 8 ± 8
Peak Tension (mg)	250 ± 29	86 ± 21 ***	- 67 ± 5
Tension at End of pulse (mg)	236 ± 29	76 ± 19 ***	- 70 ± 5
50 % Decay Time (seconds)	20.0 ± 2.9	16.1 ± 1.9	- 11 ± 10

**** P < 0.01, *** P < 0.001 compared with control response. Paired t-test.**

Proximally, the rauwolscine sensitive component was shown to be greatest when the P2X receptors were functional and smallest when the P2X receptors were blocked (Figure 7-14; Table 7-20). Distally, the rauwolscine sensitive component was not found to be different when comparing the incubation conditions (Table 7-21).

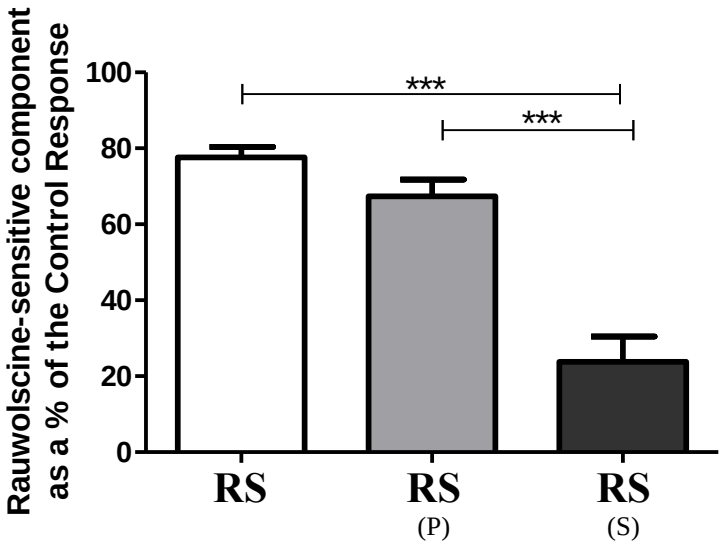

Figure 7-14: α_1-null Proximal mouse tail – the rauwolscine sensitive component at 0.5 Hz when the P2X receptors are functional (white) (n=12), prazosin sensitive component is blocked (light grey) (n=6), P2X receptors are blocked (black) (n=6).

***** P < 0.001 compared with area under the curve when the α_1-ARs are functional and the P2X receptors are blocked. One way ANOVA with Bonferonni's post-test.**

Table 7-20: α_1-null Proximal mouse tail artery - revealing the rauwolscine-sensitive (RS) component as a % of control area under the curves. Data taken from Figures 7-14 and 7-16.

	Rauwolscine-sensitive component as a % of the Control Response	
	0.5 Hz	**8 Hz**
RS	78 ± 3 ***	54 ± 5
RS (P)	67 ± 4 ***	68 ± 6
RS (S)	24 ± 7	42 ± 15

***** P < 0.001 compared with RS component when the α_1-ARs are functional and the P2X receptors are blocked. One way ANOVA with Bonferonni's post-test.**

Table 7-21: α_1-null Distal mouse tail artery response - revealing the rauwolscine-sensitive (RS) component as a % of control area under the curves.

	Rauwolscine-sensitive component as a % of the Control Response	
	0.5 Hz	**8 Hz**
RS	70 ± 5	47 ± 6
RS (P)	62 ± 5	61 ± 6
RS (S)	69 ± 47	55 ± 29

7.3.2.5 Revealing the α_2-ARs role in the response to sympathetic nerve stimulation at 8 Hz.

At 8 Hz, the response to nerve stimulation in both proximal and distal segments was inhibited by rauwolscine (100 nM) incubation. At both segments, the peak tensions were significantly reduced and the rate of rise was also reduced (Figure 7-15; Table 7-22 and 7-23). Additionally, proximal response was also reduced at the end of the stimulation period and the 50% decay time was shortened.

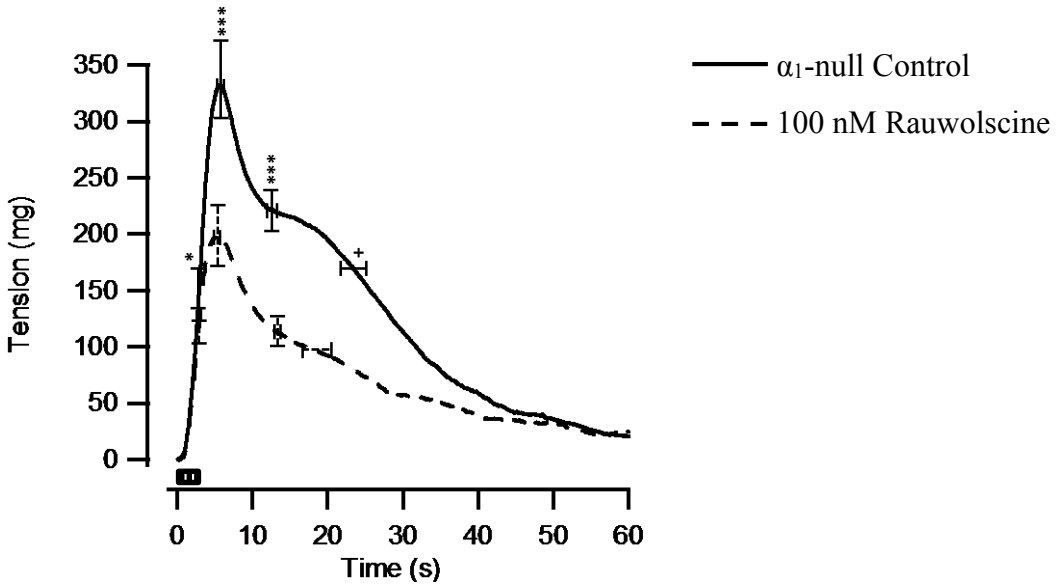

Figure 7-15: α_1-null Proximal mouse tail artery response to nerve stimulation at 8 Hz in control vessels and in the presence of the α_2-AR antagonist rauwolscine (100 nM) (n = 12).

*** P < 0.05; *** P < 0.001 compared with control response. Paired t-test.**

+ P < 0.05 compared with control time. Paired t-test.

Table 7-22: α_1-null Proximal mouse tail artery response to nerve stimulation in control and rauwolscine (100 nM) incubated vessels at 8 Hz.

Proximal 8 Hz	Contractile Response (average ± S.E.M)		
	Control	100 nM Rauwolscine (R) (n = 12)	% change following R incubation
Tension at End of pulse (mg)	120 ± 20	80 ± 12 *	- 27 ± 7
Time to Peak (seconds)	6.2 ± 0.4	5.0 ± 0.4	- 16 ± 8
Peak Tension (mg)	334 ± 40	188 ± 31 ***	- 47 ± 4
Rate of Rise (mg/s)	58 ± 9	39 ± 7 ***	- 33 ± 5
Time to Peak (2nd) (seconds)	12.9 ± 0.7	12.2 ± 0.4	- 4 ± 5
Peak Tension (2nd) (mg)	241 ± 21	112 ± 15 ***	- 55 ± 4
50 % Decay Time (seconds)	20 ± 2.1	15.1 ± 2.2 +	- 25 ± 6

*** P < 0.05, *** P < 0.001 compared with control response. Paired t-test.**

+ P < 0.05 compared with control time. Paired t-test.

Table 7-23: α_1-null Distal mouse tail artery response to nerve stimulation in control and rauwolscine (100 nM) incubated vessels at 8 Hz.

Distal 8 Hz	Contractile Response (average ± S.E.M)		
	Control	Rauwolscine (R) (n = 13)	% change following R incubation
Tension at End of pulse (mg)	73 ± 10	74 ± 9	3 ± 11
Time to Peak (seconds)	7.0 ± 1.0	5.8 ± 0.3	- 11 ± 6
Peak Tension (mg)	310 ± 26	184 ± 23 ***	- 41 ± 4
Rate of Rise (mg/s)	49 ± 5	33 ± 4 ***	- 32 ± 6
Time to Peak (2nd) (seconds)	14.8 ± 0.7	13.4 ± 0.5	- 9 ± 5
Peak Tension (2nd) (mg)	226 ± 24	118 ± 18 ***	- 47 ± 5
50 % Decay Time (seconds)	20.0 ± 2.3	14.4 ± 2.6	- 24 ± 8

***** P < 0.001 compared with control response. Paired t-test.**

Neither the proximal or distal segments displayed significant variations in rauwolscine sensitive component regardless of incubation condition. Under all conditions, the rauwolscine sensitive component represented a large portion of the control response (Figure 7-16; Tables 7-20 and 7-21).

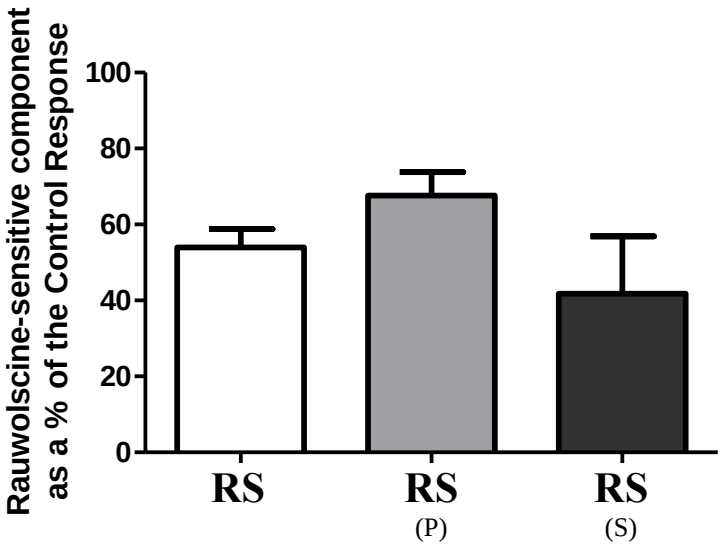

Figure 7-16: α_1-null Proximal mouse tail – the rauwolscine sensitive component at 8 Hz when the P2X receptors are functional (white) (n=12), prazosin sensitive component is blocked (light grey) (n=6), P2X receptors are blocked (black) (n=6).

7.3.2.6 Revealing the P2X receptor role in the response to sympathetic nerve stimulation at 0.5 Hz.

Proximally, suramin (1 mM) significantly reduced the peak tension and the tension at the end of the stimulation period and prolonged the time to reach the first peak (Figure 7-17; Table 7-24). The distal responses showed a similar trend but the results were not found to be significantly different (Table 7-25).

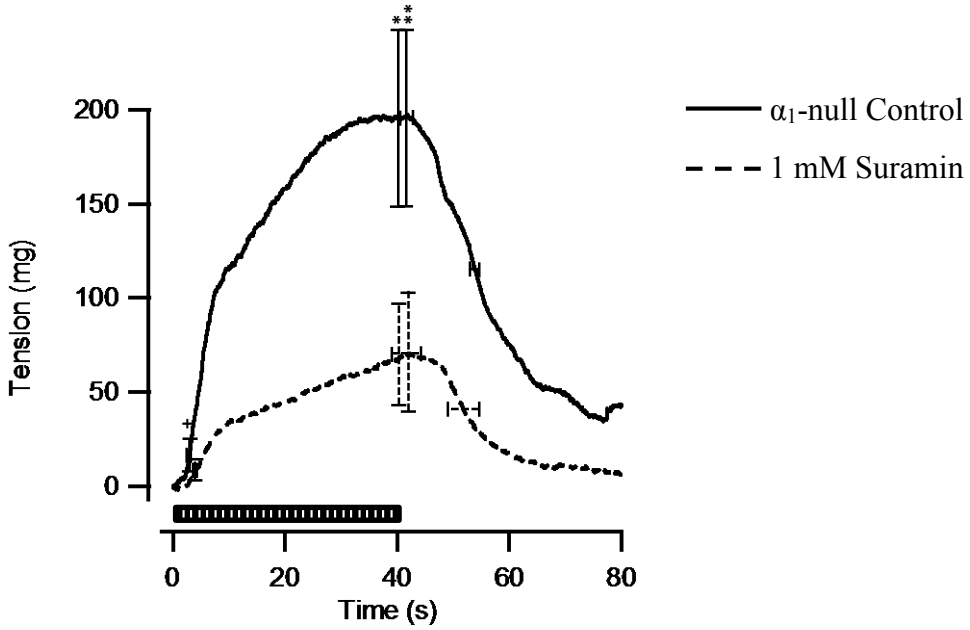

Figure 7-17: α_1-null Proximal mouse tail artery response to nerve stimulation at 0.5 Hz in control vessels and in the presence of the P2X receptor antagonist suramin (1 mM) (n = 6).

*** P < 0.05; ** P < 0.01 compared with control response. Paired t-test.**

+ P < 0.05 compared with control time. Paired t-test.

Table 7-24: α_1-null Proximal mouse tail artery response to nerve stimulation in control and suramin (1 mM) incubated vessels at 0.5 Hz.

Proximal 0.5 Hz	Contractile Response (average ± S.E.M)		
	Control	1 mM Suramin (S) (n = 6)	% change following S incubation
Time to Peak (1st) (seconds)	3.1 ± 0.2	4.2 ± 0.2 +	25 ± 9
Peak Tension (1st) (mg)	22 ± 10	11 ± 6	- 36 ± 19
Rate of Rise (mg/s)	7 ± 3	3 ± 1	- 53 ± 14
Time to Peak (seconds)	37.5 ± 1.4	36.0 ± 2.7	- 5 ± 7
Peak Tension (mg)	201 ± 54	75 ± 37 **	- 63 ± 8
Tension at End of pulse (mg)	195 ± 54	65 ± 31 *	- 70 ± 8
50 % Decay Time (seconds)	16.6 ± 0.9	13.1 ± 2.9	- 23 ± 21

*** P < 0.05; ** P < 0.01 compared with control response. Paired t-test.**

+ P < 0.05 compared with control time. Paired t-test.

Table 7-25: α_1-null Distal mouse tail artery response to nerve stimulation in control and suramin (1 mM) incubated vessels at 0.5 Hz.

Distal 0.5 Hz	Contractile Response (average ± S.E.M)		
	Control	1 mM Suramin (S) (n = 7)	% change following S incubation
Time to Peak (1st) (seconds)	3.0 ± 0.4	4.3 ± 0.5	21 ± 14
Peak Tension (1st) (mg)	41 ± 19	24 ± 16	- 36 ± 25
Rate of Rise (mg/s)	11 ± 4	4 ± 2	- 45 ± 24
Time to Peak (seconds)	31.8 ± 5.3	29.9 ± 5.0	- 5 ± 19
Peak Tension (mg)	157 ± 38	78 ± 28	- 47 ± 21
Tension at End of pulse (mg)	147 ± 37	67 ± 25	- 50 ± 21
50 % Decay Time (seconds)	20.8 ± 4.4	21.9 ± 4.9	- 0.4 ± 21

In proximal segments the suramin sensitive component was significantly greater when the α_2-ARs were functional compared with the other incubation conditions (Figure 7-18; Table 7-26 and 7-27).

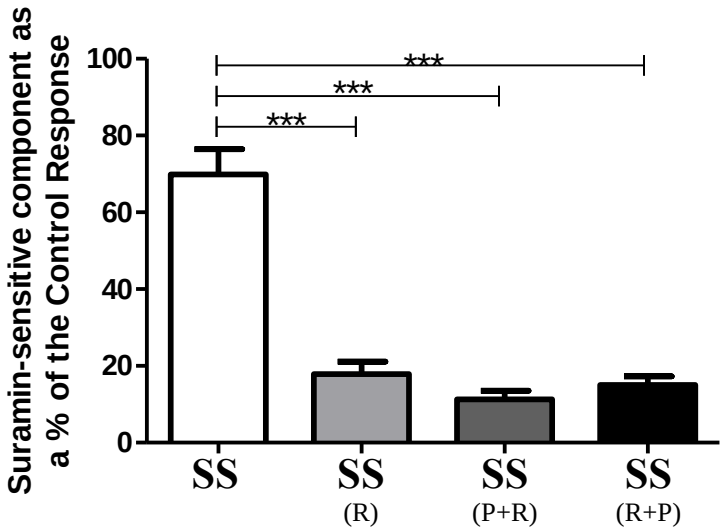

Figure 7-18: α_1-null Proximal mouse tail – the suramin sensitive component at 0.5 Hz when the α_2-ARs are functional (white) (n=6), α_2-ARs are blocked (light grey) (n=6), α_2-ARs are blocked (dark grey and black) (n=6).

***** P < 0.001 compared with SS component when the α_1- and α_2-ARs are functional. One way ANOVA with Bonferonni's post-test.**

Table 7-26: α_1-null Proximal mouse tail artery response - the suramin-sensitive (SS) component as a % of control area under the curves. Data taken from Figures 7-18 and 7-20.

	Suramin-sensitive component as a % of the Control Response	
	0.5 Hz	**8 Hz**
SS	70 ± 7	78 ± 14
SS (R)	18 ± 3 ***	33 ± 6 **
SS (P+R)	11 ± 2 ***	14 ± 2 ***
SS (R+P)	15 ± 2 ***	37 ± 2 **

**** P < 0.01; *** P < 0.001 compared with SS component when the α_2-ARs are functional. One way ANOVA with Bonferonni's post-test.**

Table 7-27: α_1-null Distal mouse tail artery response - the suramin-sensitive (SS) component as a % of control area under the curves.

	Suramin-sensitive component as a % of the Control Response	
	0.5 Hz	**8 Hz**
SS	112 ± 42	88 ± 30
SS (R)	24 ± 6	38 ± 6
SS (P+R)	17 ± 11 *	20 ± 11
SS (R+P)	19 ± 4	34 ± 8

*** P < 0.05 compared with SS component when the α_2-ARs are functional. One way ANOVA with Bonferonni's post-test.**

7.3.2.7 Revealing the P2X receptor role in the response to sympathetic nerve stimulation at 8 Hz.

Proximally, both peak tensions and the rate of rise were reduced (Figure 7-19; Table 7-28). Distally, the peak tension and the tension at the end of the stimulation period were reduced. The rate of rise was also reduced and the time to reach the peak was prolonged (Table 7-29).

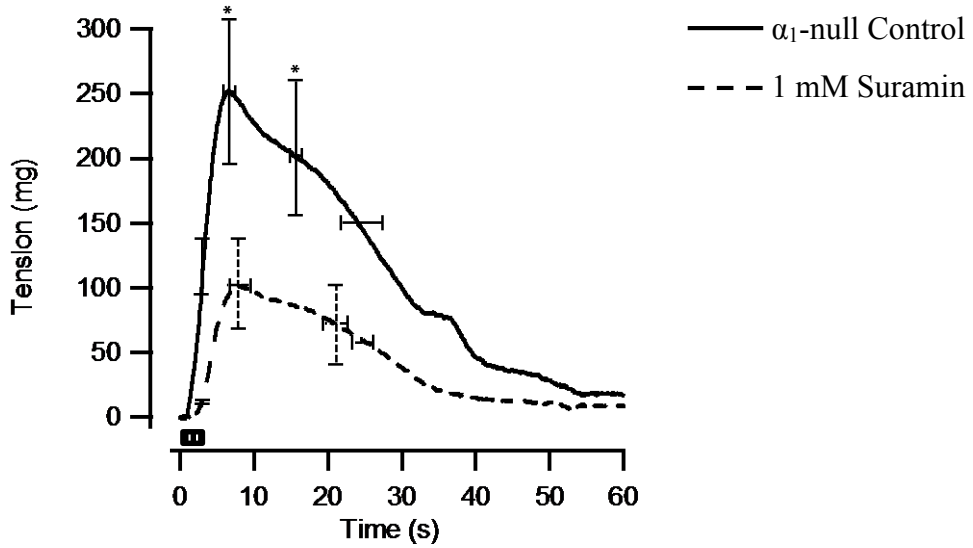

Figure 7-19: α_1-null Proximal mouse tail artery response to nerve stimulation at 8 Hz in control vessels and in the presence of the P2X receptor antagonist suramin (1 mM) (n = 6).

*** P < 0.05 compared with control response. Paired t-test.**

Table 7-28: α_1-null Proximal mouse tail artery response to nerve stimulation in control and suramin (1 mM) incubated vessels at 8 Hz.

Proximal 8 Hz	Contractile Response (average ± S.E.M)		
	Control	1 mM Suramin (S) (n = 6)	% change following S incubation
Tension at End of pulse (mg)	71 ± 25	6 ± 1	- 67 ± 18
Time to Peak (seconds)	7.3 ± 0.8	8.6 ± 1.8	7 ± 12
Peak Tension (mg)	264 ± 65	105 ± 41 *	- 52 ± 14
Rate of Rise (mg/s)	40 ± 10	13 ± 5 *	- 51 ± 21
Time to Peak (2nd) (seconds)	13.4 ± 0.9	15.6 ± 1.9	9 ± 11
Peak Tension (2nd) (mg)	213 ± 61	87 ± 35 *	- 48 ± 17
50 % Decay Time (seconds)	17.0 ± 3.3	14.6 ± 1.6	- 3 ± 17

*** P < 0.05 compared with control response. Paired t-test.**

Table 7-29: α_1-null Distal mouse tail artery response to nerve stimulation in control and suramin (1 mM) incubated vessels at 8 Hz.

Distal 8 Hz	Contractile Response (average ± S.E.M)		
	Control	Suramin (S) (n = 7)	% change following S incubation
Tension at End of pulse (mg)	83 ± 22	11 ± 2 *	- 74 ± 12
Time to Peak (seconds)	5.5 ± 0.4	6.5 ± 0.4 ++	16 ± 4
Peak Tension (mg)	245 ± 39	133 ± 38 *	- 48 ± 11
Rate of Rise (mg/s)	47 ± 9	21 ± 6 **	- 58 ± 8
Time to Peak (2nd) (seconds)	13.6 ± 0.7	14.7 ± 0.4	7 ± 4
Peak Tension (2nd) (mg)	137 ± 27	94 ± 31	- 36 ± 20
50 % Decay Time (seconds)	15.8 ± 3.6	16.0 ± 1.1	2 ± 19

*** P < 0.05, ** P < 0.01 compared with control response. Paired t-test.**

++ P < 0.01 compared with control time. Paired t-test.

Analysis of the suramin sensitive components extracted from each of the incubation conditions in proximal tail artery revealed the area under the curve when the α_2-ARs are functional to be significantly greater than the other incubation conditions (Figure 7-20; Table 7-26). This trend also occurred in distal segments although no significant differences were recorded (Table 7-27).

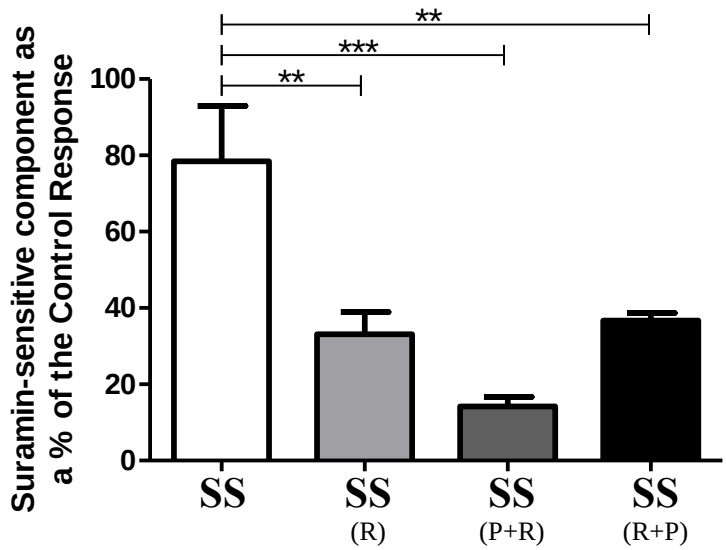

Figure 7-20: α_1-null Proximal mouse tail – the suramin sensitive component at 8 Hz when the α_2-ARs were functional (white) (n=6), α_2-ARs were blocked (light grey) (n=6), α_1- and α_2-ARs are blocked (dark grey and black) (n=6).

**** P < 0.01; *** P < 0.001 compared with SS component when the α_2-ARs receptors are functional. One way ANOVA with Bonferonni's post-test.**

7.4 Discussion

The present study was set out to determine the effect genetic removal of all three α_1-ARs had on the response to nerve stimulation. The dominant α_1-AR component was confirmed in the mouse mesenteric arteries and the possibility of compensatory mechanisms in mesenteric and tail arteries were studied.

7.4.1 Mouse Mesenteric Arteries

7.4.1.1 Comparison with WT response

The loss of the α_1-ARs was shown clearly in the response at both frequencies. Similar to the ADKO response, this response also supports previous knowledge of the α_1-ARs dominating the contraction in mesenteric arteries (Sjoblom-Widfeldt et al., 1990). The response is almost completely abolished at 2 Hz and only a small response remains at 8 Hz. Therefore, in this vessel, the response due to α_1-AR activation is not fully compensated for by another receptor. At 2 Hz, as well as a reduction in contractile response, the time taken to reach the peak was prolonged and the decay time was reduced. Therefore, the overall response was affected by loss of the α_1-ARs. In the WT vessels, no interactions were noted between the α_1-ARs and the other studied receptors and this may be the reason why the response in the α_1-null is small. If no interactions occur in the WT vessels then genetic removal of the α_1-ARs may have no influence on the other receptors and so no compensatory mechanisms would be initiated.

7.4.1.2 α_1-null Control response to Nerve Stimulation

Incubation with prazosin, rauwolscine and suramin reduced the response to nerve stimulation. However, the figures shown suggest that there is still a component of the

response remaining following co-incubation with the antagonists. On experimental days, this residual contraction was not visible on the LabChart traces and so the y-axis scale shown in the results section should be observed, as should the error bars. It was due to these small responses that the antagonist sensitive component analysis was not used, as there was potential for the response to fluctuate just below and above the baseline.

7.4.1.3 Receptor role in the Mouse Mesenteric Arteries

As the responses to nerve stimulation at 2 Hz were small, the response following treatment with any of the antagonists did not reduce the response. Combined incubation of the three antagonists was not able to reduce the response further therefore suggesting that the response was too small to statistically determine which receptors were involved in the contraction. At 8 Hz, the P2X receptors were involved in the contractile response as suramin was able to exert a change in the response. As expected, prazosin had no effect on the response. In the WT, a population of pre-junctional α_2-ARs exists, which when blocked, enhanced the response. This did not occur in the α_1-null mesenteric arteries and this is most likely due to loss of the α_1-ARs. The pre-junctional α_2-ARs may still have been blocked by rauwolscine treatment but the enhanced transmitter output would not have been able to fully exert its effect post-junctionally due to the loss of the α_1-ARs. Even the presence of the α_{1B}-ARs in the ADKO was enough to reveal these α_2-AR effects. The reduction in response to single and combined antagonist treatment in the α_1-null compared to the ADKO further supports a role for the α_{1B}-ARs. Therefore, in the mesenteric arteries, loss of the α_1-ARs considerably reduced the response and no compensatory mechanisms were revealed.

7.4.2 Mouse Proximal and Distal Tail Artery

Similar to Chapters Five and Six, the α_1-null results displayed only data from one area of the tail and only discrepancies between the segments were discussed. When comparing the WT and $\alpha_1$null responses, the proximal results were shown.

7.4.2.1 Comparison with WT

At 0.5 Hz and 8 Hz, the α_1-null vessels were able to produce a contractile response to nerve stimulation. At 0.5 Hz, the initial response to nerve stimulation was unaltered in the α_1-null vessels. This corresponds with the WT response where the P2X receptors initiate the contraction. The loss of the α_1-ARs is demonstrated by a reduction in the peak tension, a difference which was not shown in the ADKO arteries and therefore is due to loss of the α_{1B}-ARs. This may be due to a direct loss of available receptors to stimulate or it may be the loss of an interaction between receptors. Similar to the ADKO, the decay time was prolonged in the α_1-null vessels thus reaffirming the role of the α_1-ARs in ensuring completion of the response.

At 8 Hz, like in the ADKO, the loss of the α_1-ARs is seen more clearly on the response. All of the recorded tensions in the α_1-null vessels were reduced and both peak times and the decay time were prolonged, compared to the WT response. This further supports the view that the α_1-ARs contribute to the overall response.

7.4.2.2 Revealing the effect of Prazosin on the Response to Sympathetic Nerve Stimulation

In the α_1-null vessels, there should be no effect of prazosin treatment. All experiments to date have described prazosin as an α_1-AR antagonist and results suggest that only the α_1-ARs are blocked by prazosin. Also, a lack of response to prazosin at 8 Hz in the α_1-null mesenteric arteries confirms the selectivity of prazosin. However, in the α_1-null tail artery, 100 nM prazosin treatment was able to alter the nerve response and this was more clearly shown in the distal segments. Here, vessels incubated with prazosin produced a response with a prolonged time to first peak and a decreased peak tension. The most likely reason for this result is that prazosin was able to block the α_2-ARs – an effect not obvious in the WT vessels as rauwolscine incubation following α_1-AR block by prazosin always further reduced the response significantly. Therefore, the results obtained may have occurred due to a

compensatory mechanism which caused an increase in α_2-AR sensitivity in distal segments. An increased α_2-AR sensitivity in distal segments was proposed by Medgett in 1985 who studied the rat tail artery and concluded that the α_2-ARs were able to mediate more of the contractile response distally (Medgett, 1985). Therefore, if α_2-AR sensitivity was increased in the α_1-null mice, prazosin (100 nM) may be able to block some of the α_2-ARs and thus affect the response to nerve stimulation. At 8 Hz, prazosin was able to reduce the peak tensions. However, compared to the rauwolscine response, this response to nerve stimulation was only altered in a minor way and so if the receptors are able to bind prazosin, then only a small proportion of the α_2-ARs were blocked. The mouse tail artery has been implicated in thermoregulation with the main receptor involved being the α_{2C}-ARs (Chotani et al., 2000) and this receptor subtype has also been shown to bind prazosin, although at a much lower affinity than rauwolscine in the rat tail artery (Jantschak et al., 2010). When investigating the prazosin-sensitive components, following rauwolscine and suramin treatments, the remaining component was virtually abolished, therefore confirming that the prazosin effect was not due to blockade of an unknown receptor.

A similar response to prazosin incubation was shown at 8 Hz whereby the peak tension was reduced both proximally and distally. Additionally, the distal segments were again more sensitive to prazosin treatment with the tension at the end of the stimulation period reduced and the time to peak prolonged. The prazosin-sensitive components were small regardless of incubation sequence. However, there was a trend for the component to be smaller when the vessels were incubated with rauwolscine and suramin.

7.4.2.3 α_2-AR role in Mouse Tail Artery

Similar to both the WT and ADKO results, the main receptors involved in vessel contraction in the α_1-null were the α_2-ARs. In support of an increase in the α_2-AR component, particularly in distal segments, the response was affected more by rauwolscine treatment in distal segments. Proximally, only the peak tension and the tension at the end of the stimulation period were reduced. Distally, the first peak tension was also reduced. However, these responses to rauwolscine treatment were reduced compared with the WT where the response timings were also affected by α_2-AR blockade. This highlights an interaction

between the α_2- and α_1-ARs, shown in the WT analysis and lost in the α_1-null vessels. Therefore, although the α_2ARs are the main receptors involved in contraction of the tail, they require assistance from functional α_1-ARs and this is not clearly compensated for in the α_1-null vessels. When investigating the rauwolscine-sensitive component, an interaction with the P2X receptors was revealed, similar to that shown in the WT vessels whereby the rauwolscine-sensitive component was reduced when the P2X receptors were blocked. Interestingly, this interaction with the P2X receptors was not shown in distal segments. This therefore suggests than an increase in α_2-AR sensitivity distally removes the α_2-AR dependency on the P2X receptors.

At 8 Hz, rauwolscine treatment affects more of the response to nerve stimulation compared to 0.5 Hz and the results are similar regardless of location. Therefore, the α_2-ARs contribute to the overall contractile response. As was described in the ADKOs (Chapter Six), the tension recorded at the end of the stimulation period was reduced in the α_1-null but not the WT vessels. In the WT vessels, the reduction in response occurred due to prazosin treatment and so presently, this result may represent a compensatory mechanism. At 8 Hz, activation of the α_2-ARs occurred independently of the P2X receptors and was the main receptor involved in vessel contraction.

7.4.2.4 P2X receptor role in Mouse Tail Artery

At 0.5 Hz, incubation of the vessels with suramin, to block P2X receptors revealed a role for the P2X receptors in the initiation of the response as well as contributing to the overall contraction. The ability to initiate the contraction was also shown in the WT vessels. However, the reduction in peak tension, shown following suramin treatment, occurred in the α_1-null vessels but not in the WT vessels. In the WT, the latter stages of the response were driven mainly by the α_2-ARs and α_1-ARs. It is therefore possible that in the α_1-null, the P2X receptors compensate for the loss of the α_1-ARs. However, this mechanism can only occur when the α_2-ARs are active and therefore provides evidence of an interaction between these two receptors. This is similar to the ADKO response suggesting that the loss of the α_{1B}-ARs does not further alter the response.

At 8 Hz, the response to suramin treatment differed depending on the location, with the distal segments being more suramin sensitive and less dependent on the α_2-ARs. If the α_2-AR sensitivity is increased distally and not dependent on the P2X receptors being active, the P2X receptors may have adapted in the α_1-null to be independent of the α_2-ARs in distal segments. Proximally, suramin treatment was still able to reduce the contractile response. However, the response was dependent on the α_2-ARs being active.

7.4.3 Conclusion

In summary, the presence of α_2-ARs and P2X receptors has been confirmed in the mesenteric and tail arteries of α_1-null mice. The presence of a contractile response in both of these vessels confirms that activation of the remaining receptors can result in vasoconstriction. Similar to the ADKO results, the loss of the α_1-ARs is most clearly shown in the mesenteric arteries. As the α_1-ARs were shown to contribute most to the contraction of the mesenteric arteries in the WT, this result is understandable and also confirms that no other receptor was capable of fully compensating for the lost response. Evidence of minor compensatory mechanisms were revealed in the tail artery where the sensitivity of the α_2-ARs appears to be increased, particularly in distal segments as the vessel response was altered following prazosin treatment. This effect was most likely due to activation of α_{2C}-ARs. At 0.5 Hz, there was evidence to suggest P2X receptor activation compensating for the loss of the α_1-ARs and potential P2X receptor adaptation in distal segments, at 8 Hz. In conclusion, the development of the α_1-null mice has confirmed the importance of the α_1-ARs in smooth muscle contraction, particularly in mesenteric arteries. It has also been revealed that in the KO animals, other receptors can compensate for the loss of the knocked-out receptor. The pharmacology was somewhat simplified, however the unexpected effect of prazosin and the compensatory mechanisms made it difficult to determine the exact roles of the receptors involved in smooth muscle contraction.

The two vessels studied highlight the differences in receptor population that can occur throughout the vasculature. The results from the α_1-null mice provide a useful framework, along with the WT and ADKO results, for the study of independent receptor activation and receptor interactions. The responses to nerve stimulation in the mouse mesenteric arteries

were shown to be mainly α_1-AR mediated with no obvious interactions with the other receptors, and so can be utilised to demonstrate the importance of α_1-ARs. Conversely, the responses to nerve stimulation in the mouse tail artery were shown to be mainly α_2-AR mediated with clear interactions with α_1-ARs and P2X receptors. Therefore this vessel can be utilised to study receptor interactions in a vessel where the α_1-AR mediated response is not crucial to vessel contraction. The treatment of primary hypertension with α_1-AR antagonists has been largely unsuccessful. The results shown presently indicate that this may be due to differences in receptor population and receptor interactions throughout the vasculature. Further investigations utilising the mesenteric and tail artery may help in the development of novel therapies for treating this disorder.

Chapter Eight

General Discussion

Activation of post-junctional α_1-ARs has been shown throughout the vasculature to be responsible for sympathetic vasoconstriction and so can contribute to the control of arterial blood pressure. However, treatment of primary hypertension using α_1-AR antagonists has been largely unsuccessful, unless therapy is combined with another blood pressure (BP) lowering agent (Chapman et al., 2010). Therefore, a greater understanding of the various receptors in the vasculature is required in order to improve patient response to BP treatment. This has been difficult due to the complex pharmacology present in many blood vessels whereby synergy and interactions between receptors prevents clear assessment of the individual receptor roles. The results presented in this thesis utilised mouse mesenteric and tail arteries as evidence suggested that they contained different proportions of α_1- and α_2-ARs as well as a P2X receptor population (Gitterman and Evans, 2001; Brock et al., 2006) (Bao et al., 1990; Bao and Stjarne, 1993). Transgenic mice lacking at least one α_1-AR subtype have been developed and the α_{1AD}-AR KO and α_1-null mice were utilised here to determine the effects that loss of some or all of the α_1-ARs has on the response to nerve stimulation in the aforementioned vessels. Comparing with WT results and using selective antagonists it was hoped that the findings would provide a clearer representation of the functional role of the three main vasoconstrictor receptors; α_1-, α_2-ARs and P2X receptors. This will hopefully guide the development of novel therapies targeted at the studied receptors.

8.1 Systolic Blood Pressure

Initially, the systolic blood pressure was measured from WT, ADKO, and α_1-null mice to determine whether loss of some or all of the α_1-ARs has a direct effect on lowering BP as has been shown in other studies (Rokosh and Simpson, 2002; Hosoda et al., 2005; Sanbe et al., 2007; Tanoue et al., 2002). However, the present results indicated that the α_1-ARs were either not implicated in blood pressure maintenance or, another receptor was able to compensate for the loss. It was also concluded that, under the circumstances, the mice may have been more agitated and so this may have masked the BP at rest. Nonetheless, if the mice were agitated, it would suggest that, under pressure, the effect on vascular tone is similar between the strains.

8.2 Calcitonin Gene-Related Peptide (CGRP)

As well as a dense plexus of sympathetic nerve terminals, primary afferent sensory nerve terminals are present in the adventitia of many arteries (Kawasaki et al., 1988; Sneddon and Burnstock, 1984) and activation of receptors present on the nerves can lead to release of potent vasodilators including CGRP (Brain et al., 1985; Tornebrandt et al., 1987; Uddman et al., 1986). It was proposed that if CGRP was released during electrical field stimulation, then under the parameters of stimulation utilised, a CGRP effect may prevent the full contractile effect from being visualised. Therefore, all vessels were incubated with capsaicin, which depletes the sensory nerves of CGRP (Caterina et al., 1997) and responses before and after capsaicin treatment compared in WT, ADKO and α_1-null mesenteric and tail arteries. A CGRP effect was not noted in the mesenteric arteries from each strain, nor in the WT and α_1-null tail artery. However, the peak response at 0.5 Hz in the ADKO tail artery was enhanced following capsaicin treatment. This response was not shown statistically in the WT or the α_1-null tail artery, yet there was a trend for the response to increase following capsaicin treatment. Therefore, increasing the experimental number should clarify capsaicin's effect in the mouse tail artery.

8.3 Receptor role in Mouse Mesenteric Arteries

Previous studies in the rat mesenteric arteries implicated the main role in the contractile response to be due to activation of the α_1-ARs with a P2X receptor influence and modulation via activation of pre-junctional α_2-ARs (Angus et al., 1988; Gitterman and Evans, 2001; Brock et al., 2006). The results shown presently, in the mouse mesenteric arteries, supports the previous observations in the rat. Activation of the α_1-ARs predominates in the contractile response and shows no definite interactions with the other receptors. Activation of P2X receptors contributes to the initiation of the response and activation of pre-junctional α_2-ARs modulates transmitter release. The P2X receptor response is partly dependent on the presence of active α_2-ARs (Chapter Five). In the ADKO, the remaining α_{1B}-ARs were not shown to contribute to the contractile response. As the loss of the α_1-ARs are not compensated for by other receptors, and the SBP remains unchanged, this would suggest that activation of these receptors, in the mouse mesenteric arteries, are not crucial in the maintenance of vascular tone. This is surprising as the mesenteric arteries provide a large

framework of peripheral vessels. However, it is possible than compensatory mechanisms occur in the superior mesenteric artery or on the smaller divisions of the mesenteric arcades.

8.4 Receptor role in the Mouse Tail Artery

In the rat tail artery, the α_1- and α_2-ARs have been shown to contribute to the slow portion of the nerve response, with activation of P2X receptors producing the initial contraction (Sneddon and Burnstock, 1984; Bao et al., 1990). The results presented here demonstrate a strong role for the α_2-ARs in the contractile response to nerve stimulation. However, the large contractile response is due, in part, to interactions with the α_1-ARs and P2X receptors. The KO vessel response to nerve stimulation was affected in the tail artery but not as much as in the mesenteric arteries. There was some evidence of pre-junctional α_2-ARs with blockade of the receptors increasing the rate at which the response occurred but not enhancing the size of the response. Initiation of the response occurred due to activation of P2X receptors and α_1-ARs. Unlike in the mesenteric arteries, the KO tail artery responses displayed compensatory mechanisms. There was an increase in P2X receptor response and an interaction between the α_2-ARs and P2X receptors which compensated for the loss of the interaction between the α_1- and α_2-ARs in the WT strain. Responses in the ADKO tail artery revealed a role for the α_{1B}-ARs in initiation of the response with interactions greater at the lower frequency. The loss of the α_1ARs revealed a complex relationship between proximal and distal segments. As this is an α_2-AR dominated vessel, the response to nerve stimulation wouldn't have been expected to be as affected by α_1-AR removal in comparison to the mesenteric arteries. However, as removal of the α_1-ARs revealed compensatory mechanisms, the pharmacology remained complex.

8.5 Future Research

It has been proposed that α_1-AR activation is crucial in the maintenance of vascular tone. However, the poor performance of α_1-AR antagonists in the treatment of primary hypertension suggests more complex mechanisms are involved. Results presented here

support this idea, that there is more than one main receptor involved in vessel contraction and this may change depending on the vessel. Therefore, greater insight is required into the individual receptors roles in various vessels to determine whether the α_1-ARs are crucial in blood pressure maintenance. For example, the mesenteric artery results described presently indicate a dramatic reduction in response to nerve stimulation that doesn't appear to have implications on mouse survival. However, the arteries studied were first order mesenteric arteries and so investigations into the other mesenteric arteries, particularly the superior artery, may reveal a compensatory mechanism. Furthermore, complex interactions in the mouse tail artery which changed in response to frequency and/or vessel location made it difficult to elucidate the exact receptor roles as the KO animals produced varying responses. Therefore, a more detailed analysis of the tail artery is required whereby the changes in receptor role along the length of the tail can be determined. The myography protocol used presently could be further utilised in experiments involving the superior mesenteric artery and the whole tail artery. Visualisation techniques such as confocal laser scanning microscopy and fluorescent drugs would establish the location of the α-ARs. This would be particularly useful in the tail artery which has yet to be studied in this way. Utilising these techniques on other vessels will help elucidate the complex pharmacology and further reveal drug targets in the control of hypertension and other vascular concerns such as Raynaud's syndrome.

8.6 General Conclusions

The mouse mesenteric and tail arteries have not been utilised fully in previous studies concerning stimulation of the nerves, and so a number of conclusions and novel findings that have not been reported elsewhere, can be derived from the studies presented in the previous chapters.

1. The α_1-, α_2-ARs and P2X receptors have been shown to be involved in the contractile response to nerve stimulation in mouse mesenteric and tail arteries with no evidence of involvement from other receptors.
2. The α_1-AR mediated contractile response was dominant in the mesenteric arteries and was not fully compensated for in the KO animals.

3. The α_2-AR mediated contractile response was dominant in both proximal and distal tail artery segments and loss of the α_1-ARs only marginally affected the response in the KO vessels.
4. A novel role in the initiation of the contractile response for the α_{1B}-ARs was revealed in the ADKO tail artery.
5. Interactions between the receptors occurred more in the tail than in the mesenteric arteries.
6. Use of the α_1-AR KO mice allowed, for the first time, minor compensatory mechanisms to be detected in both vessels, and these mechanisms changed depending on the stimulation parameters and the location of the vessel. This made analysis of the results complex.

Reference List

Ahlquist, R. P. (1948) A Study of the Adrenotropic Receptors. *American Journal of Physiology,* 153**,** 586-600.

Alexander, S. P., Benson, H. E., Faccenda, E., Pawson, A. J., Sharman, J. L., Spedding, M., Peters, J. A. & Harmar, A. J. (2013) The Concise Guide to Pharmacology 2013/14: G Protein-Coupled Receptors. *Br J Pharmacol,* 170**,** 1459-581.

Angus, J. A., Broughton, A. & Mulvany, M. J. (1988) Role of Alpha-Adrenoceptors in Constrictor Responses of Rat, Guinea-Pig and Rabbit Small Arteries to Neural Activation. *Journal of Physiology-London,* 403**,** 495-510.

Bailey, S. R., Eid, A. H., Mitra, S., Flavahan, S. & Flavahan, N. A. (2004) Rho Kinase Mediates Cold-Induced Constriction of Cutaneous Arteries - Role of Alpha 2c-Adrenoceptor Translocation. *Circulation Research,* 94**,** 1367-1374.

Bao, J. X., Eriksson, I. E. & Stjarne, L. (1990) Neurotransmitters and Prejunctional and Postjunctional Receptors Involved in the Vasoconstrictor Response to Sympathetic-Nerve Stimulation in Rat Tail Artery. *Acta Physiologica Scandinavica,* 140**,** 467-479.

Bao, J. X., Gonon, F. & Stjarne, L. (1993a) Frequency- and Train Length-Dependent Variation in the Roles of Postjunctional Alpha 1- and Alpha 2-Adrenoceptors for the Field Stimulation-Induced Neurogenic Contraction of Rat Tail Artery. *Naunyn Schmiedebergs Arch Pharmacol,* 347**,** 601-16.

Bao, J. X., Gonon, F. & Stjarne, L. (1993b) Frequency-Dependent and Train Length-Dependent Variation in the Roles of Postjunctional Alpha-1-Adrenoceptor and Alpha-2-Adrenoceptor for the Field Stimulation-Induced Neurogenic Contraction of Rat Tail Artery. *Naunyn-Schmiedebergs Archives of Pharmacology,* 347**,** 601-616.

Bao, J. X. & Stjarne, L. (1993) Dual Contractile Effects of Atp Released by Field Stimulation Revealed by Effects of Alpha,Beta-Methylene Atp and Suramin in Rat Tail Artery. *British Journal of Pharmacology,* 110**,** 1421-1428.

Brain, S. D., Williams, T. J., Tippins, J. R., Morris, H. R. & Macintyre, I. (1985) Calcitonin Gene-Related Peptide Is a Potent Vasodilator. *Nature,* 313**,** 54-6.

Brock, J. A. & Cunnane, T. C. (1999) Effects of Ca2+ Concentration and Ca2+ Channel Blockers on Noradrenaline Release and Purinergic Neuroeffector Transmission in Rat Tail Artery. *British Journal of Pharmacology,* 126**,** 11-18.

Brock, J. A. & Tan, J. H. C. (2004) Selective Modulation of Noradrenaline Release by Alpha(2)-Adrenoceptor Blockade in the Rat-Tail Artery in Vitro. *British Journal of Pharmacology,* 142**,** 267-274.

Brock, J. A., Yeoh, M. & Mclachlan, E. M. (2006) Enhanced Neurally Evoked Responses and Inhibition of Norepinephrine Reuptake in Rat Mesenteric Arteries after Spinal Transection. *American Journal of Physiology-Heart and Circulatory Physiology,* 290**,** H398-H405.

Brown, C. M., Mackinnon, A. C., Mcgrath, J. C., Spedding, M. & Kilpatrick, A. T. (1990a) Alpha-2-Adrenoceptor Subtypes and Imidazoline-Like Binding-Sites in the Rat-Brain. *British Journal of Pharmacology,* 99**,** 803-809.

Brown, C. M., Mackinnon, A. C., Mcgrath, J. C., Spedding, M. & Kilpatrick, A. T. (1990b) Heterogeneity of Alpha-2-Adrenoceptors in Rat Cortex but Not Human Platelets Can Be Defined by 8-Oh-Dpat, Ru-24969 and Methysergide. *British Journal of Pharmacology,* 99**,** 481-486.

Burnstock (1972) Purinergic Nerves. *Pharmacological Reviews,* 24**,** 509-581.

Burnstock, G. (1976) Purinergic Receptors. *Journal of Theoretical Biology,* 62**,** 491-503.

Burnstock, G., Campbell, G., Satchell, D. & Smythe, A. (1970) Evidence That Adenosine Triphosphate or a Related Nucleotide Is Transmitter Substance Released by Ono-Adrenergic Inhibitory Nerves in Gut. *British Journal of Pharmacology,* 40**,** 668-88.

Burnstock, G., Smythe, A. & Satchell, D. G. (1972) Comparison of Excitatory and Inhibitory Effects of Non-Adrenergic, Non-Cholinergic Nerve-Stimulation and Exogenously Applied Atp on a Variety of Smooth Muscle Preparations from Different Vertebrate Species. *British Journal of Pharmacology,* 46**,** 234-42.

Burnstock, G. & Williams, M. (2000) P2 Purinergic Receptors: Modulation of Cell Function and Therapeutic Potential. *Journal of Pharmacology and Experimental Therapeutics,* 295**,** 862-869.

Bylund, D. B. (1985) Heterogeneity of Alpha-2 Adrenergic-Receptors. *Pharmacology Biochemistry and Behavior,* 22**,** 835-843.

Bylund, D. B., Rayprenger, C. & Murphy, T. J. (1988) Alpha-2a and Alpha-2b Adrenergic-Receptor Subtypes - Antagonist Binding in Tissues and Cell-Lines Containing Only One Subtype. *Journal of Pharmacology and Experimental Therapeutics,* 245**,** 600-607.

Caterina, M. J., Schumacher, M. A., Tominaga, M., Rosen, T. A., Levine, J. D. & Julius, D. (1997) The Capsaicin Receptor: A Heat-Activated Ion Channel in the Pain Pathway. *Nature,* 389**,** 816-824.

Cavalli, A., Lattion, A. L., Hummler, E., Nenniger, M., Pedrazzini, T., Aubert, J. F., Michel, M. C., Yang, M., Lembo, G., Vecchione, C., Mostardini, M., Schmidt, A., Beermann, F. & Cotecchia, S. (1997) Decreased Blood Pressure Response in Mice Deficient of the Alpha(1b)-Adrenergic Receptor. *Proceedings of the National Academy of Sciences of the United States of America,* 94**,** 11589-11594.

Chapman, N., Chen, C. Y., Fujita, T., Hobbs, F. D., Kim, S. J., Staessen, J. A., Tanomsup, S., Wang, J. G. & Williams, B. (2010) Time to Re-Appraise the Role of Alpha-1 Adrenoceptor Antagonists in the Management of Hypertension? *J Hypertens,* 28**,** 1796-803.

Chotani, M. A., Flavahan, S., Mitra, S., Daunt, D. & Flavahan, N. A. (2000) Silent Alpha(2c)-Adrenergic Receptors Enable Cold-Induced Vasoconstriction in Cutaneous Arteries. *Am J Physiol Heart Circ Physiol,* 278**,** H1075-83.

Church, D. M., Goodstadt, L., Hillier, L. W., Zody, M. C., Goldstein, S., She, X., Bult, C. J., Agarwala, R., Cherry, J. L., Dicuccio, M., Hlavina, W., Kapustin, Y., Meric, P., Maglott, D., Birtle, Z., Marques, A. C., Graves, T., Zhou, S., Teague, B., Potamousis, K., Churas, C., Place, M., Herschleb, J., Runnheim, R., Forrest, D., Amos-Landgraf, J., Schwartz, D. C., Cheng, Z., Lindblad-Toh, K., Eichler, E. E. & Ponting, C. P. (2009) Lineage-Specific Biology Revealed by a Finished Genome Assembly of the Mouse. *PLoS Biol,* 7**,** e1000112.

Coates, J., Jahn, U. & Weetman, D. F. (1982) The Existence of a New Subtype of Alpha-Adrenoceptor on the Rat Anococcygeus Is Revealed by Sgd 101/75 and Phenoxybenzamine. *Br J Pharmacol,* 75**,** 549-52.

Cotecchia, S., Schwinn, D. A., Randall, R. R., Lefkowitz, R. J., Caron, M. G. & Kobilka, B. K. (1988) Molecular Cloning and Expression of the Cdna for the Hamster Alpha 1-Adrenergic Receptor. *Proc Natl Acad Sci U S A,* 85**,** 7159-63.

Crassous, P. A., Flavahan, S. & Flavahan, N. A. (2009) Acute Dilation to Alpha(2)-Adrenoceptor Antagonists Uncovers Dual Constriction and Dilation Mediated by Arterial Alpha(2)-Adrenoceptors. *British Journal of Pharmacology,* 158**,** 1344-1355.

Dale, H. H. (1906) On Some Physiological Actions of Ergot. *J Physiol,* 34**,** 163-206.

Daly, C. J., Cotecchia, S. & Mcgrath, J. C. (1998) Low Frequency Electrical Field Stimulation Elicits Responses in Segments of Mouse Tail Artery Which Are Slower in Alpha1b-Knockout Mice Than in Control Mice. *Naunyn-Schmiedebergs Archives of Pharmacology,* 358**,** R600-R600.

Daly, C. J., Deighan, C., Mcgee, A., Mennie, D., Ali, Z., Mcbride, M. & Mcgrath, J. C. (2002) A Knockout Approach Indicates a Minor Vasoconstrictor Role for Vascular Alpha(1b)-Adrenoceptors in Mouse. *Physiological Genomics,* 9**,** 85-91.

Deighan, C., Methven, L., Naghadeh, M. M., Wokoma, A., Macmillan, J., Daly, C. J., Tanoue, A., Tsujimoto, G. & Mcgrath, J. C. (2005) Insights into the Functional Roles of Alpha(1)-Adrenoceptor Subtypes in Mouse Carotid Arteries Using Knockout Mice. *British Journal of Pharmacology,* 144**,** 558-565.

Dhall, U., Cowen, T., Haven, A. J. & Burnstock, G. (1986) Perivascular Noradrenergic and Peptide-Containing Nerves Show Different Patterns of Changes During Development and Ageing in the Guinea-Pig. *J Auton Nerv Syst,* 16**,** 109-26.

Docherty, J. R., Macdonald, A. & Mcgrath, J. C. (1979) Further Sub-Classification of Alpha-Adrenoceptors in the Cardiovascular System, Vas Deferens and Anococcygeus of the Rat [Proceedings]. *Br J Pharmacol,* 67**,** 421p-422p.

Docherty, J. R. & Mcgrath, J. C. (1980) A Comparison of Pre-Junctional and Post-Junctional Potencies of Several Alpha-Adrenoceptor Agonists in the Cardiovascular-System and Anococcygeus Muscle of the Rat - Evidence for 2 Types of Post-Junctional Alpha-Adrenoceptor. *Naunyn-Schmiedebergs Archives of Pharmacology,* 312**,** 107-116.

Drew, G. M. (1985) What Do Antagonists Tell Us About Alpha-Adrenoceptors? *Clin Sci (Lond),* 68 Suppl 10**,** 15s-19s.

Dunn, P. M. & Blakeley, A. G. H. (1988) Suramin - a Reversible P2-Purinoceptor Antagonist in the Mouse Vasdeferens. *British Journal of Pharmacology,* 93**,** 243-245.

Dunn, W. R., Hardy, T. A. & Brock, J. A. (2003) Electrophysiological Effects of Activating the Peptidergic Primary Afferent Innervation of Rat Mesenteric Arteries. *British Journal of Pharmacology,* 140**,** 231-238.

Ellis, J. L. & Burnstock, G. (1989) Modulation of Neurotransmission in the Guinea-Pig Vas Deferens by Capsaicin: Involvement of Calcitonin Gene-Related Peptide and Substance P. *Br J Pharmacol,* 98**,** 707-13.

Evans, R. J. & Kennedy, C. (1994) Characterization of P-2-Purinoceptors in the Smooth-Muscle of the Rat Tail Artery - a Comparison between Contractile and Electrophysiological Responses. *British Journal of Pharmacology,* 113**,** 853-860.

Fisher, L. A., Kikkawa, D. O., Rivier, J. E., Amara, S. G., Evans, R. M., Rosenfeld, M. G., Vale, W. W. & Brown, M. R. (1983) Stimulation of Noradrenergic Sympathetic Outflow by Calcitonin Gene-Related Peptide. *Nature,* 305**,** 534-6.

Flavahan, N. A. & Mcgrath, J. C. (1984) Are Human Vascular Alpha-Adrenoceptors Atypical. *Journal of Cardiovascular Pharmacology,* 6**,** 208-210.

Flavahan, N. A. & Vanhoutte, P. M. (1986) Alpha-1-Adrenoceptor Subclassification in Vascular Smooth-Muscle. *Trends in Pharmacological Sciences,* 7**,** 347-349.

Ford, A. P., Williams, T. J., Blue, D. R. & Clarke, D. E. (1994) Alpha 1-Adrenoceptor Classification: Sharpening Occam's Razor. *Trends Pharmacol Sci,* 15**,** 167-70.

Forray, C., Bard, J. A., Wetzel, J. M., Chiu, G., Shapiro, E., Tang, R., Lepor, H., Hartig, P. R., Weinshank, R. L., Branchek, T. A. & Et Al. (1994) The Alpha 1-Adrenergic Receptor That Mediates Smooth Muscle Contraction in Human Prostate Has the Pharmacological Properties of the Cloned Human Alpha 1c Subtype. *Mol Pharmacol,* 45**,** 703-8.

Fujii, H., Takatori, S., Zamami, Y., Hashikawa-Hobara, N., Miyake, N., Tangsucharit, P., Mio, M. & Kawasaki, H. (2012) Adrenergic Stimulation-Released 5-Ht Stored in Adrenergic Nerves Inhibits Cgrpergic Nerve-Mediated Vasodilatation in Rat Mesenteric Resistance Arteries. *British Journal of Pharmacology,* 166**,** 2084-2094.

Fujimori, A., Saito, A., Kimura, S. & Goto, K. (1990) Release of Calcitonin Gene-Related Peptide (Cgrp) from Capsaicin-Sensitive Vasodilator Nerves in the Rat Mesenteric Artery. *Neurosci Lett,* 112**,** 173-8.

Fujiwara, H., Hashikawa-Hobara, N., Wake, Y., Takatori, S., Goda, M., Higuchi, H., Zamami, Y., Tangsucharit, P. & Kawasaki, H. (2012) Neurogenic Vascular Responses in Male Mouse Mesenteric Vascular Beds. *J Pharmacol Sci,* 119**,** 260-70.

Furchgott, R. F. (1967) The Pharmacological Differentiation of Adrenergic Receptors. *Ann N Y Acad Sci,* 139**,** 553-70.

Gitterman, D. P. & Evans, R. J. (2001) Nerve Evoked P2x Receptor Contractions of Rat Mesenteric Arteries; Dependence on Vessel Size and Lack of Role of L-Type Calcium Channels and Calcium Induced Calcium Release. *Br J Pharmacol,* 132**,** 1201-8.

Goldenberger, D., Perschil, I., Ritzler, M. & Altwegg, M. (1995) A Simple "Universal" DNA Extraction Procedure Using Sds and Proteinase K Is Compatible with Direct Pcr Amplification. *Genome Research,* 4**,** 368-370.

Graham, R. M., Perez, D. M., Hwa, J. & Piascik, M. T. (1996) Alpha(1)-Adrenergic Receptor Subtypes - Molecular Structure, Function, and Signaling. *Circulation Research,* 78**,** 737-749.

Guimaraes, S. & Nunes, J. P. (1990) The Effectiveness of Alpha-2-Adrenoceptor Activation Increases from the Distal to the Proximal Part of the Veins of Canine Limbs. *British Journal of Pharmacology,* 101**,** 387-393.

Hanft, G. & Gross, G. (1989) Subclassification of Alpha 1-Adrenoceptor Recognition Sites by Urapidil Derivatives and Other Selective Antagonists. *Br J Pharmacol,* 97**,** 691-700.

Hansen, M. A., Dutton, J. L., Balcar, V. J., Barden, J. A. & Bennett, M. R. (1999) P2x (Purinergic) Receptor Distributions in Rat Blood Vessels. *Journal of the Autonomic Nervous System,* 75**,** 147-155.

Hosoda, C., Koshimizu, T. A., Tanoue, A., Nasa, Y., Oikawa, R., Tomabechi, T., Fukuda, S., Shinoura, H., Oshikawa, S., Takeo, S., Kitamura, T., Cotecchia, S. & Tsujimoto, G. (2005) Two Alpha1-Adrenergic Receptor Subtypes Regulating the Vasopressor Response Have Differential Roles in Blood Pressure Regulation. *Mol Pharmacol,* 67**,** 912-22.

Huidobro-Toro, J. P. & Donoso, M. V. (2004) Sympathetic Co-Transmission: The Coordinated Action of Atp and Noradrenaline and Their Modulation by Neuropeptide Y in Human Vascular Neuroeffector Junctions. *European Journal of Pharmacology,* 500**,** 27-35.

Hunter, J. C., Fontana, D. J., Hedley, L. R., Jasper, J. R., Lewis, R., Link, R. E., Secchi, R., Sutton, J. & Eglen, R. M. (1997) Assessment of the Role of Alpha(2)-Adrenoceptor Subtypes in the Antinociceptive, Sedative and Hypothermic Action of Dexmedetomidine in Transgenic Mice. *British Journal of Pharmacology,* 122**,** 1339-1344.

Hussain, M. B. & Marshall, I. (1997) Characterization of Alpha(1)-Adrenoceptor Subtypes Mediating Contractions to Phenylephrine in Rat Thoracic Aorta, Mesenteric Artery and Pulmonary Artery. *British Journal of Pharmacology,* 122**,** 849-858.

Jaenisch, R. (1976) Germ Line Integration and Mendelian Transmission of Exogenous Moloney Leukemia-Virus. *Proceedings of the National Academy of Sciences of the United States of America,* 73**,** 1260-1264.

Jaenisch, R. (1979) Moloney Leukemia-Virus Gene-Expression and Gene Amplification in Preleukemic and Leukemic Balb-Mo Mice. *Virology,* 93**,** 80-90.

Jaenisch, R. & Mintz, B. (1974) Simian Virus 40 DNA Sequences in DNA of Healthy Adult Mice Derived from Preimplantation Blastocysts Injected with Viral DNA. *Proceedings of the National Academy of Sciences of the United States of America,* 71**,** 1250-1254.

Janig, W. 2006. *Integrative Action of the Autonomic Nervous System: Neurobiology of Homeostasis*.

Jantschak, F., Popp, A. M., Hofmann, R. A., Villalon, C. M., Centurion, D. & Pertz, H. H. (2010) Postjunctional Alpha(2c)-Adrenoceptors Mediate Vasoconstriction in Rat Tail Artery: Influence of Precontraction and Temperature on Vasoreactivity. *Naunyn-Schmiedebergs Archives of Pharmacology,* 382**,** 487-497.

Kable, J. W., Murrin, L. C. & Bylund, D. B. (2000) In Vivo Gene Modification Elucidates Subtype-Specific Functions of Alpha(2)-Adrenergic Receptors. *Journal of Pharmacology and Experimental Therapeutics,* 293**,** 1-7.

Kasakov, L. & Burnstock, G. (1983) The Use of the Slowly Degradable Analog Alpha Beta Methylene Atp to Produce De Sensitization of the P-2 Purinoceptor Effect on Nonadrenergic Noncholinergic Responses of the Guinea-Pig Urinary Bladder. *European Journal of Pharmacology,* 86**,** 291-294.

Kawasaki, H., Nuki, C., Saito, A. & Takasaki, K. (1990) Adrenergic Modulation of Calcitonin Gene-Related Peptide (Cgrp)-Containing Nerve-Mediated Vasodilation in the Rat Mesenteric Resistance Vessel. *Brain Research,* 506**,** 287-290.

Kawasaki, H., Takasaki, K., Saito, A. & Goto, K. (1988) Calcitonin Gene-Related Peptide Acts as a Novel Vasodilator Neurotransmitter in Mesenteric Resistance Vessels of the Rat. *Nature,* 335**,** 164-7.

Kobilka, B. K., Matsui, H., Kobilka, T. S., Yangfeng, T. L., Francke, U., Caron, M. G., Lefkowitz, R. J. & Regan, J. W. (1987) Cloning, Sequencing, and Expression of the Gene Coding for the Human-Platelet Alpha-2-Adrenergic Receptor. *Science,* 238**,** 650-656.

Lachnit, W. G., Tran, A. M., Clarke, D. E. & Ford, A. (1997) Pharmacological Characterization of an Alpha(1a)-Adrenoceptor Mediating Contractile Responses to Noradrenaline in Isolated Caudal Artery of Rat. *British Journal of Pharmacology,* 120**,** 819-826.

Lakhlani, P. P., Macmillan, L. B., Guo, T. Z., Mccool, B. A., Lovinger, D. M., Maze, M. & Limbird, L. E. (1997) Substitution of a Mutant Alpha(2a)-Adrenergic Receptor Via ''Hit and Run'' Gene Targeting Reveals the Role of This Subtype in Sedative, Analgesic, and Anesthetic-Sparing Responses in Vivo. *Proceedings of the National Academy of Sciences of the United States of America,* 94**,** 9950-9955.

Lamont, C. & Wier, W. G. (2002) Evoked and Spontaneous Purinergic Junctional Ca2+ Transients (Jcats) in Rat Small Arteries. *Circulation Research,* 91**,** 454-456.

Langer, S. Z. (1974) Presynaptic Regulation of Catecholamine Release. *Biochem Pharmacol,* 23**,** 1793-800.

Lattimer, N. & Rhodes, K. F. (1985) A Difference in the Affinity of Some Selective Alpha-2-Adrenoceptor Antagonists When Compared on Isolated Vasa Deferentia of Rat and Rabbit. *Naunyn-Schmiedebergs Archives of Pharmacology,* 329**,** 278-281.

Lee, T. J., Hume, W. R., Su, C. & Bevan, J. A. (1978) Neurogenic Vasodilation of Cat Cerebral Arteries. *Circulation Research,* 42**,** 535-42.

Lin, F., Owens, W. A., Chen, S., Stevens, M. E., Kesteven, S., Arthur, J. F., Woodcock, E. A., Feneley, M. P. & Graham, R. M. (2001) Targeted Alpha1a-Adrenergic Receptor Overexpression Induces Enhanced Cardiac Contractility but Not Hypertrophy. *Circulation Research,* 89**,** 343-350.

Link, R. E., Desai, K., Hein, L., Stevens, M. E., Chruscinski, A., Bernstein, D., Barsh, G. S. & Kobilka, B. K. (1996) Cardiovascular Regulation in Mice Lacking Alpha(2)-Adrenergic Receptor Subtypes B and C. *Science,* 273**,** 803-805.

Lomasney, J. W., Cotecchia, S., Lorenz, W., Leung, W. Y., Schwinn, D. A., Yang-Feng, T. L., Brownstein, M., Lefkowitz, R. J. & Caron, M. G. (1991) Molecular Cloning and Expression of the Cdna for the Alpha 1a-Adrenergic Receptor. The Gene for Which Is Located on Human Chromosome 5. *J Biol Chem,* 266**,** 6365-9.

Lomasney, J. W., Lorenz, W., Allen, L. F., King, K., Regan, J. W., Yangfeng, T. L., Caron, M. G. & Lefkowitz, R. J. (1990) Expansion of the Alpha-2-Adrenergic Receptor Family - Cloning and Characterization of a Human Alpha-2-Adrenergic Receptor Subtype, the Gene for Which Is Located on Chromosome-2. *Proceedings of the National Academy of Sciences of the United States of America,* 87**,** 5094-5098.

Lundbaek, J. A., Birn, P., Tape, S. E., Toombes, G. E., Sogaard, R., Koeppe, R. E., 2nd, Gruner, S. M., Hansen, A. J. & Andersen, O. S. (2005) Capsaicin Regulates Voltage-Dependent Sodium Channels by Altering Lipid Bilayer Elasticity. *Mol Pharmacol,* 68**,** 680-9.

Martinez-Salas, S. G., Campos-Peralta, J. M., Pares-Hipolito, J., Gallardo-Ortiz, I. A., Ibarra, M. & Villalobos-Molina, R. (2007) Alpha(1a)-Adrenoceptors Predominate in the Control of Blood Pressure in Mouse Mesenteric Vascular Bed. *Autonomic & Autacoid Pharmacology,* 27**,** 137-142.

Martinez, L., Carmona, L. & Villalobos-Molina, R. (1999) Vascular Alpha(1d)-Adrenoceptor Function Is Maintained During Congestive Heart Failure after Myocardial Infarction in the Rat. *Archives of Medical Research,* 30**,** 290-297.

Mcgrath, J. C. (1982) Evidence for More Than One Type of Post-Junctional Alpha-Adrenoceptor. *Biochemical Pharmacology,* 31**,** 467-484.

Medgett, I. C. (1985) Alpha-2-Adrenoceptors Mediate Sympathetic Vasoconstriction in Distal Segments of Rat Tail Artery. *European Journal of Pharmacology,* 108**,** 281-287.

Methven, L., Mcbride, M., Wallace, G. A. & Mcgrath, J. C. (2009a) The Alpha(1b/D)-Adrenoceptor Knockout Mouse Permits Isolation of the Vascular Alpha(1a)-Adrenoceptor and Elucidates Its Relationship to the Other Subtypes. *British Journal of Pharmacology,* 158**,** 209-224.

Methven, L., Simpson, P. C. & Mcgrath, J. C. (2009b) Alpha(1a/B)-Knockout Mice Explain the Native Alpha(1d)-Adrenoceptor's Role in Vasoconstriction and Show That Its Location Is Independent of the Other Alpha(1)-Subtypes. *British Journal of Pharmacology,* 158**,** 1663-1675.

Milano, C. A., Dolber, P. C., Rockman, H. A., Bond, R. A., Venable, M. E., Allen, L. F. & Lefkowitz, R. J. (1994) Myocardial Expression of a Constitutively Active Alpha(1b)-Adrenergic Receptor in Transgenic Mice Induces Cardiac-Hypertrophy. *Proceedings of the National Academy of Sciences of the United States of America,* 91**,** 10109-10113.

Minneman, K. P. (1988) Alpha-1-Adrenergic Receptor Subtypes, Inositol Phosphates, and Sources of Cell Ca-2+. *Pharmacological Reviews,* 40**,** 87-119.

Morrison, J. F. B., Dhanasekaran, S. & Howarth, F. C. (2009) Neuropeptide Y and Cgrp Concentrations in the Rat Tail Artery: Effects of Age and Two Types of Diabetes. *Peptides,* 30**,** 710-714.

Morrow, A. L. & Creese, I. (1986) Characterization of Alpha 1-Adrenergic Receptor Subtypes in Rat Brain: A Reevaluation of [3h]Wb4104 and [3h]Prazosin Binding. *Mol Pharmacol,* 29**,** 321-30.

Morton, J. S. 2006. *Novel in Vitro Models to Investigate Pharmacological Targets in Genital Resistance Vasculature.* PhD, University of Glasgow.

Msghina, M., Gonon, F. & Stjarne, L. (1999) Facilitation and Depression of Atp and Noradrenaline Release from Sympathetic Nerves of Rat Tail Artery. *Journal of Physiology-London,* 515**,** 523-531.

Msghina, M., Mermet, C., Gonon, F. & Stjarne, L. (1992) Electrophysiological and Electrochemical Analysis of the Secretion of Atp and Noradrenaline from the Sympathetic-Nerves in Rat Tail Artery - Effects of Alpha-2-Adrenoceptor Agonists and Antagonists and Noradrenaline Reuptake Blockers. *Naunyn-Schmiedebergs Archives of Pharmacology,* 346**,** 173-186.

Mulvany, M. J. & Halpern, W. (1976) Mechanical Properties of Vascular Smooth Muscle Cells in Situ. *Nature,* 260**,** 617-9.

Muramatsu, I., Ohmura, T., Kigoshi, S., Hashimoto, S. & Oshita, M. (1990) Pharmacological Subclassification of Alpha 1-Adrenoceptors in Vascular Smooth Muscle. *Br J Pharmacol,* 99**,** 197-201.

Murphy, T. J. & Bylund, D. B. (1988) Characterization of Alpha-2 Adrenergic-Receptors in the Ok Cell, an Opossum Kidney-Cell Line. *Journal of Pharmacology and Experimental Therapeutics,* 244**,** 571-578.

Mutafova-Yambolieva, V. N. & Keef, K. D. (2001) Frequency Dependent Alpha(2)-Adrenoceptor Mediated Modulation of Excitatory Junction Potentials in Guinea-Pig Mesenteric Artery. *European Journal of Pharmacology,* 411**,** 123-127.

O'connell, T. D., Ishizaka, S., Nakamura, A., Swigart, P. M., Rodrigo, M. C., Simpson, G. L., Cotecchia, S., Rokosh, D. G., Grossman, W., Foster, E. & Simpson, P. C. (2003) The Alpha(1a/C)- and Alpha(1b)-Adrenergic Receptors Are Required for Physiological Cardiac Hypertrophy in the Double-Knockout Mouse. *Journal of Clinical Investigation,* 111**,** 1783-1791.

Perez, D. M., Piascik, M. T. & Graham, R. M. (1991) Solution-Phase Library Screening for the Identification of Rare Clones: Isolation of an Alpha 1d-Adrenergic Receptor Cdna. *Mol Pharmacol,* 40**,** 876-83.

Petrash, A. C. & Bylund, D. B. (1986) Alpha-2 Adrenergic-Receptor Subtypes Indicated by H-3 Yohimbine Binding in Human-Brain. *Life Sciences,* 38**,** 2129-2137.

Pipili, E. (1986) A Study on the Postjunctional Excitatory Alpha-Adrenoceptor Subtypes in the Mesenteric Arterial Bed of the Rat. *Journal of Autonomic Pharmacology,* 6**,** 125-132.

Powell, C. E. & Slater, I. H. (1958) Blocking of Inhibitory Adrenergic Receptors by a Dichloro Analog of Isoproterenol. *J Pharmacol Exp Ther,* 122**,** 480-8.

Rajanayagam, M. a. S. & Medgett, I. C. (1987) Greater Activation of Smooth-Muscle Alpha-2 Adrenoceptors by Epinephrine in Distal Than in Proximal Segments of Rat Tail Artery. *Journal of Pharmacology and Experimental Therapeutics,* 240**,** 989-997.

Ralevic, V. & Burnstock, G. (1990) Postjunctional Synergism of Noradrenaline and Adenosine 5'-Triphosphate in the Mesenteric Arterial Bed of the Rat. *European Journal of Pharmacology,* 175**,** 291-299.

Regan, J. W., Kobilka, T. S., Yangfeng, T. L., Caron, M. G., Lefkowitz, R. J. & Kobilka, B. K. (1988) Cloning and Expression of a Human-Kidney Cdna for an Alpha-2-Adrenergic Receptor Subtype. *Proceedings of the National Academy of Sciences of the United States of America,* 85**,** 6301-6305.

Rokosh, D. G. & Simpson, P. C. (2002) Knockout of the Alpha 1a/C-Adrenergic Receptor Subtype: The Alpha 1a/C Is Expressed in Resistance Arteries and Is Required to Maintain Arterial Blood Pressure. *Proceedings of the National Academy of Sciences of the United States of America,* 99**,** 9474-9479.

Rosenfeld, M. G., Mermod, J.-J., Amara, S. G., Swanson, L. W., Sawchenko, P. E., Rivier, J., Vale, W. W. & Evans, R. M. (1983) Production of a Novel Neuropeptide Encoded by the Calcitonin Gene Via Tissue-Specific Rna Processing. *Nature,* 304**,** 129-135.

Ross, K. S., Haites, N. E. & Kelly, K. F. (1990) Repeated Freezing and Thawing of Peripheral Blood and DNA in Suspension: Effects on DNA Yield and Integrity. *Journal of Medical Genetics,* 27**,** 569-570.

Ruffolo, R. R., Nichols, A. J., Stadel, J. M. & Hieble, J. P. (1991) Structure and Function of Alpha-Adrenoceptors. *Pharmacological Reviews,* 43**,** 475-505.

Ruffolo, R. R. & Yaden, E. L. (1984) Existence of Spare Alpha-1-Adrenoceptors, but Not Alpha-2-Adrenoceptors, for Respective Vasopressor Effects of Cirazoline and B-Ht 933 in the Pithed Rat. *Journal of Cardiovascular Pharmacology,* 6**,** 1011-1019.

Rummery, N. M., Brock, J. A., Pakdeechote, P., Ralevic, V. & Dunn, W. R. (2007) Atp Is the Predominant Sympathetic Neurotransmitter in Rat Mesenteric Arteries at High Pressure. *Journal of Physiology-London,* 582**,** 745-754.

Sallinen, J., Haapalinna, A., Macdonald, E., Viitamaa, T., Lahdesmaki, J., Rybnikova, E., Pelto-Huikko, M., Kobilka, B. K. & Scheinin, M. (1999) Genetic Alteration of the Alpha(2)-Adrenoceptor Subtype C in Mice Affects the Development of Behavioral Despair and Stress-Induced Increases in Plasma Corticosterone Levels. *Molecular Psychiatry,* 4**,** 443-452.

Sallinen, J., Link, R. E., Haapalinna, A., Viitamaa, T., Kulatunga, M., Sjoholm, B., Macdonald, E., Peltohuikko, M., Leino, T., Barsh, G. S., Kobilka, B. K. & Scheinin, M. (1997) Genetic Alteration of Alpha(2c)-Adrenoceptor Expression in Mice: Influence on Locomotor, Hypothermic, and Neurochemical Effects of Dexmedetomidine, a Subtype-Nonselective Alpha(2)-Adrenoceptor Agonist. *Molecular Pharmacology,* 51**,** 36-46.

Sanbe, A., Tanaka, Y., Fujiwara, Y., Miyauchi, N., Mizutani, R., Yamauchi, J., Cotecchia, S., Koike, K., Tsujimoto, G. & Tanoue, A. (2009) Enhanced Vascular Contractility in Alpha1-Adrenergic Receptor-Deficient Mice. *Life Sciences,* 84**,** 713-718.

Sanbe, A., Tanaka, Y., Fujiwara, Y., Tsumura, H., Yamauchi, J., Cotecchia, S., Koike, K., Tsujimoto, G. & Tanoue, A. (2007) Alpha(1)-Adrenoceptors Are Required for Normal Male Sexual Function. *British Journal of Pharmacology,* 152**,** 332-340.

Schwinn, D. A., Lomasney, J. W., Lorenz, W., Szklut, P. J., Fremeau, R. T., Jr., Yang-Feng, T. L., Caron, M. G., Lefkowitz, R. J. & Cotecchia, S. (1990) Molecular Cloning and Expression of the Cdna for a Novel Alpha 1-Adrenergic Receptor Subtype. *J Biol Chem,* 265**,** 8183-9.

Shafaroudi, M. M., Mcbride, M., Deighan, C., Wokoma, A., Macmillan, J., Daly, C. J. & Mcgrath, J. C. (2005) Two "Knockout" Mouse Models Demonstrate That Aortic Vasodilatation Is Mediated Via Alpha2a-Adrenoceptors Located on the Endothelium. *J Pharmacol Exp Ther,* 314**,** 804-10.

Sheykhzade, M., Gupta, S., Sorensen, T., Sorensen, O. A., Koch, H., Boonen, H. C., Back, O. & Fjalland, B. (2011) Characterization of Capsaicin Induced Responses in Mice Vas Deferens: Evidence of Cgrp Uptake. *Eur J Pharmacol,* 667**,** 375-82.

Sjoblom-Widfeldt, N., Gustafsson, H. & Nilsson, H. (1990) Transmitter Characteristics of Small Mesenteric Arteries from the Rat. *Acta Physiol Scand,* 138**,** 203-12.

Sneddon, P. & Burnstock, G. (1984) Atp as a Co-Transmitter in Rat Tail Artery. *European Journal of Pharmacology,* 106**,** 149-152.

Starke, K., Montel, H., Gayk, W. & Merker, R. (1974) Comparison of Effects of Clonidine on Presynaptic and Postsynaptic Adrenoceptors in Rabbit Pulmonary-Artery - Alpha-Sympathomimetic Inhibition of Neurogenic Vasoconstriction. *Naunyn-Schmiedebergs Archives of Pharmacology,* 285**,** 133-150.

Tan, J. H., Al Abed, A. & Brock, J. A. (2007) Inhibition of K-Atp Channels in the Rat Tail Artery by Neurally Released Noradrenaline Acting on Postjunctional Alpha(2)-Adrenoceptors. *Journal of Physiology-London,* 581**,** 757-765.

Tanoue, A., Nasa, Y., Koshimizu, T., Shinoura, H., Oshikawa, S., Kawai, T., Sunada, S., Takeo, S. & Tsujimoto, G. (2002) The Alpha(Ld)-Adrenergic Receptor Directly Regulates Arterial Blood Pressure Via Vasoconstriction. *Journal of Clinical Investigation,* 109**,** 765-775.

Tornebrandt, K., Nobin, A. & Owman, C. (1987) Contractile and Dilatory Action of Neuropeptides on Isolated Human Mesenteric Blood Vessels. *Peptides,* 8**,** 251-6.

Uberti, M. A., Hall, R. A. & Minneman, K. P. (2003) Subtype-Specific Dimerization of Alpha(1)-Adrenoceptors: Effects on Receptor Expression and Pharmacological Properties. *Molecular Pharmacology,* 64**,** 1379-1390.

Uddman, R., Edvinsson, L., Ekblad, E., Hakanson, R. & Sundler, F. (1986) Calcitonin Gene-Related Peptide (Cgrp): Perivascular Distribution and Vasodilatory Effects. *Regul Pept,* 15**,** 1-23.

Vargas, H. M. & Gorman, A. J. (1995) Vascular Alpha-1-Adrenergic Receptor Subtypes in the Regulation of Arterial-Pressure. *Life Sciences,* 57**,** 2291-2308.

Vial, C. & Evans, R. J. (2002) P2x(1) Receptor-Deficient Mice Establish the Native P2x Receptor and a P2y(6)-Like Receptor in Arteries. *Molecular Pharmacology,* 62**,** 1438-1445.

Villalobos-Molina, R., Martinez-Salas, S. G., Campos-Peralta, J. M., Pares-Hipolito, J., Gallardo-Ortiz, I. A. & Ibarra, M. (2006) Alpha(1a)-Adrenoceptors Control Blood Pressure in the Mouse Mesenteric Vascular Bed. *Acta Pharmacologica Sinica,* 27**,** 158-158.

Voets, T., Droogmans, G., Wissenbach, U., Janssens, A., Flockerzi, V. & Nilius, B. (2004) The Principle of Temperature-Dependent Gating in Cold- and Heat-Sensitive Trp Channels. *Nature,* 430**,** 748-754.

Wang, L.-H., Luo, M., Wang, Y. & Wang, D. H. (2006) Impaired Vasodilation in Response to Perivascular Nerve Stimulation in Mesenteric Arteries of Trpv1-Null Mutant Mice. *Journal of Hypertension,* 24**,** 2399-2408.

Weiss, R. J., Webb, R. C. & Smith, C. B. (1983) Alpha-2 Adrenoreceptors on Arterial Smooth-Muscle - Selective Labeling by Clonidine-H-3. *Journal of Pharmacology and Experimental Therapeutics,* 225**,** 599-605.

Wharton, J., Gulbenkian, S., Mulderry, P. K., Ghatei, M. A., Mcgregor, G. P., Bloom, S. R. & Polak, J. M. (1986) Capsaicin Induces a Depletion of Calcitonin Gene-Related Peptide (Cgrp)-Immunoreactive Nerves in the Cardiovascular System of the Guinea Pig and Rat. *J Auton Nerv Syst,* 16**,** 289-309.

Wimalawansa, S. J. & Macintyre, I. (1988) Calcitonin Gene-Related Peptide and Its Specific Binding Sites in the Cardiovascular System of Rat. *International Journal of Cardiology,* 20**,** 29-37.

Wu, D. Q., Katz, A., Lee, C. H. & Simon, M. I. (1992) Activation of Phospholipase-C by Alpha-1-Adrenergic Receptors Is Mediated by the Alpha-Subunits of Gq Family. *Journal of Biological Chemistry,* 267**,** 25798-25802.

Young, P., Berge, J., Chapman, H. & Cawthorne, M. A. (1989) Novel Alpha-2-Adrenoceptor Antagonists Show Selectivity for Alpha-2a-Adrenoceptor and Alpha-2b-Adrenoceptor Subtypes. *European Journal of Pharmacology,* 168**,** 381-386.

Zaidi, M., Bevis, P. J., Girgis, S. I., Lynch, C., Stevenson, J. C. & Macintyre, I. (1985) Circulating Cgrp Comes from the Perivascular Nerves. *Eur J Pharmacol,* 117**,** 283-4.

Zuscik, M. J., Chalothorn, D., Hellard, D., Deighan, C., Mcgee, A., Daly, C. J., Waugh, D. J., Ross, S. A., Gaivin, R. J., Morehead, A. J., Thomas, J. D., Plow, E. F., Mcgrath, J. C., Piascik, M. T. & Perez, D. M. (2001) Hypotension, Autonomic Failure, and Cardiac Hypertrophy in Transgenic Mice Overexpressing the Alpha 1b-Adrenergic Receptor. *J Biol Chem,* 276**,** 13738-43.